Convection with Chemical Reaction, and Waves in Double Porosity Materials

AL-SULAIMI, BUSHRA,HABARAS,SHABIT

Convection with Chemical Reaction, and Waves in Double Porosity Materials

Bushra Al-Sulaimi

A Thesis presented for the degree of
Doctor of Philosophy

Applied Mathematics and Numerical Analysis
Department of Mathematical Sciences
University of Durham
England

January 2017

Dedicated to

My Father, May God rest his soul, and My Mother

with Love and Gratitude.

Convection with Chemical Reaction, and Waves in Double Porosity Materials

Bushra Al-Sulaimi

Submitted for the degree of Doctor of Philosophy
January 2017

Abstract

We consider two cases of solid skeleton of porous materials: fixed skeleton saturated with fluid in motion and deformed skeleton.

In the first case, we study a problem involving the onset of thermosolutal convection in a fluid saturated porous media when the solute concentration is subject to a chemical reaction in which the solubility of the dissolved mineral is a function of temperature, particularly the effect of a reaction rate on the stability of the systems. We consider the Darcy model, the Brinkman model, and the Darcy model with anisotropic permeability and thermal diffusivity. Moreover, in all models the systems are subjected to heat on the lower boundary and salt on the upper or lower boundary.

In chapter 2 we show that the solutions to the Darcy and the Brinkman thermosolutal convection depend continuously on the reaction term when the chemical equilibrium is a linear function in temperature by establishing *a priori* bounds. While in chapter 3 we show continuous dependence of the solution to the Brinkman thermosolutal convection on reaction using *a priori* bounds for the solution when the chemical equilibrium function is an arbitrary function of temperature.

In chapter 4 we investigate the effect of the reaction terms on the onset of stability in a Darcy type porous medium using the energy method. We use the D^2 Chebyshev Tau technique to solve the associated system of equations and the cor-

responding boundary conditions. We obtain the energy stability boundaries for different values of the reaction terms and compare them with the linear instability boundaries obtained by Pritchard & Richardson [83]. We find that the two boundaries do not coincide when there is reaction and a region of potential sub-critical instability occur.

In chapter 5 we use the energy method to obtain the non-linear stability boundaries for thermosolutal convection porous medium of a Brinkman type with reaction. We implement the compound matrix technique to solve the associated system of equations with the corresponding boundary conditions. We compare the non-linear stability boundaries for different values of the reaction terms and the Brinkman coefficient with the relevant linear instability boundaries obtained by Wang & Tan [124]. Our investigation shows that a region of potential sub-critical instability may appear as we increase the reaction rate.

We study the effect of the mechanical anisotropy parameter and the thermal anisotropy parameter on the stability of a Darcy reactive thermosolutal porous medium in chapter 6 using the energy method. Particularly, we restrict consideration to horizontal isotropy in mechanical and thermal properties of the porous skeleton. We find that the anisotropic permeability has opposite effect to that of the thermal anisotropy parameter on the stability on the system.

In the second case, deformed solid skeleton, we study wave motion in elastic materials of double porosity structure.

In chapter 7 we derive the amplitude and describe the behaviour of a one-dimensional acceleration wave based on an internal strain energy function. The overall situation is complicated as a wave moves in a three-dimensional body, therefore in chapter 8 we investigate the propagation of an acceleration wave in three-dimensional fully non-linear model.

Declaration

The work in this thesis is based on research carried out at the University of Durham, the Department of Mathematical Sciences, the Applied Mathematics and Numerical Analysis Group, England. No part of this thesis has been submitted elsewhere for any other degree or qualification and it is all my own work with the exception of chapter 3 which contains work published in collaboration with Prof. Brian Straughan in [109]. Chapters 4 and 5 contain work published in [1] and [2] respectively. Part of the material in chapter 6 has been selected to be considered for publication in a special issue of Computational Thermal Sciences: An International Journal. Chapters 2, 7, and 8 may be submitted for publication in due course.

Acknowledgements

My thanks go to my supervisor Prof. B. Straughan for his support and encouragement.

Thanks to Dr. Anthony Yeates for his help, Imran M. for preparing the LaTeX template used for this thesis, and the Applied Mathematics and Numerical Analysis Group at the Mathematical Sciences Department, University of Durham.

Many thanks also to Prof. Ibrahim A. Eltayeb and Dr. Mahmood Al-Sulaimi, my family, Hassan, and my friends Anum, Iman, Khadija, Yesoul, Rafia, and Samia for their support.

I would like to acknowledge the Ministry of Higher Education, Muscat, Sultanate of Oman, for the scholarship and the financial support and the Ministry of Manpower and the Higher College of Technology, Muscat.

Contents

Abstract **iii**

Declaration **v**

Acknowledgements **vi**

1 Introduction **1**

1.1 Notations and Preliminaries 6

1.2 Bénard Problem and Navier-Stokes Equations 8

1.2.1 Basic Equations 8

1.2.2 Bénard Problem 9

1.2.3 Perturbations and Non-dimensionalisations 10

1.2.4 Boundary Conditions 11

1.2.5 Linear Instability 13

1.2.6 Exchange of Stabilities 13

1.2.7 The Nonlinear Stability 15

1.3 Overview 17

2 Continuous Dependence of Darcy and Brinkman Convection on Reaction **23**

2.1 Introduction 23

2.2 Basic Equations 23

2.3 A priori Estimates 25

2.3.1 A priori bounds for $\|T\|^2$, $\|C\|^2$, $\int_0^t \|T\|^2 ds$, $\int_0^t \|C\|^2 ds$, $\int_0^t \|\nabla C\|^2 ds$, $\int_0^t \|\nabla T\|^2 ds$ 25

2.3.2 Bounds for the $Sup_{\Omega\times[0,\tau]}|C|$ and $Sup_{\Omega\times[0,\tau]}|T|$ 32
2.4 Convergence of K(p) 41
2.5 Continuous Dependence on the Reaction Term 41

3 Structural Stability for Brinkman Convection With Reaction 45
3.1 Introduction 45
3.2 Basic Equations 45
3.3 A priori Estimates 47
3.4 Continuous Dependence on the Reaction 53

4 The Energy Stability of Darcy Thermosolutal Convection with Reaction 55
4.1 Introduction 55
4.2 Basic Equations 56
4.3 The Linear Instability Analysis 58
4.4 The Non-Linear Energy Stability Analysis 61
4.5 The Numerical Method 67
4.6 Numerical Results and Conclusion 69
4.6.1 Heated below and salted above system 69
4.6.2 Heated and salted below system 70

5 The Energy Stability of Brinkman Thermosolutal Convection with Reaction 80
5.1 Introduction 80
5.2 Basic Equations 81
5.3 Linear Instability Theory 84
5.4 Nonlinear Energy Stability Theory 85
5.5 The Numerical Method 89
5.5.1 The D^2 Chebyshev Tau method for the linear theory 89
5.5.2 The Compound Matrix technique for the energy theory 91
5.6 Numerical Results and Conclusion 92
5.6.1 Heated below salted above system 93

5.6.2 Heated and Salted Below system 95

6 Thermosolutal Convection in a Darcy Porous Medium with Anisotropic Permeability and Thermal Diffusivity 104

6.1 Introduction 104
6.2 Basic Equations 105
6.3 Linear Instability Theory 108
6.4 Non-Linear Energy Stability Theory 108
6.5 Numerical Method 112
6.6 Numerical Results and Conclusions 114
6.6.1 Salted above system 114
6.6.2 Salted below system 119

7 One-Dimensional Acceleration Waves in Non-Linear Double Porosity Materials 134

7.1 Introduction 134
7.2 Basic Equations 136
7.3 Acceleration Waves 138
7.4 Amplitude Equation 141
7.5 Special Case: Given Strain Energy Function 145

8 Three-Dimensional Acceleration Waves in Non-Linear Double Porosity Materials 149

8.1 Introduction 149
8.2 Acceleration Waves 150

9 Conclusions and Future Work 157

Appendix 172

A Useful Expressions 172

A.1 The Proof of *lemma 1* 172
A.2 The Proof of *lemma 2* 174

B The Chebyshev Tau Method **176**

B.1 Chebyshev Polynomials 176

B.2 Roots and Extrema 177

B.3 Orthogonality 178

B.4 Chebyshev Differential Matrices 179

B.5 Application of Chebyshev Tau Method 185

C The Compound Matrix Method **188**

List of Figures

4.1 Linear instability and Energy stability boundaries for the salted above Darcy convection problem for different values of the reaction rates h and η. 74

4.2 Linear instability and Energy stability boundaries for the salted above Darcy convection problem when the difference between h and η is huge. 75

4.3 Linear instability and Energy stability boundaries for the salted below Darcy convection problem for different values of h and η. 77

4.4 Linear instability and Energy stability boundaries for the salted below Darcy convection problem $\varepsilon = 3$. 77

4.5 Linear instability and Energy stability boundaries for the salted below Darcy convection problem for $\varepsilon = 2$. 78

4.6 Linear instability and Energy stability boundaries for the salted below Darcy convection problem for $\varepsilon = 5$. 79

5.1 Linear instability and energy stability boundaries for the salted above Brinkman convection problem for different values of the reaction rates h and η. 94

5.2 Linear instability and energy stability boundaries for the salted above Brinkman convection problem. The difference between the values of the reaction rates h and η is large. 96

5.3 Linear instability and energy stability boundaries for the salted above Brinkman convection problem when the Brinkman constant $\tilde{\gamma}$ is 0.5. . 97

5.4 Linear instability and energy stability boundaries for the salted above Brinkman convection problem when the Brinkman constant $\tilde{\gamma}$ is 2. . . 98

5.5 Linear instability and energy stability boundaries for the salted above Brinkman convection problem for different values of the Brinkman constant, $\tilde{\gamma} = 0.5, 1, 2$. 99
5.6 Linear instability and energy stability boundaries for the salted below Brinkman convection problem for different values of the reaction rates h and η. 100
5.7 Linear instability and energy stability boundaries for the salted below Brinkman convection problem. The difference between the values of the reaction rates h and η is large. 101
5.8 Linear instability and energy stability boundaries for the salted below Brinkman convection problem when the Brinkman constant $\tilde{\gamma}$ is 0.5. . 102
5.9 Linear instability and energy stability boundaries for the salted below Brinkman convection problem when the Brinkman constant $\tilde{\gamma}$ is 2. . . 103

6.1 Linear instability and energy stability boundaries for the salted above Darcy convection problem for different values of the anisotropic parameters when there is no reaction. 117
6.2 Linear instability and energy stability boundaries for the salted above Darcy convection problem with anisotropic effect for $\alpha = 0.5$, $\chi = 10$ and different values of the reaction rates h and η. 118
6.3 Linear instability and energy stability boundaries for the salted above Darcy convection problem with anisotropic effect for $\alpha = 1$. 124
6.4 Linear instability and energy stability boundaries for the salted above Darcy convection problem with anisotropic effect for $\alpha = 0.5$. 125
6.5 Linear instability and energy stability boundaries for the salted above Darcy convection problem with anisotropic effect for $\chi = 10$. 126
6.6 The energy stability boundaries for the salted above Darcy convection problem with anisotropic effect for $\alpha = 1$, $h = 20$, $\eta = 0$. The figure shows the effect of increasing the vertical permeability component, K_z.127

6.7 The energy stability boundaries for the salted above Darcy convection problem with anisotropic effect for $\chi = 10$, $h = 20$, $\eta = 0$. The figure shows the effect of increasing the vertical thermal diffusivity component, k_{Tz}. 127

6.8 Linear instability and energy stability boundaries for the salted below Darcy convection problem with anisotropic effect for $\alpha = 0.5$, $\chi = 10$ and different values of the reaction rates h and η. 128

6.9 Linear instability and energy stability boundaries for the salted below Darcy convection problem with anisotropic effect for $\alpha = 0.5$. 129

6.10 Linear instability and energy stability boundaries for the salted below Darcy convection problem with anisotropic effect for $\chi = 10$. 130

6.11 Linear instability and energy stability boundaries for the salted below Darcy convection problem with anisotropic effect for $\alpha = 0.5$, and $\chi = 10$ for different values of ϵ. 131

6.12 Linear instability and energy stability boundaries for the salted below Darcy convection problem with anisotropic effect for $\alpha = 0.5$ and $\epsilon = 3$. 132

6.13 Linear instability and energy stability boundaries for the salted below Darcy convection problem with anisotropic effect for $\chi = 10$ and $\epsilon = 3$. 133

List of Tables

4.1 Critical Rayleigh numbers of linear theory, Ra_L, and nonlinear energy theory, Ra_E for the salted above Darcy convection problem, with their respective critical wave numbers a_L, a_E when there is No Reaction *i.e.* $h = \eta = 0$. λ is the coupling parameter. 70

4.2 Critical Rayleigh numbers of linear theory, Ra_L, and nonlinear energy theory, Ra_E for the salted above Darcy convection problem, with their respective critical wave numbers a_L, a_E when $h = 5$ *and* $\eta = 3$. λ is the coupling parameter. 71

4.3 Critical Rayleigh numbers of linear theory, Ra_L, and nonlinear energy theory, Ra_E for the salted above Darcy convection problem, with their respective critical wave numbers a_L, a_E when $h = 20$ *and* $\eta = 16$. λ is the coupling parameter. 76

5.1 Some numerical values obtained for the linear boundary Ra_L and energy boundary Ra_E temperature Rayleigh number with corresponding salt Rayleigh number R_s and the the corresponding critical wave numbers a_L and a_E when $\tilde{\gamma} = 1$, $h = 9$ and $\eta = 6$ in the case of heated below salted above system. 95

6.1 Some numerical values obtained for the linear boundary Ra_L and the energy boundary Ra_E with corresponding salt Rayleigh number R_s and the the corresponding critical wave numbers a_L and a_E when $\alpha = 1$, $h = 20$ and $\eta = 0$ in the case of heated below salted above system. For two cases of the mechanical anisotropy parameter χ, $\chi = 2$ and $\chi = 10$. 116

6.2 Some numerical values obtained for the linear boundary Ra_L and the energy boundary Ra_E with corresponding salt Rayleigh number R_s and the the corresponding critical wave numbers a_L and a_E when $\chi = 10$, $h = 0$ and $\eta = 20$ in the case of heated below salted below system. For two cases of the thermal anisotropy parameter α, $\alpha = 0.5$ and $\alpha = 1$. 122

6.3 Some numerical values obtained for the linear boundaries Ra_L with corresponding salt Rayleigh number R_s and the the corresponding critical wave numbers a_L when $\alpha = 0.5$, $\chi = 10$, $h = 20$ and $\eta = 0$ in the case of heated below salted below system. For two cases of the porosity ϵ, $\epsilon = 3$ and $\epsilon = 5$. 123

Chapter 1

Introduction

Porous media studies are of great interest and well investigated by many researchers due to their wide range of applications in sciences and engineering, such as material science, filtration, petroleum engineering, etc. The Darcy and the Brinkman equations are often considered to be the equations governing the flow of fluid in porous media. The Darcy equation describes the proportionality of the velocity and the pressure gradient in the direction of flow. To describe a porous flow situation when the porosity is large, the Darcy equation is usually replaced by the Brinkman equation, cf. Straughan [99].

Normally, a fluid in a horizontal porous medium subjected to a heat on the upper boundary will remain in a stable state. Alternatively, if a fluid is exposed to heat on the lower boundary, the fluid in the lower part of the layer will expand and this gives rise to a buoyancy force which once it exceeds the gravitational force acting downward will give rise to instability. This is the thermal convection problem. Thermal convection in porous media problems and stability analysis returns back to Horton & Rogers [40] and Lapwood [52] who examined the change of stability of fluid in a porous medium subject to a vertical temperature gradient. This problem which is well known as the Horton-Rogers-Lapwood problem was revisited by Nield & Barletta [70] in which the effects of pressure work and viscous dissipation were included.

However, there is another kind of convection in porous media studies. Ther-

mosolutal convection or thermochemical convection is the process in which both temperature and some dissolved mineral contribute to the buoyancy of the fluid, it is also referred to as double-diffusive convection. If the fluid exposed to heat and salt on the lower boundary and the salt concentration with the presence of a sufficient heat lead to a chemical reaction so that the reaction, in the form of a buoyancy force, overcomes the gravitational force acting downward then the system will be unstable. While if the fluid exposed to heat on the lower boundary and salt on the upper boundary, then the system may be stable or unstable according to whether the salt concentration with the presence of enough heat from the lower boundary will lead to a strong chemical reaction, in the form of a buoyancy force, to overcome the gravitational force. The state of instability is translated as convective periodic cells covering the whole horizontal plane. For example, the Rayleigh-Bénard convection cells take the shape of hexagons.

The problem of thermosolutal convection in a horizontal layer of porous material saturated with an incompressible fluid has attracted the attention of many writers, see e.g. the account in Straughan [100]. An important class of such problems involving a chemical reaction with the solute has attracted recent attention, with Pritchard & Richardson [83] tackling the problem in a Darcy porous layer, Wang & Tan [124] analysing the analogous problem in a Brinkman porous layer, while Malashetty & Biradar [60] studied the equivalent problem in a Darcy layer but when the permeability and thermal conductivity are anisotropic. All of these writers assumed the chemical equilibrium function which arises in the conservation law for evolution of the solute field is linear in the temperature field.

This thesis consists of three parts related to porous media and stability. To be clear on what we mean by stability, we observe that asymptotic stability of a solution to partial differential equation means that the solution decays with time for all possible disturbances. The system is called unstable if for any perturbation the solution grows with time and will not return to the normal or original state, cf. Straughan [99, 100, 103].

The first part, chapters 2 - 3, represents the qualitative analyses of stability. A mathematical model such as these involved in the convection studies mentioned above, [83], [124], [60], is only reasonable if one can establish respectable properties of the solutions to the equations governing the model. The question of continuous dependence of the solution on the reaction rate is one which belongs to the general class of structural stability problems. Structural stability(or continuous dependence on the model itself) is one of major importance and it may be argued that it is as or more important than the widely accepted notion of stability as continuous dependence upon the initial data, cf. Hirsch & Smale [39]. Within the field of continuum mechanics Knops & Payne [48] made a major contribution studying structural stability in elasticity, and the same writers improved their estimates in Knops & Payne [49]. Further continuous dependence on modelling in continuum mechanics is due to the work of Payne [74–76], Payne, Song & Straughan [78], Straughan & Hutter [110], Lin & Payne [53, 54], Tu & Lin [118], Liu, Du & Lin [57] and Straughan [102]. Since then there have been very many articles dealing with questions of structural stability in continuum mechanics many of these are described and/or reviewed by Payne & Straughan [79–81], Gentile & Straughan [36] and in the books of Straughan [100, 103]. The qualitative analysis is needed to assess models before the numerical work and therefore the first part of this thesis is devoted to precisely this goal.

The second part, chapters 4 - 6, represents the quantitative stability analyses of the models. It is an investigation on the onset of double diffusive convection or thermosolutal convection in the Darcy and the Brinkman porous media. In particular, we are considering the effect of chemical reaction on the stability of fluid flow in saturated porous media of Darcy and Brinkman types. Nield [69] carried out the first linear instability analysis of a double-diffusive system in a porous layer. He showed that the oscillatory instability may be possible when a strongly stabilizing solute gradient is opposed by a destabilizing thermal gradient. He used a Fourier series method to obtain the eigenvalue equation which involves the thermal and so-

lutal Rayleigh numbers. Then subsequent development of Nield [69] work is carried out by Rudraiah *et al.* [92].

Wollkind & Frisch [125] carried out the earliest analysis of reactive effects on convection in a fluid layer. They investigated the stability to infinitesimal disturbances of a horizontal layer of dissociating fluid heated from below or above. They used a normal mode linear perturbation analysis. Their result shows that for a nonreactive fluid layer heated from below there is a slight departure in the onset of convective instability from the classical Bénard problem. The same authors extended the linear perturbation problem in Wollkind & Frisch [126] to include a nonlinear stability analysis of a horizontal layer of dissociating fluid, heated from above or below. Then Bdzil & Frisch [8] did a complementary work in which they performed a linear stability analysis where the fluid was catalysed at the lower boundary of the layer. The same writers developed the previous work in Bdzil & Frisch [9] and simultaneously a similar work carried by Gutkowicz-Krusin & Ross [38]. See also Nield & Bejan [71], Ingham & Pop [44, 45], Vafai [121, 122] and Vadasz [120]. Many recent studies in double and multi-component convection are accomplished by Rionero [85–87, 89].

Regarding reactive convection in a porous medium, the first study was due to Steinberg & Brand [96, 97]. They presented a linear instability analysis of a reactive binary mixture in a rectangular box with fast chemical reaction in a porous medium heated from below or from above. More studies were carried out by Gatica *et al.* [33, 34], Viljoen *et al.* [123] and Malashetty & Gaikwad [59]. Pritchard & Richardson [83] explored a model similar to that of Steinberg & Brand [96,97]. They considered the Darcy model to study the onset of thermosolutal convection of a binary fluid in a horizontal porous layer subject to fixed temperatures and chemical equilibrium on the bounding surfaces, when the solubility of the dissolved component depends on temperature. They used a linear instability analysis to study and develop understanding on how the dissolution or precipitation of the solute affects the onset of convection. Wang & Tan [124] extended the previous work of Pritchard & Richardson [83], in which Wang & Tan [124] considered the Darcy-Brinkman

model for a sparsely packed porous medium. They discussed how the onset of double-diffusive convection varies with the Darcy number, the Lewis number and the reaction term. They derived a non-dimensional model of double-diffusive convection with thermally controlled equilibrium solubility on the basis of the Brinkman model. Then, they used the normal mode analysis to carry out a linear instability analysis.

Recently, many research articles investigated convection in anisotropic porous materials. A well documented review of research articles on convective flows in anisotropic porous media can be found in Storesletten [98]. Malashetty *et al.* [31, 32, 61] studied the onset of double diffusive convection in anisotropic porous media with different effects, like rotation, cross-diffusion effects, and soret effect. Recently, Malashetty & Biradar [60] studied the onset of double diffusive reaction convection in anisotropic porous layer of Darcy type. Srivastava & Bera [95] considered the onset of thermosolutal reaction convection in a couple-stress fluid saturated anisotropic porous medium. Gaikwad & Begum [30] investigated the onset of a rotating double-diffusive reaction convection in anisotropic Darcy type porous medium. The authors in the six articles mentioned above used a linear theory and a weak non-linear theory to study the stability. The linear analysis is based on the normal mode technique, while the non-linear analysis is based on a truncated Fourier series representation.

We are studying non-linear stability using an energy stability technique which is used extensively by, for example, Amendola & Fabrizio [3], Amendola *et al.* [4, 5], Capone *et al.* [15,16,18], Capone & De Luca [17], De Luca [24], De Luca & Rionero [25], Lombardo & Mulone [58], Rionero *et al.* [88,90,91], and Straughan [99,100,105]. The aim of our study is to obtain the nonlinear stability boundaries below which the solution is globally stable using the energy method and to investigate the effect of the chemical reaction on the onset of stability.

The third part of this thesis, chapters 7 - 8, deals with acceleration waves be-

haviour in non-linear elastic double porosity materials. This direction of study takes our attention due to its great importance in real life situations, for example, in civil engineering and geophysics.

1.1 Notations and Preliminaries

Let Ω be a bounded domain in $\mathbb{R}^3$ with boundary Γ smooth enough to allow the application of the *Divergence Theorem*. Throughout this thesis we use standard indicial notations and Einstein summation convention is used for repeated indices, where Roman indices run from 1 to 3 and subscript $,i$ denoting $\partial/\partial x_i$ and subscript $,t$ denoting $\partial/\partial t$. Standard vector and tensor notations also used throughout, for example, the divergence of a vector field is defined by

$$div\ \mathbf{v} \equiv v_{i,i} \equiv \frac{\partial v_i}{\partial x_i} \equiv \Sigma_{i=1}^{i=3} \frac{\partial v_i}{\partial x_i}.$$

The Laplace operator acting on a general function f is defined by

$$\Delta f = f_{,ii} = \frac{\partial^2 f}{\partial x^2} + \frac{\partial^2 f}{\partial y^2} + \frac{\partial^2 f}{\partial z^2}.$$

Moreover, the horizontal Laplacian is defined by

$$\Delta^* = \Delta - \frac{\partial^2}{\partial z^2} = \frac{\partial^2}{\partial x^2} + \frac{\partial^2}{\partial y^2},$$

from which we define a new operator D to be

$$D = \frac{d}{dz}.$$

In addition we denote the inner product on the space $L^2(\Omega)$ by $(\cdot, \cdot)$ and we denote the associated norm by $\|\cdot\|$. For example, if f and $g \in L^2(\Omega)$, then

$$(f, g) = \int_\Omega fg\ dV,$$

and the norm of a function f is defined by

$$\|f\| = \sqrt{\int_\Omega f^2\ dV}.$$

For later purposes, we recall the following inequalities,

Poincaré inequality is defined as

$$\|f\| \leq C\|\nabla f\| \ , \tag{1.1.1}$$

for functions f which vanish on at least a part of Γ and C is a constant depending on Ω. While Cauchy-Schwarz inequality is

$$\int_\Omega fg \ dx \leq \left(\int_\Omega f^2 dx\right)^{1/2} \left(\int_\Omega g^2 dx\right)^{1/2},$$

or in terms of L^2 norm and inner product notation it may be written in the form

$$|\langle f, g\rangle| \leq \|f\|\|g\|. \tag{1.1.2}$$

The Arithmetic-Geometric Mean inequality is

$$ab \leq \frac{1}{2\alpha}a^2 + \frac{\alpha}{2}b^2, \ \ for \ any \ a, b, \alpha > 0. \tag{1.1.3}$$

The Young's Inequality is

$$ab \leq \frac{a^p}{p} + \frac{b^q}{q} \ , \tag{1.1.4}$$

where a and b are nonnegative real numbers and p and q are positive real numbers such that

$$\frac{1}{p} + \frac{1}{q} = 1.$$

Moreover, the Sobolev inequality is defined as

$$\|f\|_4 \leq \xi\|\nabla f\| \ , \tag{1.1.5}$$

for $\xi > 0$ depending on Ω, and for functions f which are zero on at least a part of Γ.

To this end, we recall two *lemmas*, which are useful in our subsequent analysis. The first one arises from a Rellich identity, Payne & Weinberger [82], and may be found in Payne & Straughan [80], inequality$(A10)$.

Lemma 1 Let ϕ be a harmonic function in Ω with boundary values M, *i.e.*

$$\begin{aligned} &\Delta\phi = 0 \ in \ \Omega, \\ &\phi = M(\mathbf{x}, t) \ on \ \Gamma. \end{aligned} \tag{1.1.6}$$

Then one may derive explicit constants c_1 and c_2 such that

$$\|\nabla\phi\|^2 + c_1 \oint_\Gamma \left(\frac{\partial\phi}{\partial n}\right)^2 dA \leq c_2 \oint_\Gamma |\nabla_s M|^2 dA \tag{1.1.7}$$

where $\boldsymbol{n}$ is the unit normal vector and ∇_s denotes the gradient in suitable orthogonal tangential directions to the unit normal.

The second *lemma* may be found in Payne & Straughan [80], inequality($A12$).

Lemma 2 Let ψ be the torsion function which satisfies the boundary value problem

$$\begin{aligned} &\Delta\psi = -1 \ , \ in \ \Omega \\ &\psi = 0 \ , \ on \ \Gamma. \end{aligned} \tag{1.1.8}$$

Then by the maximum principle $\psi > 0$ in Ω, and for a function ϕ satisfying problem (1.1.6) one has

$$2\,(\psi\nabla\phi, \nabla\phi) + \|\phi\|^2 \leq \psi_1 \oint_\Gamma M^2 dA, \tag{1.1.9}$$

where

$$\psi_1 = max_\Gamma |\frac{\partial\psi}{\partial n}|. \tag{1.1.10}$$

The reader may refer to appendix A for the proofs of the two *lemmas*.

1.2 Bénard Problem and Navier-Stokes Equations

While we are interested in the effect of a chemical reaction it is useful to introduce the basic equations for thermal convection in a viscous fluid without such a reaction.

1.2.1 Basic Equations

In general, the equations for evolution of the velocity $\mathbf{v}$ and pressure p, have the following forms of the Navier-Stokes equations

$$\rho\,(v_{i,t} + v_j v_{i,j}) = -p_{,i} + \mu\Delta v_i - g k_i \rho \ , \tag{1.2.1}$$

$$v_{i,i} = 0, \tag{1.2.2}$$

where ρ is the density, g is the gravity, μ is the effective viscosity, and $k_i = (0, 0, 1)$. In general, the density of the fluid changes with temperature. Then we adopt a linear relation for the density of form

$$\rho(T) = \rho_0 [1 - \alpha [T - T_0]], \tag{1.2.3}$$

here α is the coefficient of thermal expansion and ρ_0 and T_0 are constants. Then we adopt a Boussinesq approximation which roughly states that we cannot ignore the temperature in the expansion term $gk_i\rho$ in (1.2.1) but we may ignore the temperature in the inertia term $\rho(v_{i,t} + v_j v_{i,j})$. In this case we may replace equation (1.2.1) by

$$\rho_0 (v_{i,t} + v_j v_{i,j}) = -p_{,i} + \mu \Delta v_i - g k_i \rho_0 (1 - \alpha[T - T_0]). \tag{1.2.4}$$

The transport of heat equation is

$$T_{,t} + v_i T_{,i} = k \Delta T \ , \tag{1.2.5}$$

where k is the heat effective diffusivity.

1.2.2 Bénard Problem

The whole system consists of equations (1.2.4), (1.2.2), and (1.2.5) as follows

$$\begin{aligned} \rho_0 (v_{i,t} + v_j v_{i,j}) =& - p_{,i} + \mu \Delta v_i - g k_i \rho_0 (1 - \alpha[T - T_0]) \ , \\ v_{i,i} =& 0 \ , \\ T_{,t} + v_i T_{,i} =& k \Delta T. \end{aligned} \tag{1.2.6}$$

Equations (1.2.6) is a system of 5 equations in 5 unknowns, v_1, v_2, v_3, p, and T. We will use the standard Bénard problem for system (1.2.6) to explain the method used to find the stability and instability boundaries.

As the temperature gradient acts vertically, we consider T to depend on z only. In the steady state we are looking for

$$\bar{v_i} \equiv 0 \ , \ \bar{T} = \bar{T}(z) \ , \ \bar{p} = \bar{p}(z). \tag{1.2.7}$$

$\bar{T}$ depends only on z, so equation $(1.2.6)_3$ is $k\Delta\bar{T} = 0$, which reduces to $d^2\bar{T}/dz^2 = 0$, in which the solution is $\bar{T} = az + b$. Using the boundary conditions

$$v_i = 0 \ on \ z = 0, 1 \ ,$$

$$\bar{T} = T_L \ on \ z = 0 \ ,$$

$$\bar{T} = T_U \ on \ z = d \ ,$$

where the parameters T_L and T_U are constants and $T_L > T_U$, imply $b = T_L$ and $a = -(T_L - T_U)/d = -\beta$, here β is the temperature gradient. Then

$$\bar{T} = -\beta z + T_L.$$

Moreover, $\bar{p}$ depends on z, reduces the momentum equation to

$$\frac{d\bar{p}}{dz} = -g\rho_0\alpha\beta z - g\rho_0 \left(1 - \alpha[T_L - T_0]\right),$$

which gives a quadratic form of solution for $\bar{p}$

$$\bar{p}(z) = -\frac{1}{2}g\rho_0\alpha\beta z^2 - g\rho_0 \left(1 - \alpha[T_L - T_0]\right) z + A \ ,$$

where A is an arbitrary constant.

1.2.3 Perturbations and Non-dimensionalisations

To study the stability, we have to introduce perturbations to the steady state in the form

$$v_i = \bar{v}_i + u_i \ , \ T = \bar{T} + \theta, \ p = \bar{p} + \pi.$$

Employing these into the system (1.2.6) with the use of the steady solution, gives the full system of perturbation equations in terms of u_i, π, θ, in the form

$$\begin{aligned} u_{i,t} + u_j u_{i,j} =& -\frac{1}{\rho_0}\pi_{,i} + g\alpha k_i\theta + \nu\Delta u_i \ , \\ u_{i,i} =& 0 \ , \\ \theta_{,t} + u_i\theta_{,i} =& \beta w + k\Delta\theta \ , \end{aligned} \tag{1.2.8}$$

where $\nu = \mu/\rho_0$ and $w = u_3$.

By introducing the non-dimensionalisations

$$\mathbf{x} = \mathbf{x}^* d, \ t = t^*\frac{d^2}{\nu}, \ u_i = u_i^*\frac{\nu}{d}, \ \pi = \pi^*\frac{\rho_0\nu^2}{d^2}, \ \theta = \theta^*\sqrt{\frac{\nu^3\beta}{gkd^2\alpha}},$$

the system of non-dimensional perturbation equations is, after dropping the "*",

$$\begin{aligned} u_{i,t} + u_j u_{i,j} &= -\pi_{,i} + \Delta u_i + Rk_i\theta \ , \\ u_{i,i} &= 0 \ , \\ Pr\,(\theta_{,t} + u_i\theta_{,i}) &= Rw + \Delta\theta \ , \end{aligned} \tag{1.2.9}$$

where $Pr = \nu/k$ is the Prandtl number, and the Rayleigh number Ra is defined by $Ra = R^2 = d^4 g\alpha\beta/k\nu$. The corresponding boundary conditions are

$$w_{,zz} = w = \theta = 0 \ on \ z = 0, 1. \tag{1.2.10}$$

1.2.4 Boundary Conditions

We have to introduce the derivation of two kinds of boundary conditions due to the importance of distinguishing between the use of them in different systems of porous media. For example, in chapters (4) and (6), we assumed the porous medium has low porosity structure in which the Darcy model is applicable. While in chapters (3) and (5), we assumed that the porous medium has a high porosity structure in which the Brinkman model is relevant. The Darcy model requires just one velocity boundary condition because it has no velocity derivative terms. On the other hand, the Brinkman model contains velocity derivatives term of second order which requires two velocity boundary conditions.

Fixed (No-Slip) Boundary Conditions

To derive the no-slip boundary, we assume that the fluid has zero velocity at the boundary, *i.e.* $v_i = 0$. Then we have that

$$\begin{aligned} u &= 0 \ , \\ v &= 0 \ , \\ w &= 0 \ on \ z = 0, 1 \ , \end{aligned} \tag{1.2.11}$$

and we know that in Ω,

$$\frac{\partial u}{\partial x} + \frac{\partial v}{\partial y} + \frac{\partial w}{\partial z} = 0,$$

therefore by continuity,

$$\frac{\partial u}{\partial x} + \frac{\partial v}{\partial y} + \frac{\partial w}{\partial z} = 0 \ on \ \Gamma. \tag{1.2.12}$$

By differentiating $(1.2.11)_1$ w.r.t x and $(1.2.11)_2$ w.r.t y, implies that $\partial u/\partial x = \partial v/\partial y = 0$ *on* $z = 0, 1$. Using this result in (1.2.12) leads to $\partial w/\partial z = 0$ *on* $z = 0, 1$. It follows that the no-slip boundary conditions for w are

$$w = 0,\ w_{,z} = 0,\ on\ z = 0, 1.$$

Stress-Free Boundary Conditions

For a free-surface the stress vector $t_i = 0$ on the boundary, *i.e.* $t_i = t_{ij}n_j = 0$ *on* $z = 0, 1$, where

$$t_{ij} = 2\mu d_{ij} - \pi\delta_{ij}\ , \tag{1.2.13}$$

is the stress tensor and $d_{ij} = 1/2(u_{i,j} + u_{j,i})$, and again we assume that the fluid velocity at the boundary is zero, $w = 0$ *on* $z = 0, 1$. Since we need to obtain the boundary conditions for w, we set $j = 3$ in (1.2.13), then when $i = 1$ and $i = 2$, (1.2.13) gives

$$t_{13} = \mu(u_{1,3} + u_{3,1}) = \mu(\frac{\partial u}{\partial z} + \frac{\partial w}{\partial x}) = 0\ on\ \Gamma\ , \tag{1.2.14}$$

and

$$t_{23} = \mu(u_{2,3} + u_{3,2}) = \mu(\frac{\partial v}{\partial z} + \frac{\partial w}{\partial y}) = 0\ on\ \Gamma\ , \tag{1.2.15}$$

where we have used the fact that $\delta_{ij} = 0,\ if\ i \neq j$.

But $w_{,x} = 0$ *on* Γ and $w_{,y} = 0$ *on* Γ. Using these in (1.2.14) and (1.2.15) we obtain

$$\begin{aligned} u_{,z} &= 0\ on\ \Gamma\ , \\ v_{,z} &= 0\ on\ \Gamma. \end{aligned} \tag{1.2.16}$$

We know that $u_{,x} + v_{,y} + w_{,z} = 0$ *on* Γ, by differentiation w.r.t. z, gives

$$u_{,xz} + v_{,yz} + w_{,zz} = 0\ on\ \Gamma. \tag{1.2.17}$$

Employing (1.2.16) in (1.2.17) gives

$$u_{,zx} = 0\ ,\quad v_{,yz} = 0\ ,\ on\ \Gamma\ ,$$

then

$$w_{,zz} = 0\ on\ \Gamma.$$

It follows that the stress-free boundary conditions for w are

$$w = 0\ ,\ w_{,zz} = 0\ ,\ on\ z = 0, 1.$$

1.2.5 Linear Instability

To find the linear instability boundaries of the system (1.2.9), we have to drop the nonlinear terms

$$\begin{aligned} u_{i,t} =& -\pi_{,i} + \Delta u_i + Rk_i\theta \ , \\ u_{i,i} =& 0 \ , \\ Pr\theta_{,t} =& Rw + \Delta\theta. \end{aligned} \tag{1.2.18}$$

Because system (1.2.18) is linear, using separation of variables, we may write

$$u_i = e^{\sigma t}u_i(\mathbf{x}) \ , \ \pi = e^{\sigma t}\pi(\mathbf{x}) \ , \ \theta = e^{\sigma t}\theta(\mathbf{x}) \ , \tag{1.2.19}$$

where σ is the growth rate. The terms in (1.2.19) are called Fourier modes and the full solution is a combination of modes, *i.e.* $u_i(\mathbf{x},t) = \Sigma_{m=1}^{\infty} e^{\sigma_m t}u_i^m(\mathbf{x})$. We will consider only (1.2.19) because one term is sufficient for instability.
Employing (1.2.19) in (1.2.18) gives

$$\begin{aligned} \sigma u_i =& -\pi_{,i} + \Delta u_i + Rk_i\theta \ , \\ u_{i,i} =& 0 \ , \\ Pr\ \sigma\theta =& Rw + \Delta\theta. \end{aligned} \tag{1.2.20}$$

1.2.6 Exchange of Stabilities

The idea is that the growth rate σ is complex, $\sigma = \sigma_r + i\sigma_i$ with $\sigma_r \ , \ \sigma_i \in \mathbb{R}$. The principle of exchange of stabilities holds if $\sigma_i \neq 0 \Rightarrow \sigma_r < 0$. If $\sigma_r > 0$ then the system is unstable for all possible perturbations and any instability in this case is called an overstable oscillation. The instability boundaries therefore occur when $\sigma_r = 0$. While if $\sigma_i = 0$ always, *i.e.* $\sigma \in \mathbb{R}$, then exchange of stabilities always holds, cf. Straughan [100] and Chandrasekhar [19].

When thermal convection commences, the fluid is seen to form regular patterns known as convection cells and these are periodic in the (x,y) plane. We assume that $\mathbf{u}$, θ, p have an $(x,y)-$dependence consistent with one that has a repetitive shape that tiles the plane, such as two-dimensional rolls or hexagons. The hexagon solution was originally given by Christopherson [22] namely,

$$u(x,y) = \cos\frac{1}{2}a(\sqrt{3}x + y) + \cos\frac{1}{2}a(\sqrt{3}x - y) + \cos ay \ . \tag{1.2.21}$$

In particular, the $(x, y)-$dependence is consistent with a wavenumber, a, for which u satisfies the relation $\Delta^* u = -a^2 u$, where Δ^* is defined in section(1.1). Whatever shape the cell has in the $(x, y)-$plane, its Cartesian product with $(0, 1)$ is the period cell V.

Let V be a period cell for the solution and let system (1.2.20) be complex, *i.e.* $u_i = u_i^r + iu_i^i$, with similar expression for θ. Multiply equation $(1.2.20)_1$ by $u_i^* = u_i^r - iu_i^i$, which is the complex conjugate of u_i, and integrate over V. Likewise multiply equation $(1.2.20)_3$ by $\theta^* = \theta^r - i\theta^i$ and integrate over V, where $\|\mathbf{u}\|^2 = \int_V u_i u_i^* dV$ and $\|\theta\|^2 = \int_V \theta\theta^* dV$. Considering the periodicity in the x and y directions and adding the results, we find that

$$\begin{aligned} \sigma\left(\|\mathbf{u}\|^2 + Pr\|\theta\|^2\right) = &- \|\nabla\mathbf{u}\|^2 - \|\nabla\theta\|^2 \\ &+ R\left[(\theta w^*) + (w\theta^*)\right] \ , \end{aligned} \tag{1.2.22}$$

where $\theta w^* + w\theta^* = 2\left(\theta_r w_r + \theta_i w_i\right) \in \mathbb{R}$. Since $\sigma = \sigma_r + i\sigma_i$, by considering the imaginary part of (1.2.22), *i.e.* $\sigma_i\left(\|\mathbf{u}\|^2 + Pr\|\theta\|^2\right) = 0$, because $\left(\|\mathbf{u}\|^2 + Pr\|\theta\|^2\right) \neq 0$ implies that $\sigma_i = 0$. Therefore $\sigma \in \mathbb{R}$. We are interested to find the boundary where σ changes from negative to positive. Therefore, we set $\sigma = 0$ in (1.2.20) and the system reduces to

$$\begin{aligned} \pi_{,i} =& \Delta u_i + Rk_i\theta \ , \\ u_{i,i} =& 0 \ , \\ 0 =& Rw + \Delta\theta. \end{aligned} \tag{1.2.23}$$

Taking the double curl of $(1.2.23)_1$ reduces system (1.2.23) to

$$\begin{aligned} \Delta^2 w + R\Delta^*\theta =& 0 \ , \\ \Delta\theta + Rw =& 0, \end{aligned} \tag{1.2.24}$$

where Δ^* is the horizontal Laplacian. Write $w = W(z)f(x, y)$ and $\theta = \Theta(z)f(x, y)$, where f is a plane tiling function of the form $f(x, y) = e^{i(lx+my)}$ and $\Delta^* f = -(l^2 + m^2)f = -a^2 f$; a is the wave number. Then system (1.2.24) is

$$\begin{aligned} \left(D^2 - a^2\right)^2 W - Ra^2\Theta =& 0 \ , \\ \left(D^2 - a^2\right)\Theta + RW =& 0 \ , \end{aligned} \tag{1.2.25}$$

which is an eigenvalue problem for eigenvalue R, where $D = d/dz$ and $\Delta = D^2 - a^2$. Considering the boundary conditions, we may write $W = \hat{W}\sin n\pi z$ and $\Theta = \hat{\Theta}\sin n\pi z$. Employing these, system (1.2.25) may be written in a matrix form as

$$\begin{pmatrix} \Lambda^2 & -Ra^2 \\ R & -\Lambda \end{pmatrix} \begin{pmatrix} \hat{W} \\ \hat{\Theta} \end{pmatrix} = 0 \ ,$$

where $\Lambda = n^2\pi^2 + a^2$. Setting the determinant of the matrix to zero gives

$$R^2 = \frac{(n^2\pi^2 + a^2)^3}{a^2}.$$

To find the value of R for which the instability first occurs, we have to minimise R^2 in n^2 to find that the minimum is when $n = 1$, further minimization in a^2 yields $a^2_{crit} = \pi^2/2$, and the corresponding minimum R value is $R^2_{crit} = 27\pi^4/4$.
This linear value of R guarantees instability, *i.e.* for all $R > R_{crit}$ the system is unstable but we can not determine whether the system is stable or not for $R < R_{crit}$ using the linear method. Therefore, we will use the energy method to obtain the nonlinear boundary below which the solution is stable.

1.2.7 The Nonlinear Stability

For the problem in hand (1.2.9), Straughan [99] used the energy method to find the nonlinear stability boundary. Considering a period cell V, multiply equation $(1.2.9)_1$ by u_i and equation $(1.2.9)_3$ by θ and integrate over the domain using the integration by parts, the divergence theorem and the suitable inequalities. Then, form the energy identity by adding the obtained equations

$$\frac{dE}{dt} = RI - D \ , \tag{1.2.26}$$

where

$$\begin{aligned} E(t) =& \frac{1}{2}\|\mathbf{u}\|^2 + \frac{Pr}{2}\|\theta\|^2 \ , \\ D(t) =& \|\nabla\mathbf{u}\|^2 + \|\nabla\theta\|^2 \ , \\ I(t) =& 2\,(\theta, w)\,. \end{aligned}$$

Define R_E by

$$\frac{1}{R_E} = \max_H \frac{I}{D} \ , \tag{1.2.27}$$

where $H = \{(u_i, \theta) | u_i, \theta \in H^1(V), u_i = 0, \theta = 0 \; on \; \Gamma\}$, and u_i, θ are periodic in x and y. Returning to the energy identity

$$\begin{aligned} \frac{dE}{dt} &= R\frac{I}{D}D - D \\ &\leq RD \max_H \left(\frac{I}{D}\right) - D \\ &= \frac{R}{R_E}D - D \\ &= -D\left(1 - \frac{R}{R_E}\right). \end{aligned}$$

Now, if $R < R_E$, then $1-(R/R_E) > 0$, say that $1-(R/R_E) = (R_E-R)/R_E = a_1 > 0$, implies

$$\frac{dE}{dt} \leq -a_1 D. \tag{1.2.28}$$

Using the Poincaré's inequality, one can find a bound for D, and then from (1.2.28) we obtain

$$\frac{dE}{dt} \leq -a_1 D \leq -2a_1 k\pi^2 E(t) = \mu_1 E(t) \; , \tag{1.2.29}$$

where $k = min\{\frac{1}{Pr}, 1\}$. Integrating (1.2.29) yields

$$E(t) \leq E(0)e^{-\mu_1 t}. \tag{1.2.30}$$

Inequality (1.2.30) shows that $E(t) \to 0$ as $t \to \infty$, and then $\|\mathbf{u}(t)\|^2 \to 0$, and $\|\theta(t)\|^2 \to 0$ as $t \to \infty$.

The maximum (1.2.27) requires $R_E\delta I - \delta D = 0$. Using Calculus of variation, we obtain the following Euler-Lagrange equations

$$\begin{aligned} \Delta u_i + R_E\theta k_i &= \lambda_{i,i} \; , \\ u_{i,i} &= 0 \; , \\ \Delta\theta + R_E w &= 0. \end{aligned} \tag{1.2.31}$$

These are the same as the linear instability equations (1.2.23). Thus in this case, the linear instability Rayleigh number is equivalent to the nonlinear stability Rayleigh number, *i.e.* $R_L \equiv R_E$. This means that, for the problem in hand the linear instability boundary coincide with the nonlinear stability boundary and that there is no region of potential sub-critical instability. The system is stable for $R^2 < 27\pi^4/4$ and it is unstable for $R^2 > 27\pi^4/4$. Which is not always the case, in general $R_L > R_E$.

In chapters (4), (5) and (6) we investigate thermosolutal convection models where the two boundaries do not coincide and a region of potential sub-critical instability reveals.

1.3 Overview

Our work in chapters 2-6 is an extension of the work done by Pritchard and Richardson [83]. Indeed, we are working on the model proposed by them and a generalization. We consider the system of basic equations for double diffusive convection in porous media of Brinkman and Darcy type with a chemical reaction in a domain $\Omega \times (0, \tau)$ for some $\tau < \infty$.

Our models consist of either the Darcy equation with the density in the buoyancy term as a function of temperature and salt concentration

$$p_{,i} = -\frac{\mu}{K} v_i - \rho_0[1 - \alpha_T(T - T_0) + \alpha_C(C - C_0)]gk_i \ , \tag{1.3.1}$$

or the analogous Brinkman equation

$$p_{,i} = -\frac{\mu}{K} v_i + \lambda \Delta v_i - \rho_0[1 - \alpha_T(T - T_0) + \alpha_C(C - C_0)]gk_i \ , \tag{1.3.2}$$

the continuity equation

$$v_{i,i} = 0 \ , \tag{1.3.3}$$

the advection-diffusion equation for the transport of heat

$$\frac{1}{M} T_{,t} + v_i T_{,i} = k_T \Delta T \ , \tag{1.3.4}$$

and the advection-diffusion equation for the transport of salt with reaction term

$$\hat{\phi} C_{,t} + v_i C_{,i} = \hat{\phi} k_C \Delta C + \hat{k}[C_{eq}(T) - C] \ , \tag{1.3.5}$$

where the quantities p, v_i, T, C are pressure, velocity, temperature and salt concentration, K is the matrix permeability, μ is the fluid viscosity, ρ_0 is the fluid density. The coefficients k_C, k_T are the molecular diffusivity of the solute through the fluid and the effective diffusivity of the heat through the saturated medium, respectively. The quantity M is the ratio of the heat capacity of the fluid to the heat capacity of the medium, the matrix porosity $\hat{\phi}$ is the ratio of the volume of the fluid

to the total volume of the fluid and the solid, $\hat{k}$ is the reaction coefficient, and $C_{eq}(T) = f_0 + f_1(T - T_0)$ in Pritchard & Richardson [83] and Wang & Tan [124], where f_0, f_1 and T_0 are constants. Moreover, g is the gravity, $\mathbf{k} = (0, 0, 1)$ and α_T and α_C are the thermal and solutal expansion coefficients respectively. The term λ is the effective viscosity (Brinkman coefficient), for Darcy type problem $\lambda = 0$ and for Brinkman type problem $\lambda \neq 0$.

We impose the following boundary conditions for the Darcy model

$$\begin{aligned} &T = T_L \text{ on } z = 0 \text{ and } T = T_U \text{ on } z = d, \\ &v_i n_i = 0 \text{ on } z = 0 \text{ and } z = d \ , \\ &C = C_L \text{ on } z = 0 \text{ and } C = C_U \text{ on } z = d \ , \end{aligned} \tag{1.3.6}$$

while the analogous boundary conditions for Brinkman are

$$\begin{aligned} &T = T_L \text{ on } z = 0 \text{ and } T = T_U \text{ on } z = d, \\ &v_i = 0 \text{ on } z = 0 \text{ and } z = d \ , \\ &C = C_L \text{ on } z = 0 \text{ and } C = C_U \text{ on } z = d \ , \end{aligned} \tag{1.3.7}$$

with $T_L > T_U$ since our systems are heated below, where T_L, T_U, C_L, C_U all constants and $\mathbf{n}$ is the unit normal vector to Γ. Moreover, the fluid occupying a horizontal layer $(x, y) \in \mathcal{R}^2, z \in (0, d)$ and the equations are taken in the domain $\mathcal{R}^2 \times (0, d) \times \{t > 0\}$.

The reason for imposing the boundary condition $v_i n_i = 0$ for Darcy and $v_i = 0$ for Brinkman is that, the Darcy model only has the term v_i which does not require specification of each component of the velocity vector only the normal component. The Brinkman system has the Δv_i term which because of the second derivatives requires specification of all components of the velocity vector.
For the salted above porous medium $C_U > C_L$ while $C_L > C_U$ for the salted below case. Following Pritchard & Richardson [83], Wang & Tan [124], and [60, 95], it is assumed that the equilibrium solute concentration is a linear function of temperature so that $C_{eq}(T) = f_0 + f_1(T - T_0)$. The following lines will explain in detail how the form of $\bar{C}(z)$ is obtained and the key point in which Pritchard & Richardson [83] and Wang & Tan [124] *assume* that $C_{eq}(\bar{T}) = \bar{C}(z)$.

In the steady state, we look for

$$\begin{aligned} \bar{v}_i &= 0, \\ \bar{T} &= \bar{T}(z), \\ \bar{C} &= \bar{C}(z). \end{aligned} \tag{1.3.8}$$

Equation (1.3.3) is automatically satisfied *i.e.*,

$$\bar{v}_{i,i} = \frac{\partial \bar{v}_1}{\partial x} + \frac{\partial \bar{v}_2}{\partial y} + \frac{\partial \bar{v}_3}{\partial z} = 0 \ ,$$

since $\bar{v}_i = (\bar{v}_1, \bar{v}_2, \bar{v}_3) = (0, 0, 0)$. Now considering equation (1.3.4), $\bar{T}$ is a function of z and so $\partial \bar{T}/\partial t = 0$, also $\bar{v}_i = 0$ therefore $\bar{v}_i \partial \bar{T}/\partial x_i = 0$, and so we are left with $\frac{\partial^2 \bar{T}}{\partial x^2} + \frac{\partial^2 \bar{T}}{\partial y^2} + \frac{\partial^2 \bar{T}}{\partial z^2} = 0$, therefore $d^2\bar{T}/dz^2 = 0$, which has the form of solution, $\bar{T}(z) = \mu_1 z + \mu_2$, where μ_1 and μ_2 are constants of integration and we have to find them using the boundary conditions (1.3.6), $\bar{T}(0) = T_L$ and $\bar{T}(d) = T_U$. It follows that

$$\bar{T}(z) = T_L - \left(\frac{T_L - T_U}{d} \right) z \ \ ; \ \ T_L > T_U \ .$$

Which can be written as

$$\bar{T}(z) = -\beta_T z + T_L \ ; \ \beta_T = \frac{T_L - T_U}{d}. \tag{1.3.9}$$

Considering equation (1.3.5), we know that $\bar{C} = \bar{C}(z)$ and $\bar{v}_i = 0$, which implies that $\partial \bar{C}/\partial t = 0$, $\bar{v}_i \partial \bar{C}/\partial x_i = 0$, and $\Delta \bar{C} = d^2\bar{C}/dz^2$, so we have left with

$$\frac{d^2 \bar{C}}{dz^2} + \frac{\hat{k}}{\hat{\phi} k_C} \left[C_{eq} \left(\bar{T} \right) - \bar{C} \right] = 0. \tag{1.3.10}$$

Suppose that $C_{eq}(\bar{T})$ is a linear function in $\bar{T}$, *i.e.* $\exists \ \mu_3 \ , \ \mu_4$ *such that*

$$C_{eq}(\bar{T}) = \mu_3 \bar{T} + \mu_4.$$

Put $A^2 = \frac{\hat{k}}{\hat{\phi} k_C}$, then equation (1.3.10) becomes

$$\bar{C}'' - A^2 \bar{C} = -A^2 C_{eq}(\bar{T}) = -A^2 \left(\mu_3 \bar{T} + \mu_4 \right) = -A^2 \left[\mu_3 \left\{ \beta_T z + T_L \right\} + \mu_4 \right].$$

So, the steady state solution for $\bar{C}(z)$ is found from

$$\bar{C}'' - A^2 \bar{C} = -A^2 \mu_3 \beta_T z - A^2 \left(\mu_3 T_L + \mu_4 \right)$$

which can be written in the following form

$$\bar{C}'' - A^2\bar{C} = -\mu_5 z - \mu_6 \tag{1.3.11}$$

The solution to equation (1.3.11) will be the following

$$\bar{C}(z) = \mu_9 \sinh(Az) + \mu_{10}\cosh(Az) + \bar{C}_{particular\ solution}. \tag{1.3.12}$$

Try $\bar{C}_{particular\ solution} = \mu_7 z + \mu_8$, where μ_7 and μ_8 are constants, substitute in (1.3.11) and equate the like terms in order to find the values of μ_7 and μ_8. Therefore the solution (1.3.12) will be

$$\bar{C}(z) = \mu_9 \sinh(Az) + \mu_{10}\cosh(Az) + \frac{\mu_5}{A^2}z + \frac{\mu_6}{A^2}.$$

Employing the boundary conditions (1.3.6), $\bar{C}(0) = C_L$ and $\bar{C}(d) = C_U$, the following values of μ_{10} and μ_9 are obtained

$$\mu_{10} = C_L - \frac{\mu_6}{A^2},$$

$$\mu_9 = \frac{C_U - \frac{\mu_5 d}{A^2} - \frac{\mu_6}{A^2} - \left(C_L - \frac{\mu_6}{A^2}\right)\cosh(Ad)}{\sinh(Ad)}.$$

Hence

$$\begin{aligned}\bar{C}(z) =& \frac{C_U - \frac{\mu_5 d}{A^2} - \frac{\mu_6}{A^2} - \left(C_L - \frac{\mu_6}{A^2}\right)\cosh(Ad)}{\sinh(Ad)}\sinh(Az) \\ &+ \left[C_L - \frac{\mu_6}{A^2}\right]\cosh(Az) + \frac{\mu_5}{A^2}z + \frac{\mu_6}{A^2}.\end{aligned} \tag{1.3.13}$$

The steady state solution for $\bar{C}(z)$, equation (1.3.13), is quite complicated. The key point is that, for the Darcy model of Pritchard & Richardson [83] and also for the Brinkman model of Wang & Tan [124] they *assumed* that $C_{eq}(\bar{T}(z)) = \bar{C}(z)$. So that $\Delta\bar{C} = 0$, then $\mu_3\bar{T} + \mu_4 = \bar{C}(z)$. Hence, by employing equation (1.3.9), $\bar{C}(z) = -\mu_3\beta_T z + \mu_4 + \mu_3 T_L$, which can be written as

$$\bar{C}(z) = -\mu_{11}z + \mu_{12}. \tag{1.3.14}$$

To find the values of the constants μ_{11} and μ_{12}, the boundary conditions (1.3.6) have to be employed, $\bar{C}(0) = C_L$ and $\bar{C}(d) = C_U$, to obtain

$$\bar{C}(z) = -\beta_C z + C_L \ ; \ \beta_C = \frac{C_L - C_U}{d}. \tag{1.3.15}$$

Since in the steady state $\partial\bar{p}/\partial x = \partial\bar{p}/\partial y = 0$, the momentum equation (1.3.1), becomes

$$\frac{\partial\bar{p}}{\partial z} = -g\rho_0[1 - \alpha_T(\bar{T} - T_0) + \alpha_C(\bar{C} - C_0)]. \tag{1.3.16}$$

Using the solutions (1.3.9) and (1.3.15), the momentum equation (1.3.16) will be

$$\frac{\partial\bar{p}}{\partial z} = -g\rho_0[1 - \alpha_T(T_L - \beta_T z - T_0) + \alpha_C(-\beta_C z + C_L - C_0)]. \tag{1.3.17}$$

Integration of (1.3.17) gives $\bar{p}$ as a quadratic function of z of the form

$$\bar{p}(z) = \mu_{13}z^2 + \mu_{14}z + \mu_{15} \ ,$$

where μ_{13} , μ_{14} , and μ_{15} are constants of integration.

In chapter 2 we show continuous dependence of the solutions to the Darcy and the Brinkman thermosolutal convection models on reaction when the chemical equilibrium is a linear function in temperature. While in chapter 3 we prove continuous dependence of the solution to the Brinkman thermosolutal convection on reaction when the chemical equilibrium is an arbitrary function of the temperature.

Chapters (4 - 6) represent quantitative data analysis. In chapter 4 we assume that the porous medium has low porosity structure and therefore, we use the Darcy thermosolutal convection system with the presence of reaction to study the onset of stability and the effect of increasing the reaction rate on the critical Rayleigh number. When the porosity is high, we replace the Darcy equation with the Brinkman equation and we study the effect of the reaction rate and the Brinkman coefficient on the stability of the system. This is the content of chapter 5. Moreover, we assume that the porous skeletons in chapters 4 and 5 are fully isotropic, which is not always the case. Therefore, in chapter 6 we study the onset of thermosolutal convection with reaction in a Darcy porous medium with anisotropic permeability and thermal diffusivity. Particularly, we investigate the effect of the horizontal isotropy in the mechanical and the thermal diffusivity tenors on the stability of the system.

In the last two chapters (7-8), we move away from convective fluid motion and we turn our attention to studying the behaviour of the acceleration waves in nonlinear

elastic materials. But we are still in the field of porous media studies, particularly in materials of double porosity structures. In chapter 7 we obtain the amplitude and the behaviour of a one dimensional acceleration wave, while in chapter 8 we investigate the behaviour of a three dimensional acceleration wave.

Chapter 2

Continuous Dependence of Darcy and Brinkman Convection on Reaction

2.1 Introduction

In the current chapter, we analyse the general structure stability for a problem of continuous dependence on the reaction term for a model of flow in a porous medium of a Brinkman and/or a Darcy type for double diffusive convection by establishing *a priori* bounds for the solution. In the model we adopt, the chemical equilibrium is taken to be a linear function in temperature. We consider a saturated porous medium occupying a bounded three-dimensional domain Ω with boundary Γ smooth enough to allow the application of the Divergence Theorem.

2.2 Basic Equations

We are investigating systems of equations consisting of either the Darcy equation or the Brinkman equation with the density in the buoyancy force depending on the temperature and salt concentration, the conservation of mass, the energy balance and the conservation of solute equation. For the problem in hand, where $\mathbf{x} \in \Omega$ and t denote the time, such that $0 < t < \mathcal{T}$ for some $\mathcal{T} < \infty$, the Darcy system with the

corresponding boundary and initial conditions may be written as

$$\begin{aligned} \frac{\partial p}{\partial x_i} &= RTg_i - R_sCg_i - v_i, \\ \frac{\partial v_i}{\partial x_i} &= 0, \\ \frac{\partial T}{\partial t} + v_i\frac{\partial T}{\partial x_i} &= \Delta T, \\ \epsilon_1\frac{\partial C}{\partial t} + Lev_i\frac{\partial C}{\partial x_i} &= \Delta C + lT - hC, \end{aligned} \tag{2.2.1}$$

with boundary conditions

$$T = T_B,\ C = C_B,\ v_i n_i = 0 \ on\ \Gamma \times [0, \mathcal{T}) \tag{2.2.2}$$

and initial conditions

$$T(\mathbf{x}, 0) = T_0(\mathbf{x}),\ C(\mathbf{x}, 0) = C_0(\mathbf{x}),\ \mathbf{x} \in \Omega. \tag{2.2.3}$$

The analogous Brinkman system is

$$\begin{aligned} \frac{\partial p}{\partial x_i} &= RTg_i - R_sCg_i - v_i + \lambda\Delta v_i, \\ \frac{\partial v_i}{\partial x_i} &= 0, \\ \frac{\partial T}{\partial t} + v_i\frac{\partial T}{\partial x_i} &= \Delta T, \\ \epsilon_1\frac{\partial C}{\partial t} + Lev_i\frac{\partial C}{\partial x_i} &= \Delta C + lT - hC, \end{aligned} \tag{2.2.4}$$

and the corresponding boundary conditions are

$$T = T_B,\ C = C_B,\ v_i = 0 \ on\ \Gamma \times [0, \mathcal{T}) \tag{2.2.5}$$

and initial conditions

$$T(\mathbf{x}, 0) = T_0(\mathbf{x}),\ C(\mathbf{x}, 0) = C_0(\mathbf{x}),\ \mathbf{x} \in \Omega. \tag{2.2.6}$$

Where g_i is vector representing the gravity field and we may assume that

$$|g| \leq G \tag{2.2.7}$$

for some constant G, without loss of generality and ϵ_1 is a positive constant. The quantities p, v_i, T, C are pressure, velocity, temperature and salt concentration, R

and R_s are Rayleigh numbers for temperature and salt respectively, l and h are the reaction terms, Le is the Lewis number, and λ is the effective viscosity term (the Brinkman coefficient), for Darcy type problem $\lambda = 0$ and for Brinkman type $\lambda \neq 0$. Therefore, I will handle the general case and I will work on system (2.2.4) and the corresponding boundary and initial data (2.2.5) and (2.2.6). The term lT represents the chemical equilibrium function, C_{eq}, in Pritchard & Richardson [83], Wang & Tan [124] and Malashetty & Biradar [60]. Moreover, T_B, C_B, T_0 and C_0 are prescribed functions and $\mathbf{n}$ is the unit normal vector to Γ. Throughout, we let $\|.\|_p$ denote the norm on $L^p(\Omega)$, $p > 2$. Moreover, let the boundary-initial value problem comprised of equations (2.2.4)-(2.2.6) be denoted by $\mathcal{P}$.

2.3 A priori Estimates

To show continuous dependence of the solutions to (2.2.1) and (2.2.4) on the reaction terms h and l, we need estimates for the temperature T and salt concentration C.

2.3.1 A priori bounds for $\|T\|^2$, $\|C\|^2$, $\int_0^t \|T\|^2 ds$, $\int_0^t \|C\|^2 ds$, $\int_0^t \|\nabla C\|^2 ds$, $\int_0^t \|\nabla T\|^2 ds$

To find the estimate for C, we introduce a function $\Phi(\mathbf{x}, t)$ as a solution to the boundary value problem

$$\Delta\Phi = 0 \ in \ \Omega, \tag{2.3.1}$$

$$\Phi = C_B \ on \ \Gamma, \tag{2.3.2}$$

and similarly, to find the estimate for T, we have to introduce a function $\Theta(\mathbf{x}, t)$ as a solution to the boundary value problem

$$\Delta\Theta = 0 \ in \ \Omega, \tag{2.3.3}$$

$$\Theta = T_B \ on \ \Gamma. \tag{2.3.4}$$

The reason for introducing these functions is, because we know that on the boundary Γ, the term $(C - \Phi) = 0$. Therefore using integration by parts and with the aid of

the *Divergence Theorem*, we show

$$\int_\Omega (C-\Phi)\,\Delta C dx = \int_\Omega \nabla\left[(C-\Phi)\,\nabla C\right] dx - \int_\Omega \nabla C.\nabla\,(C-\Phi)\,dx.$$

Applying the *Divergence Theorem* to the first term on the right hand side, we obtain

$$\int_\Omega (C-\Phi)\,\Delta C dx = \oint_\Gamma \frac{\partial C}{\partial n}\,(C-\Phi)\,dA - \int_\Omega |\nabla C|^2 dx + \int_\Omega \nabla C.\nabla\Phi dx. \tag{2.3.5}$$

Since $C-\Phi=0$ on Γ the boundary term is zero. Then, the last term of (2.3.5) is

$$\int_\Omega \nabla C.\nabla\Phi dx = \int_\Omega \nabla\,(C\nabla\Phi)\,dx - \int_\Omega C\Delta\Phi dx. \tag{2.3.6}$$

Since $\Delta\Phi=0$ in Ω the second term on the right is zero, we see

$$\int_\Omega \nabla C.\nabla\Phi dx = \oint_\Gamma C\frac{\partial\Phi}{\partial n} dA. \tag{2.3.7}$$

Thus, putting (2.3.7) into (2.3.5), we find

$$\int_\Omega (C-\Phi)\,\Delta C dx = -\int_\Omega |\nabla C|^2 dx + \oint_\Gamma C\frac{\partial\Phi}{\partial n} dA.$$

The same reason applies for introducing the function Θ. Now, we form the combinations

$$\int_0^t\int_\Omega (C-\Phi)\,(\epsilon_1 C_{,s} + Lev_i C_{,i} - \Delta C - lT + hC)\,dxds = 0, \tag{2.3.8}$$

and

$$\int_0^t\int_\Omega (T-\Theta)\,(T_{,s} + v_i T_{,i} - \Delta T)\,dxds = 0, \tag{2.3.9}$$

where t is some number such that $0<t\le\tau$.

Next, integrate by parts in (2.3.8) and employ the boundary condition (2.3.2) to obtain

$$\begin{aligned}&\frac{1}{2}\epsilon_1\|C\|^2 - \frac{1}{2}\epsilon_1\|C_0\|^2 + \int_0^t \|\nabla C\|^2 ds - \int_0^t (C, lT)\,ds + \int_0^t (C, hC)\,ds\\ &- \epsilon_1\,(\Phi, C) + \epsilon_1\,(\Phi_0, C_0) + \epsilon_1\int_0^t (\Phi_{,s}, C)\,ds - Le\int_0^t\int_\Omega \Phi v_i C_{,i} dxds\\ &- \int_0^t \oint_\Gamma C\frac{\partial\Phi}{\partial n} dA ds + \int_0^t (\Phi, lT)\,ds - \int_0^t (\Phi, hC)\,ds = 0.\end{aligned} \tag{2.3.10}$$

We now multiply equation $(2.2.4)_1$ by v_i, integrate over Ω and employ the the *Poincaré Inequality* and *Cauchy-Schwarz Inequality* to see

$$\|\mathbf{v}\|^2 + \lambda_1\lambda\|\mathbf{v}\|^2 \le \|\mathbf{v}\|^2 + \lambda\|\nabla\mathbf{v}\|^2 \le RG\|T\|\|\mathbf{v}\| + R_sG\|C\|\|\mathbf{v}\|,$$

which implies

$$(1+\lambda_1\lambda)\,\|\mathbf{v}\| \le RG\|T\| + R_sG\|C\|, \tag{2.3.11}$$

where λ_1 is a constant depends on the geomerty of the domain. Squaring both sides of (2.3.11) and then applying the *Arithmetic-Geometric Mean Inequality* gives

$$(1+\lambda_1\lambda)^2\,\|\mathbf{v}\|^2 \le R^2G^2\|T\|^2 + 2RR_sG^2\left(\frac{1}{2\gamma}\|T\|^2 + \frac{\gamma}{2}\|C\|^2\right) + R_s^2G^2\|C\|^2,$$

where $\gamma > 0$ is a constant to be selected. If we choose $\gamma = \frac{R_s}{R}$, we obtain

$$(1+\lambda_1\lambda)^2\,\|\mathbf{v}\|^2 \le 2R^2G^2\|T\|^2 + 2R_s^2G^2\|C\|^2. \tag{2.3.12}$$

Then, we have to bound the cubic term in equation (2.3.10). To do this, let Φ_m be the maximum of C_B on $\Gamma\times[0,\tau]$ which exists by the *maximum principle* (Protter and Weinberger [84]). Then,

$$\begin{aligned}\int_0^t\int_\Omega \Phi v_i C_{,i}\,dxds &\le \Phi_m\sqrt{\int_0^t\|\mathbf{v}\|^2ds\int_0^t\|\nabla C\|^2ds}\\ &\le \frac{\sqrt{2}\Phi_mG}{(1+\lambda_1\lambda)}\sqrt{\int_0^t\left(R^2\|T\|^2+R_s^2\|C\|^2\right)ds\int_0^t\|\nabla C\|^2ds},\end{aligned}$$

which implies that

$$\begin{aligned}\int_0^t\int_\Omega \Phi v_i C_{,i}\,dxds \le{}& \frac{\Phi_mG}{\sqrt{2}\,(1+\lambda_1\lambda)\,\beta_1}\left(\int_0^t R^2\|T\|^2ds + \int_0^t R_s^2\|C\|^2ds\right)\\ &+\frac{\beta_1\Phi_mG}{\sqrt{2}\,(1+\lambda_1\lambda)}\int_0^t\|\nabla C\|^2ds\end{aligned} \tag{2.3.13}$$

where we have used the *Cauchy-Schwarz Inequality*, the *Arithmetic-Geometric Mean Inequality*, inequality (2.3.11) and where $\beta_1 > 0$ is a constant to be chosen.
We now employ (2.3.13) in equation (2.3.10) and make repeated use of the *Arithmetic-Geometric Mean Inequality*, for positive constants $\beta_2,\beta_3,\beta_4,\beta_5,\beta_6,\beta_7,\beta_8$, to be selected, to see

$$\begin{aligned}A_3\|C\|^2 + A_4\int_0^t\|\nabla C\|^2ds &\le A_5\|C_0\|^2 + \frac{\epsilon_1\beta_2}{2}\|\Phi\|^2\frac{\epsilon_1\beta_3}{2}\|\Phi_0\|^2 + \frac{\epsilon_1\beta_4}{2}\int_0^t\|\Phi_{,s}\|^2ds\\ &+ \frac{1}{2}\int_0^t\oint_\Gamma\left(\frac{\partial\Phi}{\partial n}\right)^2dAds + \frac{1}{2}\int_0^t\oint_\Gamma C_B^2\,dAds\\ &+ A_6\int_0^t\|C\|^2ds + A_7\int_0^t\|T\|^2ds + A_8\int_0^t\|\Phi\|^2ds,\end{aligned}$$

where

$$\begin{aligned}
A_3 &= \frac{\epsilon_1}{2} - \frac{\epsilon_1}{2\beta_2}, \\
A_4 &= 1 - \frac{\beta_1 \Phi_m GLe}{\sqrt{2}\,(1+\lambda)}, \\
A_5 &= \frac{\epsilon_1}{2} - \frac{\epsilon_1}{2\beta_3}, \\
A_6 &= \frac{\epsilon_1}{2\beta_4} + \frac{\Phi_m GLeR_s^2}{\sqrt{2}\,(1+\lambda)\,\beta_1} + \frac{l_m\beta_5}{2} + \frac{h_m\beta_6}{2} + \frac{h_m}{2\beta_6} + \frac{h_m}{2\beta_8}, \\
A_7 &= \frac{\Phi_m GLeR^2}{\sqrt{2}\,(1+\lambda)\,\beta_1} + \frac{l_m}{2\beta_5} + \frac{l_m}{2\beta_7}, \\
A_8 &= \frac{l_m\beta_7}{2} + \frac{h_m\beta_8}{2},
\end{aligned}$$

and where h_m and l_m are the maxima of h and l. If we choose $\beta_1 = \frac{(1+\lambda)}{\sqrt{2}\Phi_m GLe}$, $\beta_2 = 2$, and $\beta_3 = \beta_4 = \beta_5 = \beta_6 = \beta_7 = \beta_8 = 1$, then

$$\begin{aligned}
\frac{\epsilon_1}{4}\|C\|^2 + \frac{1}{2}\int_0^t \|\nabla C\|^2 ds \le{}& \epsilon_1\|C_0\|^2 + \epsilon_1\|\Phi\|^2 + \frac{\epsilon_1}{2}\|\Phi_0\|^2 \\
&+ \frac{\epsilon_1}{2}\int_0^t \|\Phi_{,s}\|^2 ds + \frac{1}{2}\int_0^t \oint_\Gamma \left(\frac{\partial \Phi}{\partial n}\right)^2 dA ds \\
&+ \frac{1}{2}\int_0^t \oint_\Gamma C_B^2 dA ds + A_9 \int_0^t \|C\|^2 ds \\
&+ A_{10}\int_0^t \|T\|^2 ds + A_{11}\int_0^t \|\Phi\|^2 ds
\end{aligned} \tag{2.3.14}$$

where

$$\begin{aligned}
A_9 &= \frac{\epsilon_1}{2} + \frac{\Phi_m^2 G^2 Le^2 R_s^2}{(1+\lambda)^2} + \frac{l_m}{2} + \frac{3h_m}{2}, \\
A_{10} &= \frac{\Phi_m^2 G^2 Le^2 R^2}{(1+\lambda)^2} + l_m, \\
A_{11} &= \frac{h_m + l_m}{2}.
\end{aligned}$$

Returning to equation (2.3.9) integrating by parts and employing the boundary conditions (2.3.4), we obtain

$$\begin{aligned}
&\frac{1}{2}\|T\|^2 - \frac{1}{2}\|T_0\|^2 + \int_0^t \|\nabla T\|^2 ds - (\Theta, T) + (\Theta_0, T_0) \\
&+ \int_0^t (\Theta_{,s}, T)\, ds - \int_0^t \int_\Omega \Theta v_i T_{,i} dx ds - \int_0^t \oint_\Gamma T\frac{\partial \Theta}{\partial n} dA ds = 0.
\end{aligned} \tag{2.3.15}$$

Next, we have to bound the cubic term in equation (2.3.15) using *Cauchy-Schwarz Inequality* and inequality (2.3.11), where Θ_m is the maximum of T_B on $\Gamma \times [0, \tau]$,

$$\begin{aligned}\int_0^t \int_\Omega \Theta v_i T_{,i} dx ds &\leq \Theta_m \sqrt{\int_0^t \|\mathbf{v}\|^2 ds \int_0^t \|\nabla T\|^2 ds} \\ &\leq \frac{\sqrt{2} G \Theta_m}{(1+\lambda)} \sqrt{\int_0^t \left(R^2 \|T\|^2 + R_s^2 \|C\|^2\right) ds \int_0^t \|\nabla T\|^2 ds},\end{aligned}$$

employing the *Arithmetic-Geometric Mean Inequality*, to see

$$\begin{aligned}\int_0^t \int_\Omega \Theta v_i T_{,i} dx ds \leq & \frac{G\Theta_m}{\sqrt{2}\,(1+\lambda)\,\zeta_1} \left(\int_0^t R^2 \|T\|^2 ds + \int_0^t R_s^2 \|C\|^2 ds \right) \\ & + \frac{G\Theta_m \zeta_1}{\sqrt{2}\,(1+\lambda)} \int_0^t \|\nabla T\|^2 ds,\end{aligned}$$

where $\zeta_1 > 0$ is a constant to be chosen. Now, using (2.3.16) in (2.3.15)and make repeated use of the *Arithmetic-Geometric Mean Inequality*, we may show that

$$\begin{aligned}\frac{1}{4}\|T\|^2 + \frac{1}{2}\int_0^t \|\nabla T\|^2 ds \leq & \|T_0\|^2 + \|\Theta\|^2 + \frac{1}{2}\|\Theta_0\|^2 + \frac{1}{2}\int_0^t \|\Theta_{,s}\|^2 ds \\ & + \frac{1}{2}\int_0^t \oint_\Gamma T_B^2 dA ds + \frac{1}{2}\int_0^t \oint_\Gamma \left(\frac{\partial \Theta}{\partial n}\right)^2 dA ds \\ & + B_3 \int_0^t \|T\|^2 ds + B_4 \int_0^t \|C\|^2 ds,\end{aligned} \tag{2.3.16}$$

where

$$\begin{aligned}B_3 &= \frac{1}{2} + \frac{\Theta_m^2 G^2 R^2}{(1+\lambda_1\lambda)^2}, \\ B_4 &= \frac{\Theta_m^2 G^2 R_s^2}{(1+\lambda_1\lambda)^2},\end{aligned}$$

and where we have chosen

$$\zeta_1 = \frac{(1+\lambda_1\lambda)}{\sqrt{2} G \Theta_m}.$$

Then, we add (2.3.14) and (2.3.16), to obtain

$$\begin{aligned}&\frac{\epsilon_1}{4}\|C\|^2 + \frac{1}{4}\|T\|^2 + \frac{1}{2}\int_0^t \|\nabla C\|^2 ds + \frac{1}{2}\int_0^t \|\nabla T\|^2 ds \\ &\leq (A_9 + B_4)\int_0^t \|C\|^2 ds + (A_{10} + B_3)\int_0^t \|T\|^2 ds + E(t),\end{aligned} \tag{2.3.17}$$

where $E(t)$ is a term we will show that it is bounded by data and is defined by

$$\begin{aligned} E(t) =&\epsilon_1\|C_0\|^2 + \|T_0\|^2 + \epsilon_1\|\Phi\|^2 + \|\Theta\|^2 + \frac{\epsilon_1}{2}\|\Phi_0\|^2 + \frac{1}{2}\|\Theta_0\|^2 + \frac{\epsilon_1}{2}\int_0^t \|\Phi_{,s}\|^2 ds \\ &+ \frac{1}{2}\int_0^t \|\Theta_{,s}\|^2 ds + A_{11}\int_0^t \|\Phi\|^2 ds + \frac{1}{2}\int_0^t \oint_\Gamma C_B^2 dAds + \frac{1}{2}\int_0^t \oint_\Gamma T_B^2 dAds \\ &+ \frac{1}{2}\int_0^t \oint_\Gamma \left(\frac{\partial \Phi}{\partial n}\right)^2 dAds + \frac{1}{2}\int_0^t \oint_\Gamma \left(\frac{\partial \Theta}{\partial n}\right)^2 dAds. \end{aligned} \tag{2.3.18}$$

In order to find bounds for $E(t)$ in terms of data, we have to employ the *Rellich identity* (1.1.7) and identity (1.1.9). To explain it clearly, the following lines will show the use of these inequalities to bound each term of $E(t)$ separately.
Starting by the third term of $E(t)$ up to the last term respectively,

$$\begin{aligned} \epsilon_1\|\Phi\|^2 &\leq \epsilon_1\psi_1 \oint_\Gamma C_B^2 dA, \\ \|\Theta\|^2 &\leq \psi_1 \oint_\Gamma T_B^2 dA, \\ \frac{\epsilon_1}{2}\|\Phi_0\|^2 &\leq \frac{\epsilon_1}{2}\psi_1 \oint_\Gamma C_{0B}^2 dA, \\ \frac{1}{2}\|\Theta_0\|^2 &\leq \frac{1}{2}\psi_1 \oint_\Gamma T_{0B}^2 dA, \\ \frac{\epsilon_1}{2}\int_0^t \|\Phi_{,s}\|^2 ds &\leq \frac{\epsilon_1}{2}\psi_1 \int_0^t \oint_\Gamma C_{B,\eta}^2 dAd\eta, \\ \frac{1}{2}\int_0^t \|\Theta_{,s}\|^2 ds &\leq \frac{1}{2}\psi_1 \int_0^t \oint_\Gamma T_{B,\eta}^2 dAd\eta, \\ A_{11}\int_0^t \|\Phi\|^2 ds &\leq A_{11}\psi_1 \int_0^t \oint_\Gamma C_B^2 dAd\eta, \\ \frac{1}{2}\int_0^t \oint_\Gamma C_B^2 dAds &\leq \frac{1}{2}\int_0^t \oint_\Gamma C_B^2 dAd\eta, \\ \frac{1}{2}\int_0^t \oint_\Gamma T_B^2 dAds &\leq \frac{1}{2}\int_0^t \oint_\Gamma T_B^2 dAd\eta, \\ \frac{1}{2}\int_0^t \oint_\Gamma \left(\frac{\partial \Phi}{\partial n}\right)^2 dAds &\leq \frac{c_2}{2c_1}\int_0^t \oint_\Gamma |\nabla_s C_B|^2 dAd\eta, \\ \frac{1}{2}\int_0^t \oint_\Gamma \left(\frac{\partial \Theta}{\partial n}\right)^2 dAds &\leq \frac{c_2}{2c_1}\int_0^t \oint_\Gamma |\nabla_s T_B|^2 dAd\eta. \end{aligned}$$

In fact, we have shown that

$$E(t) \leq D(t), \tag{2.3.19}$$

where

$$\begin{aligned} D(t) =&\epsilon_1\|C_0\|^2 + \|T_0\|^2 + \epsilon_1\psi_1 \oint_\Gamma C_B^2 dA + \psi_1 \oint_\Gamma T_B^2 dA + \frac{\epsilon_1}{2}\psi_1 \oint_\Gamma C_{0B}^2 dA \\ &+ \frac{1}{2}\psi_1 \oint_\Gamma T_{0B}^2 dA + \frac{\epsilon_1}{2}\psi_1 \int_0^t \oint_\Gamma C_{B,\eta}^2 dA d\eta + \frac{1}{2}\psi_1 \int_0^t \oint_\Gamma T_{B,\eta}^2 dA d\eta \\ &+ \frac{1}{2}\int_0^t \oint_\Gamma C_B^2 dA d\eta + \frac{1}{2}\int_0^t \oint_\Gamma T_B^2 dA d\eta + \frac{c_2}{2c_1}\int_0^t \oint_\Gamma |\nabla_s C_B|^2 dA d\eta \\ &+ \frac{c_2}{2c_1}\int_0^t \oint_\Gamma |\nabla_s T_B|^2 dA d\eta + A_{11}\psi_1 \int_0^t \oint_\Gamma C_B^2 dA d\eta. \end{aligned} \tag{2.3.20}$$

Note that $D(t)$ is composed of terms which depend only on the initial and boundary data of the problem, $C_0,\ T_0,\ C_B,\ T_B$, and their known derivatives.

Then from inequality (2.3.17) we may derive

$$F_1' - k_5 F_1 \leq D, \tag{2.3.21}$$

where $k_5 = max\{A_9 + B_4, A_{10} + B_3\}$ and where we have introduced the function $F_1(t)$ defined by

$$F_1(t) = \int_0^t \left(\frac{1}{4}\|T\|^2 + \frac{\epsilon_1}{4}\|C\|^2\right) ds.$$

Upon integration of the differential inequality (2.3.21), one may show that

$$F_1 \leq D_1(t), \tag{2.3.22}$$

where

$$D_1(t) = \int_0^t D e^{k_5(t-s)} ds.$$

Furthermore, setting $D_2(t) = D + k_5 D_1$, we may use inequality (2.3.21) to find

$$F_1' = \frac{1}{4}\|T\|^2 + \frac{\epsilon_1}{4}\|C\|^2 \leq D_2,$$

which implies

$$\|T\|^2 \leq 4D_2, \tag{2.3.23}$$

$$\|C\|^2 \leq \frac{4}{\epsilon_1} D_2, \tag{2.3.24}$$

Moreover, inequality (2.3.22), implies

$$\int_0^t \|T\|^2 ds \leq 4D_1, \tag{2.3.25}$$

$$\int_0^t \|C\|^2 ds \leq \frac{4}{\epsilon_1} D_1. \tag{2.3.26}$$

Returning to inequality (2.3.17),we have that

$$F_1' + \frac{1}{2}\int_0^t \|\nabla C\|^2 ds + \frac{1}{2}\int_0^t \|\nabla T\|^2 ds \leq D_2,$$

which implies

$$\int_0^t \|\nabla C\|^2 ds \leq 2D_2, \tag{2.3.27}$$

$$\int_0^t \|\nabla T\|^2 ds \leq 2D_2. \tag{2.3.28}$$

2.3.2 Bounds for the $Sup_{\Omega\times[0,\tau]}|C|$ and $Sup_{\Omega\times[0,\tau]}|T|$

The next step is to derive bounds for $sup_{\Omega\times[0,\tau]}|C|$ and $sup_{\Omega\times[0,\tau]}|T|$. For these, we have to introduce a function $I(\mathbf{x},t)$ as a solution to the following boundary value problem

$$\Delta I = 0 \ in \ \Omega, \tag{2.3.29}$$

$$I = C_B^{2p-1} \ on \ \Gamma, \tag{2.3.30}$$

similarly, we introduce a function $H(\mathbf{x},t)$ as a solution to the boundary value problem

$$\Delta H = 0 \ in \ \Omega, \tag{2.3.31}$$

$$H = T_B^{2p-1} \ on \ \Gamma, \tag{2.3.32}$$

where $p \in N$. These are different from (2.3.1) − (2.3.4) because the boundary conditions are different. Then we form the combinations

$$\int_0^t \int_\Omega \left(C^{2p-1} - I\right)\left(\epsilon_1 C_{,s} + Lev_i C_{,i} - \Delta C - lT + hC\right) dxds = 0, \tag{2.3.33}$$

and

$$\int_0^t \int_\Omega \left(T^{2p-1} - H\right)\left(T_{,s} + v_i T_{,i} - \Delta T\right) dxds = 0. \tag{2.3.34}$$

Next, integrate the terms in equation (2.3.33) by parts and employ the boundary condition (2.3.30). For clarity, we will integrate each term separately. The first term is

$$\int_0^t \int_\Omega \epsilon_1 C^{2p-1} C_{,s} dxds = \frac{\epsilon_1}{2p}\int_\Omega C^{2p} dx - \frac{\epsilon_1}{2p}\int_\Omega C_0^{2p} dx. \tag{2.3.35}$$

The second term integrated to

$$Le\int_0^t\int_\Omega C^{2p-1}v_iC_{,i}dxds=\frac{Le}{2p}\int_0^t\int_\Omega\left[\frac{\partial}{\partial x_i}\left(v_iC^{2p}\right)-C^{2p}\frac{\partial v_i}{\partial x_i}\right]dxds,$$

employing the *Divergence Theorem* to the first term on the right, we obtain

$$Le\int_0^t\int_\Omega C^{2p-1}v_iC_{,i}dxds=\frac{Le}{2p}\int_0^t\oint_\Gamma n_iv_iC^{2p}dAds-\frac{Le}{2p}\int_0^t\int_\Omega C^{2p}v_{i,i}dxds$$

Using the boundary condition $v_i=0$ for Brinkman or $v_in_i=0$ for Darcy, the first term on the right is zero and since $v_{i,i}=0$ in Ω, the second term is also zero. Therefore, the second term is

$$Le\int_0^t\int_\Omega C^{2p-1}v_iC_{,i}dxds=0. \tag{2.3.36}$$

The third term is integrated through the following steps

$$-\int_0^t\int_\Omega C^{2p-1}\Delta Cdxds=-\int_0^t\int_\Omega\nabla\left(C^{2p-1}\nabla C\right)dxds+\int_0^t\int_\Omega\frac{\partial C^{2p-1}}{\partial x_i}\frac{\partial C}{\partial x_i}dxds,$$

applying the *Divergence Theorem* to the first term on the right, we obtain

$$-\int_0^t\int_\Omega C^{2p-1}\Delta Cdxds=-\int_0^t\oint_\Gamma n_iC^{2p-1}\nabla CdAds+\int_0^t\int_\Omega\left(2p-1\right)C^{2p-2}\frac{\partial C}{\partial x_i}\frac{\partial C}{\partial x_i}dxds,$$

which can be written as

$$\begin{aligned}&-\int_0^t\int_\Omega C^{2p-1}\Delta Cdxds\\&\quad=-\int_0^t\oint_\Gamma n_iC^{2p-1}\nabla CdAds+\left(2p-1\right)\int_0^t\int_\Omega\frac{1}{p^2}\frac{\partial C^p}{\partial x_i}\frac{\partial C^p}{\partial x_i}dxds\\&\quad=-\int_0^t\oint_\Gamma n_iC^{2p-1}\nabla CdAds+\frac{\left(2p-1\right)}{p^2}\int_0^t\int_\Omega\nabla C^p\nabla C^pdxds.\end{aligned} \tag{2.3.37}$$

The fifth term is

$$\begin{aligned}-\epsilon_1\int_0^t\int_\Omega IC_{,s}dxds&=-\epsilon_1\left[\int_\Omega\left(CI|_0^t-\int_0^tCI_{,s}ds\right)dx\right]\\&=-\epsilon_1\left(I,C\right)+\epsilon_1\left(I_0,C_0\right)+\epsilon_1\int_0^t\left(I_{,s},C\right)ds.\end{aligned} \tag{2.3.38}$$

The fourth, sixth and eighth terms are integrated in the proceeding lines. Using integration by parts, the seventh term is

$$\int_0^t\int_\Omega I\Delta Cdxds=\int_0^t\int_\Omega\nabla\left(I\nabla C\right)dxds-\int_0^t\int_\Omega\nabla I\nabla Cdxds$$

Applying the *Divergence Theorem* to the first term and making repeated use of integration by parts on the second term, we see

$$\int_0^t \int_\Omega I\Delta C dxds = \int_0^t \oint_\Gamma n_i \frac{\partial C}{\partial x_i} I dAds - \left[\int_0^t \left[\int_\Omega \frac{\partial}{\partial x_i}\left(\frac{\partial I}{\partial x_i} C\right) dx - \int_\Omega C\Delta I dx\right] ds\right]$$

again we have to use the *Divergence Theorem* in the second term. Moreover, the last term is zero since $\Delta I = 0$ in Ω. Therefore

$$\int_0^t \int_\Omega I\Delta C dxds = \int_0^t \oint_\Gamma n_i \frac{\partial C}{\partial x_i} I dAds - \int_0^t \oint_\Gamma n_i \frac{\partial I}{\partial x_i} C dAds. \tag{2.3.39}$$

Now, we employ (2.3.35), (2.3.36), (2.3.37), (2.3.38) and (2.3.39) in (2.3.33) to see that

$$\begin{aligned}\epsilon_1 \int_\Omega C^{2p} dx + \frac{2(2p-1)}{p} \int_0^t \int_\Omega C_{,i}^p C_{,i}^p dxds = \epsilon_1 \int_\Omega C_0^{2p} dx + 2p\epsilon_1 (I, C) - 2p\epsilon_1 (I_0, C_0) \\ - 2p\epsilon_1 \int_0^t (I_{,s}, C)\, ds + 2p \int_0^t \oint_\Gamma C_B \frac{\partial I}{\partial n} dAds \\ + 2p \int_0^t \int_\Omega C^{2p-1} (lT - hC)\, dxds \\ - 2p \int_0^t \int_\Omega I (lT - hC)\, dxds \\ + 2pLe \int_0^t \int_\Omega I v_i C_{,i} dxds.\end{aligned} \tag{2.3.40}$$

To move on from equation (2.3.40), we proceed as in Payne and Straughan [80] employing the steps leading to their inequalities (A21)-A(25). But we have to handle the last three terms on the right of (2.3.40). First, employing *Young's inequality* to see that

$$\begin{aligned} 2p & \int_0^t \int_\Omega C^{2p-1} (lT - hC)\, dxds \\ \leq\ & 2pl_m \left[\frac{1}{2p} \int_0^t \int_\Omega T^{2p} dxds + \frac{2p-1}{2p} \int_0^t \int_\Omega \left(C^{2p-1}\right)^{\frac{2p}{2p-1}} dxds\right] \\ +\ & 2ph_m \left[\frac{1}{2p} \int_0^t \int_\Omega C^{2p} dxds + \frac{2p-1}{2p} \int_0^t \int_\Omega \left(C^{2p-1}\right)^{\frac{2p}{2p-1}} dxds\right] \end{aligned}$$

on simplification, we obtain

$$\begin{aligned} 2p \int_0^t \int_\Omega C^{2p-1} (lT - hC)\, dxds \leq \{(2p-1)\, l_m + 2ph_m\} \int_0^t \int_\Omega C^{2p} dxds \\ + l_m \int_0^t \int_\Omega T^{2p} dxds. \end{aligned} \tag{2.3.41}$$

A further application of *Young's inequality* on the penultimate term in (2.3.40) leads to

$$\begin{aligned} 2p\int_0^t\int_\Omega I\left(lT-hC\right)dxds &\leq 2pl_m\left[\frac{1}{2p}\int_0^t\int_\Omega T^{2p}dxds+\frac{2p-1}{2p}\int_0^t\int_\Omega I^{\frac{2p}{2p-1}}dxds\right] \\ &+ 2ph_m\left[\frac{1}{2p}\int_0^t\int_\Omega C^{2p}dxds+\frac{2p-1}{2p}\int_0^t\int_\Omega I^{\frac{2p}{2p-1}}dxds\right] \end{aligned}$$

simplifying and combining the like terms

$$\begin{aligned} 2p\int_0^t\int_\Omega I\left(lT-hC\right)dxds &\leq l_m\int_0^t\int_\Omega T^{2p}dxds+h_m\int_0^t\int_\Omega C^{2p}dxds \\ &+ \left(2p-1\right)\left(l_m+h_m\right)\int_0^t\int_\Omega I^{\frac{2p}{2p-1}}dxds \end{aligned}$$

Applying identity (1.1.9) to last term of the previous inequality and using the boundary condition (2.3.30), we obtain

$$\begin{aligned} 2p\int_0^t\int_\Omega I\left(lT-hC\right)dxds \leq & l_m\int_0^t\int_\Omega T^{2p}dxds+h_m\int_0^t\int_\Omega C^{2p}dxds \\ & +\left(2p-1\right)\psi_1\left(l_m+h_m\right)\int_0^t\oint_\Gamma C_B^{2p}dxds. \end{aligned} \tag{2.3.42}$$

The last term of (2.3.40) will be

$$\begin{aligned} 2pLe\quad &\int_0^t\int_\Omega Iv_iC_{,i}dxds \leq 2pLeI_m\sqrt{\int_0^t\|\mathbf{v}\|^2ds\int_0^t\|\nabla C\|^2ds} \\ \leq\quad & 2pLeI_m\frac{\sqrt{2}G}{\left(1+\lambda_1\lambda\right)}\sqrt{\int_0^t\left(R^2\|T\|^2+R_s^2\|C\|^2\right)ds\int_0^t\|\nabla C\|^2ds}, \end{aligned}$$

where I_m denotes the maximum value of I on Γ and *Cauchy-Schwarz inequality* and inequality (2.3.11) have been employed. An application of the *Arithmetic-Geometric Mean inequality* together with (2.3.25), (2.3.26) and (2.3.27) yields

$$2pLe\int_0^t\int_\Omega Iv_iC_{,i}dxds \leq \frac{\sqrt{2}pLeGI_m}{\left(1+\lambda_1\lambda\right)}\left[4R^2D_1+\frac{4}{\epsilon_1}R_s^2D_1+2D_2\right] \tag{2.3.43}$$

Thus, combining (2.3.41), (2.3.42) and (2.3.43) in (2.3.40), to find with the aid of *Cauchy-Schwarz inequality*

$$\begin{aligned}\epsilon_1\int_\Omega C^{2p}dx \leq & \epsilon_1\int_\Omega C_0^{2p}dx + 2p\epsilon_1\left(\|I\|\|C\| + \|I_0\|\|C_0\|\right) + 2p\epsilon_1\sqrt{\int_0^t \|I_{,\eta}\|^2 d\eta \int_0^t \|C\|^2 d\eta} \\ & + 2p\sqrt{\int_0^t \oint_\Gamma C_B^2 dAd\eta \int_0^t \oint_\Gamma \left(\frac{\partial I}{\partial n}\right)^2 dAd\eta} + 2l_m\int_0^t\int_\Omega T^{2p}dxd\eta \\ & + \frac{\sqrt{2}pLeGI_m}{(1+\lambda_1\lambda)}\left[4R^2D_1 + \frac{4}{\epsilon_1}R_s^2D_1 + 2D_2\right] \\ & + \left[(2p-1)\,l_m + (2p+1)\,h_m\right]\int_0^t\int_\Omega C^{2p}dxd\eta \\ & + (2p-1)\,\psi_1\,(h_m+l_m)\int_0^t\oint_\Gamma C_B^{2p}dxd\eta.\end{aligned} \tag{2.3.44}$$

Next, we have to bound the second, third and fourth terms on the right of the previous inequality. In order to bound the second term we have to use the prescribed boundary conditions, identity (1.1.9) and inequality (2.3.24), so that the second term is

$$2p\epsilon_1\left(\|I\|\|C\| + \|I_0\|\|C_0\|\right) \leq 2p\epsilon_1\psi_1^{\frac{1}{2}}\left(\oint_\Gamma C_B^{4p-2}dA\right)^{\frac{1}{2}}\left[2\sqrt{\frac{D_2}{\epsilon_1}} + \|C_0\|\right]. \tag{2.3.45}$$

The third term is bounded by using inequality (2.3.26) together with identity (1.1.9), to obtain

$$2p\epsilon_1\sqrt{\int_0^t \|I_{,\eta}\|^2 d\eta \int_0^t \|C\|^2 d\eta} \leq 2p\epsilon_1\sqrt{\frac{4D_1}{\epsilon_1}}\left(\int_0^t \psi_1 \oint_\Gamma \left[\left(C_B^{2p-1}\right)_{,\eta}\right]^2 dAd\eta\right)^{\frac{1}{2}} \tag{2.3.46}$$

Finally, we bound the fourth term by using the *Rellich identity*

$$\begin{aligned}& 2p\sqrt{\int_0^t \oint_\Gamma C_B^2 dAd\eta \int_0^t \oint_\Gamma \left(\frac{\partial I}{\partial n}\right)^2 dAd\eta} \\ & \quad \leq 2p\sqrt{\frac{c_2}{c_1}}\left(\int_0^t \oint_\Gamma C_B^2 dAd\eta\right)^{\frac{1}{2}}\left(\int_0^t \oint_\Gamma |\nabla_s C_B^{2p-1}|^2 dAd\eta\right)^{\frac{1}{2}}.\end{aligned} \tag{2.3.47}$$

Substituting (2.3.45), (2.3.46) and (2.3.47) in (2.3.44), we find

$$\begin{aligned}
\epsilon_1 \int_\Omega C^{2p} dx \;\leq\; & \epsilon_1 \int_\Omega C_0^{2p} dx + 2p\epsilon_1 \psi_1^{\frac{1}{2}} \left(\oint_\Gamma C_B^{4p-2} dA \right)^{\frac{1}{2}} \left[2\sqrt{\frac{D_2}{\epsilon_1}} + \|C_0\| \right] \\
+ \;& 2p\epsilon_1 \sqrt{\frac{4D_1}{\epsilon_1}} \left(\int_0^t \psi_1 \oint_\Gamma \left[\left(C_B^{2p-1} \right)_{,\eta} \right]^2 dA d\eta \right)^{\frac{1}{2}} \\
+ \;& 2p \sqrt{\frac{c_2}{c_1}} \left(\int_0^t \oint_\Gamma C_B^2 dA d\eta \right)^{\frac{1}{2}} \left(\int_0^t \oint_\Gamma |\nabla_s C_B^{2p-1}|^2 dA d\eta \right)^{\frac{1}{2}} \\
+ \;& 2l_m \int_0^t \int_\Omega T^{2p} dx d\eta + \frac{\sqrt{2} p LeG C_{Bm}^{2p-1}}{(1+\lambda_1 \lambda)} \left[4R^2 D_1 + \frac{4}{\epsilon_1} R_s^2 D_1 + 2D_2 \right] \\
+ \;& \left[(2p-1)\, l_m + (2p+1)\, h_m \right] \int_0^t \int_\Omega C^{2p} dx d\eta \\
+ \;& (2p-1)\, \psi_1 \left(h_m + l_m \right) \int_0^t \oint_\Gamma C_B^{2p} dA d\eta,
\end{aligned}$$

where C_{Bm} is the maximum of C_B on Γ. To move on, we commence as in Payne and Straughan [80], going through the steps leading to their inequality $A(25)$, to find

$$\begin{aligned}
\epsilon_1 \int_\Omega C^{2p} dx \leq\; & \left[(2p-1)\, l_m + (2p+1)\, h_m \right] \int_0^t \int_\Omega C^{2p} dx d\eta + \epsilon_1 \int_\Omega C_0^{2p} dx \\
& + \frac{\sqrt{2} p LeG}{(1+\lambda_1 \lambda)\, C_{Bm}} \left[4R^2 D_1 + \frac{4}{\epsilon_1} R_s^2 D_1 + 2D_2 \right] C_{Bm}^{2p} \\
& + \frac{2p\epsilon_1 \psi_1^{\frac{1}{2}} \left[m(\Gamma) \right]^{\frac{1}{2}}}{C_{Bm}} \left(2\sqrt{\frac{D_2}{\epsilon_1}} + \|C_0\| \right) C_{Bm}^{2p} \\
& + \frac{2p\epsilon_1 \psi_1^{\frac{1}{2}} \left[t m(\Gamma) \right]^{\frac{1}{2}}}{C_{Bm}^2} \sqrt{\frac{4D_1}{\epsilon_1}} \left(\int_0^t \oint_\Gamma C_{B,\eta}^2 dA d\eta \right)^{\frac{1}{2}} C_{Bm}^{2p} \\
& + 2p \sqrt{\frac{c_2}{c_1}} \frac{\left(t m(\Gamma) \right)^{\frac{1}{2}}}{C_{Bm}} \left(\int_0^t \oint_\Gamma |\nabla_s C_B|^2 dA d\eta \right)^{\frac{1}{2}} C_{Bm}^{2p} \\
& + (2p-1)\, (h_m + l_m)\, \psi_1 t m(\Gamma) C_{Bm}^{2p} + 2l_m \int_0^t \int_\Omega T^{2p} dx d\eta,
\end{aligned} \tag{2.3.48}$$

where $m(\Gamma)$ is the surface measure of Γ.

Returning to equation (2.3.34) and performing various integration by parts, to see

$$\begin{aligned}
\int_\Omega T^{2p} dx + \frac{2\,(2p-1)}{p} \int_0^t \int_\Omega T_{,i}^p T_{,i}^p dx d\eta = & \int_\Omega T_0^{2p} dx + 2p\,(H, T) - 2p\,(H_0, T_0) \\
& - 2p \int_0^t (H_{,\eta}, T)\, d\eta + 2p \int_0^t \oint_\Gamma T_B \frac{\partial H}{\partial n} dA d\eta \\
& + 2p \int_0^t \int_\Omega H v_i T_{,i} dx d\eta.
\end{aligned} \tag{2.3.49}$$

Now, we have to handle the last term on the right of (2.3.49), where H_m is the maximum value of H on $\Gamma \times [0,\tau]$,

$$\begin{aligned} 2p \quad & \int_0^t \int_\Omega H v_i T_{,i} dx d\eta \leq 2pH_m \sqrt{\int_0^t \|v\|^2 d\eta \int_0^t \|\nabla T\|^2 d\eta} \\ \leq \quad & 2pT_{Bm}^{2p-1} \frac{\sqrt{2}G}{(1+\lambda_1\lambda)} \sqrt{\int_0^t R^2 \|T\|^2 d\eta + \int_0^t R_s^2 \|C\|^2 d\eta} \sqrt{\int_0^t \|\nabla T\|^2 d\eta}\,, \end{aligned}$$

where T_{Bm} is the maximum of T_B and where we have used the *Cauchy-Schawrz inequality* and inequality (2.3.11). We now make use of the *Arithmetic-Geometric Mean inequality* and employ (2.3.26), (2.3.25) and (2.3.28) to arrive at

$$2p \int_0^t \int_\Omega H v_i T_{,i} dx d\eta \leq \sqrt{2} p T_{Bm}^{2p-1} \frac{G}{(1+\lambda_1\lambda)} \left[4R^2 D_1 + \frac{4}{\epsilon_1} R_s^2 D_1 + 2D_2 \right]. \quad (2.3.50)$$

Employing (2.3.50) in (2.3.49) and make use of the *Cauchy-Schawrz inequality* to obtain

$$\begin{aligned} \int_\Omega T^{2p} dx \quad \leq \quad & \int_\Omega T_0^{2p} dx + 2p \left(\|H\| \|T\| + \|H_0\| \|T_0\| \right) + 2p \sqrt{\int_0^t \|H_{,\eta}\|^2 d\eta \int_0^t \|T\|^2 d\eta} \\ + \quad & \sqrt{2} p T_{Bm}^{2p-1} \frac{G}{(1+\lambda_1\lambda)} \left[4R^2 D_1 + \frac{4}{\epsilon_1} R_s^2 D_1 + 2D_2 \right] \\ + \quad & 2p \sqrt{\int_0^t \oint_\Gamma T_B^2 dA d\eta \int_0^t \oint_\Gamma \left(\frac{\partial H}{\partial n} \right)^2 dA d\eta}. \end{aligned}$$

Furthermore, using the *Rellich identity*, inequality (2.3.24) and employing the procedure leading to inequality $A(25)$ of Payne and Straughan [80], to find

$$\begin{aligned} \int_\Omega T^{2p} dx \leq & \int_\Omega T_0^{2p} dx + \frac{\sqrt{2} p G}{(1+\lambda_1\lambda)\, T_{Bm}} \left[4R^2 D_1 + \frac{4}{\epsilon_1} R_s^2 D_1 + 2D_2 \right] T_{Bm}^{2p} \\ & + \frac{2p\psi_1^{\frac{1}{2}} [m(\Gamma)]^{\frac{1}{2}}}{T_{Bm}} \left[2\sqrt{D_2} + \|T_0\| \right] T_{Bm}^{2p} \\ & + 2p \sqrt{\frac{c_2}{c_1}} \frac{(tm(\Gamma))^{\frac{1}{2}}}{T_{Bm}} \left(\int_0^t \oint_\Gamma |\nabla_s T_B|^2 dA d\eta \right)^{\frac{1}{2}} T_{Bm}^{2p} \\ & + \frac{2p\psi_1^{\frac{1}{2}} (tm(\Gamma))^{\frac{1}{2}}}{T_{Bm}^2} \sqrt{4D_1} \left(\int_0^t \oint_\Gamma T_{B,\eta}^2 dA d\eta \right)^{\frac{1}{2}} T_{Bm}^{2p}. \end{aligned} \quad (2.3.51)$$

Next, add (2.3.48) and (2.3.51) to arrive at

$$\begin{aligned} \epsilon_1 \int_\Omega C^{2p} dx + \int_\Omega T^{2p} dx \leq & \left[(2p-1)\, l_m + (2p+1)\, h_m \right] \int_0^t \int_\Omega C^{2p} dx d\eta \\ & + 2l_m \int_0^t \int_\Omega T^{2p} dx d\eta + K(p), \end{aligned} \quad (2.3.52)$$

where the value of $K(p)$ is

$$\begin{aligned}
K(p) =&\epsilon_1 \int_\Omega C_0^{2p} dx + \int_\Omega T_0^{2p} dx + \frac{\sqrt{2} pLeG}{(1+\lambda_1\lambda)\, C_{Bm}} \left[4R^2 D_1 + \frac{4}{\epsilon_1} R_s^2 D_1 + 2D_2\right] C_{Bm}^{2p} \\
&+ \frac{\sqrt{2} pG}{(1+\lambda_1\lambda)\, T_{Bm}} \left[4R^2 D_1 + \frac{4}{\epsilon_1} R_s^2 D_1 + 2D_2\right] T_{Bm}^{2p} \\
&+ \frac{2p\epsilon_1 \psi_1^{\frac{1}{2}} [m(\Gamma)]^{\frac{1}{2}}}{C_{Bm}} \left(2\sqrt{\frac{D_2}{\epsilon_1}} + \|C_0\|\right) C_{Bm}^{2p} \\
&+ \frac{2p\psi_1^{\frac{1}{2}} [m(\Gamma)]^{\frac{1}{2}}}{T_B} \left[2\sqrt{D_2} + \|T_0\|\right] T_{Bm}^{2p} \\
&+ \frac{2p\epsilon_1 \psi_1^{\frac{1}{2}} [tm(\Gamma)]^{\frac{1}{2}}}{C_{Bm}^2} \sqrt{\frac{4D_1}{\epsilon_1}} \left(\int_0^t \oint_\Gamma C_{B,\eta}^2 dA d\eta\right)^{\frac{1}{2}} C_{Bm}^{2p} \\
&+ \frac{2p\epsilon_1 \psi_1^{\frac{1}{2}} (tm(\Gamma))^{\frac{1}{2}}}{T_{Bm}^2} \sqrt{4D_1} \left(\int_0^t \oint_\Gamma T_{B,\eta}^2 dA d\eta\right)^{\frac{1}{2}} T_{Bm}^{2p} \\
&+ 2p\sqrt{\frac{c_2}{c_1}} \frac{(tm(\Gamma))^{\frac{1}{2}}}{C_{Bm}^2} \left(\int_0^t \oint_\Gamma C_B^2 dA d\eta\right)^{\frac{1}{2}} \left(\int_0^t \oint_\Gamma |\nabla_s C_B|^2 dA d\eta\right)^{\frac{1}{2}} C_{Bm}^{2p} \\
&+ 2p\sqrt{\frac{c_2}{c_1}} \frac{(tm(\Gamma))^{\frac{1}{2}}}{T_{Bm}^2} \left(\int_0^t \oint_\Gamma T_B^2 dA d\eta\right)^{\frac{1}{2}} \left(\int_0^t \oint_\Gamma |\nabla_s T_B|^2 dA d\eta\right)^{\frac{1}{2}} T_{Bm}^{2p} \\
&+ (2p-1)\,(h_m + l_m)\, \psi_1 tm(\Gamma) C_{Bm}^{2p}.
\end{aligned} \tag{2.3.53}$$

If $k_6 = max\,\{(2p-1)\, l_m + (2p+1)\, h_m, 2l_m\}$, then inequality (2.3.52) can be written as

$$\epsilon_1 \int_\Omega C^{2p} dx + \int_\Omega T^{2p} dx \leq k_6 \left[\epsilon_1 \int_0^t \int_\Omega C^{2p} dx d\eta + \int_0^t \int_\Omega T^{2p} dx d\eta\right] + K(p),$$

which can be integrated. Setting $F_2(t) = \epsilon_1 \int_0^t \int_\Omega C^{2p} dx d\eta + \int_0^t \int_\Omega T^{2p} dx d\eta$, the above differential inequality can be written as

$$F_2' - k_6 F_2 \leq K(p),$$

upon integration, we obtain

$$F_2(t) \leq \int_0^t e^{k_6(t-\eta)} K(p) d\eta,$$

which is

$$\epsilon_1 \int_0^t \int_\Omega C^{2p} dx d\eta + \int_0^t \int_\Omega T^{2p} dx d\eta \leq \int_0^t e^{k_6(t-\eta)} K(p) d\eta. \tag{2.3.54}$$

Inequality (2.3.54) implies that

$$\int_0^t \int_\Omega C^{2p} dx d\eta \leq \frac{1}{\epsilon_1} \int_0^t e^{k_6(t-\eta)} K(p) d\eta, \tag{2.3.55}$$

and

$$\int_0^t \int_\Omega T^{2p} dx d\eta \leq \int_0^t e^{k_6(t-\eta)} K(p) d\eta. \tag{2.3.56}$$

Then, we take the $\frac{1}{2p}$ power of (2.3.55) and (2.3.56), to find

$$\left[\int_0^t \int_\Omega C^{2p} dx d\eta\right]^{\frac{1}{2p}} \leq \left[\frac{1}{\epsilon_1} \int_0^t e^{k_6(t-\eta)} K(p) d\eta\right]^{\frac{1}{2p}}, \tag{2.3.57}$$

and

$$\left[\int_0^t \int_\Omega T^{2p} dx d\eta\right]^{\frac{1}{2p}} \leq \left[\int_0^t e^{k_6(t-\eta)} K(p) d\eta\right]^{\frac{1}{2p}}. \tag{2.3.58}$$

Let now $p \to \infty$ and then (2.3.57) and (2.3.58) lead to

$$sup_{\Omega\times[0,\tau]}|C| \leq max\left\{|T_0|_m, |C_0|_m, sup_{[0,\tau]}|C_{Bm}|, sup_{[0,\tau]}|T_{Bm}|\right\}$$
$$sup_{\Omega\times[0,\tau]}|T| \leq max\left\{|T_0|_m, |C_0|_m, sup_{[0,\tau]}|C_{Bm}|, sup_{[0,\tau]}|T_{Bm}|\right\}$$

We henceforth denote the right-hand sides of the above two inequalities by C_m and T_m respectively, to arrive at

$$sup_{\Omega\times[0,\tau]}|C| \leq C_m, \tag{2.3.59}$$

$$sup_{\Omega\times[0,\tau]}|T| \leq T_m. \tag{2.3.60}$$

Inequalities (2.3.59) and (2.3.60) are the a priori estimates we need for C and T.

2.4 Convergence of K(p)

In this section, we have to prove the convergence of the term $K(p)$. To do that, we have to use the fact that if $a_1 \geq a_2 \geq a_3 \geq a_4 \geq \cdots a_N \geq 0$, then

$$\begin{aligned}\left(a_1^{2p} + a_2^{2p} + a_3^{2p} + \cdots + a_N\right)^{\frac{1}{2p}} &= a_1\left[1 + \left(\frac{a_2}{a_1}\right)^{2p} + \left(\frac{a_3}{a_1}\right)^{2p} + \cdots + \left(\frac{a_N}{a_1}\right)^{2p}\right]^{\frac{1}{2p}} \\ &\leq N^{\frac{1}{2p}} a_1 = N^{\frac{1}{2p}} max\left\{a_1, a_2, a_3, \cdots, a_N\right\}.\end{aligned}$$

(See Payne and Straughan [80], page 322), in our case $N = 11$, because $K(p)$ has 11 terms. So

$$\left[\int_0^t e^{k_6(t-\eta)} K(p) d\eta\right]^{\frac{1}{2p}} \leq 11^{\frac{1}{2p}} max\left\{a_1, a_2, a_3, \cdots, a_{11}\right\}$$

As $p \to \infty$,

$$\begin{aligned}a_1 &= \left[\int_0^t \int_\Omega e^{k_6(t-\eta)} \epsilon_1 C_0^{2p} dx d\eta\right]^{\frac{1}{2p}} \to |C_0|_m \\ a_2 &= \left[\int_0^t \int_\Omega e^{k_6(t-\eta)} T_0^{2p} dx d\eta\right]^{\frac{1}{2p}} \to |T_0|_m \\ a_3 + a_5 + a_7 + a_9 &= \left[\int_0^t e^{k_6(t-\eta)} \left\{r_3 + r_5 + r_7 + r_9\right\} C_{Bm}^{\frac{1}{2p}} d\eta\right]^{\frac{1}{2p}} \to sup_{[0,\tau]}|C_{Bm}| \\ a_4 + a_6 + a_8 + a_{10} &= \left[\int_0^t e^{k_6(t-\eta)} \left\{r_4 + r_6 + r_8 + r_{10}\right\} T_{Bm}^{\frac{1}{2p}} d\eta\right]^{\frac{1}{2p}} \to sup_{[0,\tau]}|T_{Bm}| \\ a_{11} &= \left[\int_0^t e^{k_6(t-\eta)} (2p-1)\left(h_m + l_m\right) \psi_1 tm(\Gamma) C_{Bm}^{2p} d\eta\right]^{\frac{1}{2p}} \to sup_{[0,\tau]}|C_{Bm}|.\end{aligned}$$

Where $a_1, a_2, a_3, \cdots, a_{11}$ are the terms of $K(p)$ and $r_3, r_4, r_5, \cdots$ are the corresponding terms after factoring C_{Bm}^{2p} or T_{Bm}^{2p} respectively.

2.5 Continuous Dependence on the Reaction Term

To investigate continuous dependence on the reaction terms h and l, assume that we have two solutions $\{u_i, p_1, T_1, C_1\}$ and $\{v_i, p_2, T_2, C_2\}$ which satisfy (2.2.4), (2.2.5) and (2.2.6) for the same boundary and initial conditions, but for different reaction terms h_1, h_2 and l_1, l_2. Define the difference of the two solutions by,

$$w_i = u_i - v_i,\ \pi = p_1 - p_2,\ \theta = T_1 - T_2,\ \phi = C_1 - C_2,$$

and define the difference of the reaction terms by,

$$h = h_1 - h_2 \; and \; l = l_1 - l_2.$$

Then, we find that $\{w_i, \pi, \theta, \phi\}$ satisfies the boundary-initail value problem,

$$\begin{aligned} \pi_{,i} &= Rg_i\theta - R_s g_i\phi - w_i + \lambda\Delta w_i, \\ w_{i,i} &= 0, \\ \theta_{,t} + u_i\theta_{,i} + w_i T_{2,i} &= \Delta\theta, \\ \epsilon_1\phi_{,t} + Leu_i\phi_{,i} + Lew_i C_{2,i} &= \Delta\phi + lT_1 + l_2\theta - hC_1 - h_2\phi, \end{aligned} \tag{2.5.1}$$

on $\Omega \times (0, \tau]$, together with

$$w_i = 0, \; \theta = 0, \; \phi = 0, \; on \; \Gamma \times (0, \tau], \tag{2.5.2}$$

$$\theta(\mathbf{x}, 0) = 0 \; and \; \phi(\mathbf{x}, 0) = 0. \tag{2.5.3}$$

We want to estimate the solution $\{w_i, \pi, \theta, \phi\}$ in terms of h and l. Multiply equation $(2.5.1)_1$ by w_i, integrate over Ω and suppose that $|g_i| \leq G$. Using *Cauchy-Schwarz inequality* followed by the *Arithmetic-Geometric Mean inequality* the following is obtained,

$$\|\mathbf{w}\|^2 + \lambda\|\nabla\mathbf{w}\|^2 \leq \frac{RG}{2\alpha}\|\theta\|^2 + \frac{RG\alpha}{2}\|\mathbf{w}\|^2 + \frac{R_s G}{2\beta}\|\phi\|^2 + \frac{R_s G\beta}{2}\|\mathbf{w}\|^2 \; ,$$

where α,$\beta > 0$ are constants to be selected. If we choose $\alpha = \frac{1}{2RG}$ *and* $\beta = \frac{1}{2R_s G}$, we get

$$\frac{1}{2}\|\mathbf{w}\|^2 + \lambda\|\nabla\mathbf{w}\|^2 \leq R^2G^2\|\theta\|^2 + R_s^2G^2\|\phi\|^2. \tag{2.5.4}$$

Furthermore, multiply equation $(2.5.1)_3$ by θ, integrate over Ω and employ the *Cauchy-Schwarz inequality* and the *Arithmetic-Geometric Mean inequality* to obtain,

$$\frac{d}{dt}\frac{1}{2}\|\theta\|^2 \leq -\|\nabla\theta\|^2 + T_{2m}\|\mathbf{w}\|\|\nabla\theta\| \leq -\|\nabla\theta\|^2 + \frac{T_{2m}}{2\alpha_1}\|\mathbf{w}\|^2 + \frac{T_{2m}\alpha_1}{2}\|\nabla\theta\|^2 \; ,$$

where $\alpha_1 > 0$ is a constant to be chosen and T_{2m} is the maximum of T_2. Employing inequality (2.5.4) and choose $\alpha_1 = \frac{1}{T_{2m}}$ to obtain,

$$\frac{d}{dt}\frac{1}{2}\|\theta\|^2 \leq -\frac{1}{2}\|\nabla\theta\|^2 + \frac{1}{2}A_1\|\theta\|^2 + \frac{1}{2}B_1\|\phi\|^2 \; ,$$

which implies

$$\frac{d}{dt}\|\theta\|^2 \leq A_1\|\theta\|^2 + B_1\|\phi\|^2 \tag{2.5.5}$$

where $A_1 = 2T_{2m}^2 R^2 G^2$ and $B_1 = 2T_{2m}^2 R_s^2 G^2$.

Going through the same procedure, multiply equation $(2.5.1)_4$ by ϕ and integrate over Ω, to see

$$\begin{aligned}\frac{d}{dt}\frac{\epsilon_1}{2}\|\phi\|^2 = &- \|\nabla\phi\|^2 - Le\int_\Omega \frac{\partial}{\partial x_i}\left(\phi w_i C_2\right)dx + Le\int_\Omega \left(\phi w_{i,i} + \phi_{,i} w_i\right) C_2 dx \\ &+ l\left(T_1,\phi\right) + l_2\left(\theta,\phi\right) - h\left(C_1,\phi\right) - h_2\|\phi\|^2\end{aligned}$$

Applying the *Divergence Theorem* to the second term on the right and since $w_{i,i} = 0$ in Ω the third term is zero, then

$$\begin{aligned}\frac{d}{dt}\frac{\epsilon_1}{2}\|\phi\|^2 = &- \|\nabla\phi\|^2 - Le\oint_\Gamma \phi w_i n_i C_2 dA + Le\int_\Omega \phi_{,i} w_i C_2 dx \\ &+ l\left(T_1,\phi\right) + l_2\left(\theta,\phi\right) - h\left(C_1,\phi\right) - h_2\|\phi\|^2\end{aligned}$$

and since $w_i = 0$ on Γ, the second term is zero. So, we obtain

$$\begin{aligned}\frac{d}{dt}\frac{\epsilon_1}{2}\|\phi\|^2 = &- \|\nabla\phi\|^2 + Le\int_\Omega \phi_{,i} w_i C_2 dx + l\left(T_1,\phi\right) \\ &+ l_2\left(\theta,\phi\right) - h\left(C_1,\phi\right) - h_2\|\phi\|^2\end{aligned}$$

Making use of *Cauchy-Schwarz inequality*, we see

$$\begin{aligned}\frac{d}{dt}\frac{\epsilon_1}{2}\|\phi\|^2 \leq &- \|\nabla\phi\|^2 + LeC_{2m}\|\mathbf{w}\|\|\nabla\phi\| + l\|T_1\|\|\phi\| \\ &+ l_2\|\theta\|\|\phi\| + h\|C_1\|\|\phi\| + h_2\|\phi\|^2\end{aligned}$$

Using the *Arithmetic-Geometric Mean inequality* in addition to inequality (2.5.4), we find

$$\begin{aligned}\frac{d}{dt}\frac{\epsilon_1}{2}\|\phi\|^2 \leq &- \|\nabla\phi\|^2 + \frac{LeC_{2m}\alpha_2}{2}\|\nabla\phi\|^2 + \frac{LeC_{2m}R^2G^2}{\alpha_2}\|\theta\|^2 + \frac{LeC_{2m}R_s^2G^2}{\alpha_2}\|\phi\|^2 \\ &+ \frac{l\alpha_3}{2}\|\phi\|^2 + \frac{l}{2\alpha_3}\|T_1\|^2 + \frac{l_2\alpha_4}{2}\|\phi\|^2 + \frac{l_2}{2\alpha_4}\|\theta\|^2 \\ &+ \frac{h\alpha_5}{2}\|\phi\|^2 + \frac{h}{2\alpha_5}\|C_1\|^2 + h_2\|\phi\|^2\end{aligned}$$

where $\alpha_2,\ \alpha_3,\ \alpha_4,\ \alpha_5 > 0$ are constants to be chosen and C_{2m} is the maximum of C_2. If we choose $\alpha_2 = \frac{1}{LeC_{2m}}$, $\alpha_3 = \frac{2}{l}$, $\alpha_4 = \frac{2}{l_2}$ and $\alpha_5 = \frac{2}{h}$, then

$$\frac{d}{dt}\frac{\epsilon_1}{2}\|\phi\|^2 \leq -\frac{1}{2}\|\nabla\phi\|^2 + \frac{h^2}{4}\|C_1\|^2 + \frac{l^2}{4}\|T_1\|^2 + A_2\|\theta\|^2 + B_2\|\phi\|^2\ ,$$

where

$$A_2 = \frac{l_2^2}{4} + Le^2 C_{2m}^2 R^2 G^2$$

and

$$B_2 = 3 + h_2 + Le^2 C_{2m}^2 R_s^2 G^2$$

This implies that,

$$\frac{d}{dt}\epsilon_1 \|\phi\|^2 \leq \mu_1 \|\theta\|^2 + \mu_2 \|\phi\|^2 + k_1 h^2 + k_2 l^2 \ , \tag{2.5.6}$$

where $\mu_1 = 2A_2$, $\mu_2 = 2B_2$, $k_1 = \frac{\|C_1\|^2}{4}$, $k_2 = \frac{\|T_1\|^2}{4}$.
Next, add inequalities (2.5.5) and (2.5.6) to obtain

$$\frac{d}{dt}\left(\|\theta\|^2 + \epsilon_1 \|\phi\|^2\right) \leq k\left(\|\theta\|^2 + \epsilon_1 \|\phi\|^2\right) + k_3\left(h^2 + l^2\right) \ , \tag{2.5.7}$$

where $k_3 = max\left\{k_1, k_2\right\}$ and $k = max\left\{A_1 + \mu_1, B_1 + \mu_2\right\}$. Inequality (2.5.7) can be written as a differential inequality in the form

$$\frac{d}{dt}F - kF \leq k_3\left(h^2 + l^2\right) \ ,$$

where $F(t) = (\|\theta\|^2 + \epsilon_1 \|\phi\|^2)$. Upon integration, the solution will be

$$F(t) \leq \frac{k_3}{k}\left(e^{kt} - 1\right)\left(h^2 + l^2\right) \ on \ [0, \tau] \ . \tag{2.5.8}$$

Inequality (2.5.8) shows continuous dependence on the reaction terms, h and l , of θ and ϕ. To derive continuous dependence of $\mathbf{w}$, we have to employ inequality (2.5.8) in inequality (2.5.4) to see

$$\|\mathbf{w}\|^2 \leq k_4\left(\|\theta\|^2 + \epsilon_1 \|\phi\|^2\right) \leq \frac{k_4 k_3}{k}\left(e^{kt} - 1\right)\left(h^2 + l^2\right) \ on \ [0, \tau] \,, \tag{2.5.9}$$

where $k_4 = max\left\{2R^2G^2, 2R_s^2G^2\right\}$. Inequality (2.5.9) demonstrates continuous dependence also in the L^2 measure of $\mathbf{w}$.

Chapter 3

Structural Stability for Brinkman Convection With Reaction

3.1 Introduction

In this chapter we address the fundamental question of continuous dependence of the solution on the reaction rate but we allow the chemical equilibrium function to depend in an arbitrary way on the temperature field. We allow the saturated porous medium of a Brinkman type to occupy a bounded three-dimensional domain Ω, the boundary of which, Γ, is sufficiently smooth to allow application of the Divergence Theorem. This chapter may be considered as an extension or a generalization of chapter 2 in which we showed continuous dependence of the Darcy and/or the Brinkman convection on reaction *but* the chemical equilibrium was a linear function in temperature. Moreover, here we follow a different route to study the continuous dependence on reaction for the Brinkman convection problem due to the Brinkman term and the route is not applicable for the Darcy.

3.2 Basic Equations

The equations we adopt in this chapter are the Brinkman equation with the density in the buoyancy force depending on the temperature, the conservation of mass, the energy balance and the conservation of solute equation. Let $\mathbf{x} \in \Omega$ and let t denote

time, where $0 < t < \tau$ for some $\tau < \infty$ and then, without loss of generality for the problem in hand, these equations may be written as

$$\begin{aligned} \frac{\partial p}{\partial x_i} &= g_i T - h_i C - v_i + \lambda \Delta v_i, \\ \frac{\partial v_i}{\partial x_i} &= 0, \\ \frac{\partial T}{\partial t} + v_i \frac{\partial T}{\partial x_i} &= \Delta T, \\ a\frac{\partial C}{\partial t} + b v_i \frac{\partial C}{\partial x_i} &= \Delta C + L f(T) - KC, \end{aligned} \tag{3.2.1}$$

where $v_i(\mathbf{x}, t)$, $p(\mathbf{x}, t)$, $T(\mathbf{x}, t)$ and $C(\mathbf{x}, t)$ denote the velocity, pressure, temperature and solute concentration, respectively. In equations(3.2.1) g_i and h_i represent gravity functions, $\lambda > 0$ is the Brinkman coefficient, a, b are positive constants as are L and K and $f(T)$ is a known function of temperature which is bounded and differentiable for T bounded. The term $Lf(T)$ is denoted as a chemical equilibrium function, C_{eq}, in Pritchard & Richardson [83], Wang & Tan [124], and in Malashetty & Biradar [60]. Equations(3.2.1) are assumed to hold on the domain $\Omega \times (0, \tau)$ while on the boundary

$$v_i(\mathbf{x}, t) = 0, \ T = T_B(\mathbf{x}, t), \ C = C_B(\mathbf{x}, t) \tag{3.2.2}$$

on $\Gamma \times [0, \tau)$, where T_B and C_B are known functions. Equations (3.2.1) are also subject to the initial conditions

$$T(\mathbf{x}, 0) = T_0(\mathbf{x}), \ C(\mathbf{x}, 0) = C_0(\mathbf{x}), \tag{3.2.3}$$

$\mathbf{x} \in \Omega$, where T_0 and C_0 are given. The boundary-initial value problem comprised of (3.2.1), (3.2.2) and (3.2.3) will be denoted by P. In addition we suppose, without loss of generality, that

$$|\mathbf{g}| \leq 1 \ , \ |\mathbf{h}| \leq 1 \ . \tag{3.2.4}$$

For a general derivation of equations not dissimilar to (3.2.1), employing contemporary methods of continuum thermodynamics, the reader may wish to consult Morro & Straughan [68], or the interesting recent papers involving phase changes of Berti *et al.* [12], Berti *et al.* [11], Bonetti *et al.* [13], and Fabrizio *et al.* [27–29].

In many cases the reaction rates L and K are closely linked. However, we here treat the general case and so to study continuous dependence of the solution to (3.2.1),

(3.2.2) and (3.2.3) we suppose (u_i, p_1, T_1, C_1) and (v_i, p_2, T_2, C_2) are solutions to the boundary-initial value problem P for the same constants g_i, h_i, λ, a and b and for the same functions f, T_B, C_B, T_0 and C_0, but for different reaction coefficients L_1, K_1 and L_2, K_2, respectively. We define the difference variables w_i, π, θ and ϕ by

$$\begin{aligned} &w_i = u_i - v_i \ , \ \pi = p_1 - p_2, \\ &\theta = T_1 - T_2 \ , \ \phi = C_1 - C_2, \\ &l = L_1 - L_2 \ , \ k = K_1 - K_2. \end{aligned} \tag{3.2.5}$$

From equations (3.2.1)-(3.2.3) one determines the equations governing the variables (w_i, π, θ, ϕ) to be

$$\begin{aligned} &\frac{\partial \pi}{\partial x_i} = g_i\theta - h_i\phi - w_i + \lambda \Delta w_i, \\ &\frac{\partial w_i}{\partial x_i} = 0, \\ &\frac{\partial \theta}{\partial t} + u_i \frac{\partial \theta}{\partial x_i} + w_i \frac{\partial T_2}{\partial x_i} = \Delta\theta, \\ &a\frac{\partial \phi}{\partial t} + bu_i \frac{\partial \phi}{\partial x_i} + bw_i \frac{\partial C_2}{\partial x_i} = \Delta\phi + L_1\left[f(T_1) - f(T_2)\right] + lf(T_2) - K_1\phi - kC_2, \end{aligned} \tag{3.2.6}$$

on $\Omega \times (0, \tau)$, together with

$$w_i = 0 \ , \ \theta = 0 \ , \ \phi = 0, \tag{3.2.7}$$

on $\Gamma \times [0, \tau)$, and

$$\theta = 0 \ , \ \phi = 0, \tag{3.2.8}$$

for $\mathbf{x} \in \Omega$, at $t = 0$.

We wish to derive estimates which show that a suitable measure of w_i, θ and ϕ is bounded in a precise sense by a function of l and k, with the coefficients in the bound being truly *a priori* in that they depend only on τ and the boundary and initial data of the problem. Before proceeding to this goal we must derive some *a priori* estimates for the solution to equations (3.2.1), (3.2.2) and (3.2.3).

3.3 A priori Estimates

Let $\|\cdot\|_\infty$ denote the $L^\infty(\Omega)$ norm and define

$$T_m = max\left\{\|T_0\|_\infty, sup_{[0,\tau]}\|T_B\|_\infty\right\}. \tag{3.3.1}$$

then one may employ the function

$$\tilde{\psi} = [T - T_m]^+ = sup\,(T - T_m, 0)\,,$$

cf. Payne *et al.* [77] to establish that

$$sup_{\Omega\times[0,\tau]}|T(\mathbf{x},t)| \leq T_m, \tag{3.3.2}$$

where T is the temperature function in equations (3.2.1)-(3.2.3).

Let $\|\cdot\|$ and $(\cdot,\cdot)$ denote the norm and inner product in $L^2(\Omega)$ and let $\|\cdot\|_4$ denote the norm on $L^4(\Omega)$. We require *a priori* bounds for $\|C\|$, $\|C\|_4$ and $\int_0^t \|\nabla C\|^2 ds$ and now proceed to derive these. To progress with bounds for the function C in equations (3.2.1)-(3.2.3) we introduce auxiliary functions $H(\mathbf{x},t)$ and $I(\mathbf{x},t)$ which satisfy the boundary value problems

$$\begin{aligned} &\Delta H = 0\ ,\ in\ \Omega, \\ &H = C_B(\mathbf{x},t)\ ,\ on\ \Gamma \end{aligned} \tag{3.3.3}$$

and

$$\begin{aligned} &\Delta I = 0\ ,\ in\ \Omega, \\ &I = C_B^3(\mathbf{x},t)\ ,\ on\ \Gamma. \end{aligned} \tag{3.3.4}$$

We begin by forming from equation $(3.2.1)_4$ the identity

$$\begin{aligned} &a\int_0^t (C_{,s}, C-H)\,ds + b\int_0^t (v_i C_{,i}, C-H)\,ds \\ &= \int_0^t (\Delta C, C-H)\,ds + L\int_0^t (f(T), C-H)\,ds - K\int_0^t (C, C-H)\,ds. \end{aligned} \tag{3.3.5}$$

Denote the terms in this expression by $I_1 - I_5$ and then one may show after integration by parts

$$I_1 = \frac{a}{2}\left(\|C\|^2 - \|C_0\|^2\right) - a\,(H,C) + a\,(H_0,C_0) + a\int_0^t (C, H_{,s})\,ds, \tag{3.3.6}$$

where $H_0 = H(\mathbf{x},0)$.

$$I_2 = b\int_0^t (v_i C_{,i}, C)ds + -b\int_0^t (v_i C_{,i}, H)\,ds, \tag{3.3.7}$$

using the *Divergence Theorem* the first term integrated to zero and from the maximum principle the maximum of H in $\Omega\times[0,\tau]$ exists, say H_m, then using the Cauchy-Schwarz inequality

$$I_2 = -b\int_0^t (v_i C_{,i}, H)\,ds \leq H_m b\sqrt{\int_0^t \|\mathbf{v}\|^2 ds \int_0^t \|\nabla C\|^2 ds}. \tag{3.3.8}$$

Multiply equation $(3.2.1)_1$ by v_i and integrate over Ω to find after use of the Arithmetic-Geometric Mean inequality,

$$\|\mathbf{v}\|^2 + \lambda\|\nabla\mathbf{v}\|^2 \leq \frac{1}{2\alpha}\|T\|^2 + \frac{1}{2\beta}\|C\|^2 + \left(\frac{\alpha}{2} + \frac{\beta}{2}\right)\|\mathbf{v}\|^2$$

for $\alpha, \beta > 0$ at our disposal. Pick $\alpha = \beta = 1/2$ and then we find

$$\frac{1}{2}\|\mathbf{v}\|^2 + \lambda\|\nabla\mathbf{v}\|^2 \leq \|T\|^2 + \|C\|^2. \tag{3.3.9}$$

Use of this in inequality (3.3.8) allows one to show

$$I_2 \leq \sqrt{2}bH_m\sqrt{\int_0^t (\|T\|^2 + \|C\|^2)\, ds \int_0^t \|\nabla C\|^2 ds}. \tag{3.3.10}$$

After some integration by parts I_3 may be manipulated to derive

$$\begin{aligned}
I_3 =& -\int_0^t \|\nabla C\|^2 ds + \int_0^t \oint_\Gamma C\frac{\partial C}{\partial n} dA ds - \int_0^t (\Delta C, H)\, ds \\
=& -\int_0^t \|\nabla C\|^2 ds + \int_0^t \oint_\Gamma C\frac{\partial C}{\partial n} dA ds \\
& - \int_0^t \int_\Omega \frac{\partial}{\partial x_i}\left(\frac{\partial C}{\partial x_i} H\right) dx ds + \int_0^t \int_\Omega \frac{\partial C}{\partial x_i}\frac{\partial H}{\partial x_i} dx ds \\
=& -\int_0^t \|\nabla C\|^2 ds + \int_0^t \oint_\Gamma C_B \frac{\partial C}{\partial n} dA ds - \int_0^t \oint_\Gamma \frac{\partial C}{\partial n} C_B dA ds \\
& + \int_0^t \int_\Omega \frac{\partial}{\partial x_i}(CH_{,i})\, dx ds - \int_0^t \int_\Omega CH_{,ii} dx ds \\
=& -\int_0^t \|\nabla C\|^2 ds + \int_0^t \oint_\Gamma C_B \frac{\partial H}{\partial n} dA ds.
\end{aligned} \tag{3.3.11}$$

The term I_4 is bounded with the aid of the Cauchy-Schwarz inequality to see that

$$I_4 \leq L\int_0^t \|f(T)\|^2 ds + \frac{L}{2}\int_0^t \|C\|^2 ds + \frac{L}{2}\int_0^t \|H\|^2 ds. \tag{3.3.12}$$

Finally, for I_5 we have

$$I_5 \leq -K\int_0^t \|C\|^2 ds + \frac{K}{2\gamma}\int_0^t \|C\|^2 ds + \frac{K\gamma}{2}\int_0^t \|H\|^2 ds. \tag{3.3.13}$$

Now f is known and T is bounded as in (3.3.2). Thus, $\int_0^t \|f(T)\|^2 ds$ may be bounded by data (T_m). The terms in (3.3.6)-(3.3.13) in H, $H_{,s}$ and $\partial H/\partial n$ are bounded in terms of C_B by using (1.1.7) and (1.1.9). Thus, combining (3.3.6)-(3.3.13) in (3.3.5)

we may arrive at an inequality of form

$$\begin{aligned}\frac{a}{2}\|C\|^2+\int_0^t\|\nabla C\|^2ds\leq&\frac{D_1(t)}{2}+\frac{a}{2\mu_1}\|C\|^2+\frac{a}{2\mu_2}\int_0^t\|C\|^2ds\\&+\frac{bH_m}{\sqrt{2}\mu_3}\int_0^t\|C\|^2ds+\frac{bH_m\mu_3}{\sqrt{2}}\int_0^t\|\nabla C\|^2ds\\&+\frac{L}{2}\int_0^t\|C\|^2ds-K\int_0^t\|C\|^2ds+\frac{K}{2\gamma}\int_0^t\|C\|^2ds,\end{aligned}\tag{3.3.14}$$

for $\mu_1,\mu_2,\mu_3,\gamma>0$ at our disposal and where $D_1(t)$ is a data term. We pick $\gamma=1/2$, $\mu_1=2$, $\mu_3=1/\sqrt{2}bH_m$ and then from (3.3.14) we obtain

$$\frac{a}{2}\|C\|^2+\int_0^t\|\nabla C\|^2ds\leq D_1(t)+\left(\frac{a}{\mu_2}+L+2b^2H_m^2\right)\int_0^t\|C\|^2ds.\tag{3.3.15}$$

and

$$\begin{aligned}D_1=&2a\|C_0\|^2+a\psi_1\oint_\gamma C_{0B}^2dA+2b^2H_m^2\int_0^t\|T\|^2ds\\&+\int_0^t\oint_\Gamma C_B^2dAds+2L\int_0^t\|f(T)\|^2ds+2a\psi_1\oint_\Gamma C_B^2dA\\&+a\mu_2\psi_1\int_0^t\oint_\Gamma C_{B,s}^2dAds+\left(L+\frac{K}{2}\right)\psi_1\int_0^t\oint_\Gamma C_B^2dAds\\&+\frac{c_2}{c_1}\int_0^t\oint_\Gamma|\nabla_sC_B|^2dAds,\end{aligned}$$

we may integrate inequality (3.3.15) to derive

$$\int_0^t\|C(s)\|^2ds\leq\int_0^te^{\zeta_1(t-s)}D_2(s)ds,\tag{3.3.16}$$

where $D_2=2D_1/a$ and $\zeta_1=\frac{2}{\mu_2}+\frac{2L}{a}+\frac{4b^2H_m^2}{a}$. Then from (3.3.16) and (3.3.15) we find

$$\int_0^t\|\nabla C\|^2ds\leq D_3(t),\tag{3.3.17}$$

where D_3 is the data term

$$D_3=D_1+\left(\frac{a}{\mu_2}+L+2b^2H_m^2\right)\int_0^te^{\zeta_1(t-s)}D_2(s)ds,$$

together with

$$\|C(t)\|^2\leq D_2(t)+\zeta_1\int_0^te^{\zeta_1(t-s)}D_2(s)ds\equiv D_4(t).\tag{3.3.18}$$

Inequalities (3.3.16), (3.3.17) and (3.3.18) furnish data bounds (truly *a priori* bounds) for $\|C\|^2$, $\int_0^t\|C\|^2ds$ and $\int_0^t\|\nabla C\|^2ds$. It remains to bound $\|C\|_4$.

Now commence with equation $(3.2.1)_4$ and form the following identity,

$$\begin{aligned} a\int_0^t \left(C_{,s}\ ,\ C^3 - I\right) ds + b\int_0^t \left(v_i C_{,i}\ ,\ C^3 - I\right) ds \\ = \int_0^t \left(\Delta C\ ,\ C^3 - I\right) ds + L\int_0^t \left(f(T)\ ,\ C^3 - I\right) ds \\ - K\int_0^t \left(C\ ,\ C^3 - I\right) ds. \end{aligned} \tag{3.3.19}$$

Recall the definition of I in (3.3.4) and we follow a similar procedure to that leading to inequality (3.3.14) except we now employ Young's inequality to the term involving fC^3. Denote the terms in (3.3.19) by $r_1 - r_5$ and then one may show after integration by parts

$$\begin{aligned} r_1 &= \frac{a}{4}\|C\|_4^4 - \frac{a}{4}\|C_0\|_4^4 - a\int_0^t (C_{,s}, I)\, ds \\ &= \frac{a}{4}\|C\|_4^4 - \frac{a}{4}\|C_0\|_4^4 - a\,(C, I) + a\,(C_0, I_0) + a\int_0^t (C, I_{,s})\, ds, \end{aligned} \tag{3.3.20}$$

where $I_0 = I(\mathbf{x}, 0)$. From the maximum principle the maximum of I in $\Omega \times [0, \tau]$ exists, say I_m, then using the Cauchy-Schwarz inequality

$$r_2 = -b\int_0^t \int_\Omega v_i C_{,i} I dx ds \leq I_m b \sqrt{\int_0^t \|\mathbf{v}\|^2 ds \int_0^t \|\nabla C\|^2 ds}$$

Use of inequality (3.3.9) allows one to show

$$r_2 \leq \sqrt{2} I_m b \sqrt{\int_0^t \left(\|T\|^2 + \|C\|^2\right) ds \int_0^t \|\nabla C\|^2 ds}. \tag{3.3.21}$$

After some integration by parts r_3 may be manipulated to derive

$$\begin{aligned} r_3 &= \int_0^t \int_\Omega C^3 \Delta C dx ds - \int_0^t \int_\Omega I \Delta C dx ds \\ &= \int_0^t \int_\Omega \left[\nabla\left(C^3 \nabla C\right) - 3(C\nabla C)^2\right] dx ds - \int_0^t \int_\Omega I \Delta C dx ds \\ &= \int_0^t \oint_\Gamma C^3 \frac{\partial C}{\partial n} dA ds - \frac{3}{4}\int_0^t \|\nabla C^2\|^2 ds \\ &\quad - \int_0^t \int_\Omega \left[\nabla(I\nabla C) - (\nabla I \nabla C)\right] dx ds \\ &= \int_0^t \oint_\Gamma C^3 \frac{\partial C}{\partial n} dA ds - \frac{3}{4}\int_0^t \|\nabla C^2\|^2 ds - \int_0^t \oint_\Gamma I \frac{\partial C}{\partial n} dA ds \\ &\quad + \int_0^t \int_\Omega \nabla(C\nabla I) dx ds - \int_0^t \int_\Omega C \Delta I dx ds \\ &= -\frac{3}{4}\int_0^t \|\nabla C^2\|^2 ds + \int_0^t \oint_\Gamma C_B \frac{\partial I}{\partial n} dA ds \end{aligned} \tag{3.3.22}$$

The term r_4 is bounded with the aid of Young's inequality, Cauchy-Schwarz inequality and the Arithmetic-Geometric mean inequality to see that

$$r_4 \leq \frac{L}{4\varepsilon^4}\int_0^t \|f(T)\|_4^4 ds + \frac{3L\varepsilon^{4/3}}{4}\int_0^t \|C\|_4^4 ds + \frac{L}{2}\int_0^t \|f(T)\|^2 ds + \frac{L}{2}\int_0^t \|I\|^2 ds \tag{3.3.23}$$

Finally, for r_5 we have

$$r_5 \leq -K\int_0^t \|C\|_4^4 ds + \frac{K}{2}\int_0^t \|C\|^2 ds + \frac{K}{2}\int_0^t \|I\|^2 ds \tag{3.3.24}$$

Thus, combining (3.3.20)-(3.3.24) in (3.3.19) we may arrive at the inequality

$$\begin{aligned}
&\frac{a}{4}\|C\|_4^4 + \int_0^t \|\nabla C^2\|^2 ds + K\int_0^t \|C\|_4^4 ds \\
\leq &\frac{a}{4}\|C_0\|_4^4 - a(I_0, C_0) + \frac{I_m b}{2\lambda_1}\int_0^t \left(\|T\|^2 + \|C\|^2\right) ds \\
&+ \frac{I_m b}{2\lambda_1}\int_0^t \|\nabla C\|^2 ds + \int_0^t \oint_\Gamma C_B \frac{\partial I}{\partial n} dA ds \\
&+ \frac{L}{4\varepsilon^4}\int_0^t \|f(T)\|_4^4 ds + \frac{3L\varepsilon^{4/3}}{4}\int_0^t \|C\|_4^4 ds \\
&+ \frac{K}{2}\int_0^t \|C\|^2 ds + \left(\frac{K+L}{2}\right)\int_0^t \|I\|^2 ds \\
&+ \frac{L}{2}\int_0^t \|f(T)\|^2 ds + a\|I\|\|C\| \\
&+ a\sqrt{\int_0^t \|I_{,s}\| ds \int_0^t \|C\|^2 ds}\ ,
\end{aligned} \tag{3.3.25}$$

for $\varepsilon > 0$ and $\lambda_1 > 0$ to be chosen. Since we have data bounds for $\|T\|$, $\|C\|$, $\int_0^t \|\nabla C\|^2 ds$, we know C_0 and C_B, and $\|I\|$ and $\int_0^t \oint_\Gamma \left(\frac{\partial I}{\partial n}\right) dA ds$ may be estimated in terms of C_B by using *lemmas 1 and 2*, we may choose $\varepsilon = (4(K+1)/3L)^{3/4}$ and then inequality (3.3.25) furnishes directly a data bound for $\|C\|_4$ and also for $\int_0^t \|\nabla C^2\|^2 ds$. Thus, employing *lemmas 1 and 2* together with (3.3.16)-(3.3.18) and (3.3.2) we may derive data functions $D_5(t)$, $D_6(t)$ and $D_7(t)$ such that from inequality (3.3.25)

$$\int_0^t \|C\|_4^4 ds \leq \int_0^t e^{\frac{4}{a}(t-s)} D_5(t) ds\ , \tag{3.3.26}$$

$$\|C(t)\|_4^4 \leq D_5(t) + \frac{4}{a}\int_0^t e^{\frac{4}{a}(t-s)} D_5(t) ds \equiv D_6(t)\ , \tag{3.3.27}$$

and

$$\int_0^t \|\nabla C^2\|^2 ds \leq \frac{a}{4} D_5(t) + \int_0^t e^{\frac{4}{a}(t-s)} D_5(t) ds \equiv D_7(t). \tag{3.3.28}$$

3.4 Continuous Dependence on the Reaction

We firstly multiply equation $(3.2.6)_1$ by w_i and integrate over Ω using the boundary conditions to see that

$$\|\mathbf{w}\|^2 + \lambda\|\nabla\mathbf{w}\|^2 = (g_i\theta, w_i) - (h_i\phi, w_i)\,.$$

After using the Cauchy-Schwarz and Arithmetic-Geometric Mean inequalities on the right hand side we may then deduce that

$$\frac{1}{2}\|\mathbf{w}\|^2 + \lambda\|\nabla\mathbf{w}\|^2 \leq \|\theta\|^2 + \|\phi\|^2. \tag{3.4.1}$$

Next, multiply equation $(3.2.6)_3$ by θ and integrate over Ω to find after using the boundary conditions and $(3.2.6)_2$,

$$\begin{aligned}\frac{d}{dt}\frac{1}{2}\|\theta\|^2 &= -\|\nabla\theta\|^2 + \int_\Omega T_1 w_i \theta_{,i} dx \\ &\leq \frac{T_m^2}{4}\|\mathbf{w}\|^2 \\ &\leq \frac{T_m^2}{2}\left(\|\theta\|^2 + \|\phi\|^2\right)\end{aligned} \tag{3.4.2}$$

where (3.3.2) and (3.4.1) have been employed.

The next step is to form the inner product on $L^2(\Omega)$ of ϕ with equation $(3.2.6)_4$. Upon using the boundary conditions we find

$$\begin{aligned}\frac{d}{dt}\frac{a}{2}\|\phi\|^2 =& -\|\nabla\phi\|^2 + L_1\left(f(T_1) - f(T_2), \phi\right) \\ &+ l\left(f(T_2), \phi\right) - K_1\|\phi\|^2 - k\left(C_2, \phi\right) \\ &+ b\int_\Omega w_i C_2 \phi_{,i} dx\ .\end{aligned} \tag{3.4.3}$$

Using Lagrange's Theorem $f(T_1) - f(T_2) = f'(\xi)\theta$ for some $\xi \in (T_1, T_2)$ and then from (3.4.3) we may obtain

$$\begin{aligned}\frac{d}{dt}\frac{a}{2}\|\phi\|^2 \leq& -\|\nabla\phi\|^2 + L_1\left(f'(\xi)\theta, \phi\right) \\ &+ \frac{\|\phi\|^2}{2} + l^2\frac{\|f(T_2)\|^2}{2} + k^2\frac{\|C_2\|^2}{4K_1} \\ &+ \frac{b}{2\mu}\|\nabla\phi\|^2 + \frac{b\mu}{2}\|\mathbf{w}\|_4^2\|C_2\|_4^2\ ,\end{aligned} \tag{3.4.4}$$

for $\mu > 0$ at our disposal. From the Sobolev inequality, see *e.g.* Gilbarg & Trudinger [37], there is a constant $\xi_1 > 0$ depending on Ω such that

$$\|\mathbf{w}\|_4 \leq \xi_1\|\nabla\mathbf{w}\| \tag{3.4.5}$$

and we employ this on the last term on the right of (3.4.4), so that

$$\frac{b\mu}{2}\|\mathbf{w}\|_4^2\|C_2\|_4^2 \leq \frac{b\mu}{2}\xi_1^2\|\nabla\mathbf{w}\|^2\|C_2\|_4^2 \,. \tag{3.4.6}$$

Pick now $\mu = b/2$ and then from (3.4.4) and (3.4.6) we obtain

$$\begin{aligned}\frac{d}{dt}\frac{a}{2}\|\phi\|^2 \leq & L_1\left(f'(\xi)\theta,\phi\right) + \frac{\|\phi\|^2}{2} \\ & + l^2\frac{\|f(T_2)\|^2}{2} + k^2\frac{\|C_2\|^2}{4K_1} \\ & + \frac{b^2\xi_1^2}{4}\|\nabla\mathbf{w}\|^2\|C_2\|_4^2 \,.\end{aligned} \tag{3.4.7}$$

Since T is bounded it follows ξ is bounded and since we know also $f'(\xi)$ this is likewise *a priori* bounded, say by f_1, on $\Gamma\times[0,\tau]$. Likewise from (3.3.18) and (3.3.27), $\|C_2\|$ and $\|C_2\|_4$ are also *a priori* bounded on $\Omega\times[0,\tau]$. Thus, we may add (3.4.2) and (3.4.7) and use (3.4.1) to see

$$\begin{aligned}\frac{d}{dt}\left(\|\theta\|^2+\|\phi\|^2\right) \leq & T_m^2\|\theta\|^2 + T_m^2\|\phi\|^2 + \frac{2}{a}L_1f_1\|\theta\|^2 \\ & + \frac{2}{a}L_1f_1\|\phi\|^2 + \frac{\|\phi\|^2}{a} + \frac{l^2}{a}\|f(T_2)\|^2 \\ & + \frac{k^2}{2aK_1}\|C_2\|^2 + \frac{b^2\xi_1^2}{2a\lambda}\|C_2\|_4^2\left(\|\theta\|^2+\|\phi\|^2\right),\end{aligned}$$

This means that there are functions $d_1(t)$ and $d_2(t)$ which depend only on the data, Ω and Γ, such that

$$\frac{d}{dt}\left(\|\theta\|^2+\|\phi\|^2\right) \leq \delta_1\|\theta\|^2 + \delta_2\|\phi\|^2 + d_1k^2 + d_2l^2 \,. \tag{3.4.8}$$

Put $\delta = max\left\{\delta_1,\delta_2\right\}$ and then we may integrate inequality (3.4.8) to derive

$$\begin{aligned}\|\theta(t)\|^2+\|\phi(t)\|^2 \leq & \left(\int_0^t e^{\delta(t-s)}d_1(s)ds\right)k^2 \\ & + \left(\int_0^t e^{\delta(t-s)}d_2(s)ds\right)l^2 \,.\end{aligned} \tag{3.4.9}$$

Inequality (3.4.9) demonstrate continuous dependence on the reaction rates k and l and is truly *a priori* in the sense that d_1 and d_2 depend only on data. By employing inequality (3.4.1) one may directly obtain an *a priori* continuous dependence estimate in the measure of $\|\mathbf{w}(\mathbf{t})\|$ or $\|\nabla\mathbf{w}(\mathbf{t})\|$,

$$\frac{1}{2}\|\mathbf{w}\|^2 + \lambda\|\nabla\mathbf{w}\|^2 \leq \left(\int_0^t e^{\delta(t-s)}d_1(s)ds\right)k^2 + \left(\int_0^t e^{\delta(t-s)}d_2(s)ds\right)l^2 \,.$$

Chapter 4

The Energy Stability of Darcy Thermosolutal Convection with Reaction

4.1 Introduction

The work in this chapter may be considered as an extension of the work of Pritchard & Richardson [83]. We use the energy method to study the nonlinear energy stability of the Darcy convection model with reaction, where the system is either heated below and salted above or heated and salted below. The aim of this study is to discuss how the onset of thermosolutal convection varies with the reaction terms. Considering a porous medium of Darcy type occupying a bounded three-dimensional domain, we derive a perturbed dimensionless model of double-diffusive convection with reaction. Then we carry out a nonlinear stability analysis by using the energy method and we implement the D^2 Chebyshev Tau technique to solve the system. The reason behind using the energy method is because the linear instability boundary specifies the space where the solution is unstable, using the energy theory we obtain the nonlinear stability boundary below which the solution is globally stable. By globally stable we mean that the solution is stable for all initial perturbations.

4.2 Basic Equations

We consider a layer of porous porous medium saturated by a fluid, bounded by two parallel planes with distance d between them. We will carry out the analysis of two cases of the layers of porous media, heated from below, salted from above and heated and salted from below. Our model consists of Darcy equation with the density in the buoyancy term depends linearly on the temperature T and salt concentration C, the continuity equation, the advection-diffusion equation for the transport of heat and the equation for the transport of solute with reaction terms,

$$\begin{aligned} p_{,i} &= -\frac{\mu}{K}v_i - \rho_0[1-\alpha_T(T-T_0)+\alpha_C(C-C_0)]gk_i, \\ v_{i,i} &= 0, \\ \frac{1}{M}T_{,t} + v_iT_{,i} &= k_T\Delta T, \\ \hat{\phi}C_{,t} + v_iC_{,i} &= \hat{\phi}k_C\Delta C + \hat{k}[f_1(T-T_0)+f_0-C]. \end{aligned} \tag{4.2.1}$$

Where v_i, p, T, C are the velocity, pressure, temperature and salt concentration fields respectively, K is the matrix permeability, μ is the fluid viscosity, ρ_0 is the fluid density, and k_C and k_T are the molecular diffusivity of the solute through the fluid and the effective diffusivity of the heat through the saturated medium. The quantity M is the ratio of the heat capacity of the fluid to the heat capacity of the medium, $\hat{\phi}$ is the matrix porosity, $\hat{k}$ is the reaction coefficient and $f_0 + f_1(T-T_0) = C_{eq}(T)$ in Pritchard and Richardson [83] and Wang and Tan [124], where f_0, f_1 and T_0 are constants. Moreover, g is the gravity, $\mathbf{k} = (0,0,1)$ and α_T and α_C are the thermal and solutal expansion coefficients respectively. The fluid occupying a horizontal layer $(x,y) \in \mathcal{R}^2, z \in (0,d)$ and the equations (4.2.1) are taken in the domain $\mathcal{R}^2 \times (0,d) \times \{t>0\}$. The boundary conditions are

$$\begin{aligned} &v_in_i = 0 \ on \ z = 0,d, \\ &T = T_L \ on \ z = 0, \quad T = T_U \ on \ z = d, \\ &C = C_L \ on \ z = 0, \quad C = C_U \ on \ z = d, \end{aligned} \tag{4.2.2}$$

with $T_L > T_U$ since our system is heated below, where T_L, T_U, C_L, C_U all constants. For the salted above porous medium $C_U > C_L$ while $C_L > C_U$ for the salted below case. The steady solution to (4.2.1) which we are interested in studying its stability

and which satisfies (4.2.2) is

$$\begin{aligned} \bar{v}_i &= 0, \\ \bar{T}(z) &= -\beta_T z + T_L, \\ \bar{C}(z) &= -\beta_C z + C_L, \end{aligned} \tag{4.2.3}$$

where β_T and β_C are the temperature and salt gradients given by

$$\beta_T = \frac{T_L - T_U}{d} \ , \ \beta_C = \frac{C_L - C_U}{d}.$$

To analyse the stability of the solutions(4.2.3) we define perturbations (u_i, π, θ, ϕ) such that $v_i = \bar{v}_i + u_i,\ p = \bar{p} + \pi,\ T = \bar{T} + \theta,\ C = \bar{C} + \phi$. Using these perturbations in equations (4.2.1) we derive the equations governing (u_i, π, θ, ϕ) as

$$\begin{aligned} \pi_{,i} &= -\frac{\mu}{K} u_i + \rho_0 g k_i \alpha_T \theta - \rho_0 g k_i \alpha_C \phi \ , \\ u_{i,i} &= 0 \ , \\ \frac{1}{M}\theta_{,t} + u_i \theta_{,i} &= \beta_T w + k_T \Delta\theta \ , \\ \hat{\phi}\phi_{,t} + u_i \phi_{,i} &= \beta_C w + \hat{\phi} k_C \Delta\phi + \hat{k} f_1 \theta - \hat{k}\phi, \end{aligned} \tag{4.2.4}$$

where $w = u_3$. We define the length, time and velocity scales L, τ and U by $L = d,\ \tau = d/MU,\ U = k_T/d$, to non-dimensionalize equations (4.2.4). Then we introduce pressure, temperature and salt scales as

$$P = \frac{Ud\mu}{K} \ , \ T^{\sharp^2} = \frac{\mu\beta_T k_T}{\alpha_T \rho_0 g K} \ , \ C^{\sharp^2} = \frac{\mu\beta_C k_T Le}{\alpha_C \rho_0 g K \hat{\phi}},$$

where $Le = k_T/k_C$ is the Lewis number. The temperature Rayleigh number and the salt Rayleigh number are defined as

$$R = \sqrt{\frac{\beta_T d^2 K \alpha_T \rho_0 g}{k_T \mu}} \ ,$$

$$R_s = \sqrt{\frac{\beta_C d^2 K \alpha_C \rho_0 g Le}{\hat{\phi} k_T \mu}} \ \ when\ C_L > C_U \ \ or \ \ R_s = \sqrt{\frac{|\beta_C| d^2 K \alpha_C \rho_0 g Le}{\hat{\phi} k_T \mu}} \ \ when\ C_L < C_U.$$

Then, the fully nonlinear, non-dimensional form of (4.2.4) is

$$\begin{aligned} \pi_{,i} &= -u_i + R k_i \theta - R_s k_i \phi \ , \\ u_{i,i} &= 0 \ , \\ \theta_{,t} + u_i \theta_{,i} &= R w + \Delta\theta \ , \\ \varepsilon\phi_{,t} + \frac{Le}{\hat{\phi}} u_i \phi_{,i} &= \mp R_s w + \Delta\phi + h\theta - \eta\phi \ , \end{aligned} \tag{4.2.5}$$

where $\varepsilon = MLe$ and h and η are the reaction terms

$$h = \frac{\hat{k} f_1 d^2 T^\sharp}{\hat{\phi} k_C C^\sharp} \quad and \quad \eta = \frac{\hat{k} d^2}{\hat{\phi} k_C}.$$

Moreover, $+R_s$ is taken when $C_L > C_U (i.e.\ \beta_C > 0)$, which means that the system is salted from below, and $-R_s$ is taken when $C_L < C_U (i.e.\ \beta_C < 0)$, which means that the system is salted from above. The boundary conditions becomes

$$w = \theta = \phi = 0 \ on \ z = 0 \ and \ z = 1 \ . \tag{4.2.6}$$

4.3 The Linear Instability Analysis

In order to study the linear instability of the system (4.2.5) we neglect the nonlinear terms of the system and we take the third component of the double curl of equation $(4.2.5)_1$, so equation $(4.2.5)_1$ will be

$$0 = -(u_{j,ij} - \Delta u_i) + R(k_j \theta_{,ij} - k_i \Delta\theta) - R_s(k_j \phi_{,ij} - k_i \Delta\phi) \ , \tag{4.3.1}$$

using $(4.2.5)_2$ and then taking the third component, *i.e.* take $i = 3$, equation (4.3.1) will be

$$0 = \Delta w - R\Delta^* \theta + R_s \Delta^* \phi \ , \tag{4.3.2}$$

where $\Delta^* = \frac{\partial^2}{\partial x^2} + \frac{\partial^2}{\partial y^2}$. The linearized system of equations is

$$\begin{aligned} \Delta w - R\Delta^* \theta + R_s \Delta^* \phi &= 0 \ , \\ \theta_{,t} &= Rw + \Delta\theta \ , \\ \varepsilon \phi_{,t} &= \mp R_s w + \Delta\phi + h\theta - \eta\phi. \end{aligned} \tag{4.3.3}$$

Because this is linear, we consider a perturbation to the solution to (4.3.3) of the form

$$\begin{aligned} \theta &= e^{\sigma t}\theta(x_i) = e^{\sigma t}\Theta(z) f(x,y) = e^{\sigma t}\Theta_0 e^{ilx+imy} sin(n\pi z) \ , \\ w &= e^{\sigma t} w(x_i) = e^{\sigma t} W(z) f(x,y) = e^{\sigma t} W_0 e^{ilx+imy} sin(n\pi z) \ , \\ \phi &= e^{\sigma t}\phi(x_i) = e^{\sigma t}\Phi(z) f(x,y) = e^{\sigma t}\Phi_0 e^{ilx+imy} sin(n\pi z) \ , \end{aligned} \tag{4.3.4}$$

where σ is the growth rate. The terms in (4.3.4) are referred to as a Fourier modes. The full solution will be a combination of modes. Since it is sufficient for only one

destabilizing disturbance to cause instability, we will consider only (4.3.4), because by taking different values of the real numbers l and m we can determine the most destabilizing term. One can deal with other cell shapes rather than rectangles as described by (4.3.4), cf. Chandrasekhar [19] and the explanation on page13. For example the form of the solution for a hexagonal shape was given by Christopherson [22], cf. equation (1.2.21).

Then using (4.3.4) in our system (4.3.3), we obtain

$$\begin{aligned} \Delta w - R\Delta^*\theta + R_s\Delta^*\phi = 0 \ , \\ \sigma\theta = Rw + \Delta\theta \ , \\ \varepsilon\sigma\phi = \mp R_s w + \Delta\phi + h\theta - \eta\phi \ . \end{aligned} \tag{4.3.5}$$

This is an eigenvalue problem for σ to be solved subject to the boundary conditions

$$w = 0 \ , \ \theta = 0 \ , \ \phi = 0 \ on \ z = 0 \ , \ 1$$

with the periodicity in (x, y), we introduce a plane function f and a wave number a, such that

$$\Delta^* f = -a^2 f.$$

With the representations

$$w = W(z)f(x,y) \ , \ \theta = \Theta(z)f(x,y) \ , \ \phi = \Phi(z)f(x,y)$$

equations (4.3.5) reduces to solving

$$\begin{aligned} (D^2 - a^2)W + Ra^2\Theta - R_s a^2\Phi = 0 \ , \\ \sigma\Theta = RW + (D^2 - a^2)\Theta \ , \\ \varepsilon\sigma\Phi = \mp R_s W + (D^2 - a^2)\Phi + h\Theta - \eta\Phi \ , \end{aligned} \tag{4.3.6}$$

on $z \in (0, 1)$, where $D = d/dz$ and $a^2 = l^2 + m^2$. Equations (4.3.6) are to be solved subject to the boundary conditions

$$W = 0 \ , \ \Theta = 0 \ , \ \Phi = 0 \ \ on \ \ z = 0 \ , 1 \tag{4.3.7}$$

We solve equations (4.3.6) and (4.3.7) exactly by analytical means, but also numerically using a D^2-*Chebyshev Tau* numerical method, cf. Dongarra, Straughan

& Walker [26] and Straughan [101]. By writing W, Θ, Φ as a series of the form $\sin(n\pi z)$, one may derive linear instability threshold. The system (4.3.6) can be written in the following matrix form

$$\begin{pmatrix} -\Lambda & Ra^2 & -R_s a^2 \\ R & -\Lambda-\sigma & 0 \\ \mp R_s & h & -\Lambda-\eta-\sigma\varepsilon \end{pmatrix} \begin{pmatrix} W_0 \\ \Theta_0 \\ \Phi_0 \end{pmatrix} = \begin{pmatrix} 0 \\ 0 \\ 0 \end{pmatrix}$$

where $\Lambda = n^2\pi^2 + a^2$. Setting the determinant of the matrix to zero, a quadratic equation in R is obtained

$$b_1 R^2 + c_1 R + d_1 = 0 \ , \tag{4.3.8}$$

in which

$$\begin{aligned} b_1 &= a^2\Lambda + \eta a^2 + \varepsilon\sigma a^2 \ , \\ c_1 &= -R_s h a^2 \ , \\ d_1 &= \pm R_s^2 a^2(\Lambda+\sigma) - \Lambda^3 - \eta\Lambda^2 - \varepsilon\sigma\Lambda^2 - \sigma\Lambda^2 - \eta\sigma\Lambda - \varepsilon\sigma^2\Lambda. \end{aligned} \tag{4.3.9}$$

Two cases will be considered,

$case(i):\ \sigma = i\omega$, where ω is a real number, and

$case(ii):\ \sigma = 0$.

Case(i): $\sigma = i\omega$ ***(Oscillatory Mode)***

Substituting $\sigma = i\omega$ in the quadratic equation (4.3.8)-(4.3.9) and solving the equation for the real and imaginary parts of R^2, the following are obtained

$$real\ part:\ \pm R_s^2 a^2\Lambda + (a^2\Lambda + \eta a^2)R^2 - R_s h a^2 R - \Lambda^3 - \eta\Lambda^2 + \varepsilon\omega^2\Lambda = 0.$$

$$imaginary\ part:\ \pm R_s^2 a^2 + \varepsilon a^2 R^2 - \varepsilon\Lambda^2 - \Lambda^2 - \eta\Lambda = 0 \ ,$$

When there is No Reaction *i.e.* $h = \eta = 0$

$$real\ part:\ R^2 = \mp R_s^2 + \frac{\Lambda^2 - \varepsilon\omega^2}{a^2} \ ,$$

$$imaginary\ part:\ R^2 = \mp\frac{R_s^2}{\varepsilon} + \frac{(\varepsilon+1)\Lambda^2}{\varepsilon a^2} \ ,$$

minimizing firstly over n, one finds $n = 1$, and then a further minimization over a^2 yields

$$a^2_{critical} = \pi^2$$

which implies

$$R^2_{critical} = \mp\frac{R_s^2}{\varepsilon} + 4\pi^2(1 + \frac{1}{\varepsilon}).$$

Case(ii): $\sigma = 0$ ***(Stationary Mode)***

Substituting $\sigma = 0$ in the quadratic equation (4.3.8)-(4.3.9) and solving the equation for R^2, we get in the case of a reaction *i.e.* $h \neq 0$ *and* $\eta \neq 0$

$$\pm R_s^2 a^2\Lambda + (a^2\Lambda + \eta a^2)R^2 - R_s h a^2 R - \Lambda^3 - \eta\Lambda^2 = 0.$$

When there is No Reaction *i.e.* $h = \eta = 0$

$$R^2 = \mp R_s^2 + \frac{\Lambda^2}{a^2} \ ,$$

minimizing firstly over n, one finds $n = 1$, and then a further minimization over a^2 yields

$$a^2_{critical} = \pi^2 \ ,$$

which implies

$$R^2_{critical} = \mp R_s^2 + 4\pi^2.$$

The linear instability results for the Darcy-model with reaction has been discussed and analysed by Pritchard & Ritchardson [83].

4.4 The Non-Linear Energy Stability Analysis

In order to study the nonlinear stability of the Darcy model for the double diffusive convection, consider the nonlinear system of equations in the dimensionless form (4.2.5) and the corresponding boundary conditions (4.2.6). Taking into consideration the periodicity of the system and the smoothness of the boundary to allow the application of the *Divergence Theorem*. Multiply equation $(4.2.5)_1$ by u_i and integrate over V using integration by parts. Likewise, multiply equation $(4.2.5)_3$ by θ

and equation $(4.2.5)_4$ by ϕ and integrate. The following system of energy equations is obtained

$$\begin{aligned} 0 &= -\|\mathbf{u}\|^2 + R(\theta, w) - R_s(\phi, w) \ , \\ \frac{d}{dt}\frac{1}{2}\|\theta\|^2 &= R(\theta, w) - \|\nabla\theta\|^2 \ , \\ \frac{d}{dt}\frac{\varepsilon}{2}\|\phi\|^2 &= \mp R_s(\phi, w) - \|\nabla\phi\|^2 + h(\theta, \phi) - \eta\|\phi\|^2. \end{aligned} \tag{4.4.1}$$

Now we have to form the combination of the equations in system (4.4.1) as

$$(4.4.1)_1 + (4.4.1)_2 + \lambda(4.4.1)_3,$$

where λ is positive constant we are using as a coupling parameter. This leads to the energy equation

$$\begin{aligned} \frac{dE}{dt} = I - D = &- D(1 - \frac{I}{D}) \\ &\leq -D(1 - \max_H \frac{I}{D}) = -D(1 - \frac{1}{R_E}) \ , \end{aligned} \tag{4.4.2}$$

where H is the space of admissible solutions. In this case

$$H = \left\{ u_i, \theta, \phi | u_i \in L^2(V), \theta, \phi \in H^1(V) \right\},$$

subject to zero boundary conditions on $z = 0, 1$ and periodicity in the x, y directions. The nonlinear stability ensues when $R_E > 1$ which implies that $1 - 1/R_E > 0$, where

$$\frac{1}{R_E} = \max_H \frac{I}{D} \ , \tag{4.4.3}$$

and

$$\begin{aligned} E &= \frac{1}{2}\|\theta\|^2 + \frac{\varepsilon\lambda}{2}\|\phi\|^2 \ , \\ I &= 2R(\theta, w) + \lambda h(\theta, \phi) - (1 \pm \lambda) R_s(\phi, w) \ , \\ D &= \|\mathbf{u}\|^2 + \|\nabla\theta\|^2 + \lambda\|\nabla\phi\|^2 + \lambda\eta\|\phi\|^2. \end{aligned} \tag{4.4.4}$$

Inequality (4.4.2) can be written as

$$\frac{dE}{dt} \leq -a_1 D \ , \tag{4.4.5}$$

where $a_1 = 1 - 1/R_E > 0$. In order to obtain a bound for D, we have to use the Poincaré inequality

$$\begin{aligned} D &= \|\mathbf{u}\|^2 + \lambda\eta\|\phi\|^2 + \|\nabla\theta\|^2 + \lambda\|\nabla\phi\|^2 \\ &\geq \|\mathbf{u}\|^2 + \lambda\eta\|\phi\|^2 + \pi^2\|\theta\|^2 + \pi^2\lambda\|\phi\|^2 \\ &\geq \pi^2\|\theta\|^2 + \pi^2\lambda\|\phi\|^2 \\ &\geq \pi^2\|\theta\|^2 + \pi^2\lambda\frac{MLe}{MLe}\|\phi\|^2. \end{aligned} \tag{4.4.6}$$

If $MLe < 1$, then (4.4.6) implies

$$\pi^2\|\theta\|^2 + \pi^2\lambda\frac{MLe}{MLe}\|\phi\|^2 \geq \pi^2\|\theta\|^2 + \pi^2\lambda\varepsilon\|\phi\|^2. \tag{4.4.7}$$

If $MLe > 1$, then (4.4.6) implies

$$\pi^2\|\theta\|^2 + \pi^2\lambda\frac{MLe}{MLe}\|\phi\|^2 \leq \pi^2\|\theta\|^2 + \pi^2\lambda\varepsilon\|\phi\|^2. \tag{4.4.8}$$

From inequalities (4.4.7) and (4.4.8), we conclude that

$$\pi^2\|\theta\|^2 + \pi^2\lambda\varepsilon\|\phi\|^2 \geq k[\pi^2(\|\theta\|^2 + \lambda\varepsilon\|\phi\|^2)] \ , \ where\ k = min\{\frac{1}{MLe}, 1\} \tag{4.4.9}$$

Now employing inequality (4.4.9) in inequality (4.4.6), we get

$$D \geq 2k\pi^2\left(\frac{\|\theta\|^2 + \lambda\varepsilon\|\phi\|^2}{2}\right) = 2k\pi^2 E \ ,$$

So inequality (4.4.5) will be

$$\frac{dE}{dt} \leq -a_1 D \leq -2a_1 k\pi^2 E = -\mu E \ ,$$

from which

$$\frac{d}{dt}(e^{\mu t}E) \leq 0 \ ,$$

and then after integration we obtain

$$e^{\mu t}E \leq E(0).$$

Therefore,

$$E(t) \leq E(0)e^{-\mu t}. \tag{4.4.10}$$

Inequality (4.4.10) shows that under the condition $R_E > 1$, $E(t) \to 0$ as $t \to \infty$. This result according to the defined value of $E(t)$, equation $(4.4.4)_1$, proves that $\|\theta\|^2 \to 0$ and $\|\phi\|^2 \to 0$ as $t \to \infty$.

It remains to show the decay of $\|\mathbf{u}\|$. So, from the energy equation $(4.4.1)_1$ and by using the Arithmetic-Geometric Mean inequality, we have

$$\begin{aligned} \|\mathbf{u}\|^2 &= R(\theta, w) - R_s(\phi, w) \\ &\leq \frac{R}{2\alpha}\|\theta\|^2 + \frac{R\alpha}{2}\|w\|^2 + \frac{R_s}{2\beta}\|\phi\|^2 + \frac{R_s\beta}{2}\|w\|^2. \end{aligned} \tag{4.4.11}$$

Using the fact that $\|w\|^2 \leq \|\mathbf{u}\|^2$, inequality (4.4.11) will be

$$\|\mathbf{u}\|^2 \leq \left(\frac{R\alpha}{2} + \frac{R_s\beta}{2}\right)\|\mathbf{u}\|^2 + \frac{R}{2\alpha}\|\theta\|^2 + \frac{R_s}{2\beta}\|\phi\|^2 \ , \tag{4.4.12}$$

where α and β are constants to be chosen such that $R\alpha + R_s\beta = 1$, which gives $\alpha = 1/2R$ and $\beta = 1/2R_s$. According to that our inequality (4.4.12) will be,

$$\|\mathbf{u}\|^2 \leq 2R^2\|\theta\|^2 + 2R_s^2\|\phi\|^2. \tag{4.4.13}$$

Relation (4.4.13) shows that R_E^{-1} guarantees in addition to decay of $\|\theta\|$ and $\|\phi\|$, also decay of $\|\mathbf{u}\|$.

The nonlinear stability threshold is given by the variational problem (4.4.3). We have to determine the Euler-Lagrange equations and maximize in the coupling parameter λ to obtain the best value of R. The maximum problem is

$$\frac{1}{R_E} = \max_H \frac{2R(\theta, w) + \lambda h(\theta, \phi) - R_s(1 \pm \lambda)(\phi, w)}{\|\mathbf{u}\|^2 + \|\nabla\theta\|^2 + \lambda\|\nabla\phi\|^2 + \lambda\eta\|\phi\|^2}. \tag{4.4.14}$$

Rescaling ϕ by putting $\tilde{\phi} = \sqrt{\lambda}\phi$. equation (4.4.14) will be

$$\frac{1}{R_E} = \max_H \frac{2R(\theta, w) + \sqrt{\lambda}h(\theta, \tilde{\phi}) - R_s f(\lambda)(\tilde{\phi}, w)}{\|\mathbf{u}\|^2 + \|\nabla\theta\|^2 + \|\nabla\tilde{\phi}\|^2 + \eta\|\tilde{\phi}\|^2} \ , \tag{4.4.15}$$

where

$$f(\lambda) = \frac{1 \pm \lambda}{\sqrt{\lambda}}.$$

Hence, the Euler-Lagrange equations arising from (4.4.3) requires

$$\frac{d}{d\epsilon}\frac{I}{D}|_{\epsilon=0} = \delta\frac{I}{D} = 0 \ ,$$

where δ refers to the "derivative" evaluated at $\epsilon = 0$, or, upon calculation,

$$\frac{\delta I}{D} - \frac{I}{D^2}\delta D = \frac{1}{D}(\delta I - \frac{I}{D}\delta D) = \frac{1}{D}(\delta I - \frac{1}{R_E}\delta D) = 0 \ ,$$

which means that the maximum requires

$$\delta D - R_E\delta I = 0 \tag{4.4.16}$$

Let us define u_i , θ and ϕ in terms of arbitrary $C^2(0,1)$ functions, ζ_i , β and γ, with $\zeta_i(0) = \zeta_i(1) = \beta(0) = \beta(1) = \gamma(0) = \gamma(1) = 0$ and find the derivatives at $\epsilon = 0$,

where ϵ is a small parameter,

$$\begin{aligned} u_i &= u_i + \epsilon\zeta_i \ , \\ \theta &= \theta + \epsilon\beta \ , \\ \phi &= \phi + \epsilon\gamma. \end{aligned} \tag{4.4.17}$$

Thus using the defined values of I and D, equations (4.4.4), and incorporating the constrained $u_{i,i} = 0$ in I, we find

$$\delta D = -2\langle\beta\Delta\theta\rangle - 2\langle\gamma\Delta\tilde{\phi}\rangle + 2\langle\zeta_{,i}u_i\rangle + 2\eta\langle\tilde{\phi}\gamma\rangle \ , \tag{4.4.18}$$

and

$$\begin{aligned} \delta I =& 2R\langle\theta\zeta_3\rangle + 2R\langle w\beta\rangle - R_s f\langle\tilde{\phi}\zeta_3\rangle - R_s f\langle w\gamma\rangle \\ &+ \sqrt{\lambda}h\langle\theta\gamma\rangle + \sqrt{\lambda}h\langle\tilde{\phi}\beta\rangle - \langle P_{,i}\zeta_{,i}\rangle. \end{aligned} \tag{4.4.19}$$

Using (4.4.18) and (4.4.19) in equation (4.4.16), the following is obtained

$$\begin{aligned} &\langle\zeta_i, 2u_i - 2RR_E k_i\theta + R_s R_E f k_i\tilde{\phi} + R_E P_{,i}\rangle \\ &+\langle\beta, -2\Delta\theta - 2R_E Rw - \sqrt{\lambda}R_E h\tilde{\phi}\rangle \\ &+\langle\gamma, -2\Delta\tilde{\phi} + 2\eta\tilde{\phi} + R_E R_s f w - \sqrt{\lambda}R_E h\theta\rangle = 0. \end{aligned} \tag{4.4.20}$$

Since ζ_i , β and γ are arbitrary apart from the continuity and boundary condition requirements, we must have the following

$$\begin{aligned} 2u_i - 2RR_E k_i\theta + R_s R_E f k_i\tilde{\phi} &= -R_E P_{,i} \\ -2\Delta\theta - 2R_E Rw - \sqrt{\lambda}R_E h\tilde{\phi} &= 0 \\ -2\Delta\tilde{\phi} + 2\eta\tilde{\phi} + R_E R_s f w - \sqrt{\lambda}R_E h\theta &= 0. \end{aligned} \tag{4.4.21}$$

The system (4.4.21) is the Euler equations that give an eigenvalue problem for R. Taking the double Curl of equation $(4.4.21)_1$ and retaining only the third component of the resulting equation, our new system of equations will be

$$\begin{aligned} &\Delta w - RR_E\Delta^*\theta + \left(\frac{1 \pm \lambda}{2\sqrt{\lambda}}\right) R_s R_E \Delta^*\tilde{\phi} = 0 \ , \\ &\Delta\theta + R_E Rw + R_E\frac{\sqrt{\lambda}h}{2}\tilde{\phi} = 0 \ , \\ &(\Delta - \eta)\tilde{\phi} - R_E R_s\left(\frac{1 \pm \lambda}{2\sqrt{\lambda}}\right) w + R_E\frac{\sqrt{\lambda}h}{2}\theta = 0. \end{aligned} \tag{4.4.22}$$

Since $\tilde{\phi} = \sqrt{\lambda}\phi$, we can write the system (4.4.22) as

$$\begin{aligned} &\Delta w - RR_E\Delta^*\theta + \left(\frac{1 \pm \lambda}{2}\right) R_s R_E \Delta^* \phi = 0 \ , \\ &\Delta\theta + R_E R w + R_E \frac{\lambda h}{2}\phi = 0 \ , \\ &(\Delta - \eta)\phi - R_E R_s \left(\frac{1 \pm \lambda}{2\lambda}\right) w + R_E \frac{h}{2}\theta = 0. \end{aligned} \tag{4.4.23}$$

Because the system of equations (4.4.23) is linear, we may look for solutions of the form

$$\begin{aligned} w &= W(z) f(x, y) \ , \\ \theta &= \Theta(z) f(x, y) \ , \\ \phi &= \Phi(z) f(x, y) \ , \end{aligned} \tag{4.4.24}$$

where the function f satisfies $\Delta^* f = -a^2 f$ and a is a wave number, $D = d/dz$, $\Lambda = n^2\pi^2 + a^2$ and

$$\Delta = \Delta^* + \frac{\partial^2}{\partial z^2} = D^2 - a^2 = -\Lambda.$$

Substituting (4.4.24) in the system of equations (4.4.23), we obtain the following eigenvalue problem

$$\begin{aligned} &-\Lambda f W + R_E R a^2 f\Theta - \left(\frac{\lambda \pm 1}{2}\right) R_s R_E a^2 f\Phi = 0 \ , \\ &R_E R f W - \Lambda f\Theta + R_E \frac{\lambda}{2} h f\Phi = 0 \ , \\ &-R_E R_s \left(\frac{\lambda \pm 1}{2\lambda}\right) f W + R_E \frac{h}{2} f\Theta - (\Lambda + \eta) f\Phi = 0. \end{aligned} \tag{4.4.25}$$

Our system of equations (4.4.25) can be written in the following matrix form

$$\begin{pmatrix} \Lambda & -a^2 R_E R & a^2 R_E (\frac{1\pm\lambda}{2}) R_s \\ -R_E R & \Lambda & -\frac{\lambda h}{2} R_E \\ R_E R_s \left(\frac{1\pm\lambda}{2\lambda}\right) & -\frac{h}{2} R_E & \Lambda + \eta \end{pmatrix} \begin{pmatrix} W_0 \\ \Theta_0 \\ \Phi_0 \end{pmatrix} = \begin{pmatrix} 0 \\ 0 \\ 0 \end{pmatrix}$$

Setting the determinant of the matrix to zero, a quadratic equation in R is obtained

$$b_2 R^2 + c_2 R + d_2 = 0 \ , \tag{4.4.26}$$

where

$$\begin{aligned} b_2 &= 4R_E^2 a^2 (\Lambda + \eta) \ , \\ c_2 &= -2(1 \pm \lambda) R_E^3 R_s a^2 h \ , \\ d_2 &= -4\Lambda^3 - 4\eta\Lambda^2 + R_E^2 \left(\lambda h^2 + \frac{(1 \pm \lambda)^2}{\lambda} R_s^2 a^2\right) \Lambda. \end{aligned}$$

We set $R_E = 1$, since this yields the stability threshold and the quadratic equation (4.4.26) has to be solved for R in terms of the other parameters.
If there is No Reaction *i.e.* $h = \eta = 0$, then

$$R^2 = \frac{\Lambda^2}{a^2 R_E^2} - \frac{(1 \pm \lambda)^2 R_s^2}{4\lambda}. \tag{4.4.27}$$

Minimizing firstly over n, one finds $n = 1$, then a further minimization over a^2 yields

$$a^2_{critical} = \pi^2$$

which implies

$$R^2_{critical} = \frac{4\pi^2}{R_E^2} - \frac{(1 \pm \lambda)^2 R_s^2}{4\lambda}.$$

4.5 The Numerical Method

Numerically, we use the D^2 Chebyshev tau method, cf. Dongarra *et al.* [26], to solve equations (4.4.23) in the form

$$\begin{aligned}
&(D^2 - a^2)W - (\frac{1 \pm \lambda}{2})R_s R_E a^2 \Phi = -R R_E a^2 \Theta \\
&(D^2 - a^2)\Theta + R_E \frac{h\lambda}{2}\Phi = -R R_E W \\
&-R_s R_E (\frac{1 \pm \lambda}{2\lambda})W + R_E \frac{h}{2}\Theta + (D^2 - a^2 - \eta)\Phi = 0,
\end{aligned} \tag{4.5.1}$$

subject to the boundary conditions

$$w = \theta = \phi = 0 \ , \ z = 0, 1. \tag{4.5.2}$$

The functions W, Θ and Φ are expanded in terms of Chebyshev polynomials

$$W(z) = \Sigma_{n=1}^N w_n T_n(z), \ \Theta(z) = \Sigma_{n=1}^N \theta_n T_n(z), \ \Phi(z) = \Sigma_{n=1}^N \phi_n T_n(z).$$

Since $T_n(\pm 1) = (\pm 1)^n$, $T_n'(\pm 1) = (\pm 1)^{n-1} n^2$, implies that the boundary conditions (4.5.2) become

$$\begin{aligned}
&w_2 + w_4 + w_6 + \cdots + w_N = 0, \\
&w_1 + w_3 + w_5 + \cdots + w_{N-1} = 0
\end{aligned} \tag{4.5.3}$$

with similar representations for θ_n and ϕ_n

$$\begin{aligned} &\theta_2 + \theta_4 + \theta_6 + \cdots + \theta_N = 0, \\ &\theta_1 + \theta_3 + \theta_5 + \cdots + \theta_{N-1} = 0 \end{aligned} \tag{4.5.4}$$

$$\begin{aligned} &\phi_2 + \phi_4 + \phi_6 + \cdots + \phi_N = 0, \\ &\phi_1 + \phi_3 + \phi_5 + \cdots + \phi_{N-1} = 0. \end{aligned} \tag{4.5.5}$$

Therefore, the Chebyshev tau method reduces to solving the matrix system $A\mathbf{x} = RB\mathbf{x}$, where $\mathbf{x} = (w_1, w_2, \cdots, w_N, \theta_1, \cdots, \theta_N, \phi_1, \cdots, \phi_N)$ and the matrices A and B are given by

$$A = \begin{pmatrix} 4D^2 - a^2 I & 0 & -(\frac{1\pm\lambda}{2}) R_s R_E a^2 I \\ BC1 & 0 \cdots 0 & 0 \cdots 0 \\ BC2 & 0 \cdots 0 & 0 \cdots 0 \\ 0 & 4D^2 - a^2 I & R_E \frac{h\lambda}{2} I \\ 0 \cdots 0 & BC3 & 0 \cdots 0 \\ 0 \cdots 0 & BC4 & 0 \cdots 0 \\ -R_E R_s (\frac{1\pm\lambda}{2\lambda}) I & R_E \frac{h}{2} I & 4D^2 - (a^2 + \eta) I \\ 0 \cdots 0 & 0 \cdots 0 & BC5 \\ 0 \cdots 0 & 0 \cdots 0 & BC6 \end{pmatrix}$$

$$B = \begin{pmatrix} 0 & -R_E a^2 I & 0 \\ 0 \cdots 0 & 0 \cdots 0 & 0 \cdots 0 \\ 0 \cdots 0 & 0 \cdots 0 & 0 \cdots 0 \\ -R_E I & 0 & 0 \\ 0 \cdots 0 & 0 \cdots 0 & 0 \cdots 0 \\ 0 \cdots 0 & 0 \cdots 0 & 0 \cdots 0 \\ 0 & 0 & 0 \\ 0 \cdots 0 & 0 \cdots 0 & 0 \cdots 0 \\ 0 \cdots 0 & 0 \cdots 0 & 0 \cdots 0 \end{pmatrix}$$

where in the matrix A the notations $BC1, BC2$ refer to the boundary conditions (4.5.3), $BC3, BC4$ refer to (4.5.4) and $BC5, BC6$ refer to the boundary conditions (4.5.5). The matrix system is solved by the QZ algorithm, cf. Dongarra *et al.* [26].

4.6 Numerical Results and Conclusion

The critical Rayleigh number of the energy stability theory Ra_E is obtained by performing the optimization problem

$$Ra_E^2 = \max_{\lambda} \min_{a^2} R_E^2(a^2; \lambda). \tag{4.6.1}$$

While the critical Rayleigh number of the linear instability theory Ra_L has been calculated by performing the optimization

$$Ra_L^2 = \min_{a^2} R_L^2(a^2). \tag{4.6.2}$$

We analyse the numerical results of two different systems, heated below and salted above and heated and salted below, in the following subsections. The analyses supported by graphical figures.

4.6.1 Heated below and salted above system

The linear instability threshold Ra_L guarantees instability. Thus, in figure (4.1), any point in (Rs^2, R^2) space which is above the solid curve (Ra_L^2) represents an unstable solution. On the other hand, if (Rs^2, R^2) lies below the dashed curve (Ra_E^2) in figure (4.1) there is nonlinear stability for all initial perturbations. The values of Ra_L^2 in equation (4.6.2) and Ra_E^2 in equation (4.6.1) are obtained numerically using the D^2-*Chebyshev Tau* method to determine the eigenvalues. Table (4.1) shows that the linear and energy results are close to each other in the nonreactive case (*i.e.* $h = \eta = 0$). As can be noticed in figure (4.1)(a), that $Ra_L^2 = Ra_E^2$ when $h = \eta = 0$ and so we may conclude that the linear theory has covered the essential content of convection. Numerical values given in table (4.2) and table (4.3) are presented graphically in figures (4.1)(d) and (4.1)(f), respectively, and are included to show the effect of an increasing reaction rate. The linear instability boundary begins to diverge from the nonlinear stability one as the reaction rate increases. There is definitely instability if $Ra^2 > Ra_L^2$ whereas there is definitely global nonlinear stability when $Ra^2 < Ra_E^2$. Figure (4.2) shows the gap between the linear instability boundary and the energy stability boundary when the difference between the values of the reaction rates h and η is huge. As it is clear in figure (4.2)(a) that there is a

larger gap between the linear and energy boundaries when the value of h is bigger compared to the value of η. On the other hand, the two boundaries coincide when the value of h is smaller, see figure (4.2)(b). We note that increasing η for fixed

Linear Theory			Energy Theory			
Rs	Ra_L	a_L	Rs	Ra_E	a_E	λ
0.0826	6.2832	3.1	0	6.283186	3.14	1
0.2	6.28	3.14	0.5	6.263260	3.14	1
0.4	6.27	3.14	1	6.203098	3.14	1
1.865	6	3.14	2	5.956377	3.14	1
3.805	5	3.14	3	5.520727	3.14	1
4.845	4	3.14	4	4.845454	3.14	1
5.521	3	3.14	5	3.805053	3.14	1
5.956	2	3.14	6.12	1.422683	3.14	1
6.263	0.5	3.14	6.282	0.122081	3.14	1
6.2832	0	3.14	6.283	0.048361	3.14	1

Table 4.1: Critical Rayleigh numbers of linear theory, Ra_L, and nonlinear energy theory, Ra_E for the salted above Darcy convection problem, with their respective critical wave numbers a_L, a_E when there is No Reaction *i.e.* $h = \eta = 0$. λ is the coupling parameter.

h leads to the energy stability boundary being closer to the linear instability one. This is to be expected from equations (4.5.1) since $-\eta\phi$ is effectively a stabilizing term. On the other hand, in equations (4.5.1) the term $h\theta$ will generally destabilize the solution and this effect is borne out in figures (4.1) and (4.2). In particular, in figure (4.2)(a) we see that when $h = 20$ and $\eta = 1$ the gap between the nonlinear and linear thresholds is relatively large.

4.6.2 Heated and salted below system

It is instructive to write system (4.2.5) and the boundary conditions (4.2.6) for the salted below case as an abstract equation of form

$$A\mathbf{u}_t = L(\mathbf{u}) + N(\mathbf{u}),$$

Linear Theory			Energy Theory			
Rs	Ra_L	a_L	Rs	Ra_E	a_E	λ
1.5713	6.283	3.23	1	6.283186	3.14	1.69
1.5800	6.282	3.23	2	6.216381	3.25	3.77
1.5972	6.28	3.23	3	5.946768	3.32	1.82
1.6781	6.27	3.24	4	5.477767	3.38	1.42
1.8202	6.25	3.25	5	4.729768	3.43	1.24
2.4599	6.12	3.29	6	3.466519	3.45	1.12
2.8700	6	3.32	6.12	3.245767	3.45	1.11
4.7211	5	3.44	6.25	2.974599	3.45	1.09
5.6857	4	3.48	6.27	2.929212	3.45	1.09
6.2764	3	3.48	6.28	2.906083	3.45	1.09
6.6183	2	3.46	6.282	2.901421	3.45	1.09
6.7619	1	3.42	6.283	2.899085	3.45	1.09
6.7290	0	3.36	7	0.655904	3.46	1.0029

Table 4.2: Critical Rayleigh numbers of linear theory, Ra_L, and nonlinear energy theory, Ra_E for the salted above Darcy convection problem, with their respective critical wave numbers a_L, a_E when $h = 5$ *and* $\eta = 3$. λ is the coupling parameter.

where $\mathbf{u} = (u_1, u_2, u_3, \theta, \phi)$, $N(\mathbf{u})$ represents the nonlinear terms in (4.2.5) so

$$N(\mathbf{u}) = \begin{pmatrix} 0 \\ 0 \\ 0 \\ -u_i\theta_{,i} \\ -\frac{Le}{\hat{\phi}}u_i\phi_{,i} \end{pmatrix},$$

and L is the linear operator. In fact, the linear operator for (4.2.5) is

$$L = \begin{pmatrix} -1 & 0 & 0 & 0 & 0 \\ 0 & -1 & 0 & 0 & 0 \\ 0 & 0 & -1 & R & -R_s \\ 0 & 0 & R & \Delta & 0 \\ 0 & 0 & R_s & h & \Delta - \eta \end{pmatrix}.$$

If the reaction term h were not present, *i.e.* $h = 0$, then we may split L into a symmetric plus skew-symmetric parts as follows

$$L = L_s + L_A \ ,$$

where

$$L_s = \begin{pmatrix} -1 & 0 & 0 & 0 & 0 \\ 0 & -1 & 0 & 0 & 0 \\ 0 & 0 & -1 & R & 0 \\ 0 & 0 & R & \Delta & 0 \\ 0 & 0 & 0 & 0 & \Delta - \eta \end{pmatrix},$$

and

$$L_A = \begin{pmatrix} 0 & 0 & 0 & 0 & 0 \\ 0 & 0 & 0 & 0 & 0 \\ 0 & 0 & 0 & 0 & -R_s \\ 0 & 0 & 0 & 0 & 0 \\ 0 & 0 & R_s & 0 & 0 \end{pmatrix}.$$

For the salted above case, previous subsection, L_A would be zero and the analogous linear operator L would be symmetric.

Even when $h = 0$ in the salted below case, we expect some problem with non-linear energy stability theory since

$$(\mathbf{u}, L(\mathbf{u})) \neq (\mathbf{u}, L_s(\mathbf{u}))$$

where $(\cdot, \cdot)$ is the inner product on $(L^2(V))^3 \times (H^1(V))^2$ with V being a period cell for the solution. For the problem of this subsection, governed by equations (4.2.5) and (4.2.6) for the salted below case, we have two sources of anti-symmetry, the R_s term and the h term.

The results are presented graphically for different values of the reaction rates h and η in figure (4.3). As the figure shows, increasing the values of the reaction terms resulted in increasing the distance between the linear instability boundary Ra_L and the energy stability one Ra_E. Moreover, the position of the transition point where the linear instability boundary switches from stationary convection to oscillatory convection becomes lower and lower as the the reaction rates increase.

According to the curves in figure (4.3), the difference between the nonreactive case (*i.e.* $h = \eta = 0$) and the case $h = \eta = 1$ is unnoticeable compared to the case when $h = 15$ and $\eta = 9$ where the area or the gap between the linear instability boundaries increased. On the other hand, the energy boundary Ra_E remains constant for all the taken values of the reaction rates. If $Ra^2 < Ra_E^2$ there is globally nonlinear stability, whereas there is definitely instability if $Ra^2 > Ra_L^2$. To investigate the effect of each of h and η in the stability of the system, a slightly larger difference between their values is considered for different values of ε. Comparing the two cases when $h = 10$, $\eta = 1$ and $h = 1$, $\eta = 10$, as is shown in figures (4.4), (4.5) and (4.6), the linear instability boundary for $h = 10$ always lies above the linear instability boundary for $\eta = 10$ for all the chosen values of ε ($\varepsilon = 2, 3, 5$). But at a certain point (Rs^2, Ra^2) the two boundaries intersect each other and the opposite situation occurs, the linear boundary for $\eta = 10$ is above the linear boundary for $h = 10$ and the gap between them remains at a constant value as is clear in figures (4.6)(b) and (4.5)(c). This is to be expected from equations (4.5.1) since $-\eta\phi$ is a stabilizing term and $h\theta$ generally will destabilize the solution and that what is actually noticed in the figures. But then the term $+R_s w$ will dominate for the fixed values of h and η which explains what happened after the intersection. While the energy boundary remains unchanged in all cases.

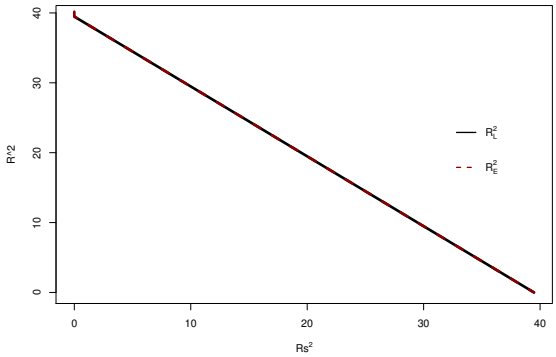

(a) $h = \eta = 0$

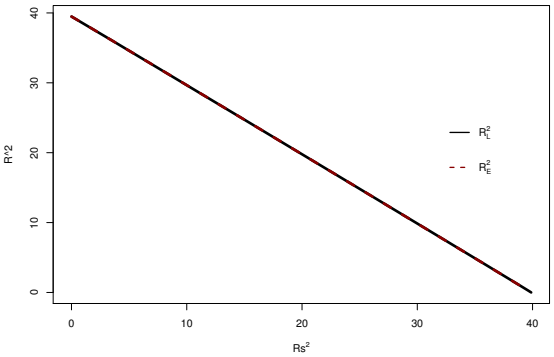

(b) $h = 0.1\ ,\ \eta = 0.2$

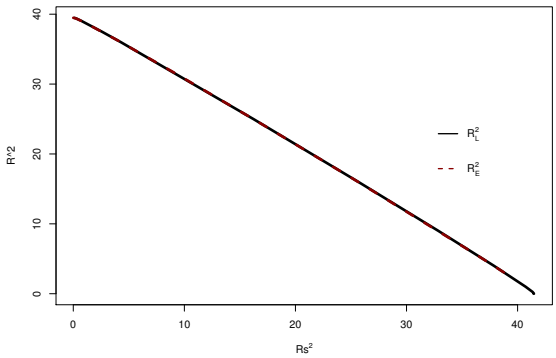

(c) $h = \eta = 1$

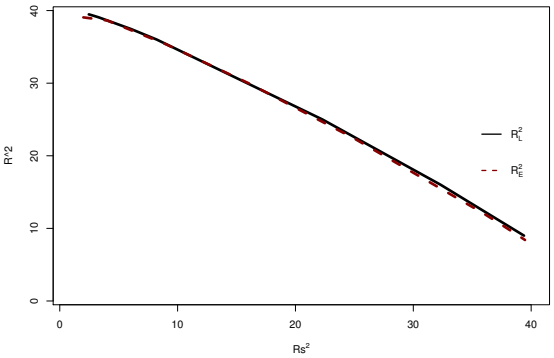

(d) $h = 5\ ,\ \eta = 3$

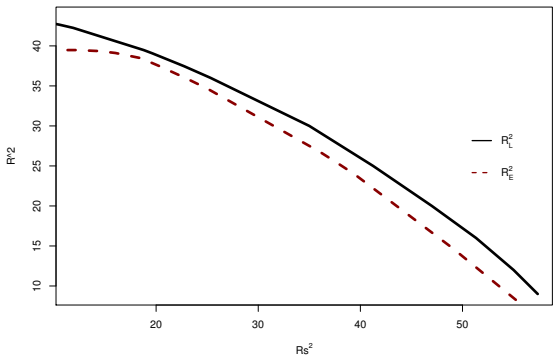

(e) $h = 15\ ,\ \eta = 9$

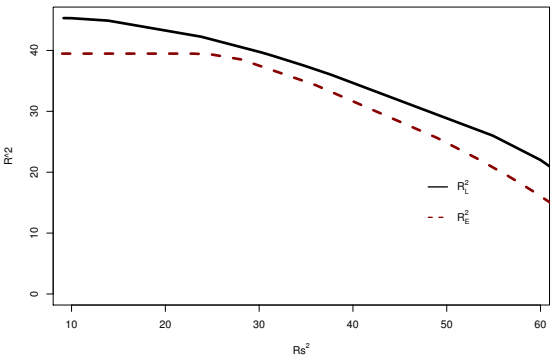

(f) $h = 20\ ,\ \eta = 16$

Figure 4.1: Linear instability and Energy stability boundaries for the salted above Darcy convection problem for different values of the reaction rates h and η.

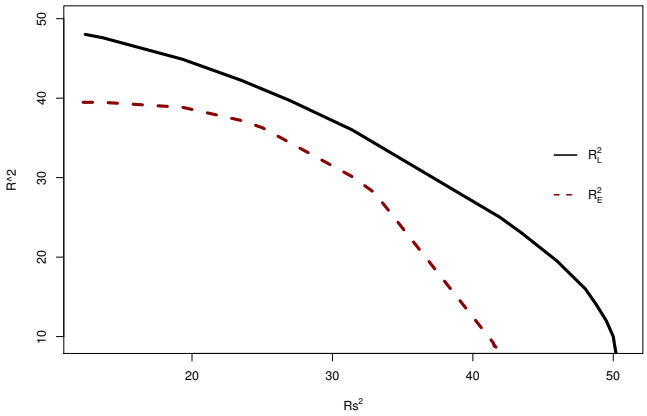

(a) $h = 20\ ,\ \eta = 1$

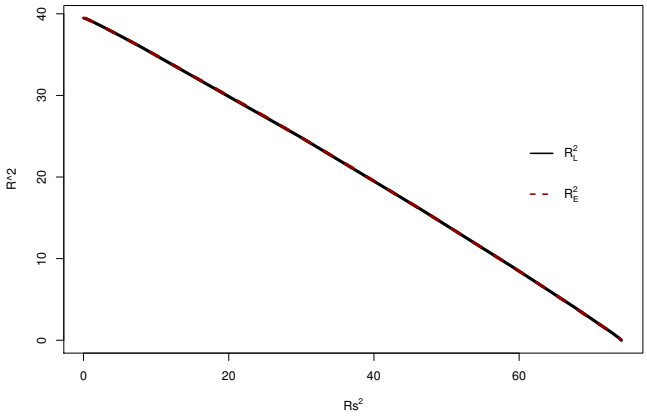

(b) $h = 1\ ,\ \eta = 20$

Figure 4.2: Linear instability and Energy stability boundaries for the salted above Darcy convection problem when the difference between h and η is huge.

Linear Theory			Energy Theory			
Rs	Ra_L	a_L	Rs	Ra_E	a_E	λ
3.024502	6.7313399	3.53	0.01	6.283186	3.14	0.0016
3.027284	6.731335	3.54	0.02	6.283186	3.14	0.0032
3.029454	6.73133	3.54	0.1	6.283186	3.14	0.016
3.039739	6.7313	3.54	0.5	6.283088	3.14	0.09
3.089217	6.731	3.55	1	6.283162	3.14	0.19
3.163901	6.73	3.56	2	6.283184	3.14	0.46
3.731663	6.7	3.68	3	6.283186	3.14	0.89
4.881631	6.5	3.94	4	6.283186	3.14	1.69
5.495110	6.3	4.08	5	6.270139	3.44	3.13
5.545822	6.28	4.1	5.8	5.972402	3.99	2.59
5.619278	6.25	4.11	6	5.858324	4.02	2.31
5.907456	6.12	4.18	7	5.061064	4.17	1.56
6.139228	6	4.24	7.3	4.712228	4.19	1.43
7.410971	5	4.5	7.5	4.432304	4.21	1.36
8.098929	4	4.57	7.8	3.898452	4.2	1.24
8.466344	3	4.53	7.9	3.670777	4.19	1.21
8.594079	2	4.41	8	3.398999	5.17	0.5
8.235507	0.02	4	8.3	1.578162	5.03	0.7
8.227812	0	4	8.5	1.517708	5.52	0.7

Table 4.3: Critical Rayleigh numbers of linear theory, Ra_L, and nonlinear energy theory, Ra_E for the salted above Darcy convection problem, with their respective critical wave numbers a_L, a_E when $h = 20$ *and* $\eta = 16$. λ is the coupling parameter.

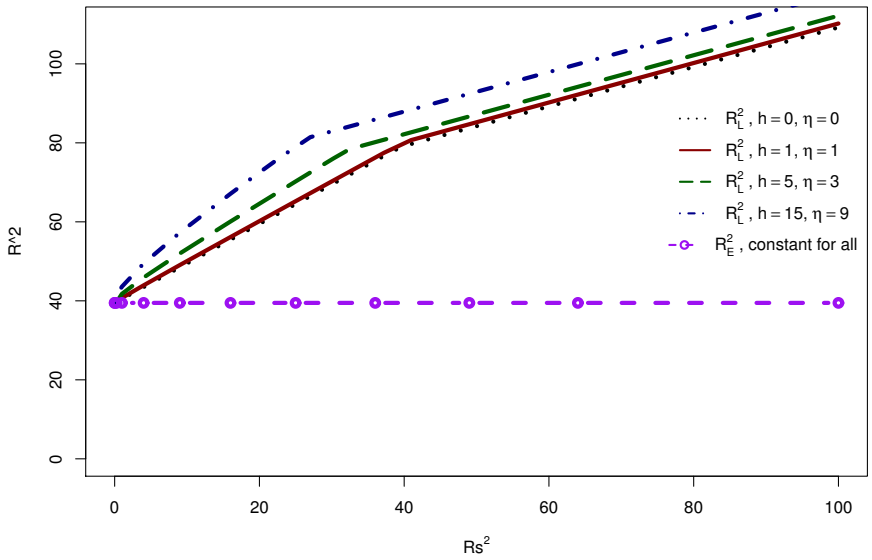

Figure 4.3: Linear instability and Energy stability boundaries for the salted below Darcy convection problem for different values of h and η.

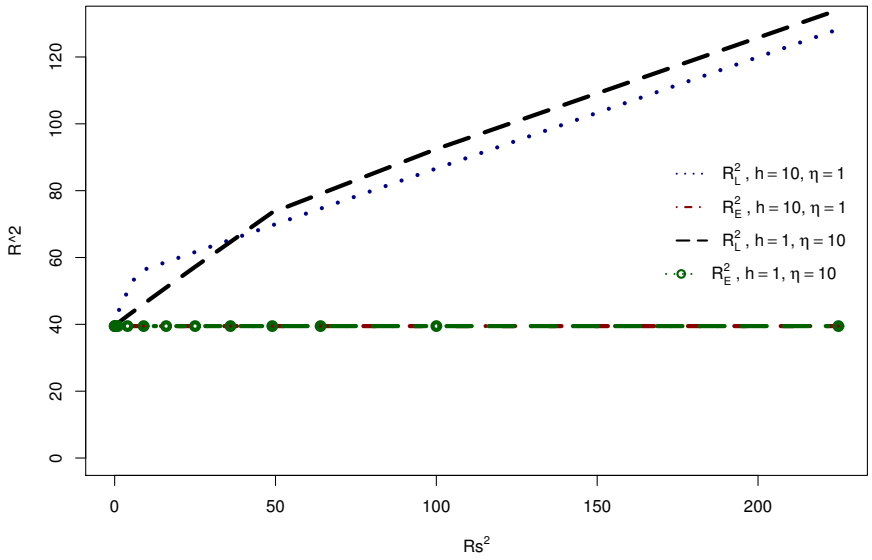

Figure 4.4: Linear instability and Energy stability boundaries for the salted below Darcy convection problem $\varepsilon = 3$.

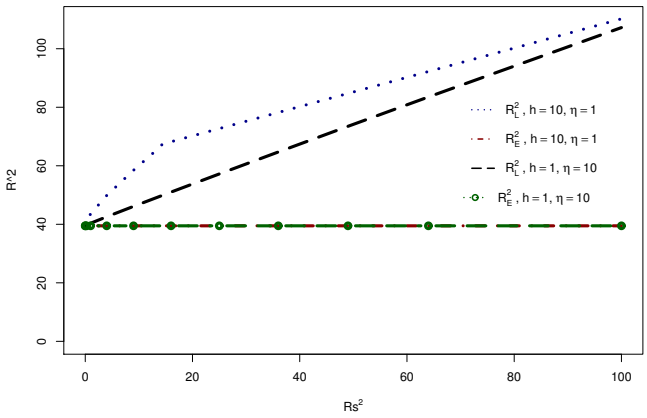

(a) $R_s = 0 : 100$

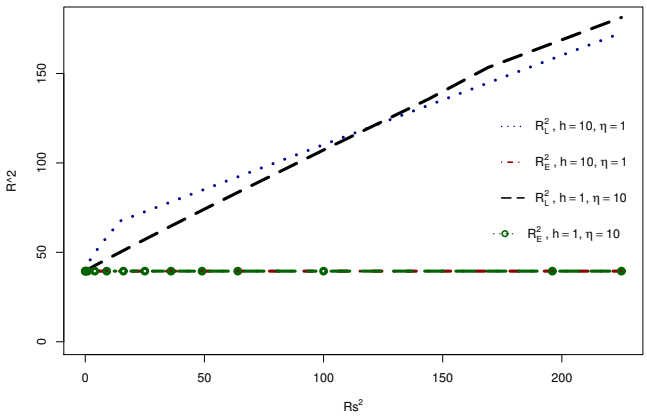

(b) $R_s = 0 : 200$

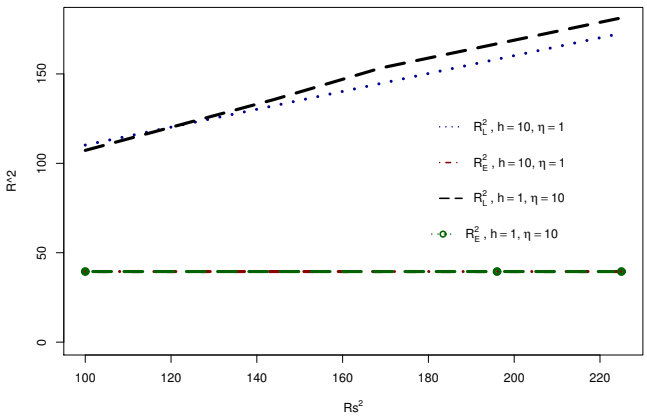

(c) $R_s = 100 : 220$

Figure 4.5: Linear instability and Energy stability boundaries for the salted below Darcy convection problem for $\varepsilon = 2$.

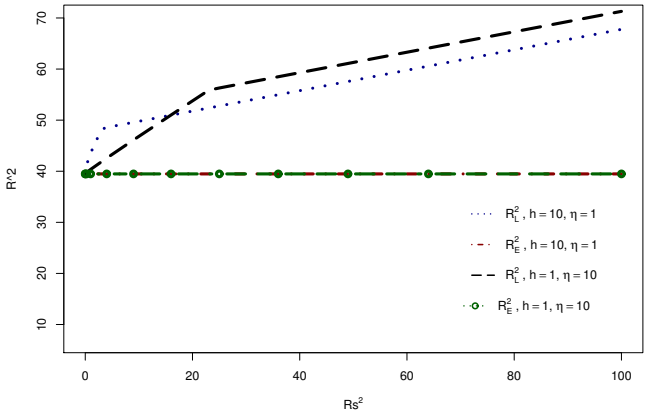

(a) $R_s = 0 : 100$

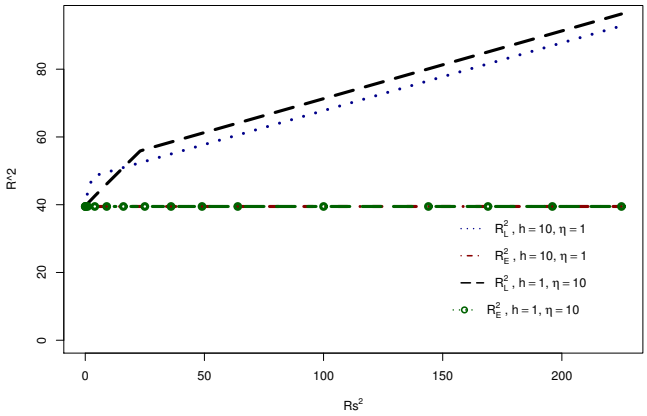

(b) $R_s = 0 : 200$

Figure 4.6: Linear instability and Energy stability boundaries for the salted below Darcy convection problem for $\varepsilon = 5$.

Chapter 5

The Energy Stability of Brinkman Thermosolutal Convection with Reaction

5.1 Introduction

This chapter may be considered as an extension of Wang and Tan [124] and Pritchard and Richardson [83]. In chapter 4 we used the energy method to carry out a nonlinear stability analysis of the Darcy thermosolutal convection with reaction. In the current chapter, the energy stability of the Brinkman thermosolutal convection with reaction is considered. We use the compound matrix numerical technique to solve the associated system of equations with the corresponding boundary conditions, in which we investigate two systems separately, the heated below-salted above system and the heated below-salted below system. We obtain the energy stability boundaries for different values of the reaction rates and compare them with the relevant linear instability boundaries. Some linear instability boundaries are obtained by Wang and Tan [124], but they do not correspond directly to what we require and hence we recompute also the linear values using the D^2 Chebyshev Tau method.

Our aim is to obtain the nonlinear stability boundaries below which the solution is globally stable by using the energy method and compare the nonlinear

boundaries with the relevant linear instability boundaries obtained by Wang and Tan [124]. Considering a porous medium of Brinkman type occupying a bounded three-dimensional domain, we discuss the variation of the onset of thermosolutal convection with the reaction rate and the Brinkman coefficient.

5.2 Basic Equations

Our model consists of Brinkman equation with the density in the buoyancy term depends linearly on the temperature T and salt concentration C, the continuity equation, the advection-diffusion equation for the transport of heat and the equation for the transport of solute with reaction terms,

$$\begin{aligned} p_{,i} &= -\frac{\mu}{K}v_i - \rho_0[1-\alpha_T(T-T_0)+\alpha_C(C-C_0)]gk_i + \lambda\Delta v_i, \\ v_{i,i} &= 0, \\ \frac{1}{M}T_{,t} + v_iT_{,i} &= k_T\Delta T, \\ \hat{\phi}C_{,t} + v_iC_{,i} &= \hat{\phi}k_C\Delta C + \hat{k}[f_1(T-T_0)+f_0-C]. \end{aligned} \tag{5.2.1}$$

Where as in the previous chapters, v_i, p, T, C are the velocity, pressure, temperature and salt concentration, K is the matrix permeability, μ is the fluid viscosity, ρ_0 is the fluid density. The coefficients k_C, k_T are the molecular diffusivity of the solute through the fluid and the effective diffusivity of the heat through the saturated medium. The quantity M is the ratio of the heat capacity of the fluid to the heat capacity of the medium, $\hat{\phi}$ is the matrix porosity, $\hat{k}$ is the reaction coefficient and $f_0 + f_1(T-T_0) = C_{eq}(T)$ in Pritchard & Richardson [83], where f_0, f_1 and T_0 are constants. Moreover, g is the gravity, $\mathbf{k} = (0,0,1)$, and α_T and α_C are the thermal and solutal expansion coefficients respectively. The equations (5.2.1) are taken in the domain $\mathcal{R}^2 \times (0,d) \times \{t>0\}$. The boundary conditions are

$$\begin{aligned} &v_i = 0 \ on \ z = 0, d, \\ &T = T_L \ on \ z = 0, \quad T = T_U \ on \ z = d, \\ &C = C_L \ on \ z = 0, \quad C = C_U \ on \ z = d, \end{aligned} \tag{5.2.2}$$

where T_L, T_U, C_L, C_U all constants, with $T_L > T_U$ since our systems are heated below. For the salted above porous medium $C_U > C_L$ while for the salted below

case $C_L > C_U$. In the steady state, we look for

$$\begin{aligned} \bar{v}_i &= 0, \\ \bar{T} &= \bar{T}(z), \\ \bar{C} &= \bar{C}(z). \end{aligned} \tag{5.2.3}$$

Equation $(5.2.1)_2$ is automatically satisfied since $\bar{v}_i = 0$. Equation $(5.2.1)_3$ will give

$$\bar{T}(z) = \mu_1 z + \mu_2,$$

using the boundary conditions $(5.2.2)_2$ implies

$$\bar{T}(z) = -\beta_T z + T_L \ ; \ \beta_T = \frac{T_L - T_U}{d}. \tag{5.2.4}$$

Considering equation $(5.2.1)_4$ we get

$$\frac{d^2\bar{C}}{dz^2} + \frac{\hat{k}}{\hat{\phi} k_C}\left[f_1(\bar{T} - T_0) + f_0 - \bar{C}\right] = 0,$$

assuming $C_{eq}(\bar{T}(z)) = \bar{C}(z)$ implies that $\Delta\bar{C} = 0$. Hence employing the boundary conditions $(5.2.2)_3$ imply

$$\bar{C}(z) = -\beta_C z + C_L \ ; \ \beta_C = \frac{C_L - C_U}{d}, \tag{5.2.5}$$

and the momentum equation $(5.2.1)_1$ becomes

$$\frac{\partial \bar{p}}{\partial z} = -g\rho_0 \left[1 - \alpha_T(T_L - \beta_T z - T_0) + \alpha_C(C_L - \beta_C z - C_0)\right] k_i. \tag{5.2.6}$$

Integration of (5.2.6) gives $\bar{p}$ as a quadratic function of z of the form

$$\bar{p}(z) = \alpha z^2 + \beta z + \gamma. \tag{5.2.7}$$

Therefore, we find the steady solution or the basic state to (5.2.1) which we are interested in studying its stability and which satisfies (5.2.2) as

$$\begin{aligned} \bar{v}_i &= 0, \\ \bar{T}(z) &= -\beta_T z + T_L, \\ \bar{C}(z) &= -\beta_C z + C_L, \end{aligned} \tag{5.2.8}$$

where β_T and β_C are the temperature and salt gradients respectively.
To analyse the stability of the solutions (5.2.8) we define perturbations (u_i, π, θ, ϕ) such that

$$\begin{aligned} v_i &= \bar{v}_i + u_i, \\ p &= \bar{p} + \pi, \\ T &= \bar{T} + \theta, \\ C &= \bar{C} + \phi \end{aligned} \tag{5.2.9}$$

Using these perturbations in equations (5.2.1) we derive the equations governing (u_i, π, θ, ϕ) as

$$\begin{aligned} \pi_{,i} &= -\frac{\mu}{K}u_i + \rho_0 g k_i \alpha_T \theta - \rho_0 g k_i \alpha_C \phi + \lambda \Delta u_i \ , \\ u_{i,i} &= 0 \ , \\ \frac{1}{M}\theta_{,t} + u_i\theta_{,i} &= \beta_T w + k_T \Delta\theta \ , \\ \hat{\phi}\phi_{,t} + u_i\phi_{,i} &= \beta_C w + \hat{\phi} k_C \Delta\phi + \hat{k} f_1 \theta - \hat{k}\phi, \end{aligned} \tag{5.2.10}$$

where $w = u_3$. To non-dimensionalize the system (5.2.10), we define the length, time and velocity scales, L, τ and U, by $L = d$, $\tau = d/MU$ and $U = k_T/d$. We introduce pressure, temperature and salt scales as

$$P = \frac{Ud\mu}{K} \ , \ T^{\sharp^2} = \frac{\mu\beta_T k_T}{\alpha_T \rho_0 g K} \ , \ C^{\sharp^2} = \frac{\mu\beta_C k_T Le}{\alpha_C \rho_0 g K \hat{\phi}},$$

where $Le = k_T/k_C$ is the Lewis number. The temperature and salt Rayleigh numbers are defined as

$$R = \sqrt{\frac{\beta_T d^2 K \alpha_T \rho_0 g}{k_T \mu}} \ ,$$

$$R_s = \sqrt{\frac{\beta_C d^2 K \alpha_C \rho_0 g Le}{\hat{\phi} k_T \mu}} \ \ when \ C_L > C_U \ \ or \ \ R_s = \sqrt{\frac{|\beta_C| d^2 K \alpha_C \rho_0 g Le}{\hat{\phi} k_T \mu}} \ \ when \ C_L < C_U.$$

Then, the fully nonlinear, perturbed dimensionless form of (5.2.10) is

$$\begin{aligned} \pi_{,i} &= -u_i + R k_i \theta - R_s k_i \phi + \tilde{\gamma} \Delta u_i \ , \\ u_{i,i} &= 0 \ , \\ \theta_{,t} + u_i\theta_{,i} &= Rw + \Delta\theta \ , \\ \varepsilon\phi_{,t} + \frac{Le}{\hat{\phi}} u_i \phi_{,i} &= \mp R_s w + \Delta\phi + h\theta - \eta\phi \ , \end{aligned} \tag{5.2.11}$$

where $\varepsilon = MLe$, $\tilde{\gamma} = \lambda K/\mu d^2$ the Brinkman coefficient and h and η are the reaction terms

$$h = \frac{\hat{k} f_1 d^2 T^\sharp}{\hat{\phi} k_C C^\sharp} \quad and \quad \eta = \frac{\hat{k} d^2}{\hat{\phi} k_C}.$$

Moreover, $+R_s$ is taken when $C_L > C_U$, which means that the system is salted from below, and $-R_s$ is taken when $C_L < C_U$, which means that the system is salted from above. The corresponding boundary conditions are

$$Dw = w = \theta = \phi = 0 \ on \ z = 0 \ and \ z = 1. \tag{5.2.12}$$

5.3 Linear Instability Theory

To study the linear instability, we drop the nonlinear terms of (5.2.11) and take the double curl of equation $(5.2.11)_1$ and retaining only the third component of the resulting equation to reduce (5.2.11) to studying the system

$$\begin{aligned} &\Delta w - R\Delta^* \theta + R_s \Delta^* \phi - \tilde{\gamma} \Delta^2 w = 0, \\ &\theta_{,t} = Rw + \Delta\theta, \\ &\varepsilon \phi_{,t} = \mp R_s w + \Delta\phi + h\theta - \eta\phi, \end{aligned} \tag{5.3.1}$$

where Δ^* is the horizontal Laplacian. Assuming a normal mode representation for w, θ and ϕ of the form $w = W(z)f(x,y)$, $\theta = \Theta(z)f(x,y)$ and $\phi = \Phi(z)f(x,y)$ where $f(x,y)$ is a plan tiling function satisfying

$$\Delta^* f = -a^2 f; \tag{5.3.2}$$

cf. Straughan [99] and a is a wave number. Using (5.3.2) and applying the normal mode representations to (5.3.1), we find

$$\begin{aligned} &(D^2 - a^2)W + Ra^2\Theta - R_s a^2 \Phi - \tilde{\gamma}(D^2 - a^2)^2 W = 0, \\ &\sigma\Theta = RW + (D^2 - a^2)\Theta, \\ &\varepsilon\sigma\Phi = \mp R_s W + (D^2 - a^2)\Phi + h\Theta - \eta\Phi, \end{aligned} \tag{5.3.3}$$

where $D = d/dz$. This is an eigenvalue problem for σ to be solved subject to the boundary conditions

$$DW = W = \Theta = \Phi = 0 \ , \ on \ z = 0, 1. \tag{5.3.4}$$

We solved system (5.3.3) with the corresponding boundary conditions (5.3.4) using the D^2 Clebyshev Tau method and the Compound Matrix technique. Detailed numerical results for the heated below-salted above and heated below-salted below are reported separately in the subsections (5.6.1) and (5.6.2). We determined the critical Rayleigh number given by $Ra_L^2 = min_{a^2} R^2(a^2)$ where for all $R^2 > Ra_L^2$ the system is unstable.

5.4 Nonlinear Energy Stability Theory

In order to study the nonlinear stability of the Brinkman model for the double diffusive convection, consider the nonlinear system of equations in the dimensionless form (5.2.11) and the corresponding boundary conditions (5.2.12). Taking into consideration the periodicity of the system and the smoothness of the boundary to allow the application of the *Divergence Theorem*. Multiply equation $(5.2.11)_1$ by u_i and integrate over V using integration by parts. Likewise, multiply equation $(5.2.11)_3$ by θ and equation $(5.2.11)_4$ by ϕ and integrate. The following energy equations are obtained

$$\begin{aligned} 0 &= -\|\mathbf{u}\|^2 + R(\theta, w) - R_s(\phi, w) - \tilde{\gamma}\|\nabla \mathbf{u}\|^2 \ , \\ \frac{d}{dt}\frac{1}{2}\|\theta\|^2 &= R(\theta, w) - \|\nabla\theta\|^2 \ , \\ \frac{d}{dt}\frac{\varepsilon}{2}\|\phi\|^2 &= \mp R_s(\phi, w) - \|\nabla\phi\|^2 + h(\theta, \phi) - \eta\|\phi\|^2. \end{aligned} \tag{5.4.1}$$

Then we form the combination of the equations in system (5.4.1) as

$$(5.4.1)_1 + (5.4.1)_2 + \lambda(5.4.1)_3,$$

where λ a coupling parameter. This leads to the energy equation

$$\begin{aligned} \frac{dE}{dt} = I - D = &- D(1 - \frac{I}{D}) \\ &\leq -D(1 - \max_H \frac{I}{D}) = -D(1 - \frac{1}{R_E}) \ , \end{aligned} \tag{5.4.2}$$

where H is the space of admissible solutions. Namely

$$H = \left\{ u_i, \theta, \phi \in H^1(V) : u_i = \theta = \phi = 0 \ on \ z = 0, 1 \right\},$$

and

$$\begin{aligned}
&\frac{1}{R_E} = max_H \frac{I}{D},\\
&E = \frac{1}{2}\|\theta\|^2 + \frac{\varepsilon\lambda}{2}\|\phi\|^2 \ ,\\
&I = 2R(\theta, w) + \lambda h(\theta, \phi) - (1 \pm \lambda)R_s(\phi, w) \ ,\\
&D = \|\mathbf{u}\|^2 + \|\nabla\theta\|^2 + \lambda\|\nabla\phi\|^2 + \lambda\eta\|\phi\|^2 + \tilde{\gamma}\|\nabla\mathbf{u}\|^2.
\end{aligned} \tag{5.4.3}$$

The nonlinear stability ensues when $R_E > 1$ which implies that $1 - 1/R_E > 0$. Inequality (5.4.2) can be written as

$$\frac{dE}{dt} \leq -a_1 D \ , \tag{5.4.4}$$

where $a_1 = 1 - 1/R_E > 0$. Then, using the Poincaré inequality in order to obtain a bound for D

$$\begin{aligned}
D &= \|\mathbf{u}\|^2 + \lambda\eta\|\phi\|^2 + \|\nabla\theta\|^2 + \lambda\|\nabla\phi\|^2 + \tilde{\gamma}\|\nabla\mathbf{u}\|^2\\
&\geq \|\mathbf{u}\|^2 + \lambda\eta\|\phi\|^2 + \pi^2\|\theta\|^2 + \pi^2\lambda\|\phi\|^2 + \pi^2\tilde{\gamma}\|\mathbf{u}\|^2\\
&\geq \pi^2\|\theta\|^2 + \pi^2\lambda\|\phi\|^2\\
&\geq \pi^2\|\theta\|^2 + \pi^2\lambda\frac{MLe}{MLe}\|\phi\|^2\\
&\geq 2k\pi^2\left(\frac{\|\theta\|^2 + \lambda\varepsilon\|\phi\|^2}{2}\right) = 2k\pi^2 E,
\end{aligned} \tag{5.4.5}$$

where $k = min\left\{\frac{1}{MLe}, 1\right\}$. Then inequality (5.4.4) will be

$$\frac{dE}{dt} \leq -a_1 D \leq -2a_1 k\pi^2 E = -\mu E \ ,$$

from which

$$\frac{d}{dt}(e^{\mu t}E) \leq 0 \ ,$$

integration leads to

$$E(t) \leq E(0)e^{-\mu t} \tag{5.4.6}$$

Inequality (5.4.6) shows that under the condition $R_E > 1$, $E(t) \to 0$ as $t \to \infty$. This result according to equation $(5.4.3)_2$, proves that $\|\theta\|^2 \to 0$ and $\|\phi\|^2 \to 0$ as $t \to \infty$. To show the decay of $\|\mathbf{u}\|$, we have to use the Poincaré inequality and the Arithmetic-Geometric Mean inequality in the energy equation $(5.4.1)_1$ to obtain

$$\begin{aligned}
\|\mathbf{u}\|^2 &= R(\theta, w) - R_s(\phi, w) - \tilde{\gamma}\|\nabla\mathbf{u}\|^2\\
&\leq R(\theta, w) - R_s(\phi, w) - \tilde{\gamma}\pi^2\|\mathbf{u}\|^2
\end{aligned} \tag{5.4.7}$$

which can be written as

$$\begin{aligned}(1+\tilde{\gamma}\pi^2)\|\mathbf{u}\|^2 &\leq R(\theta,w)-R_s(\phi,w)\\ &\leq \frac{R}{2\alpha}\|\theta\|^2+\frac{R\alpha}{2}\|w\|^2+\frac{R_s}{2\beta}\|\phi\|^2+\frac{R_s\beta}{2}\|w\|^2.\end{aligned} \tag{5.4.8}$$

Using the fact that $\|w\|^2 \leq \|\mathbf{u}\|^2$, inequality (5.4.8) is

$$(1+\tilde{\gamma}\pi^2)\|\mathbf{u}\|^2 \leq \left(\frac{R\alpha}{2}+\frac{R_s\beta}{2}\right)\|\mathbf{u}\|^2+\frac{R}{2\alpha}\|\theta\|^2+\frac{R_s}{2\beta}\|\phi\|^2\ , \tag{5.4.9}$$

where α and β are constants to be chosen such that $R\alpha + R_s\beta = 1$, which gives $\alpha = 1/2R$ and $\beta = 1/2R_s$. According to our choice of α and β, inequality (5.4.9) will be

$$(\frac{1}{2}+\tilde{\gamma}\pi^2)\|\mathbf{u}\|^2 \leq R^2\|\theta\|^2+R_s^2\|\phi\|^2, \tag{5.4.10}$$

which shows that R_E^{-1} guarantees in addition to the decay of $\|\theta\|$ and $\|\phi\|$, also decay of $\|\mathbf{u}\|$.

Turning our attention to the maximization problem $(5.4.3)_1$, we have to determine the Euler-Lagrange equations in order to solve it. The maximum problem is

$$\frac{1}{R_E}=\max_H \frac{2R(\theta,w)+\lambda h(\theta,\phi)-R_s(1\pm\lambda)(\phi,w)}{\|\mathbf{u}\|^2+\|\nabla\theta\|^2+\lambda\|\nabla\phi\|^2+\lambda\eta\|\phi\|^2+\tilde{\gamma}\|\nabla\mathbf{u}\|^2}. \tag{5.4.11}$$

Rescaling ϕ by putting $\tilde{\phi}=\sqrt{\lambda}\phi$. equation (5.4.11) will be

$$\frac{1}{R_E}=\max_H \frac{2R(\theta,w)+\sqrt{\lambda}h(\theta,\tilde{\phi})-R_s f(\lambda)(\tilde{\phi},w)}{\|\mathbf{u}\|^2+\|\nabla\theta\|^2+\|\nabla\tilde{\phi}\|^2+\eta\|\tilde{\phi}\|^2+\tilde{\gamma}\|\nabla\mathbf{u}\|^2}\ , \tag{5.4.12}$$

where

$$f(\lambda)=\frac{1\pm\lambda}{\sqrt{\lambda}}.$$

Hence, the Euler-Lagrange equations arising from $(5.4.3)_1$ requires

$$\frac{d}{d\epsilon}\frac{I}{D}|_{\epsilon=0}=\delta\frac{I}{D}=0\ ,$$

where δ refers to the "derivative" evaluated at $\epsilon = 0$, or, upon calculation,

$$\frac{\delta I}{D}-\frac{I}{D^2}\delta D=\frac{1}{D}(\delta I-\frac{I}{D}\delta D)=\frac{1}{D}(\delta I-\frac{1}{R_E}\delta D)=0\ ,$$

which means that the maximum requires

$$\delta D - R_E\delta I = 0, \tag{5.4.13}$$

to obtain the Euler equations that give an eigenvalue problem for R. Let ζ, β and γ be arbitrary fixed $C^2(V)$ functions that satisfy the boundary conditions and define neighbouring functions $u_i = u_i + \epsilon\zeta_i$, $\theta = \theta + \epsilon\beta$, $\tilde{\phi} = \tilde{\phi} + \epsilon\gamma$. Hence

$$\begin{aligned}\delta I =& 2R(\zeta_3, \theta) + 2R(w, \beta) - R_s f(\lambda)(\zeta_3, \tilde{\phi}) - R_s f(\lambda)(w, \gamma) \\ &+ \sqrt{\lambda} h(\gamma, \theta) + \sqrt{\lambda} h(\beta, \tilde{\phi}) - (\zeta_i, P_{,i})\end{aligned} \tag{5.4.14}$$

and

$$\delta D = -2\tilde{\gamma}(\Delta u_i, \zeta_i) - 2(\Delta\theta, \beta) - 2(\Delta\tilde{\phi}, \gamma) + 2(u_i, \zeta_i) + 2\eta(\tilde{\phi}, \gamma). \tag{5.4.15}$$

Thus, the Euler-Lagrange equations arise from the variational problem $(5.4.3)_1$ are

$$\begin{aligned} 2u_i - 2RR_E k_i\theta + R_s R_E f k_i\tilde{\phi} - 2\tilde{\gamma}\Delta u_i &= -R_E P_{,i} \\ -2\Delta\theta - 2R_E R w - \sqrt{\lambda} R_E h\tilde{\phi} &= 0 \\ -2\Delta\tilde{\phi} + 2\eta\tilde{\phi} + R_E R_s f w - \sqrt{\lambda} R_E h\theta &= 0, \end{aligned} \tag{5.4.16}$$

where P is a Lagrange multiplier. To remove the Lagrange multiplier, we take the double Curl of equation $(5.4.16)_1$ and retaining only the third component of the resulting equation to reduce (5.4.16) to studying the system

$$\begin{aligned} &\Delta w - RR_E\Delta^*\theta + \left(\frac{1 \pm \lambda}{2}\right) R_s R_E \Delta^*\phi - \tilde{\gamma}\Delta^2 w = 0 \ , \\ &\Delta\theta + R_E R w + R_E \frac{\lambda h}{2}\phi = 0 \ , \\ &(\Delta - \eta)\phi - R_E R_s \left(\frac{1 \pm \lambda}{2\lambda}\right) w + R_E \frac{h}{2}\theta = 0, \end{aligned} \tag{5.4.17}$$

where $\Delta^* = \partial^2/\partial x^2 + \partial^2/\partial y^2$ is the horizontal Laplacian. Introducing the normal mode representation as presented in section 5.3, system (5.4.17) becomes

$$\begin{aligned} &(D^2 - a^2)W - \tilde{\gamma}(D^2 - a^2)^2 W + a^2 R_E R\Theta - a^2 R_E R_s \left(\frac{1 \pm \lambda}{2}\right)\Phi = 0, \\ &R_E R W + (D^2 - a^2)\Theta + \left(\frac{h\lambda}{2}\right) R_E \Phi = 0, \\ &R_E R_s \left(\frac{1 \pm \lambda}{2\lambda}\right) W - \frac{h}{2} R_E\Theta + \eta\Phi - (D^2 - a^2)\Phi = 0. \end{aligned} \tag{5.4.18}$$

The Laplace operator is equivalent to $\Delta = D^2 - a^2$, where $D = \partial/\partial z$. The corresponding boundary conditions are

$$DW = W = \Theta = \Phi = 0 \ , \ on \ z = 0, 1. \tag{5.4.19}$$

We can determine the critical Rayleigh number given by $Ra_E^2 = \max_\lambda \min_{a^2} R^2(a^2, \lambda)$, where for all $R^2 < Ra_E^2$ the system is stable.

5.5 The Numerical Method

We used the D^2 Chebyshev Tau method, cf. Dongarra *et al.* [26], and the Compound Matrix technique to find the bound for the linear instability theory, system (5.3.3) and the corresponding boundary conditions (5.3.4). Both methods give exactly the same solution. For the energy theory I have used the Compound Matrix technique.

5.5.1 The D^2 Chebyshev Tau method for the linear theory

In this subsection, I describe the D^2 Chebyshev Tau method and in the next subsection I will describe the Compound Matrix method since I used it for the energy stability theory.

Using the D^2 Chebyshev to solve (5.3.3) subject to (5.3.4), we have to introduce a variable χ such that $\chi = \Delta w$. Then, equations (5.3.3) will be

$$\begin{aligned}
&(D^2 - a^2)W - \chi = 0,\\
&\tilde{\gamma}(D^2 - a^2)\chi - \chi - a^2 R\Theta + a^2 R_s\Phi = 0,\\
&(D^2 - a^2)\Theta + RW = \sigma\Theta,\\
&(D^2 - a^2)\Phi - \eta\Phi + h\Theta \mp R_s W = \varepsilon\sigma\Phi.
\end{aligned} \tag{5.5.1}$$

The functions W, χ, Θ and Φ are expanded in terms of Chebyshev polynomials

$$W(z) = \Sigma_{n=1}^{N} w_n T_n(z),\ \chi(z) = \Sigma_{n=1}^{N} \chi_n T_n(z),\ \Theta(z) = \Sigma_{n=1}^{N} \theta_n T_n(z),\ \Phi(z) = \Sigma_{n=1}^{N} \phi_n T_n(z).$$

Since $T_n(\pm 1) = (\pm 1)^n$, $T_n'(\pm 1) = (\pm 1)^{n-1} n^2$, implies that the boundary conditions (5.3.4) become

$$\begin{aligned}
&w_2 + w_4 + w_6 + \cdots + w_N = 0,\\
&w_1 + w_3 + w_5 + \cdots + w_{N-1} = 0
\end{aligned} \tag{5.5.2}$$

with similar representations for θ_n and ϕ_n

$$\begin{aligned}
&\theta_2 + \theta_4 + \theta_6 + \cdots + \theta_N = 0,\\
&\theta_1 + \theta_3 + \theta_5 + \cdots + \theta_{N-1} = 0,
\end{aligned} \tag{5.5.3}$$

$$\begin{aligned}
&\phi_2 + \phi_4 + \phi_6 + \cdots + \phi_N = 0,\\
&\phi_1 + \phi_3 + \phi_5 + \cdots + \phi_{N-1} = 0,
\end{aligned} \tag{5.5.4}$$

while the boundary condition $Dw = 0$ becomes

$$\begin{aligned} &2^2 w_2 + 4^2 w_4 + 6^2 w_6 + \cdots + N^2 w_N = 0, \\ &w_1 + 3^2 w_3 + 5^2 w_5 + \cdots + (N-1)^2 w_{N-1} = 0 \end{aligned} \tag{5.5.5}$$

Therefore, the Chebyshev Tau method reduces to solving the matrix system $A\mathbf{x} = \sigma B\mathbf{x}$, where $\mathbf{x} = (w_1, w_2, \cdots, w_N, \chi_1, \chi_2, \cdots, \chi_N, \theta_1, \cdots, \theta_N, \phi_1, \cdots, \phi_N)$ and the matrices A and B are given by

$$A = \begin{pmatrix} 4D^2 - a^2 I & -I & 0 & 0 \\ BC1 & 0\cdots 0 & 0\cdots 0 & 0\cdots 0 \\ BC2 & 0\cdots 0 & 0\cdots 0 & 0\cdots 0 \\ 0 & 4D^2 - a^2 I - \frac{I}{\tilde{\gamma}} & -a^2 R\frac{I}{\tilde{\gamma}} & a^2 R_s \frac{I}{\tilde{\gamma}} \\ BC7 & 0\cdots 0 & 0\cdots 0 & 0\cdots 0 \\ BC8 & 0\cdots 0 & 0\cdots 0 & 0\cdots 0 \\ RI & 0 & 4D^2 - a^2 I & 0 \\ 0\cdots 0 & 0\cdots 0 & BC3 & 0\cdots 0 \\ 0\cdots 0 & 0\cdots 0 & BC4 & 0\cdots 0 \\ \mp R_s I & 0 & hI & 4D^2 - (a^2+\eta)I \\ 0\cdots 0 & 0\cdots 0 & 0\cdots 0 & BC5 \\ 0\cdots 0 & 0\cdots 0 & 0\cdots 0 & BC6 \end{pmatrix}$$

$$B = \begin{pmatrix} 0 & 0 & 0 & 0 \\ 0\cdots 0 & 0\cdots 0 & 0\cdots 0 & 0\cdots 0 \\ 0\cdots 0 & 0\cdots 0 & 0\cdots 0 & 0\cdots 0 \\ 0 & 0 & 0 & 0 \\ 0\cdots 0 & 0\cdots 0 & 0\cdots 0 & 0\cdots 0 \\ 0\cdots 0 & 0\cdots 0 & 0\cdots 0 & 0\cdots 0 \\ 0 & 0 & I & 0 \\ 0\cdots 0 & 0\cdots 0 & 0\cdots 0 & 0\cdots 0 \\ 0\cdots 0 & 0\cdots 0 & 0\cdots 0 & 0\cdots 0 \\ 0 & 0 & 0 & \varepsilon I \\ 0\cdots 0 & 0\cdots 0 & 0\cdots 0 & 0\cdots 0 \\ 0\cdots 0 & 0\cdots 0 & 0\cdots 0 & 0\cdots 0 \end{pmatrix}$$

where in the matrix A the notations $BC1, BC2$ refer to the boundary conditions (5.5.2), $BC3, BC4$ refer to (5.5.3) , $BC5, BC6$ refer to (5.5.4) and $BC7, BC8$ refer to the boundary conditions (5.5.5). We solved the matrix system by the QZ algorithm, cf. Dongarra *et al.* [26].

5.5.2 The Compound Matrix technique for the energy theory

To employ the compound matrix method, cf. Lindsay & Straughan [56], we have to write system (5.4.18) as

$$\begin{aligned} D^4W &= -a^4W + 2a^2D^2W - \frac{a^2}{\tilde{\gamma}}W + \frac{1}{\tilde{\gamma}}D^2W + R_ER\frac{a^2}{\tilde{\gamma}}\Theta - \frac{a^2}{\tilde{\gamma}}\left(\frac{1\pm\lambda}{2}\right)R_ER_s\Phi, \\ D^2\Theta &= a^2\Theta - R_ERW - \left(\frac{h\lambda}{2}\right)R_E\Phi, \\ D^2\Phi &= \left(a^2+\eta\right)\Phi - \frac{h}{2}R_E\Theta + \left(\frac{1\pm\lambda}{2\lambda}\right)R_ER_sW. \end{aligned} \tag{5.5.6}$$

The compound matrix for (5.5.6) works with the 4×4 minors of the 8×4 solution matrix formed from

$$\begin{aligned} U_1 &= (W_1, W_1', W_1'', W_1''', \Theta_1, \Theta_1', \Phi_1, \Phi_1'), \\ U_2 &= (W_2, W_2', W_2'', W_2''', \Theta_2, \Theta_2', \Phi_2, \Phi_2'), \\ U_3 &= (W_3, W_3', W_3'', W_3''', \Theta_3, \Theta_3', \Phi_3, \Phi_3'), \\ U_4 &= (W_4, W_4', W_4'', W_4''', \Theta_4, \Theta_4', \Phi_4, \Phi_4'). \end{aligned} \tag{5.5.7}$$

The solutions U_i for $i = 1, 2, 3, 4$ are independent solutions to (5.5.6) for different initial values, U_i's correspond to solutions for starting values

$$(0,0,1,0,0,0,0,0)^T \ , \ (0,0,0,1,0,0,0,0)^T,$$

$$(0,0,0,0,0,1,0,0)^T \ , \ (0,0,0,0,0,0,0,1)^T,$$

respectively. We define $C_4^8 = 70$ new variables $y_1, \cdots, y_{70}$ as the 4×4 minors. For example

$$y_1 = \begin{vmatrix} W_1 & W_2 & W_3 & W_4 \\ W_1' & W_2' & W_3' & W_4' \\ W_1'' & W_2'' & W_3'' & W_4'' \\ W_1''' & W_2''' & W_3''' & W_4''' \end{vmatrix}$$

implies that $y_1 = W_1 W_2' W_3'' W_4''' + \cdots$, which gives 24 terms for y_1. So, the idea is to derive $y_2, \cdots, y_{70}$ similarly and then obtain differential equations for the y_i's by differentiation. There is no need to write out the whole determinant each time. The first term, y_1, suffices. The 70 variables are included in Appendix C. By differentiating each y_i and substituting from equations (5.5.6) we obtain differential equations for the y_i's, see Appendix C. These equations are integrated numerically from 0 *to* 1. We keep the boundary conditions (5.4.19) at $z = 0$ and replace the ones at $z = 1$ by

$$W_1''(0) = W_2'''(0) = \Theta_3'(0) = \Phi_4'(0) = 1, \tag{5.5.8}$$

which using the y_i's yields the initial condition for the y_i''s as

$$y_{60}(0) = 1. \tag{5.5.9}$$

Using y_i's, the final condition which satisfies (5.4.19) is seen to be

$$y_{11}(1) = 0. \tag{5.5.10}$$

The eigenvalue R is varied until (5.5.10) is satisfied to some pre-assigned tolerance. For more details on the compound matrix method and it's application on solving boundary value problems, the reader may refer to the books of Straughan, chapter 19 of Straughan [99] and chapter 9 of Straughan [100], and the article by Lindsay & Straughan [56].

5.6 Numerical Results and Conclusion

In this section, analysis of the numerical results of two different systems, heated below-salted above and heated below-salted below separately is reported in the fol-

lowing subsections. Numerical data and graphical figures are included to support the analysis.

5.6.1 Heated below salted above system

The numerical integration is carried out for different values of the reaction rates, h *and* η and different values of the Brinkman coefficient $\tilde{\gamma}$. We found that when the layer is heated below and salted above in the case of no reaction *i.e.* $h = \eta = 0$ and when Brinkman coefficient $\tilde{\gamma} = 1$ that the numerical methods used give exactly the same values for Ra_L and Ra_E. The graphical representation of these values shows that the linear instability threshold coincide with the energy stability threshold as it is clear in figure $(5.1)(a)$ and that there is no region of subcritical instability. As we increase the values of the reaction rates h and η, the linear instability boundary starts to diverge from the energy stability boundary. Figure (5.1) shows the effect of increasing the values of the reaction rates, as we increase the values of h and η, the gap between the boundaries increases. Any point (Rs^2, Ra^2) in the space above the linear instability boundary, the solid line Ra_L^2, represents a region where the system is unstable because the linear instability boundary guarantees instability. On the other hand, if (Rs^2, Ra^2) lies below the energy stability boundary, the dashed line Ra_E^2, represents the space where the system is definitely stable. Note that as the reaction rates increase, the peak of the linear instability curve moves to a higher position resulting in a wider region of possible subcritical instability between the energy stability threshold and the linear instability threshold. Moreover, there is a slight noticeable decrease in the energy stability threshold as the values of $R_s \to +\infty$. Table 5.1 represents some numerical values obtained.

To study the effect of each one of h and η on the stability of the system, a bigger difference between their values is considered. It has been noticed that when h is bigger compared to η, the region of possible subcritical instability is wider and increasing the value of h implies more divergence of the linear instability boundary from the energy stability boundary and a movement of the peak value of the linear instability threshold to a higher position, as figure $(5.2)(a)$ *and* (c) shows. Com-

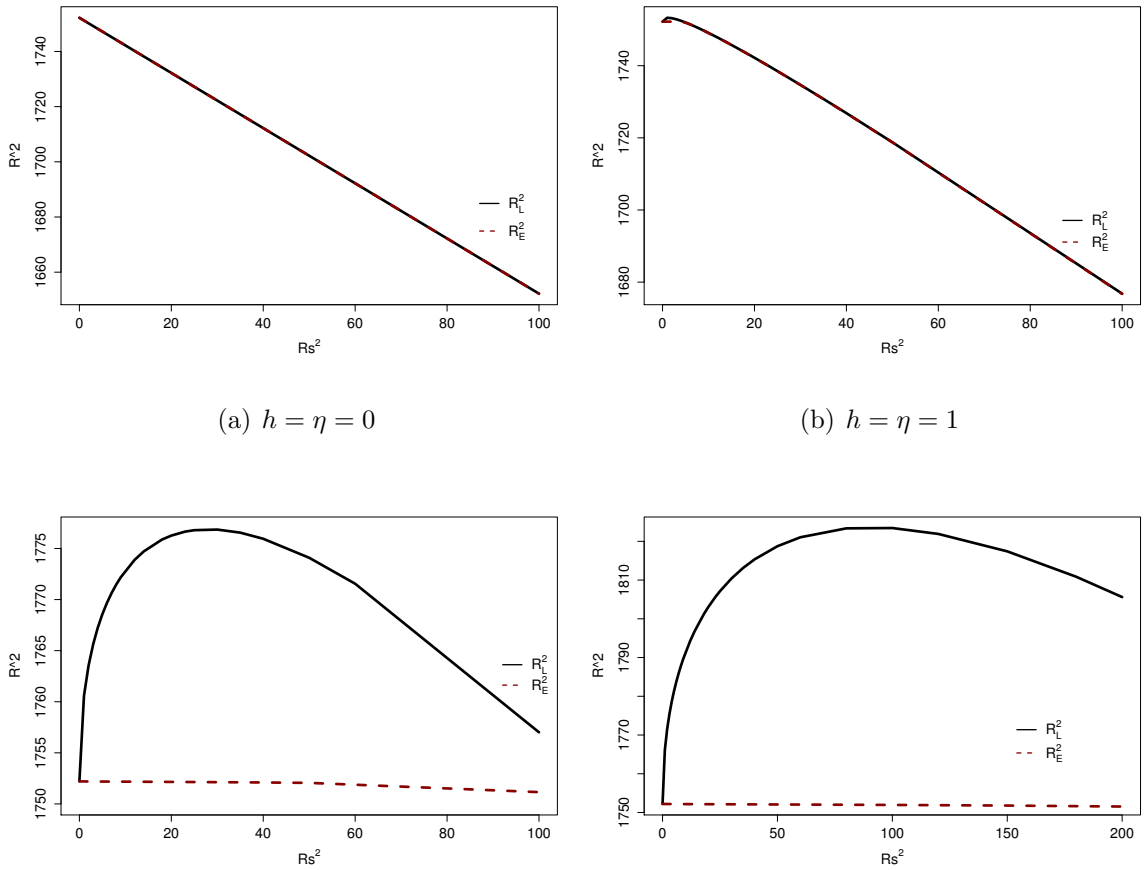

(a) $h = \eta = 0$

(b) $h = \eta = 1$

(c) $h = 5\ ,\ \eta = 3$

(d) $h = 9\ ,\ \eta = 6$

Figure 5.1: Linear instability and energy stability boundaries for the salted above Brinkman convection problem for different values of the reaction rates h and η.

pared to the case when η has a bigger value than h, the linear and energy boundaries coincide, figure (5.2)(b) *and* (d) and the linear boundary covers the content of stability. This is expected, as system (5.2.11) shows that $h\Theta$ is a destabilizing term while $-\eta\Phi$ is a stabilizing term.

Examining the effect of different values of the Brinkman coefficient (effective viscosity term) on the stability boundaries, reveals that increasing the value of $\tilde{\gamma}$ results in a wider space of global stability below the energy stability threshold and a wider region of potential subcritical instability. The effect of different values of $\tilde{\gamma}(= 0.5, 2)$ are presented graphically in figures (5.3), (5.4) and (5.5).

R_s^2	a_L	Ra_L^2	a_E	Ra_E^2	λ
1	3.13	1766.156	3.12	1752.197	0.055
3	3.13	1775.442	3.12	1752.187	0.099
5	3.14	1781.378	3.12	1752.179	0.132
6	3.14	1783.775	3.12	1752.175	0.146
12	3.15	1794.255	3.12	1752.157	0.220
20	3.15	1803.123	3.12	1752.137	0.304

Table 5.1: Some numerical values obtained for the linear boundary Ra_L and energy boundary Ra_E temperature Rayleigh number with corresponding salt Rayleigh number R_s and the the corresponding critical wave numbers a_L and a_E when $\tilde{\gamma} = 1$, $h = 9$ and $\eta = 6$ in the case of heated below salted above system.

5.6.2 Heated and Salted Below system

It is instructive to write system (5.2.11) and the boundary conditions (5.2.12) for the salted below case as an abstract equation of form

$$A\mathbf{u}_t = L(\mathbf{u}) + N(\mathbf{u}),$$

where $\mathbf{u} = (u_1, u_2, u_3, \theta, \phi)$, $N(\mathbf{u})$ represents the nonlinear terms in (5.2.11) so

$$N(\mathbf{u}) = \begin{pmatrix} 0 \\ 0 \\ 0 \\ -u_i\theta_{,i} \\ -\frac{Le}{\hat{\phi}}u_i\phi_{,i} \end{pmatrix},$$

and L is the linear operator. In fact, the linear operator for (5.2.11) is

$$L = \begin{pmatrix} -1+\tilde{\gamma}\Delta & 0 & 0 & 0 & 0 \\ 0 & -1+\tilde{\gamma}\Delta & 0 & 0 & 0 \\ 0 & 0 & -1+\tilde{\gamma}\Delta & R & -R_s \\ 0 & 0 & R & \Delta & 0 \\ 0 & 0 & R_s & h & \Delta-\eta \end{pmatrix}.$$

We may split L into a symmetric plus skew-symmetric parts as follows

$$L = L_s + L_A \ ,$$

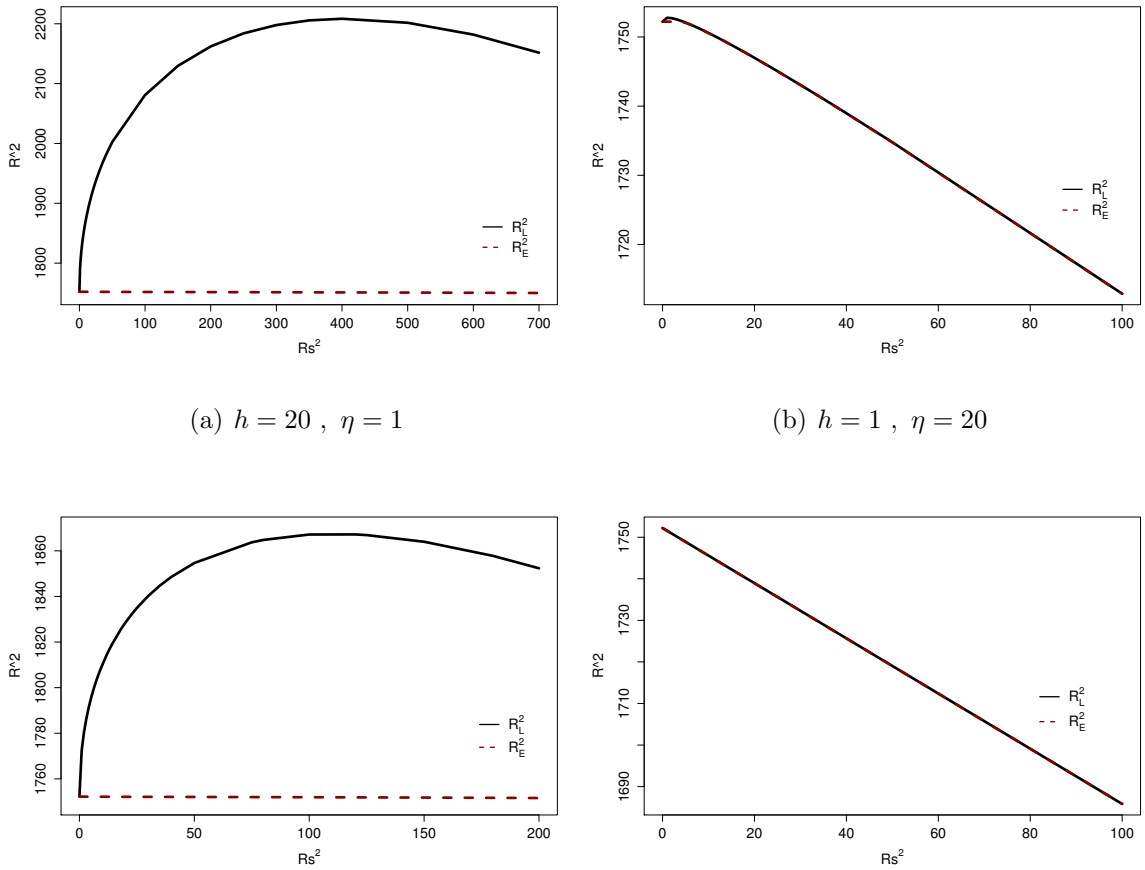

(a) $h = 20\ ,\ \eta = 1$

(b) $h = 1\ ,\ \eta = 20$

(c) $h = 10\ ,\ \eta = 0$

(d) $h = 0\ ,\ \eta = 10$

Figure 5.2: Linear instability and energy stability boundaries for the salted above Brinkman convection problem. The difference between the values of the reaction rates h and η is large.

where

$$L_s = \begin{pmatrix} -1+\tilde{\gamma}\Delta & 0 & 0 & 0 & 0 \\ 0 & -1+\tilde{\gamma}\Delta & 0 & 0 & 0 \\ 0 & 0 & -1+\tilde{\gamma}\Delta & R & 0 \\ 0 & 0 & R & \Delta & \frac{h}{2} \\ 0 & 0 & 0 & \frac{h}{2} & \Delta-\eta \end{pmatrix},$$

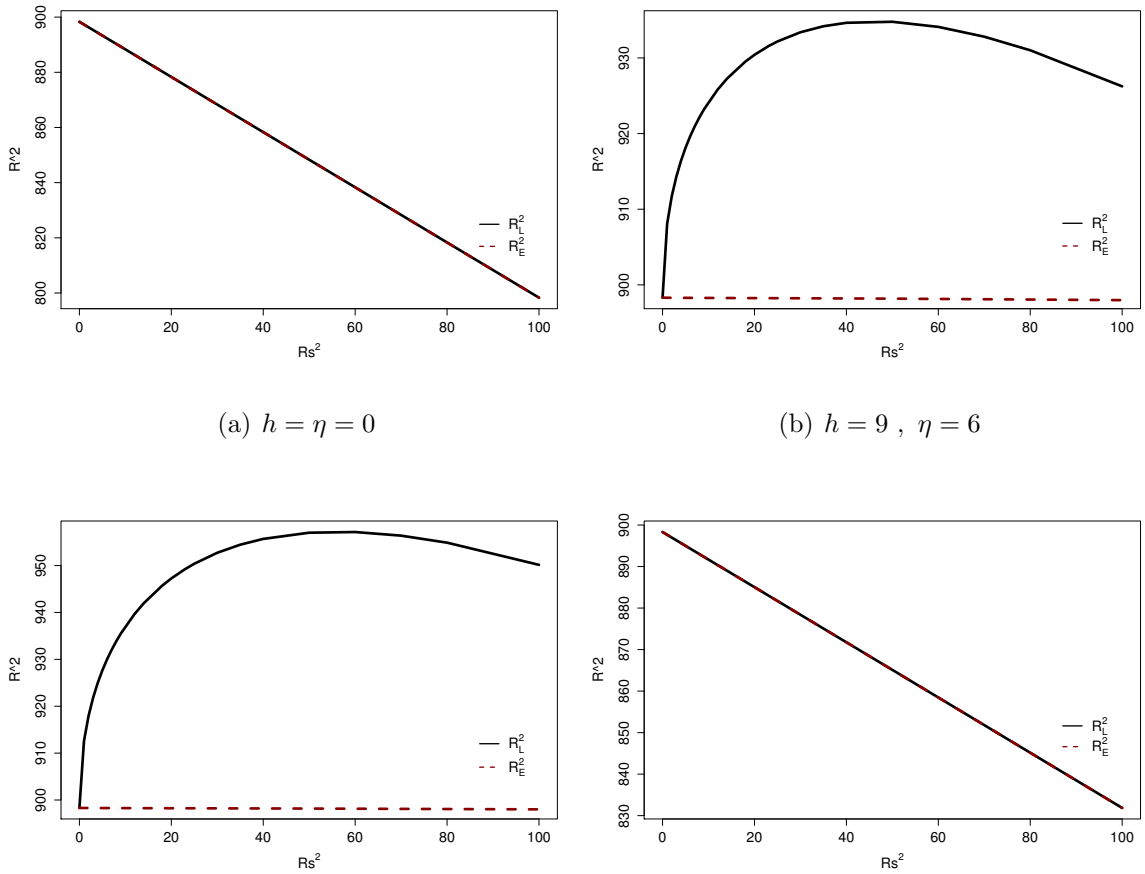

(a) $h = \eta = 0$

(b) $h = 9\ ,\ \eta = 6$

(c) $h = 10\ ,\ \eta = 0$

(d) $h = 0\ ,\ \eta = 10$

Figure 5.3: Linear instability and energy stability boundaries for the salted above Brinkman convection problem when the Brinkman constant $\tilde{\gamma}$ is 0.5.

and

$$L_A = \begin{pmatrix} 0 & 0 & 0 & 0 & 0 \\ 0 & 0 & 0 & 0 & 0 \\ 0 & 0 & 0 & 0 & -R_s \\ 0 & 0 & 0 & 0 & -\frac{h}{2} \\ 0 & 0 & R_s & \frac{h}{2} & 0 \end{pmatrix}.$$

For the salted above case, see the previous subsection, L_A would be zero and the analogous linear operator L would be symmetric.

Even when $h = 0$ in the salted below case, we expect some problem with non-linear energy stability theory since

$$(\mathbf{u}, L(\mathbf{u})) \neq (\mathbf{u}, L_s(\mathbf{u}))$$

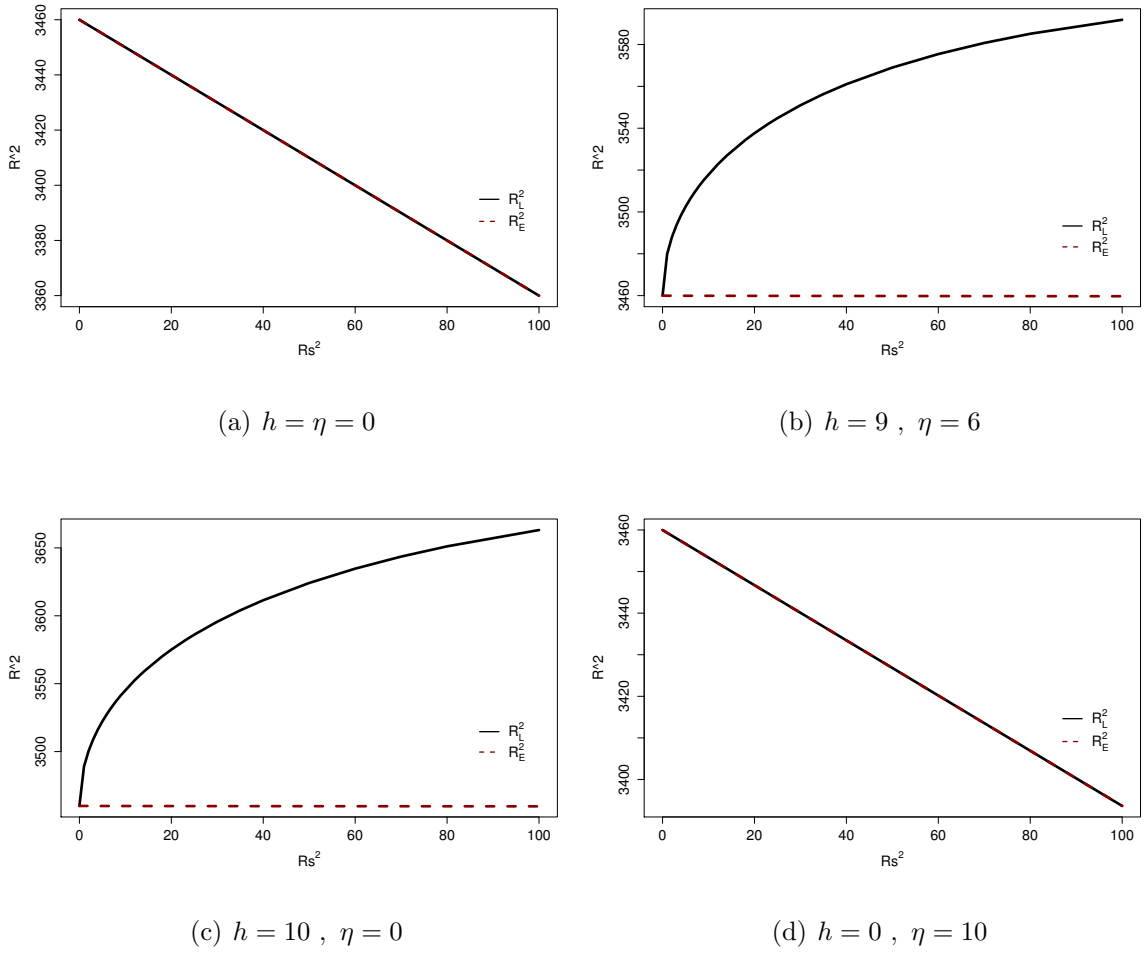

(a) $h = \eta = 0$

(b) $h = 9\ ,\ \eta = 6$

(c) $h = 10\ ,\ \eta = 0$

(d) $h = 0\ ,\ \eta = 10$

Figure 5.4: Linear instability and energy stability boundaries for the salted above Brinkman convection problem when the Brinkman constant $\tilde{\gamma}$ is 2.

where $(\cdot, \cdot)$ is the inner product on $(H^1(V))^5$ with V being a period cell for the solution. For the problem of this subsection, governed by equations (5.2.11) and (5.2.12) for the salted below case, we have two sources of anti-symmetry, the R_s term and the h term.

The numerical values are presented graphically for different values of the reaction rates h and η in figure (5.6). It has been noticed that as the reaction rate increases, the gap between the linear instability and energy stability boundaries increases due to the divergence of the linear threshold yielding a wider region of potential subcritical instability. Whereas, the energy stability threshold is approximately constant or more precisely it is decreasing unnoticeably as shown in figures (5.6) and (5.7). As expected from system (5.2.11) one sees that $h\Theta$ will destabilize the system while

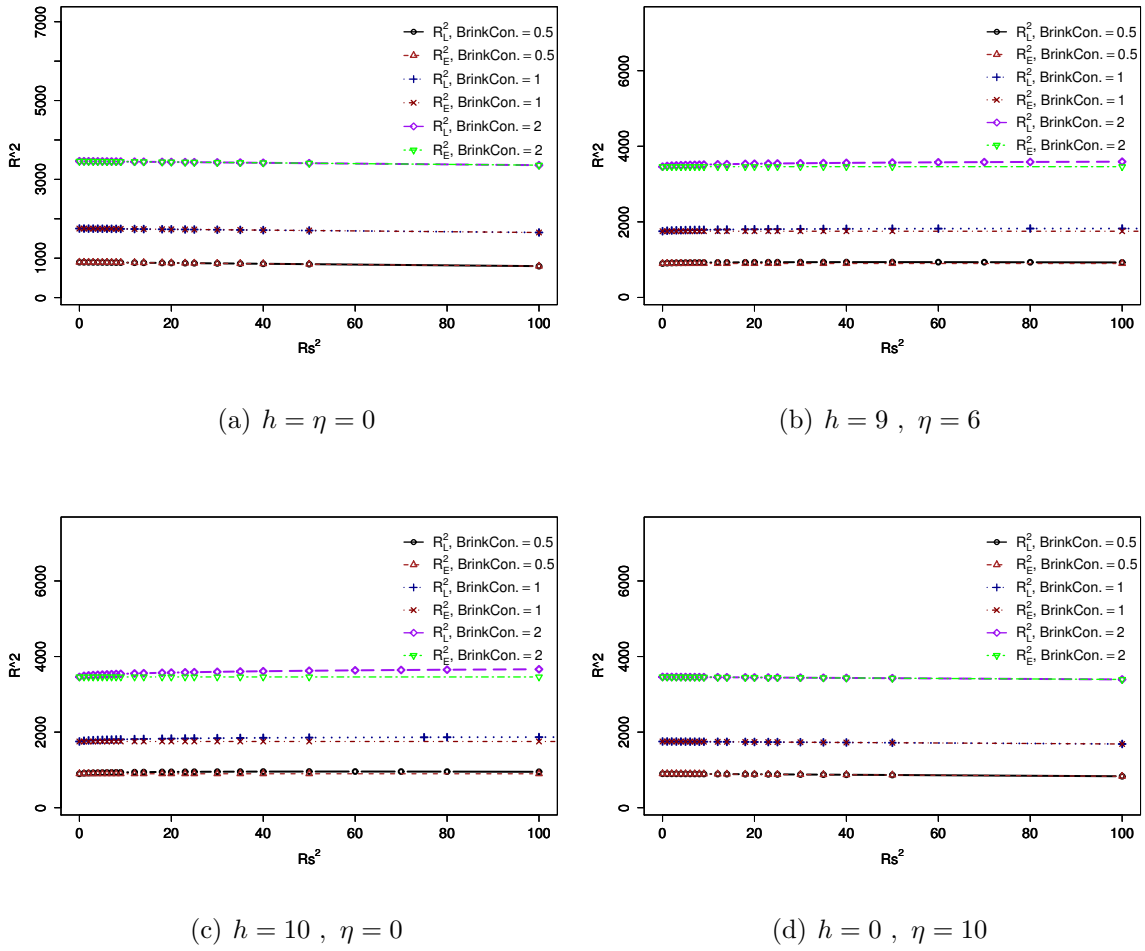

(a) $h = \eta = 0$ (b) $h = 9\ ,\ \eta = 6$

(c) $h = 10\ ,\ \eta = 0$ (d) $h = 0\ ,\ \eta = 10$

Figure 5.5: Linear instability and energy stability boundaries for the salted above Brinkman convection problem for different values of the Brinkman constant, $\tilde{\gamma} = 0.5, 1, 2$.

$-\eta\Phi$ will stabilize the system which is clear and shown in figure (5.7) *i.e,* when the value of h is smaller compared to η the space of possible subcritical instability is less compared to the case when h is larger than η. The effect of changing the value of $\tilde{\gamma}$ can be noticed in figure (5.8) for $\tilde{\gamma} = 0.5$ and figure (5.9) for $\tilde{\gamma} = 2$. The gap between the boundaries increases and the space of global stability is wider as $\tilde{\gamma}$ increases.
The numerical values and their graphical representations show that the linear instability theory does not necessarily represent accurately the onset of convection and we may explain that this is due to the two sources of anti-symmetry the R_s term and the h term. By this we mean that the linear instability boundary is definitely a threshold for instability, but in this case, it may be possible for instability to arise

with a Rayleigh number below the linear instability boundary.

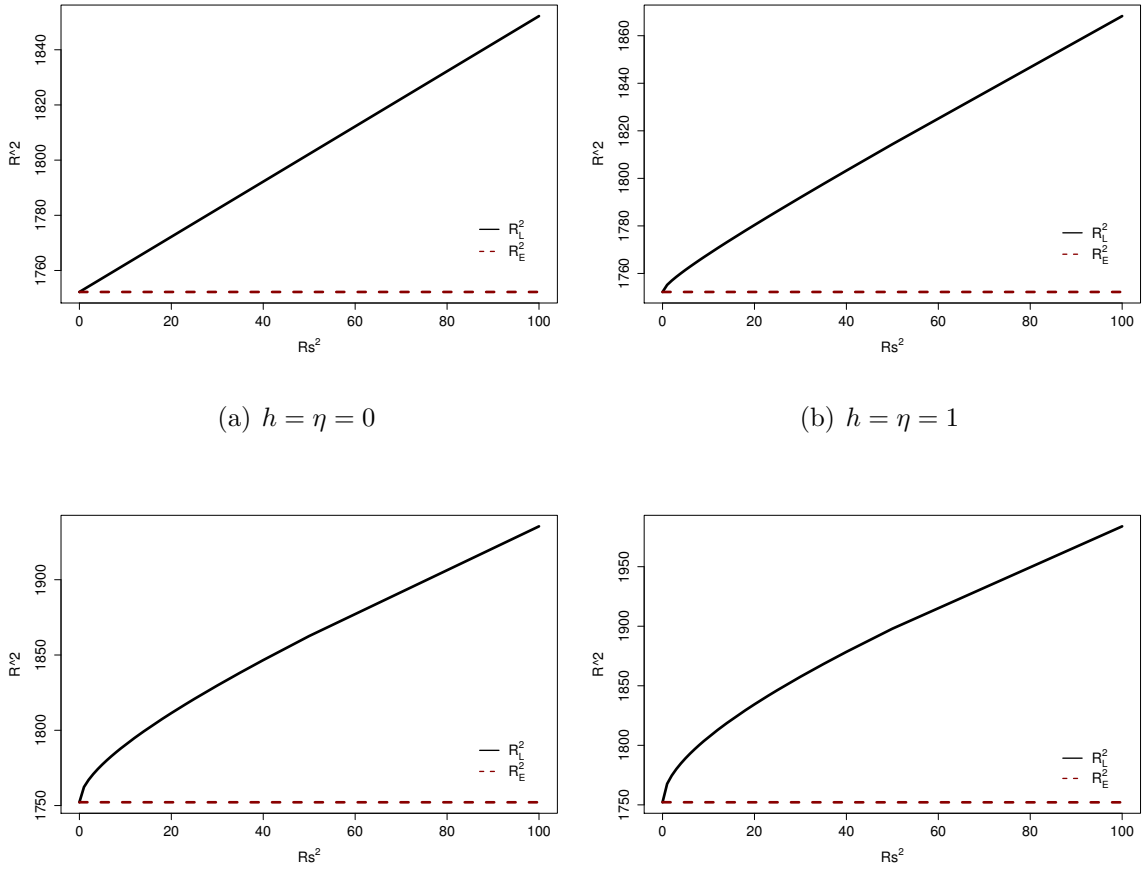

(a) $h = \eta = 0$ (b) $h = \eta = 1$

(c) $h = 5\ ,\ \eta = 3$ (d) $h = 9\ ,\ \eta = 6$

Figure 5.6: Linear instability and energy stability boundaries for the salted below Brinkman convection problem for different values of the reaction rates h and η.

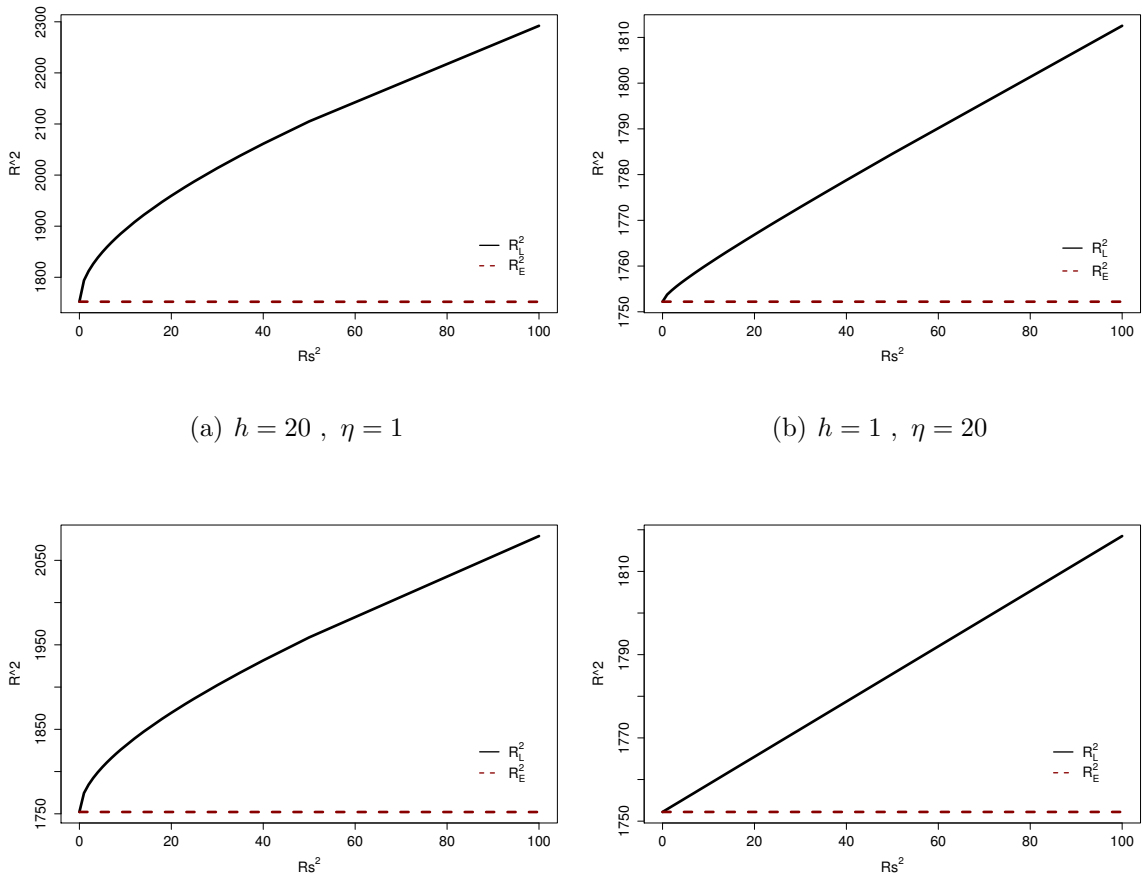

(a) $h = 20$, $\eta = 1$

(b) $h = 1$, $\eta = 20$

(c) $h = 10$, $\eta = 0$

(d) $h = 0$, $\eta = 10$

Figure 5.7: Linear instability and energy stability boundaries for the salted below Brinkman convection problem. The difference between the values of the reaction rates h and η is large.

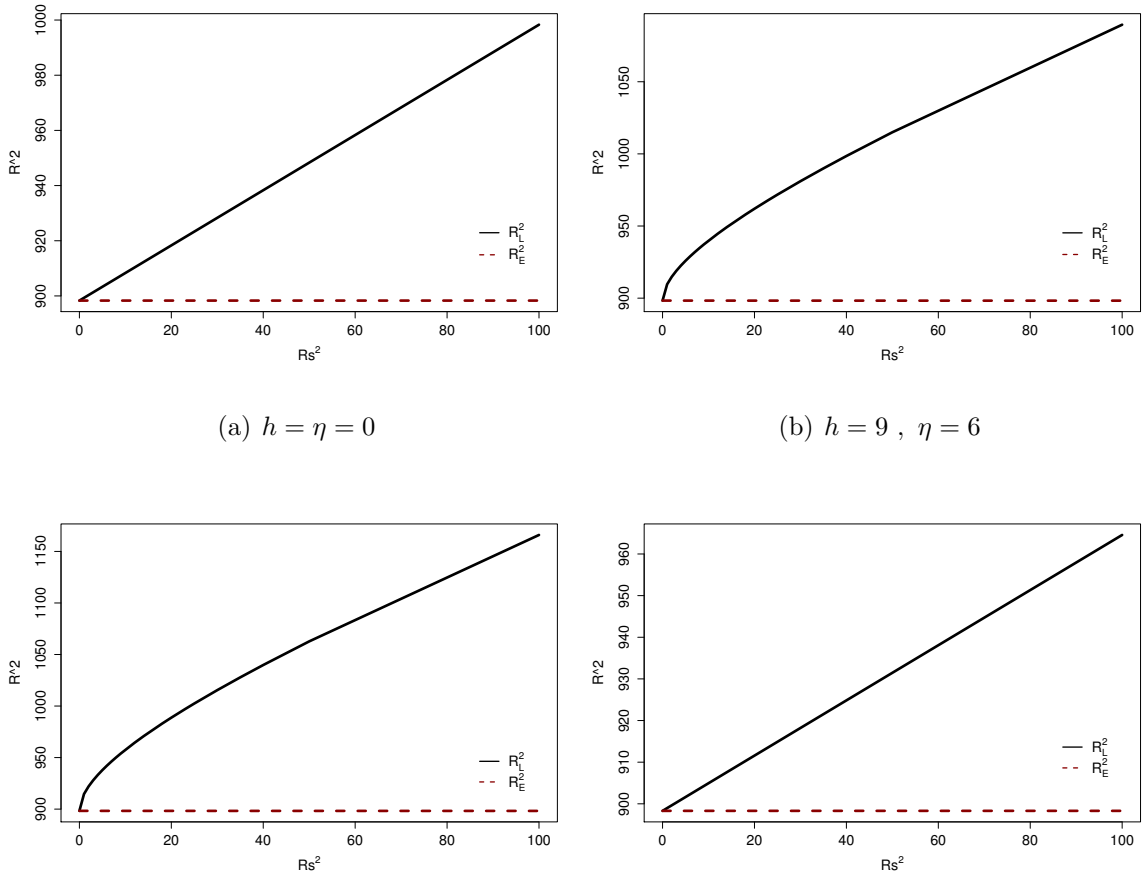

(a) $h = \eta = 0$

(b) $h = 9\ ,\ \eta = 6$

(c) $h = 10\ ,\ \eta = 0$

(d) $h = 0\ ,\ \eta = 10$

Figure 5.8: Linear instability and energy stability boundaries for the salted below Brinkman convection problem when the Brinkman constant $\tilde{\gamma}$ is 0.5.

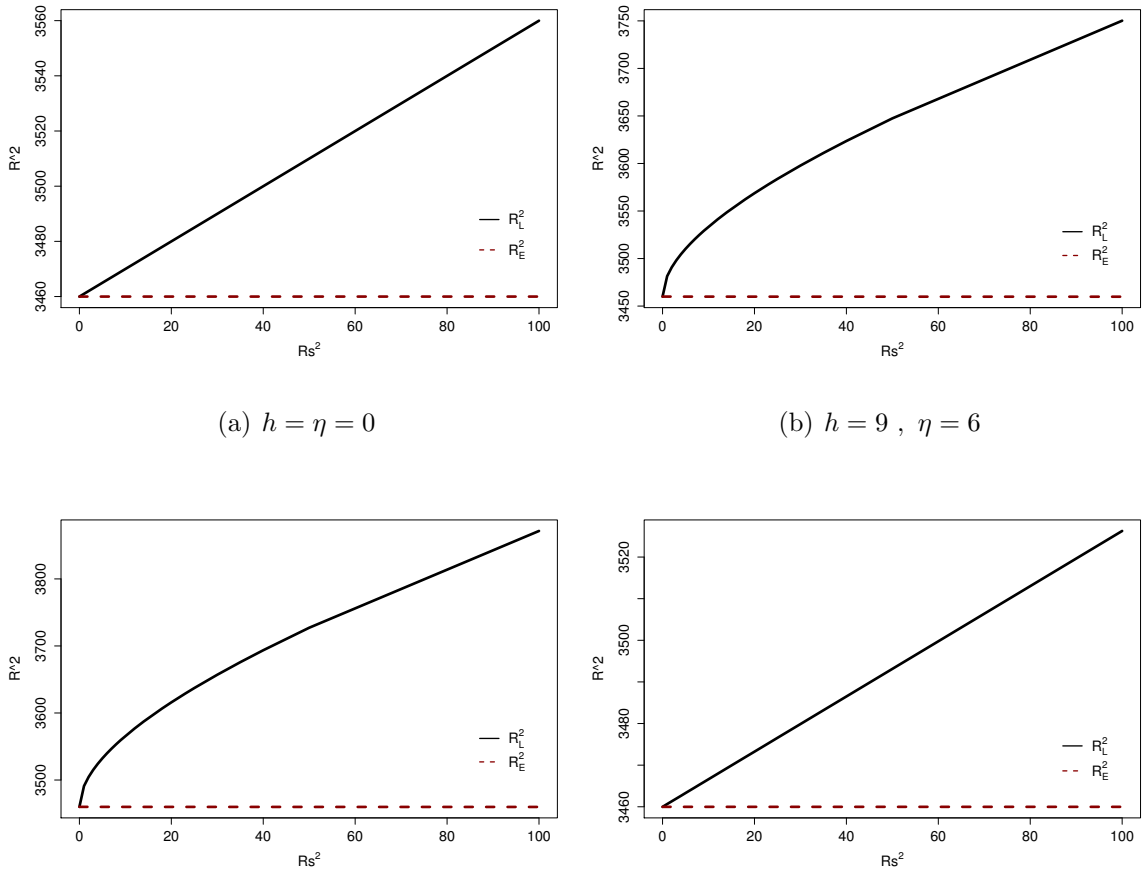

(a) $h = \eta = 0$

(b) $h = 9\ ,\ \eta = 6$

(c) $h = 10\ ,\ \eta = 0$

(d) $h = 0\ ,\ \eta = 10$

Figure 5.9: Linear instability and energy stability boundaries for the salted below Brinkman convection problem when the Brinkman constant $\tilde{\gamma}$ is 2.

Chapter 6

Thermosolutal Convection in a Darcy Porous Medium with Anisotropic Permeability and Thermal Diffusivity

6.1 Introduction

In chapters 4 and 5 we used the energy method to study the non-linear stability of the Darcy and the Brinkman thermosoultal convection with reaction, respectively, where the porous media were isotropic. Malashetty and Biradar [60] studied the onset of the double-diffusive reaction convection in an anisotropic porous medium of a Darcy type considering a model similar to that of Pritchard and Richardson [83]. They analysed the linear and weak non-linear stability of a reactive binary mixture in a horizontal porous layer with anisotropic permeability and thermal diffusivity. The work in this chapter may be considered as an extension of Malashetty and Biradar [60]. Our concern is to use the energy method to study the nonlinear stability aspect of the problem. The aim of the study is to obtain the non-linear stability boundaries below which the solution is globally stable. We analyse and compare the effects of the reaction terms, the anisotropic permeability, and thermal diffusivity tensors on the onset of stability with the relevant results obtained by

Malashetty and Biradar [60].

6.2 Basic Equations

We consider an anisotropic porous layer of Darcy model for the momentum equation with the density ρ being a linear function in temperature T and salt concentration C. In addition we need the continuity equation, the advection-diffusion equation for the transport of heat and the advection-diffusion equation for the transport of solute with reaction. The governing system of equations is

$$\begin{aligned} \mu v_i &= -K_{ij}p_{,j} - K_{ij}k_j g\rho_0[1 - \alpha_T(T - T_0) + \alpha_C(C - C_0)], \\ v_{i,i} &= 0, \\ \frac{1}{\tilde{M}}T_{,t} + v_i T_{,i} &= (k_{Tij}T_{,j})_{,i}, \\ \hat{\phi}C_{,t} + v_i C_{,i} &= \hat{\phi}k_C\Delta C + \hat{k}[f_1(T - T_0) + f_0 - C], \end{aligned} \tag{6.2.1}$$

where as mentioned in the previous chapters, $v_i, p, T, C, \mu, \rho_0$ are the velocity, pressure, temperature, salt concentration, the fluid viscosity and the fluid density respectively. Moreover, $K = K_x ii + K_y jj + K_z kk$ is the permeability tensor, $k_T = k_{Tx}ii + k_{Ty}jj + k_{Tz}kk$ is the thermal diffusivity tensor, k_C is the molecular diffusivity of the solute through the fluid and $\hat{k}$ is the reaction rate. The system is taken in the domain $\mathcal{R}^2 \times (0, d) \times \{t > 0\}$, and the corresponding boundary conditions are

$$\begin{aligned} &v_i n_i = 0 \ on \ z = 0, d, \\ &T = T_L \ on \ z = 0, \ and \ T = T_U \ on \ z = d, \\ &C = C_L \ on \ z = 0, \ and \ C = C_U \ on \ z = d. \end{aligned} \tag{6.2.2}$$

Where $T_L > T_U$ since we are considering the heated below case, while $C_U > C_L$ for the salted above system and $C_L > C_U$ for the salted below system. The steady state

whose stability is under investigation is

$$\begin{aligned}
\bar{v}_i =& 0, \\
\bar{T}(z) =& -\beta_T z + T_L, \\
\bar{C}(z) =& -\beta_C z + C_L, \\
\bar{p}(z) =& -\frac{1}{2} g\rho_0(\alpha_T\beta_T - \alpha_C\beta_C)z^2 \\
& - g\rho_0[1 - \alpha_T(T_L - T_0) + \alpha_C(C_L - C_0)]z + p_0,
\end{aligned} \tag{6.2.3}$$

where $\beta_T = (T_L - T_U)/d$, $\beta_C = (C_L - C_U)/d$, and p_0 is the pressure at $z = 0$.

To study the stability, we introduce perturbations (u_i, π, θ, ϕ) to the steady solutions (6.2.3) in such a way that

$$\begin{aligned}
v_i &= \bar{v}_i + u_i, \\
p &= \bar{p} + \pi, \\
T &= \bar{T} + \theta, \\
C &= \bar{C} + \phi
\end{aligned} \tag{6.2.4}$$

Substituting (6.2.4) in (6.2.1) and using (6.2.3) we derive the equations governing (u_i, π, θ, ϕ) as

$$\begin{aligned}
\mu u_i &= K_{ij}k_j g\rho_0\alpha_T\theta - K_{ij}k_j g\rho_0\alpha_C\phi - K_{ij}\pi_{,j} \ , \\
u_{i,i} &= 0 \ , \\
\frac{1}{\tilde{M}}\theta_{,t} + u_i\theta_{,i} &= \beta_T w + (k_{Tij}\theta_{,j})_{,i} \ , \\
\hat{\phi}\phi_{,t} + u_i\phi_{,i} &= \beta_C w + \hat{\phi}k_C\Delta\phi + \hat{k}f_1\theta - \hat{k}\phi,
\end{aligned} \tag{6.2.5}$$

where $w = u_3$. We introduce an inverse permeability tensor M_{ij} which satisfies

$$M_{ij}K_{jk} = \delta_{ik},$$

where

$$M_{ij} = \begin{pmatrix} \kappa & 0 & 0 \\ 0 & \kappa & 0 \\ 0 & 0 & \kappa_3 \end{pmatrix} \ ; \ \kappa \neq \kappa_3.$$

In terms of the inverse permeability tensor M_{ij}, equations (6.2.5) are equivalent to

$$\begin{aligned} M_{ij}\mu u_j &= -\pi_{,i} + k_i g\rho_0\alpha_T\theta - k_i g\rho_0\alpha_C\phi \ , \\ u_{i,i} &= 0 \ , \\ \frac{1}{\tilde{M}}\theta_{,t} + u_i\theta_{,i} &= \beta_T w + (k_{Tij}\theta_{,j})_{,i} \ , \\ \hat{\phi}\phi_{,t} + u_i\phi_{,i} &= \beta_C w + \hat{\phi}k_C\Delta\phi + \hat{k}f_1\theta - \hat{k}\phi. \end{aligned} \tag{6.2.6}$$

To non-dimensionalize equations (6.2.6), we define the non-dimensional variables

$$\begin{aligned} &\pi = P\pi^*, \ u_i = Uu_i^*, \ \theta = T^\sharp\theta^*, \\ &\phi = C^\sharp\phi^*, \ x_i = dx_i^*, \ t = \tau t^*. \end{aligned} \tag{6.2.7}$$

Employing (6.2.7) in (6.2.6), choose the time, velocity, pressure, temperature and salt scales as

$$\begin{aligned} \tau = \frac{d}{\tilde{M}U} \ , \ U = \frac{k_{Tz}}{d} \ , \ P = dU\mu \ , \\ T^{\sharp^2} = \frac{\beta_T\mu k_{Tz}}{g\rho_0\alpha_T} \ , \ C^{\sharp^2} = \frac{\beta_C\mu k_{Tz}}{g\rho_0\alpha_C} \ , \end{aligned}$$

and define the temperature and salt Rayleigh numbers by

$$R = \sqrt{\frac{g\rho_0\alpha_T\beta_T d^2}{\mu k_{Tz}}},$$

$$R_s = \sqrt{\frac{g\rho_0\alpha_C|\beta_C|d^2Le}{\mu k_{Tz}\hat{\phi}}} \ when \ C_L < C_U \ or \ R_s = \sqrt{\frac{g\rho_0\alpha_C\beta_C d^2Le}{\mu k_{Tz}\hat{\phi}}} \ when \ C_L > C_U,$$

where $Le = k_{Tz}/k_C$ is the Lewis number.

The non-linear, non-dimensional system of equations, after dropping the stars, is

$$\begin{aligned} M_{ij}u_j &= -\pi_{,i} + k_i R\theta - k_i R_s\phi \ , \\ u_{i,i} &= 0 \ , \\ \theta_{,t} + u_i\theta_{,i} &= Rw + \alpha\Delta^*\theta + D^2\theta \ , \\ \varepsilon\phi_{,t} + \frac{Le}{\hat{\phi}}u_i\phi_{,i} &= \mp R_s w + \Delta\phi + h\theta - \eta\phi \ , \end{aligned} \tag{6.2.8}$$

where $\alpha = k_{Tx}/k_{Tz}$, $\varepsilon = \tilde{M}Le$, $D = d/dz$, Δ^* is the horizontal Laplacian and h and η are the reaction coefficients

$$h = \frac{\hat{k}f_1T^\sharp d^2Le}{k_{Tz}C^\sharp\hat{\phi}} \ and \ \eta = \frac{\hat{k}d^2Le}{k_{Tz}\hat{\phi}}.$$

Moreover, $-R_s$ for the salted above system and $+R_s$ for the salted below system. The corresponding boundary conditions are

$$u_i n_i = 0 \ , \ \theta = 0 \ , \ \phi = 0 \ at \ z = 0, 1 \ , \tag{6.2.9}$$

with $\{u_i, \theta, \phi\}$ satisfying a plane tiling periodicity in (x, y) direction.

6.3 Linear Instability Theory

In order to study the linear instability, we drop the non-linear terms in system (6.2.8) and retain the third component of the double curl of equation $(6.2.8)_1$ to reduce (6.2.8)-(6.2.9) to investigating the system

$$\begin{aligned} -\kappa w_{,zz} - \kappa_3 \Delta^* w &= -R\Delta^* \theta + R_s \Delta^* \phi \ , \\ \theta_{,t} &= Rw + \alpha \Delta^* \theta + D^2 \theta \ , \\ \varepsilon \phi_{,t} &= \mp R_s w + \Delta \phi + h\theta - \eta \phi \ . \end{aligned} \tag{6.3.1}$$

Following the same procedure as in the previous chapters and assuming a normal mode representation, system (6.3.1) is

$$\begin{aligned} &(D^2 - \frac{a^2 \kappa_3}{\kappa}) W + \frac{a^2}{\kappa} R\Theta - \frac{a^2}{\kappa} R_s \Phi = 0 \ , \\ &\sigma \Theta = RW + (D^2 - a^2 \alpha)\Theta \ , \\ &\varepsilon \sigma \Phi = \mp R_s W + (D^2 - a^2 - \eta)\Phi + h\Theta \ . \end{aligned} \tag{6.3.2}$$

Equations (6.3.2) are to be solved subject to the boundary conditions

$$W = \Theta = \Phi = 0 \ on \ z = 0, 1 \ , \tag{6.3.3}$$

using D^2 Chebyshev-Tau method, cf. Dongarra *et al.* [26]. The numerical method and the analysis are presented in sections 6.5 and 6.6.

6.4 Non-Linear Energy Stability Theory

Returning to the non-linear, non-dimensional perturbed system of equations (6.2.8) and the corresponding boundary conditions (6.2.9). Multiplying equation $(6.2.8)_1$ by

u_i, equation $(6.2.8)_3$ by θ and equation $(6.2.8)_4$ by ϕ and integrate over the domain using integration by parts to obtain the following system of balance equations

$$\begin{aligned} &-(M_{ij}u_j, u_i) + R(\theta, w) - R_s(\phi, w) = 0 \ , \\ &\frac{d}{dt}\frac{1}{2}\|\theta\|^2 = R(\theta, w) - \alpha\|\nabla\theta\|^2 - (1-\alpha)\|\theta_{,z}\|^2 \ , \\ &\frac{d}{dt}\frac{\varepsilon}{2}\|\phi\|^2 = \mp R_s(\phi, w) - \|\nabla\phi\|^2 + h(\theta, \phi) - \eta\|\phi\|^2. \end{aligned} \tag{6.4.1}$$

We form the combination of equations (6.4.1) as

$$(6.4.1)_1 + (6.4.1)_2 + \lambda(6.4.1)_3,$$

where λ is a coupling parameter, to derive the energy identity in the form

$$\frac{dE}{dt} = I - D \ , \tag{6.4.2}$$

where

$$\begin{aligned} &E(t) = \frac{1}{2}\|\theta\|^2 + \frac{\varepsilon\lambda}{2}\|\phi\|^2 \ , \\ &I = 2R(\theta, w) + \lambda h(\theta, \phi) - (1 \pm \lambda)R_s(\phi, w) \ , \\ &D = (M_{ij}u_j, u_i) + \alpha\|\nabla\theta\|^2 + (1-\alpha)\|\theta_{,z}\|^2 + \lambda\|\nabla\phi\|^2 + \lambda\eta\|\phi\|^2. \end{aligned} \tag{6.4.3}$$

Then, provided that $R_E > 1$

$$\frac{dE}{dt} \leq -D(1 - \frac{1}{R_E}) \tag{6.4.4}$$

is an energy inequality which follows from the energy identity (6.4.2).

Where

$$\frac{1}{R_E} = \max_H \frac{I}{D} \ , \tag{6.4.5}$$

and

$$H = \{u_i, \theta, \phi \ | u_i \in L^2(V), \ \theta, \phi \in H^1(V), \ u_{i,i} = 0 \ \textit{and} \ u_i, \theta, \phi \ \textit{are periodic in} \ x, y\}.$$

We can show

$$(M_{ij}u_j, u_i) \geq \kappa_0\|\mathbf{u}\|^2 \ ; \ \kappa_0 = \min\{\kappa, \kappa_3\} \ ,$$

and

$$\begin{aligned} D &\geq \kappa_0\|\mathbf{u}\|^2 + \alpha\pi^2\|\theta\|^2 + (1-\alpha)\|\theta_{,z}\|^2 + \lambda\pi^2\|\phi\|^2 + \lambda\eta\|\phi\|^2 \\ &\geq \alpha\pi^2\|\theta\|^2 + \pi^2\lambda\|\phi\|^2 \\ &\geq \alpha\pi^2\|\theta\|^2 + \pi^2\lambda\frac{\tilde{M}Le}{\tilde{M}Le}\|\phi\|^2 \\ &\geq 2k\pi^2\left(\frac{\|\theta\|^2 + \lambda\varepsilon\|\phi\|^2}{2}\right) = 2k\pi^2 E(t) \ , \end{aligned}$$

where $k = \min\{\frac{1}{\alpha \tilde{M} Le}, 1\}$. Then from (6.4.4) we may derive the inequality

$$\frac{dE}{dt} \leq -2a_1 k\pi^2 E(t) \ ,$$

where the coefficient a_1 is defined by

$$a_1 = \frac{R_E - 1}{R_E}.$$

Upon integration we obtain

$$E(t) \leq E(0)e^{-2a_1 k\pi^2 t},$$

which shows that $E(t) \to 0$ as $t \to \infty$. Therefore $\|\theta(t)\| \to 0$ and $\|\phi(t)\| \to 0$ as $t \to \infty$ according to $(6.4.3)_1$.

To show the decay of $\|\mathbf{u}\|$, we have to employ the Arithmetic-Geometric Mean inequality in $(6.4.1)_1$

$$\kappa_0 \|\mathbf{u}\|^2 \leq (M_{ij}u_j, u_i) \leq \frac{R}{2\alpha_1}\|\theta\|^2 + \frac{R\alpha_1}{2}\|w\|^2 + \frac{R_s}{2\beta_1}\|\phi\|^2 + \frac{R_s\beta_1}{2}\|w\|^2, \tag{6.4.6}$$

using the fact $\|w\|^2 \leq \|\mathbf{u}\|^2$ in the previous inequality leads to

$$\left(\kappa_0 - \frac{R\alpha_1 + R_s\beta_1}{2}\right)\|\mathbf{u}\|^2 \leq \frac{R}{2\alpha_1}\|\theta\|^2 + \frac{R_s}{2\beta_1}\|\phi\|^2. \tag{6.4.7}$$

Inequality (6.4.7) shows the decay of $\|\mathbf{u}\|^2$ under the condition

$$\kappa_0 - \frac{R\alpha_1 + R_s\beta_1}{2} > 0.$$

Regarding the maximum equation (6.4.5), the nonlinear stability threshold is given by the variational problem

$$\frac{1}{R_E} = \max_H \frac{I}{D} = \max_H \frac{2R(\theta, w) - (1 \pm \lambda)R_s(\phi, w) + h\lambda(\theta, \phi)}{(M_{ij}u_j, u_i) + \alpha\|\nabla\theta\|^2 + (1-\alpha)\|\theta_{,z}\|^2 + \lambda\|\nabla\phi\|^2 + \eta\lambda\|\phi\|^2}. \tag{6.4.8}$$

We have to determine the Euler-Lagrange equations and maximize in the coupling parameter λ. Rescaling ϕ by putting $\tilde{\phi} = \sqrt{\lambda}\phi$, equation (6.4.8) will be

$$\frac{1}{R_E} = \max_H \frac{2R(\theta, w) - R_s f(\lambda)(\tilde{\phi}, w) + h\sqrt{\lambda}(\theta, \tilde{\phi})}{(M_{ij}u_j, u_i) + \alpha\|\nabla\theta\|^2 + (1-\alpha)\|\theta_{,z}\|^2 + \|\nabla\tilde{\phi}\|^2 + \eta\|\tilde{\phi}\|^2}, \tag{6.4.9}$$

where

$$f(\lambda) = \frac{1 \pm \lambda}{\sqrt{\lambda}}.$$

Hence, the Euler-Lagrange equations require

$$\frac{d}{d\epsilon}\frac{I}{D}|_{\epsilon=0} = \delta\left(\frac{I}{D}\right) = 0 \ ,$$

which means the maximum requires

$$\delta D - R_E \delta I = 0 \ . \tag{6.4.10}$$

Let us define $u_i, \theta, \tilde{\phi}$ in terms of arbitrary $C^2(0,1)$ functions, ζ_i, β and γ with $\zeta_i(0) = \zeta_i(1) = \beta(0) = \beta(1) = \gamma(0) = \gamma(1) = 0$ and consider solutions of the form

$$u_i = u_i + \epsilon\zeta_i \ , \ \theta = \theta + \epsilon\beta \ , \ \tilde{\phi} = \tilde{\phi} + \epsilon\gamma.$$

By standard calculation, the Euler-Lagrange equations which arise from the variational problem (6.4.5) are

$$\begin{aligned} &2M_{ij}u_j - 2RR_E k_i\theta + R_s R_E f(\lambda)k_i\tilde{\phi} + R_E P_{,i} = 0 \ , \\ &-2\alpha\Delta\theta - 2(1-\alpha)\theta_{,zz} - 2RR_E w - \sqrt{\lambda}hR_E\tilde{\phi} = 0 \ , \\ &-2\Delta\tilde{\phi} + 2\eta\tilde{\phi} - \sqrt{\lambda}hR_E\theta + R_s R_E f(\lambda)w = 0 \ . \end{aligned} \tag{6.4.11}$$

Rescaling $\tilde{\phi}$ again, system (6.4.11) can be written as

$$\begin{aligned} &\left(\frac{1\pm\lambda}{2}\right)R_s R_E k_i\phi - RR_E k_i\theta + M_{ij}u_j = -\frac{R_E}{2}P_{,i} \ , \\ &\alpha\Delta\theta + (1-\alpha)\theta_{,zz} + RR_E w + \frac{\lambda}{2}hR_E\phi = 0 \ , \\ &\Delta\phi - \eta\phi + \frac{h}{2}R_E\theta - R_s R_E\left(\frac{1\pm\lambda}{2\lambda}\right)w = 0 \ . \end{aligned} \tag{6.4.12}$$

Taking the double curl of $(6.4.12)_1$ and retaining just the third component, our system will be

$$\begin{aligned} &-\left(\frac{1\pm\lambda}{2}\right)R_s R_E\Delta^*\phi + RR_E\Delta^*\theta - \kappa w_{,zz} - \kappa_3\Delta^* w = 0 \ , \\ &\alpha\Delta\theta + (1-\alpha)\theta_{,zz} + RR_E w + \frac{\lambda}{2}hR_E\phi = 0 \ , \\ &\Delta\phi - \eta\phi + \frac{h}{2}R_E\theta - R_s R_E\left(\frac{1\pm\lambda}{2\lambda}\right)w = 0 \ . \end{aligned} \tag{6.4.13}$$

Assuming normal mode solutions, as in the previous chapters, system (6.4.13) gives rise to

$$\begin{aligned} &\left(D^2 - \frac{a^2\kappa_3}{\kappa}\right)W + \frac{a^2}{\kappa}RR_E\Theta - \left(\frac{1\pm\lambda}{2}\right)\frac{a^2}{\kappa}R_s R_E\Phi = 0 \ , \\ &RR_E W + \left(D^2 - a^2\alpha\right)\Theta + \frac{\lambda h}{2}R_E\Phi = 0 \ , \\ &-R_s R_E\left(\frac{1\pm\lambda}{2\lambda}\right)W + \frac{h}{2}R_E\Theta + \left(D^2 - a^2 - \eta\right)\Phi = 0 \ , \end{aligned} \tag{6.4.14}$$

and the corresponding boundary conditions are

$$W = \Theta = \Phi = 0 \;\; at \; z = 0, 1 \; . \tag{6.4.15}$$

We solved system (6.4.14)-(6.4.15) numerically using the D^2 Chebyshev Tau method as explained in the next section.

6.5 Numerical Method

Following the procedure of chapters 4 and 5, the functions W, Θ, and Φ and the boundary conditions are expanded in terms of Chebyshev polynomials, cf. Dongarra *et al.* [26]. Therefore, for the linear theory, system (6.3.2)-(6.3.3), the Chebyshev Tau method reduces to solving the matrix system $A_1\mathbf{x} = \sigma B_1\mathbf{x}$, where $\mathbf{x} = (w_1, w_2, \cdots, w_N, \theta_1, \cdots, \theta_N, \phi_1, \cdots, \phi_N)$ and the matrices A_1 and B_1 are given by

$$A_1 = \begin{pmatrix} 4D^2 - a^2\frac{\kappa_3}{\kappa}I & \frac{a^2}{\kappa}RI & -\frac{a^2}{\kappa}R_sI \\ BC1 & 0\cdots 0 & 0\cdots 0 \\ BC2 & 0\cdots 0 & 0\cdots 0 \\ RI & 4D^2 - a^2\alpha I & 0 \\ 0\cdots 0 & BC3 & 0\cdots 0 \\ 0\cdots 0 & BC4 & 0\cdots 0 \\ \mp R_sI & hI & 4D^2 - (a^2+\eta)I \\ 0\cdots 0 & 0\cdots 0 & BC5 \\ 0\cdots 0 & 0\cdots 0 & BC6 \end{pmatrix},$$

$$B_1 = \begin{pmatrix} 0 & 0 & 0 \\ 0\cdots 0 & 0\cdots 0 & 0\cdots 0 \\ 0\cdots 0 & 0\cdots 0 & 0\cdots 0 \\ 0 & I & 0 \\ 0\cdots 0 & 0\cdots 0 & 0\cdots 0 \\ 0\cdots 0 & 0\cdots 0 & 0\cdots 0 \\ 0 & 0 & \varepsilon I \\ 0\cdots 0 & 0\cdots 0 & 0\cdots 0 \\ 0\cdots 0 & 0\cdots 0 & 0\cdots 0 \end{pmatrix}.$$

While for the nonlinear theory, system (6.4.14)-(6.4.15), the Chebyshev Tau method reduces to solving the matrix system $A_2\mathbf{x} = RB_2\mathbf{x}$, where the matrices A_2 and B_2 are given by

$$A_2 = \begin{pmatrix} 4D^2 - a^2\frac{\kappa_3}{\kappa}I & 0 & -(\frac{1\pm\lambda}{2})\frac{a^2}{\kappa}R_sR_EI \\ BC1 & 0\cdots0 & 0\cdots0 \\ BC2 & 0\cdots0 & 0\cdots0 \\ 0 & 4D^2 - a^2\alpha I & \frac{\lambda h}{2}R_EI \\ 0\cdots0 & BC3 & 0\cdots0 \\ 0\cdots0 & BC4 & 0\cdots0 \\ -R_sR_E(\frac{1\pm\lambda}{2\lambda})I & \frac{h}{2}R_EI & 4D^2 - (a^2+\eta)I \\ 0\cdots0 & 0\cdots0 & BC5 \\ 0\cdots0 & 0\cdots0 & BC6 \end{pmatrix},$$

$$B_2 = \begin{pmatrix} 0 & -\frac{a^2}{\kappa}R_EI & 0 \\ 0\cdots0 & 0\cdots0 & 0\cdots0 \\ 0\cdots0 & 0\cdots0 & 0\cdots0 \\ -R_EI & 0 & 0 \\ 0\cdots0 & 0\cdots0 & 0\cdots0 \\ 0\cdots0 & 0\cdots0 & 0\cdots0 \\ 0 & 0 & 0 \\ 0\cdots0 & 0\cdots0 & 0\cdots0 \\ 0\cdots0 & 0\cdots0 & 0\cdots0 \end{pmatrix},$$

where in both systems $BC1, BC2, BC3, BC4, BC5$ and $BC6$ represent the boundary conditions in expanded form of Chebychev polynomials, *i.e.*

$$\begin{aligned} BC1 :& w_2 + w_4 + w_6 + \cdots + w_N = 0, \\ BC2 :& w_1 + w_3 + w_5 + \cdots + w_{N-1} = 0, \\ BC3 :& \theta_2 + \theta_4 + \theta_6 + \cdots + \theta_N = 0, \\ BC4 :& \theta_1 + \theta_3 + \theta_5 + \cdots + \theta_{N-1} = 0, \\ BC5 :& \phi_2 + \phi_4 + \phi_6 + \cdots + \phi_N = 0, \\ BC6 :& \phi_1 + \phi_3 + \phi_5 + \cdots + \phi_{N-1} = 0. \end{aligned} \tag{6.5.1}$$

We solved the matrix systems by the QZ algorithm, cf. Dongarra *et al.* [26] and Straughan [99].

6.6 Numerical Results and Conclusions

6.6.1 Salted above system

Numerically, the results show the coincidence of the linear instability boundary and the energy stability boundary for different values of the anisotropy parameters when there is no reaction, $h = \eta = 0$. As figure (6.1) shows that there is no region of potential subcritical instabilities. To investigate the effect of increasing the reaction rates, different values of h *and* η are implemented for $\alpha = k_{Tx}/k_{Tz} = 0.5$ and $\chi = K_z/K_x = 10$. Increasing the reaction rates, see figure (6.2), results in a wider gap between the linear instability and nonlinear energy stability boundaries, and therefore, a wider space of potential subcritical instability.

To study the effect of each of h and η on the onset of convection, a large difference between their values is implemented for different values of α and χ as figures (6.3) and (6.4) show. For all chosen values of α and χ, when η is larger than h the two boundaries coincide, which is expected from system $(6.2.8)_4$ as $-\eta\phi$ is a stabilizing term but the region of stability varies due to the effect of the anisotropy parameters α and χ. On the other hand, implementing larger values of h than η for different cases of α and χ, reveals regions of potential subcritical instability which is a result of a divergence of the energy stability boundaries(dashed lines) and the linear instability boundaries(continuous lines) from each other, which is also expected from system $(6.2.8)_4$ as $+h\theta$ is a destabilizing term.

The effect of the thermal anisotropic parameter $\alpha = k_{Tx}/k_{Tz}$ and the mechanical anisotropic parameter $\chi = K_z/K_x$ may be interpreted as follows: When $\chi < 1$, keeping the vertical permeability constant $K_z = 1$ and decreasing the horizontal permeability K_x, lowers the the energy stability boundary and the linear instability boundary indicating that the effect is destabilizing as figure $(6.3)(a, c), (b, d)$ shows. When $\chi > 1$, keeping the horizontal permeability constant $K_x = 1$ and increasing the vertical permeability K_z, shifts the two boundaries to higher positions indicating

that the effect is stabilizing, as is clear in figure (6.3)$(e, g), (f, h)$. Figure (6.4) is included as a support of the above interpretation when $\alpha = 0.5$ while figure (6.3) is when $\alpha = 1$. Moreover, the numerical values obtained reveal that increasing the mechanical anisotropy parameter, shifts the minimum of the Rayleigh number towards smaller values of the wave number. For example, from table (6.1) we observe that when $R_s^2 = 14$, $\chi = 2$, $a_L = 3.5$ whereas for the same value of R_s but $\chi = 10$, we have $a_L = 2.16$. This indicates that the cell width increases with increasing mechanical anisotropy parameter.

Figure (6.5) indicates the effect of the thermal anisotropy parameter $\alpha = k_{Tx}/k_{Tz} \leq 1$ for fixed values of the mechanical anisotropy parameter χ and reaction rates h and η which can be interpreted as follows.

Keeping the horizontal thermal diffusivity constant, $k_{Tx} = 1$, and increasing the vertical thermal diffusivity, k_{Tz}, lowering the two boundaries which results in smaller definite stable space below the energy stability boundary(dashed lines), see figure (6.5)$(a, c), (b, d)$, as an indication of a destabilization effect. Note that the effect of the thermal anisotropy parameter α is opposite to that of the mechanical anisotropy parameter χ when $\chi > 1$. This result agrees with the finding of Malashetty and Biradar [60].

We conclude that the reaction rates may stabilize or destabilize according to the values of each of the reaction terms h and η. h plays the role of destabilizing while η plays the role of stabilizing. When the vertical permeability is high ($\chi > 1$), the system is more stable. While decreasing the horizontal permeability for fixed vertical permeability such that ($\chi < 1$), the system will be more unstable. When the vertical component of the thermal diffusivity is high ($\alpha < 1$), the system is more unstable. While increasing the horizontal component of the thermal diffusivity for fixed vertical component of the themal diffusivity such that ($\alpha < 1$), the system will be more stable. The results reveal the opposite effect of the anisotropic parameters when the vertical components are higher, as fig.(6.6) and fig.(6.7) show. This finding agrees with the conclusions of [60], [31], and [62].

$\chi = 2$					$\chi = 10$				
R_s^2	a_L	Ra_L^2	a_E	Ra_E^2	R_s^2	a_L	Ra_L^2	a_E	Ra_E^2
0	2.64	57.524295	2.64	57.524296	0	1.77	170.98696	1.77	170.98694
1	2.84	65.867328	2.47	47.728294	1	1.84	191.04848	1.7	150.33782
2	2.93	68.841697	2.42	43.309404	2	1.88	199.25623	1.68	141.54712
5	3.13	73.662351	2.31	34.178499	5	1.97	215.18329	1.63	123.86981
7	3.24	75.450431	2.27	29.564022	7	2.01	222.86906	1.62	115.00238
10	3.36	77.054094	2.22	23.809327	10	2.08	232.23865	1.59	103.86712
12	3.43	77.634638	2.19	20.527959	12	2.12	237.51810	1.58	97.388428
14	3.5	77.925078	2.17	17.593690	14	2.16	242.22792	1.57	91.478747
18	3.61	77.835481	2.14	12.584275	18	2.23	250.33498	1.55	80.961612
20	3.66	77.520858	2.13	10.447675	20	2.27	253.86249	1.54	76.217504
25	3.76	76.114746	2.11	6.0404112	25	2.35	261.48666	1.52	65.521436
30	3.84	73.984800	2.1	2.8499080	30	2.43	267.74073	1.5	56.177642
35	3.91	71.258474	2.11	0.8246665	35	2.5	272.91206	1.5	47.932140

Table 6.1: Some numerical values obtained for the linear boundary Ra_L and the energy boundary Ra_E with corresponding salt Rayleigh number R_s and the the corresponding critical wave numbers a_L and a_E when $\alpha = 1$, $h = 20$ and $\eta = 0$ in the case of heated below salted above system. For two cases of the mechanical anisotropy parameter χ, $\chi = 2$ and $\chi = 10$.

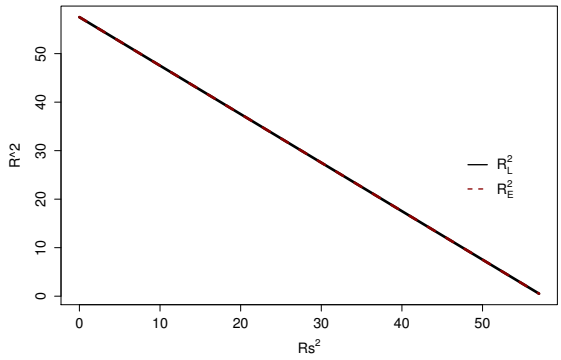

(a) $\alpha = 1$, $\chi = 2$

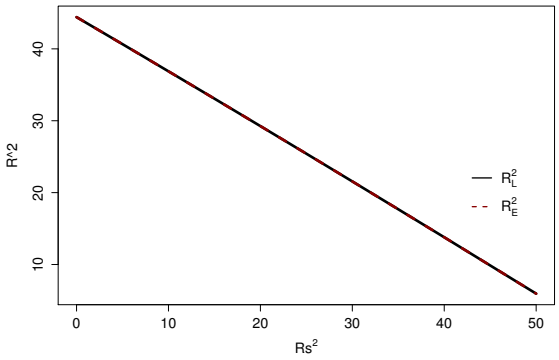

(b) $\alpha = 0.5$, $\chi = 2$

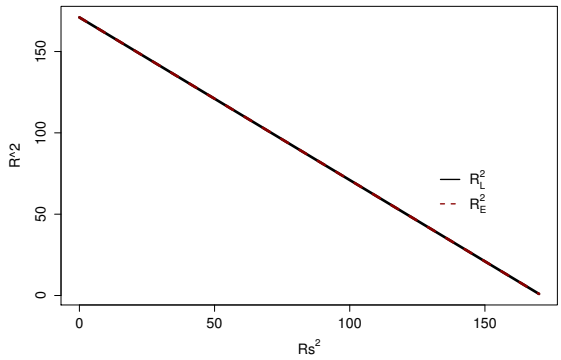

(c) $\alpha = 1$, $\chi = 10$

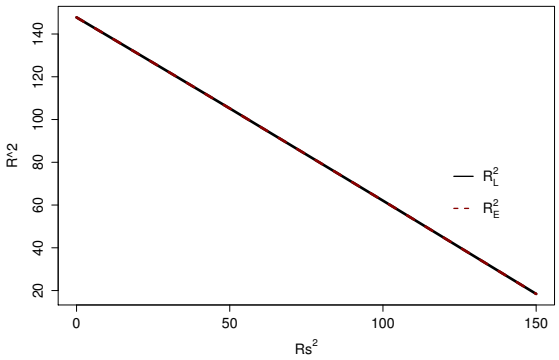

(d) $\alpha = 0.5$, $\chi = 10$

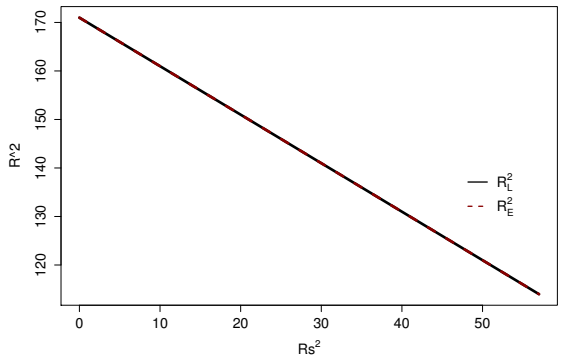

(e) $\alpha = 1$, $\chi = 0.1$

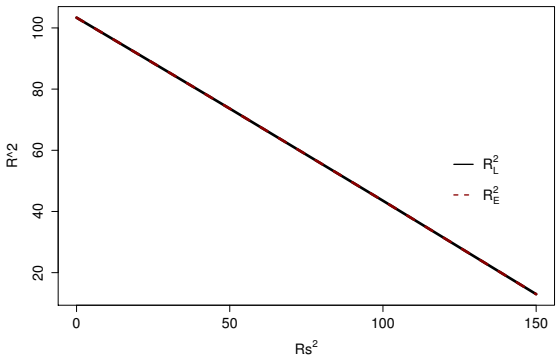

(f) $\alpha = 0.5$, $\chi = 0.1$

Figure 6.1: Linear instability and energy stability boundaries for the salted above Darcy convection problem for different values of the anisotropic parameters when there is no reaction.

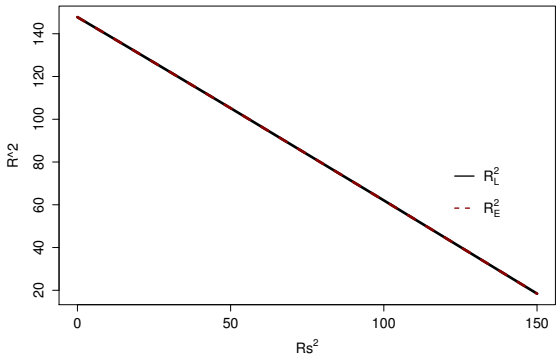

(a) $h = 0$ *and* $\eta = 0$

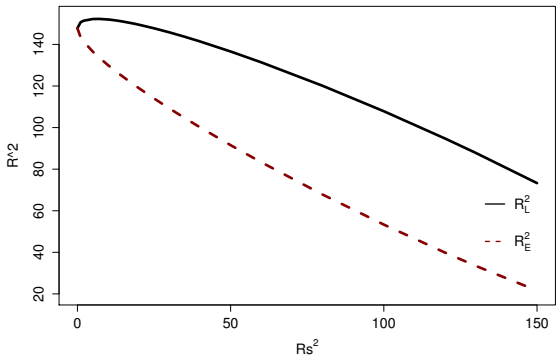

(b) $h = 5$ *and* $\eta = 3$

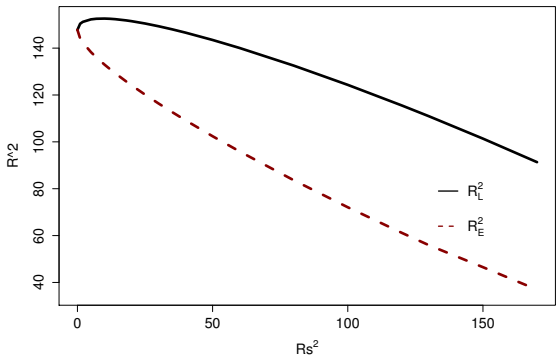

(c) $h = 6$ *and* $\eta = 9$

Figure 6.2: Linear instability and energy stability boundaries for the salted above Darcy convection problem with anisotropic effect for $\alpha = 0.5$, $\chi = 10$ and different values of the reaction rates h and η.

6.6.2 Salted below system

It is instructive to write system (6.2.8) for the salted below case as an abstract equation of the form

$$A\mathbf{u}_t = L(\mathbf{u}) + N(\mathbf{u}),$$

where, as in the previous chapters, $\mathbf{u} = (u_1, u_2, u_3, \theta, \phi)$, $N(\mathbf{u})$ represents the non-linear terms and $L(\mathbf{u})$ represents the linear terms as

$$N(\mathbf{u}) = \begin{pmatrix} 0 \\ 0 \\ 0 \\ -u_i\theta_{,i} \\ -\frac{Le}{\hat{\phi}}u_i\phi_{,i} \end{pmatrix},$$

and

$$L = \begin{pmatrix} -M_{11} & 0 & 0 & 0 & 0 \\ 0 & -M_{22} & 0 & 0 & 0 \\ 0 & 0 & -M_{33} & R & -R_s \\ 0 & 0 & R & \alpha\Delta^* + D^2 & 0 \\ 0 & 0 & R_s & h & \Delta - \eta \end{pmatrix}.$$

If $h = 0$, then we may write L as a symmetric plus skew-symmetric parts as

$$L = L_s + L_A,$$

where

$$L_s = \begin{pmatrix} -M_{11} & 0 & 0 & 0 & 0 \\ 0 & -M_{22} & 0 & 0 & 0 \\ 0 & 0 & -M_{33} & R & 0 \\ 0 & 0 & R & \alpha\Delta^* + D^2 & 0 \\ 0 & 0 & 0 & 0 & \Delta - \eta \end{pmatrix},$$

and

$$L_A = \begin{pmatrix} 0 & 0 & 0 & 0 & 0 \\ 0 & 0 & 0 & 0 & 0 \\ 0 & 0 & 0 & 0 & -R_s \\ 0 & 0 & 0 & 0 & 0 \\ 0 & 0 & R_s & 0 & 0 \end{pmatrix}.$$

For the salted above case L_A would be zero and the linear operator would be symmetric. For the salted below case, the problem of this subsection, even when $h = 0$, $(\mathbf{u}, L(\mathbf{u})) \neq (\mathbf{u}, L_s(\mathbf{u}))$. So for the problem in hand we have two sources of anti-symmetry, the R_s term and the h term.

The numerical results are presented graphically in which the effect of the reaction rates, the mechanical anisotropy parameter and the thermal anisotropy parameter in the stability of the system is investigated. The effect of reaction is shown in figure (6.8). In contrast to the salted above case, the linear instability boundary and the energy stability boundary do not coincide even when the reaction does not present, $h = \eta = 0$, *i.e.* there is always a region of potential subcritical instability. As the value of the reaction rate increases the space below the energy stability boundary(dashed line) decreases whenever the value of h is greater than η value which explains that h is a destabilizing term while η has a stabilizing effect.

The effect of the anisotropic permeability parameter $\chi = K_z/K_x$ can be explained as follows. When $\chi < 1$, keeping the vertical permeability constant $K_z = 1$ and decreasing the horizontal permeability K_x, lowers the energy stability boundary as well as the linear instability boundary, which results in a smaller definite stable space below the energy stability boundary as figure $(6.9)(a, c), (b, d)$ shows, indicating that the effect, according to the energy stability theory, is destabilizing. When $\chi > 1$, increasing the vertical permeability K_z and keeping the horizontal permeability constant $K_x = 1$, shifts the two boundaries to a higher position, resulting in a wider definite stable space below the energy stability boundary, indicating that the effect is stabilizing as is clear in figure $(6.9)(e, g), (f, h)$. Furthermore, we notice that increasing the mechanical anisotropy parameter, shifts the minimum of the Rayleigh number towards smaller values of the wave number, indicating that the cell width increases with increasing mechanical anisotropy parameter.

Figure (6.10) indicates the effect of the thermal anisotropy parameter $\alpha = k_{Tx}/k_{Tz} \leq 1$ for fixed values of $\chi = 10$, h and η. Similar to the salted above case, it is noticed that the thermal anisotropy parameter has opposite effect to that of the mechanical anisotropy parameter when the mechanical anisotropy parameter is greater than 1. Keeping the horizontal thermal diffusivity constant $k_{Tx} = 1$

and increasing the vertical thermal diffusivity k_{Tz}, shifts the two boundaries to a lower position indicating that the effect is destabilizing which is presented in figure $(6.10)(a, c), (b, d)$. Moreover, we find that increasing the thermal anisotropy parameter shifts the minimum of the Rayleigh number towards smaller values of the wave number. For example, from table (6.2) we observe that when $R_s^2 = 5$, $\alpha = 0.5$, $a_L = 2.1$ whereas for the same R_s value but $\alpha = 1$ one has $a_L = 1.76$. This indicates that the cell width increases with increasing thermal anisotropy parameter. It is noticed that the effects of the mechanical and thermal anisotropy parameters on the onset of double-diffusive convection discussed above are in agreement with the results obtained by Malashetty and Biradar [60], Gaikwad *et al.* [31] and Malashetty and Swamy [62].

Over-stability may be obtained due to the strong effect of the porosity ϵ on the oscillatory behaviour of the flow as demonstrated by Mamou [63]. Hence, its effect is investigated in figure (6.11). Increasing the porosity precipitates the transition to oscillatory convection, shifting the minimum of the Rayleigh number towards a bigger value of the wave number indicating that the cell width decreases with increasing porosity. For example, from table (6.3) we observe that when $R_s^2 = 10$, $\epsilon = 3$, $a_L = 1.99$ whereas for the same R_s value but $\epsilon = 5$ one has $a_L = 2.02$.

Figure (6.12) shows the effect of the mechanical anisotropy parameter χ and figure (6.13) presents the effect of the thermal anisotropy parameter α for fixed values of the reaction rates $h = 20$ and $\eta = 0$ when the porosity $\epsilon = 3$. The effects are exactly the same as for the case when $\epsilon = 1$ discussed above and presented graphically in figures (6.8), (6.9) and (6.10) and in agreement with Malashetty *et al.* [60].

$\alpha = 0.5$					$\alpha = 1$				
R_s^2	a_L	Ra_L^2	a_E	Ra_E^2	R_s^2	a_L	Ra_L^2	a_E	Ra_E^2
0	2.1	147.76908	2.1	147.76908	0	1.77	170.98696	1.77	170.98696
1	2.1	148.12131	2.1	147.76908	1	1.77	171.38094	1.77	170.98696
2	2.1	148.47355	2.1	147.76908	2	1.77	171.77493	1.77	170.98696
5	2.1	149.53027	2.1	147.76908	5	1.76	172.95496	1.77	170.98696
7	2.1	150.23475	2.1	147.76908	7	1.76	173.74164	1.77	170.98696
10	2.1	151.29146	2.1	147.76908	10	1.76	174.92165	1.77	170.98696
12	2.1	151.99594	2.1	147.76908	12	1.76	175.70832	1.77	170.98696
14	2.09	152.70026	2.1	147.76908	14	1.76	176.49499	1.77	170.98696
18	2.09	154.10849	2.1	147.76908	18	1.75	178.06612	1.77	170.98696
20	2.09	154.81261	2.1	147.76908	20	1.75	178.85149	1.77	170.98696
25	2.09	156.57289	2.1	147.76908	25	1.75	180.81494	1.77	170.98696
30	2.09	158.33319	2.1	147.76908	30	1.74	182.77671	1.77	170.98696
35	2.09	160.09348	2.1	147.76908	35	1.74	184.73694	1.77	170.98696
40	2.08	161.85299	2.1	147.76908	40	1.74	186.69717	1.77	170.98696
50	2.08	165.37177	2.1	147.76908	50	1.73	190.61156	1.77	170.98696
60	2.07	168.89030	2.1	147.76908	60	1.72	194.52177	1.77	170.98696
70	2.07	172.40728	2.1	147.76908	70	1.71	198.42803	1.77	170.98696
80	2.07	175.92425	2.1	147.76908	80	1.71	202.32929	1.77	170.98696
90	2.06	179.43982	2.1	147.76908	90	1.70	206.22549	1.77	170.98696
120	2.05	189.98285	2.1	147.76908	120	1.68	217.89006	1.77	170.98696
150	2.04	200.51952	2.1	147.76908	150	1.66	229.51770	1.77	170.98696

Table 6.2: Some numerical values obtained for the linear boundary Ra_L and the energy boundary Ra_E with corresponding salt Rayleigh number R_s and the the corresponding critical wave numbers a_L and a_E when $\chi = 10$, $h = 0$ and $\eta = 20$ in the case of heated below salted below system. For two cases of the thermal anisotropy parameter α, $\alpha = 0.5$ and $\alpha = 1$.

$\epsilon = 3$			$\epsilon = 5$		
R_s^2	a_L	Ra_L^2	R_s^2	a_L	Ra_L^2
0	2.1	147.7690755	0	2.1	147.7690755
1	2.25	166.2869491	1	2.25	166.2869491
2	2.32	174.8063078	2	2.32	174.8063078
5	2.5	193.0438038	5	2.02	183.5537000
7	1.99	207.9504079	7	2.02	183.9537000
10	1.99	208.9504079	10	2.02	184.5537000
12	1.99	209.6170746	12	2.02	184.9537000
14	1.99	210.2837412	14	2.02	185.3537000
18	1.99	211.6170746	18	2.02	186.1537000
20	1.99	212.2837412	20	2.02	186.5537000
25	1.99	213.9504079	25	2.02	187.5537000
30	1.99	215.6170746	30	2.02	188.5537000
35	1.99	217.2837412	35	2.02	189.5537000
40	1.99	218.9504079	40	2.02	190.5537000
50	1.99	222.2837412	50	2.02	192.5537000
60	1.99	225.6170746	60	2.02	194.5537000
70	1.99	228.9504079	70	2.02	196.5537000
80	1.99	232.2837412	80	2.02	198.5537000
90	1.99	235.6170746	90	2.02	200.5537000
120	1.99	245.6170746	120	2.02	206.5537000
150	1.99	255.6170746	150	2.02	212.5537000

Table 6.3: Some numerical values obtained for the linear boundaries Ra_L with corresponding salt Rayleigh number R_s and the the corresponding critical wave numbers a_L when $\alpha = 0.5$, $\chi = 10$, $h = 20$ and $\eta = 0$ in the case of heated below salted below system. For two cases of the porosity ϵ, $\epsilon = 3$ and $\epsilon = 5$.

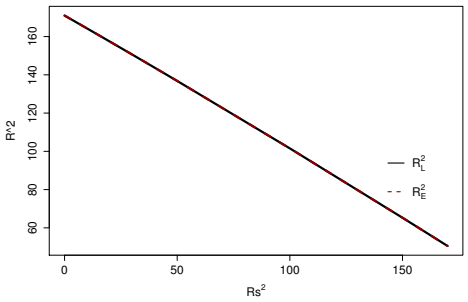

(a) $h = 0$ *and* $\eta = 20$, $\chi = 0.1$

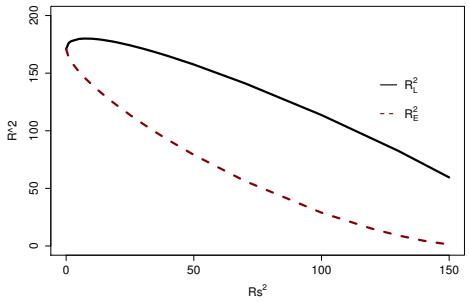

(b) $h = 20$ *and* $\eta = 0$, $\chi = 0.1$

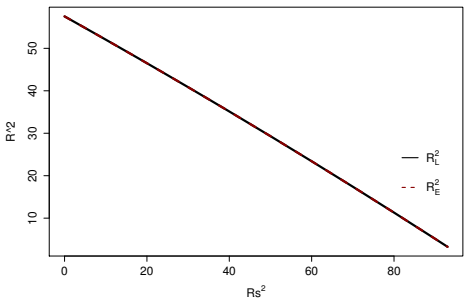

(c) $h = 0$ *and* $\eta = 20$, $\chi = 0.5$

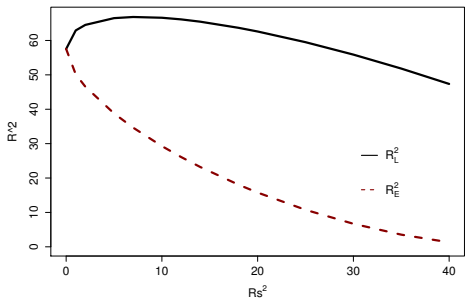

(d) $h = 20$ *and* $\eta = 0$, $\chi = 0.5$

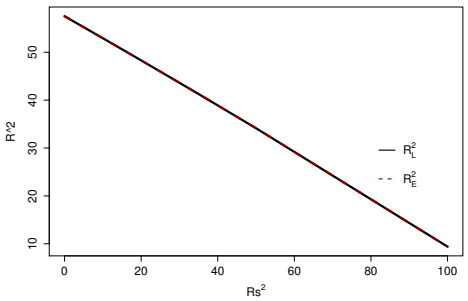

(e) $h = 0$ *and* $\eta = 20$, $\chi = 2$

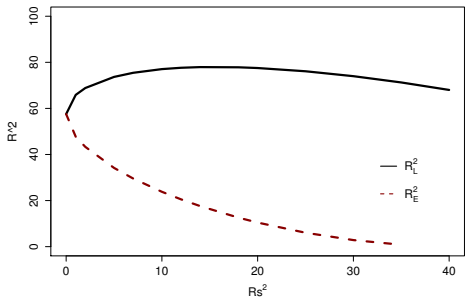

(f) $h = 20$ *and* $\eta = 0$, $\chi = 2$

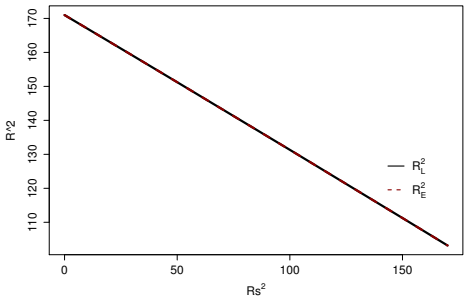

(g) $h = 0$ *and* $\eta = 20$, $\chi = 10$

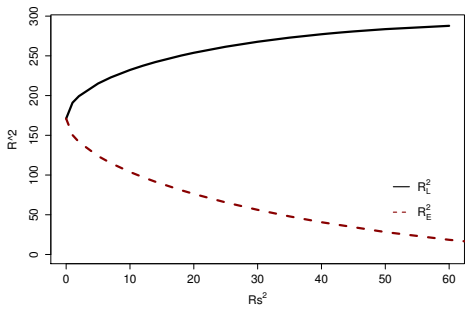

(h) $h = 20$ *and* $\eta = 0$, $\chi = 10$

Figure 6.3: Linear instability and energy stability boundaries for the salted above Darcy convection problem with anisotropic effect for $\alpha = 1$.

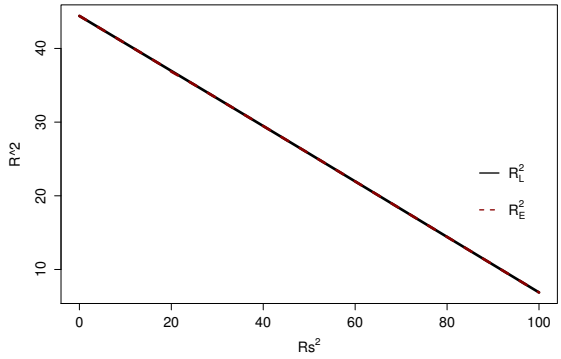

(a) $h = 0$ *and* $\eta = 20$, $\chi = 2$

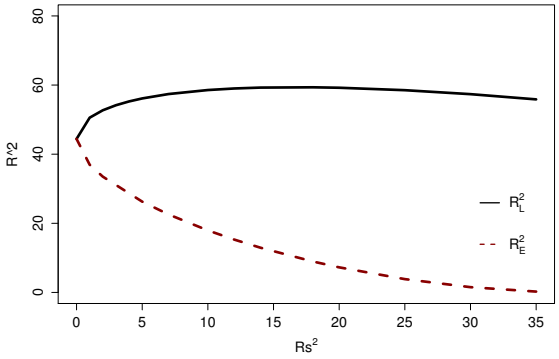

(b) $h = 20$ *and* $\eta = 0$, $\chi = 2$

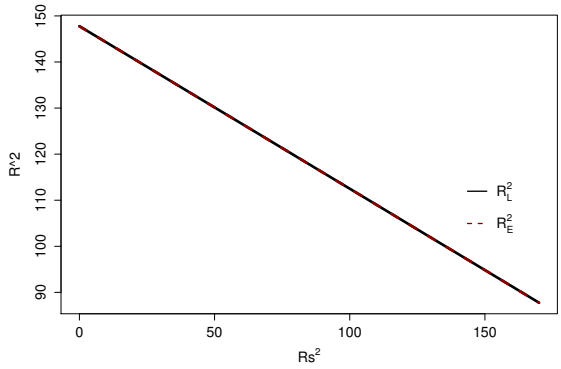

(c) $h = 0$ *and* $\eta = 20$, $\chi = 10$

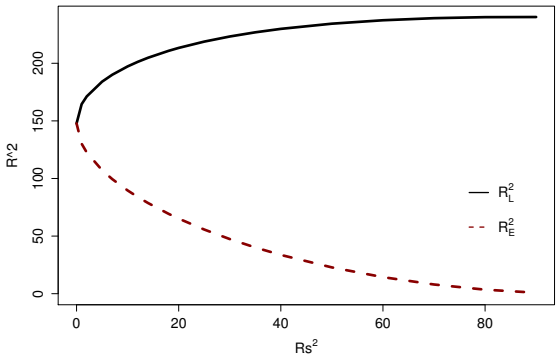

(d) $h = 20$ *and* $\eta = 0$, $\chi = 10$

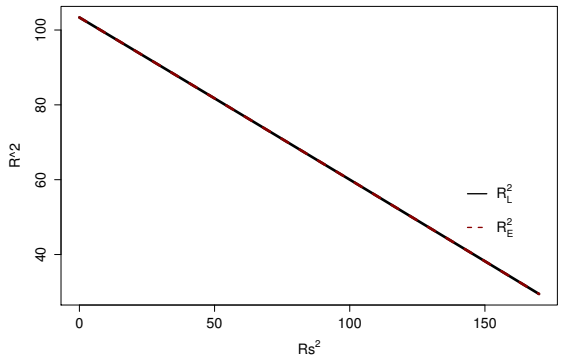

(e) $h = 0$ *and* $\eta = 20$, $\chi = 0.1$

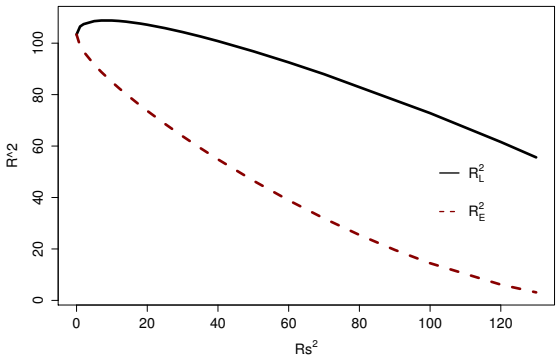

(f) $h = 20$ *and* $\eta = 0$, $\chi = 0.1$

Figure 6.4: Linear instability and energy stability boundaries for the salted above Darcy convection problem with anisotropic effect for $\alpha = 0.5$.

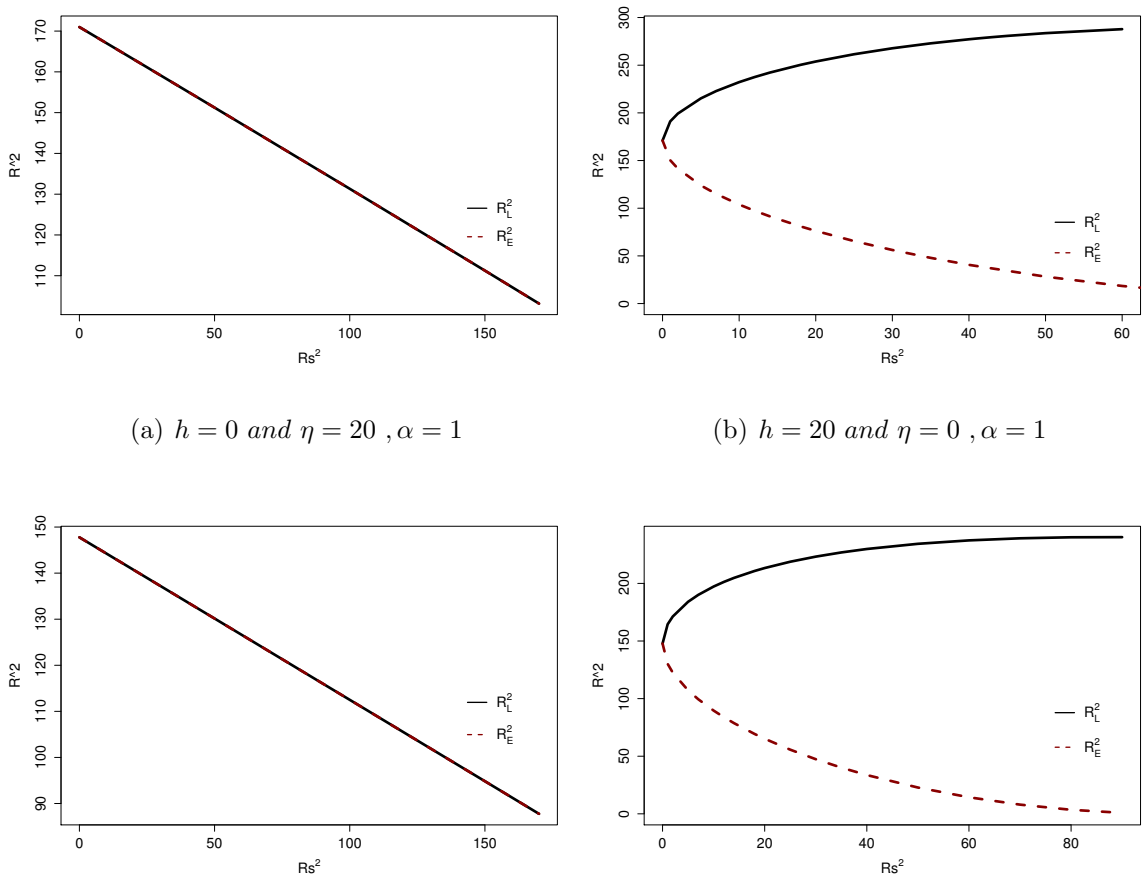

(a) $h = 0$ *and* $\eta = 20$, $\alpha = 1$

(b) $h = 20$ *and* $\eta = 0$, $\alpha = 1$

(c) $h = 0$ *and* $\eta = 20$, $\alpha = 0.5$

(d) $h = 20$ *and* $\eta = 0$, $\alpha = 0.5$

Figure 6.5: Linear instability and energy stability boundaries for the salted above Darcy convection problem with anisotropic effect for $\chi = 10$.

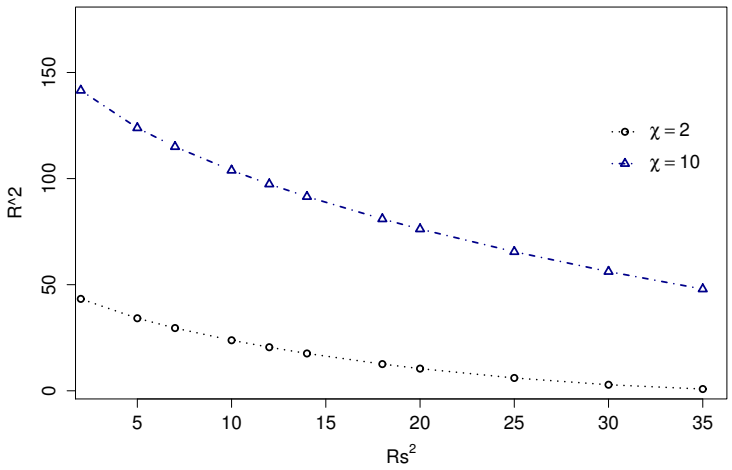

Figure 6.6: The energy stability boundaries for the salted above Darcy convection problem with anisotropic effect for $\alpha = 1$, $h = 20$, $\eta = 0$. The figure shows the effect of increasing the vertical permeability component, K_z.

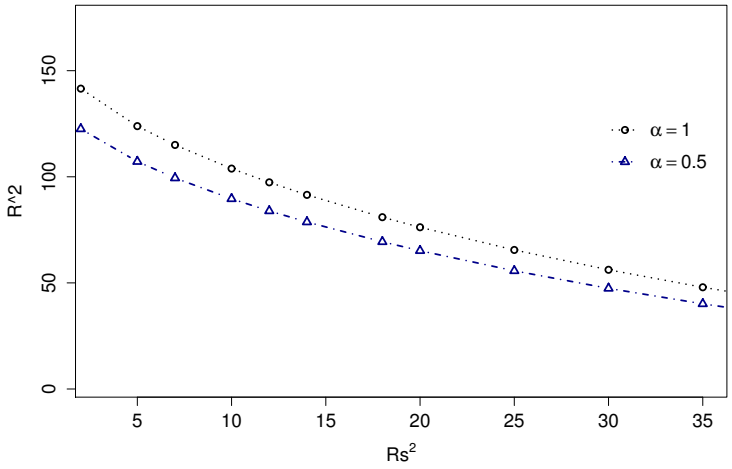

Figure 6.7: The energy stability boundaries for the salted above Darcy convection problem with anisotropic effect for $\chi = 10$, $h = 20$, $\eta = 0$. The figure shows the effect of increasing the vertical thermal diffusivity component, k_{Tz}.

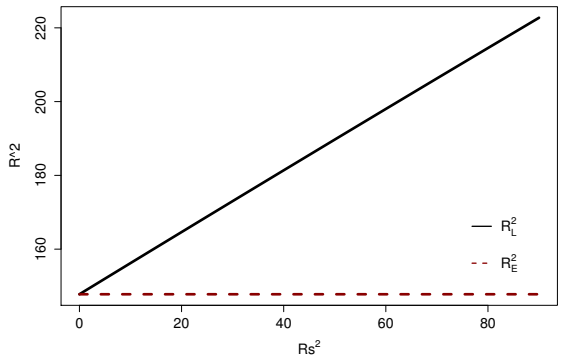

(a) $h = 0$ *and* $\eta = 0$

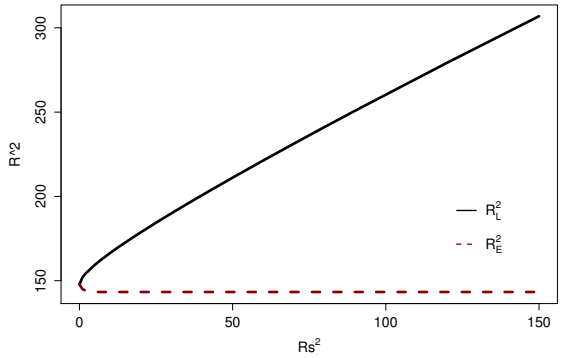

(b) $h = 5$ *and* $\eta = 3$

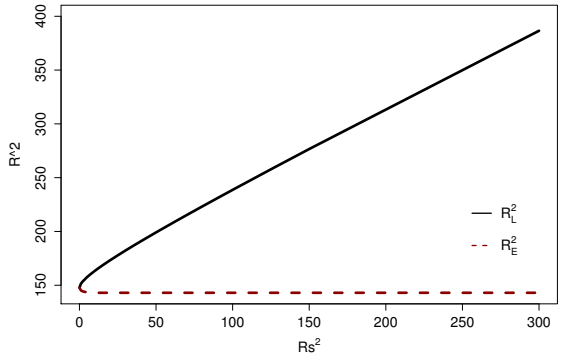

(c) $h = 6$ *and* $\eta = 9$

Figure 6.8: Linear instability and energy stability boundaries for the salted below Darcy convection problem with anisotropic effect for $\alpha = 0.5$, $\chi = 10$ and different values of the reaction rates h and η.

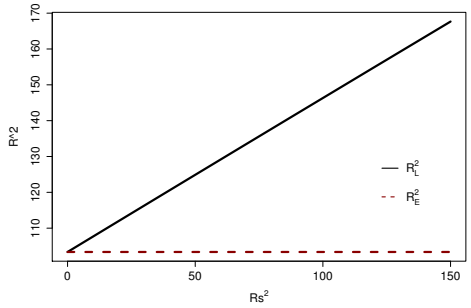

(a) $h = 0$ *and* $\eta = 20$, $\chi = 0.1$

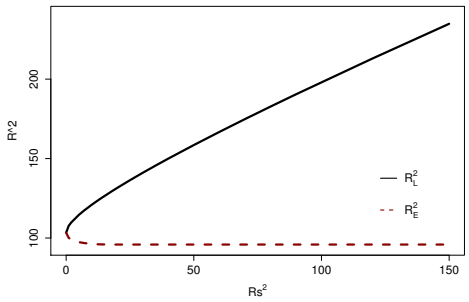

(b) $h = 20$ *and* $\eta = 0$, $\chi = 0.1$

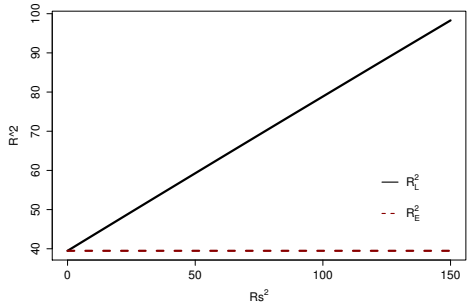

(c) $h = 0$ *and* $\eta = 20$, $\chi = 0.5$

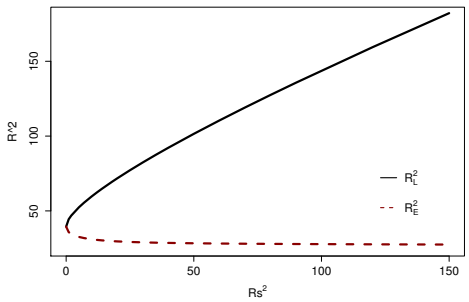

(d) $h = 20$ *and* $\eta = 0$, $\chi = 0.5$

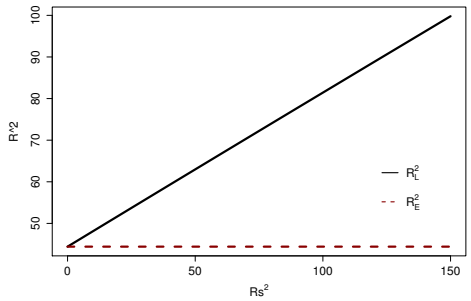

(e) $h = 0$ *and* $\eta = 20$, $\chi = 2$

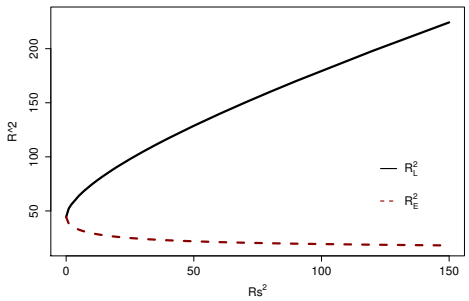

(f) $h = 20$ *and* $\eta = 0$, $\chi = 2$

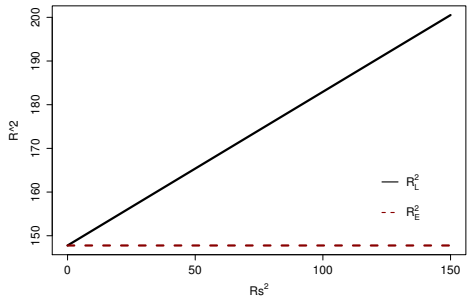

(g) $h = 0$ *and* $\eta = 20$, $\chi = 10$

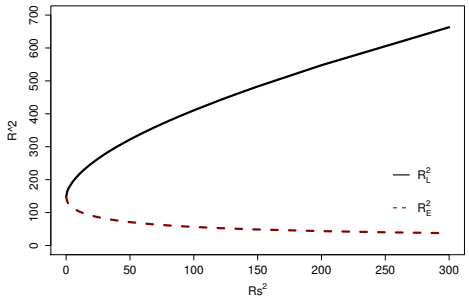

(h) $h = 20$ *and* $\eta = 0$, $\chi = 10$

Figure 6.9: Linear instability and energy stability boundaries for the salted below Darcy convection problem with anisotropic effect for $\alpha = 0.5$.

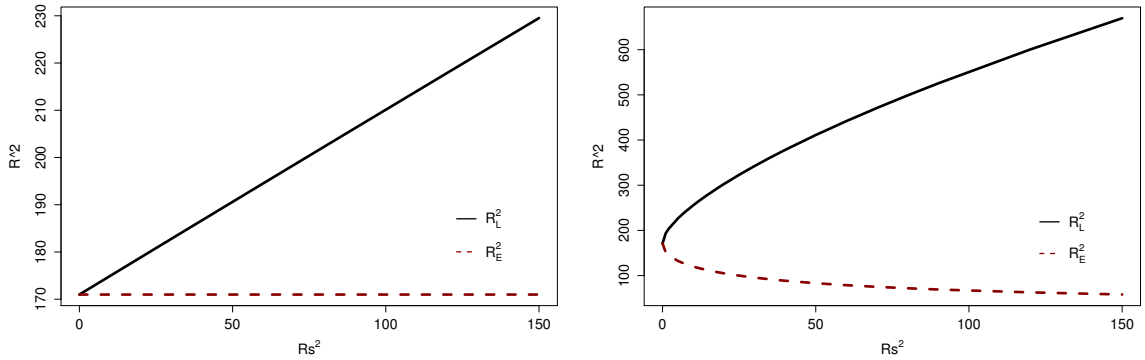

(a) $h = 0$ *and* $\eta = 20$, $\alpha = 1$

(b) $h = 20$ *and* $\eta = 0$, $\alpha = 1$

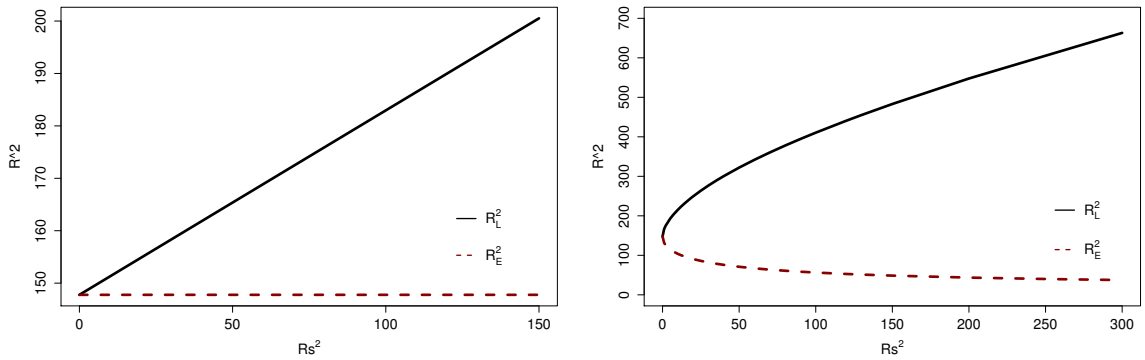

(c) $h = 0$ *and* $\eta = 20$, $\alpha = 0.5$

(d) $h = 20$ *and* $\eta = 0$, $\alpha = 0.5$

Figure 6.10: Linear instability and energy stability boundaries for the salted below Darcy convection problem with anisotropic effect for $\chi = 10$.

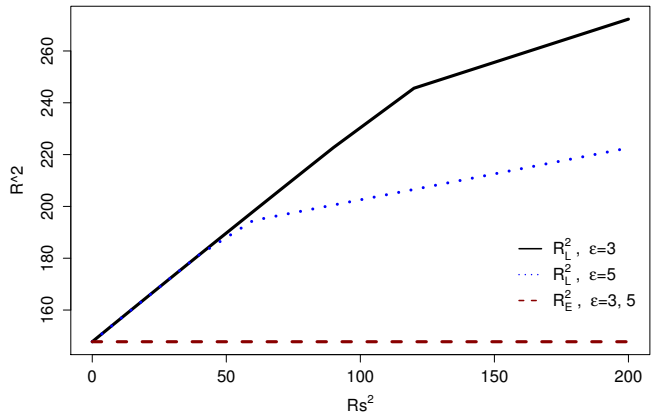

(a) $h = \eta = 0$

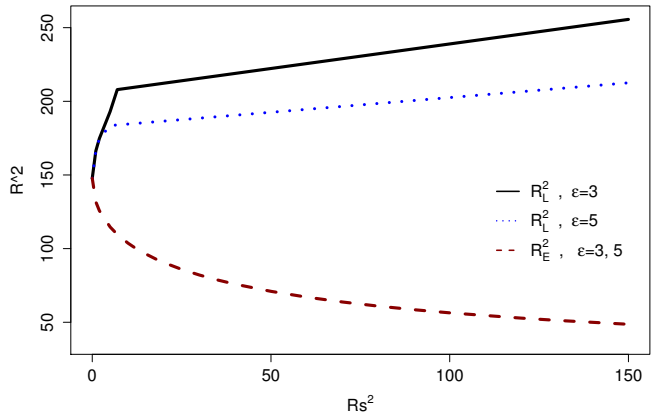

(b) $h = 20$ *and* $\eta = 0$

Figure 6.11: Linear instability and energy stability boundaries for the salted below Darcy convection problem with anisotropic effect for $\alpha = 0.5$, and $\chi = 10$ for different values of ϵ.

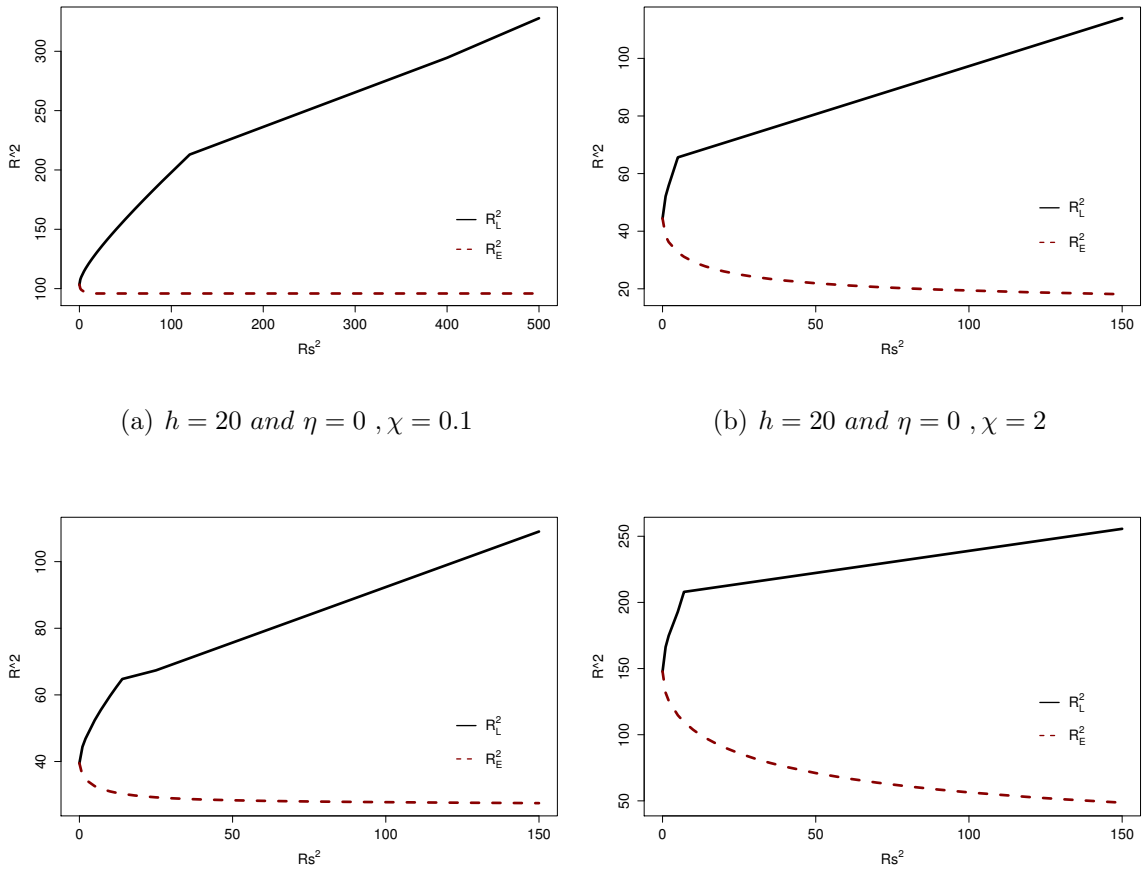

(a) $h = 20$ *and* $\eta = 0$, $\chi = 0.1$

(b) $h = 20$ *and* $\eta = 0$, $\chi = 2$

(c) $h = 20$ *and* $\eta = 0$, $\chi = 0.5$

(d) $h = 20$ *and* $\eta = 0$, $\chi = 10$

Figure 6.12: Linear instability and energy stability boundaries for the salted below Darcy convection problem with anisotropic effect for $\alpha = 0.5$ and $\epsilon = 3$.

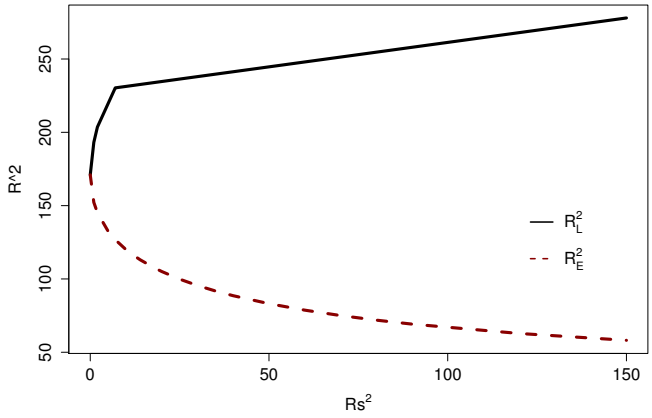

(a) $h = 20$ *and* $\eta = 0$, $\alpha = 1$

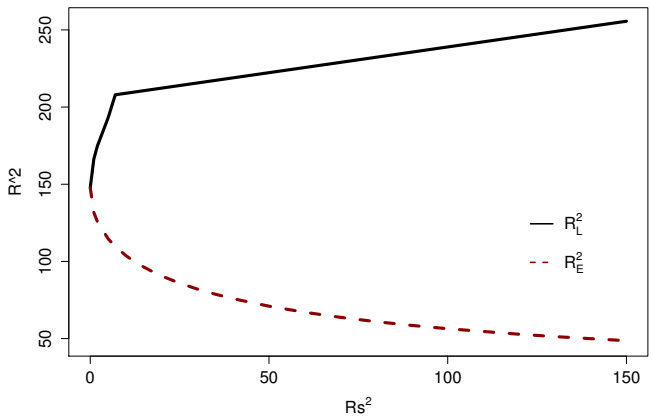

(b) $h = 20$ *and* $\eta = 0$, $\alpha = 0.5$

Figure 6.13: Linear instability and energy stability boundaries for the salted below Darcy convection problem with anisotropic effect for $\chi = 10$ and $\epsilon = 3$.

Chapter 7

One-Dimensional Acceleration Waves in Non-Linear Double Porosity Materials

7.1 Introduction

In this chapter we move away from the content of the previous five chapters although we still remain in the remit of porous media. In the previous cases the solid skeleton of the porous material remains fixed while the fluid moves. However, when one is dealing with waves it is arguable that one should consider deformation of the elastic skeleton itself. Therefore, we now change direction and study wave motion in an elastic body but we allow the body to have a double porosity structure.

Elastic double porosity materials play a considerable interest recently and are available in abundance in nature. There are relatively large pores called macro pores, but additionally fissures or cracks, which are pores on a much small scale, and these are known as micro pores. To the macro pores there is an associated pressure field and another pressure field is associated to the micro pores. An example of such double porosity, macro and micro, structure is presented in the photographs of Masin et al. [65]. Double porosity materials are of great importance in civil engineering, in geophysics, in petroleum recovery, and the subject of attention in modelling gas production via the technique of fracking, cf. Kim and Moridis [47] and Sarma and

Aziz [93].

Modelling double porosity elastic materials begins with Barenblatt et al. [7], in which they presented the basic concepts of the motion of liquids. Under certain assumptions, Barenblatt et al. [7] obtained an expression for the intensity of the transfer of liquid between the fissures and the pores. Recently, the work of Barenblatt et al. [7] has been employed and generalised by many researchers, cf. Berryman and Wang [10], Masters et al. [66], Zhao and Chen [127], Gentile and Straughan [35], Jeong et al. [46], Straughan [104, 106], Ciarletta et al. [23], Svanadze [112, 113], Iesan [41], Kumar et al. [50], Marin et al. [64], Scarpetta and Svanadze [94], and Tsagareli and Bitsadze [117].

Berryman and Wang [10] generalised the quasi-static results to incorporate wave propagation effect and conclude that the double porosity dual-permeability analysis has the capability to explain both wave propagation and attenuation in earth materials. Ciarletta et al. [23] considered the coupled linear theory of flow and deformation processes of the double porosity media. They established the basic properties of linear harmonic plane waves and they proved the uniqueness theorems for classical solutions of the boundary value problems of steady vibrations. Gentile and Straughan [35] proposed a model for a nonlinear elastic body with a double porosity structure. They allow the strain energy function and the macro and micro porosity structures' effective permeabilities to be general nonlinear functions of the deformation gradient, macro and micro pressure gradients and of the macro and micro pressures themselves. They developed the analysis of a fully nonlinear acceleration wave and derived and completely analysed the amplitude equation for an acceleration wave in the one-dimensional case for a wave moving into a constant strain and constant macro and micro pressures state. Iesan [41] investigated a linear theory of elastic solids with a double porosity structure using the method of potentials to study the basic boundary-value problems. Then he established some existence and uniqueness results.

Recently, many investigations are carried out in thermoelastic materials with double porosity structure, see e.g. Svanadze [113], Scarpetta and Svanadze [94], Iesan and Quintanilla [42], Iesan [43], chapter 7 of Straughan [100], see also Straughan

[108] and the references therein. Svanadze [113] considered the linear theory of thermoelasticity for solids with isotropic double porosity. He formulated a wide class of boundary value problems of steady vibrations and proved the uniqueness theorems for classical solutions of these problems. Scarpetta and Svanadze [94] investigated the linear quasi-static theory of thermoelasticity. They obtained the Green's formulas and established the formulas of integral representations of classical solutions and they proved the uniqueness theorems. Iesan and Quintanilla [42] generalised the idea of Nunziato and Cowin theory [72] of materials with voids to derive theory of thermoelastic solids with double porosity structure. They proved the uniqueness of solutions by using the logarithmic convexity arguments, cf. Ames and Straughan [6] page.17, and they investigated the deformation of an elastic space with a spherical cavity.

Gentile and Straughan [35] described acceleration wave behaviour in a non-linear elastic body with a double porosity structure by employing a non-linear elasticity theory with double porosity based on an internal strain energy function which is a general function of the constitutive variables. Here, we are analysing a more general acceleration wave than Gentile and Straughan [35] in which the fluxes satisfy the same constitutive theory as the internal strain energy function. Gentile and Straughan [35] chose a special form for the fluxes.

7.2 Basic Equations

Let ϖ be a body deformed from a reference configuration at time $t = 0$ into a new configuration at time t. Denote the points in the reference configuration by X. The mapping to the new configuration denoted by

$$x = x(X, t). \tag{7.2.1}$$

By referring to the reference configuration, the displacement u of a typical particle moving from X in the reference configuration to x at time t is

$$u(X, t) = x(X, t) - X \ . \tag{7.2.2}$$

The deformation gradient tensor is

$$F_X = \frac{\partial x}{\partial X} \ , \tag{7.2.3}$$

which leads to the displacement gradient

$$u_X = \frac{\partial u}{\partial X} = \frac{\partial x}{\partial X} - \frac{\partial X}{\partial X} = F_X - 1 \ . \tag{7.2.4}$$

We consider the theory of double porosity elastic materials based on an internal strain energy function W. The basic equations for double porosity elastic materials involve the elastic displacement, $u(X,t)$, a fluid pressure associated with the macro pores, $p(X,t)$, and a fluid pressure associated with the fissures, $q(X,t)$. The governing equations in 1-Dimension are the momentum equation, an equation which arises from a Darcy law connected to the macro pores and an equation which comes from a Darcy law connected to the micro pores. The basic system of equations is

$$\begin{aligned} \rho\ddot{u} =& \frac{\partial}{\partial X}\left(\frac{\partial W}{\partial u_X}\right) - \frac{\partial}{\partial X}\left(\beta p\right) - \frac{\partial}{\partial X}\left(\gamma q\right), \\ \alpha\dot{p} =& \frac{\partial J}{\partial X} - \lambda(p-q) - \beta\frac{\partial \dot{u}}{\partial X}, \\ \beta_1\dot{q} =& \frac{\partial M}{\partial X} + \lambda(p-q) - \gamma\frac{\partial \dot{u}}{\partial X}, \end{aligned} \tag{7.2.5}$$

where ρ is the density, β and γ are constitutive functions of p and q which couple equations (7.2.5), $\lambda > 0$ is the interaction coefficient, the inertia coefficients $\alpha > 0$ and $\beta_1 > 0$ are constants. Throughout we employ standard notation, subscript $,X$ denotes $\partial/\partial X$ with X fixed and a superposed dot denotes $\partial/\partial t$, namely, partial differentiation with respect to time. The terms J and M are the fluxes associated to the pressures p and q, which satisfy the same constitutive theory as W.

For constitutive theory we use the list of variables

$$\chi = u_X,\ p_X,\ q_X,\ p,\ q \ ,$$

and suppose that

$$W = W(\chi),\ J = J(\chi)\ and\ M = M(\chi). \tag{7.2.6}$$

7.3 Acceleration Waves

We need the compatibility relations to study and analyse the acceleration waves. The compatibility relations may be found in Truesdell and Toupin [116] and Chen [21]. We define an acceleration wave for the system (7.2.5) as a surface S such that $u(X,t)$, $p(X,t)$, $q(X,t)$ and their first derivatives are continuously differentiable everywhere but the functions $\ddot{u}, \dot{u}_{,X}, u_{,XX}, \ddot{p}, \dot{p}_{,X}, p_{XX}, \ddot{q}, \dot{q}_{,X}$ *and* $q_{,XX}$ and their higher derivatives suffer a finite discontinuities. The jump of a function across the wave,$[f]$, is defined as

$$[f] = f^+ - f^-, \tag{7.3.1}$$

where

$$f^+ = \lim_{X \to S^+},$$

and

$$f^- = \lim_{X \to S^-}.$$

The amplitudes $a(t)$, $P(t)$, $Q(t)$ of the acceleration wave are defined by

$$a(t) = [\ddot{u}],\ P(t) = [\ddot{p}(t)],\ Q(t) = [\ddot{q}(t)]. \tag{7.3.2}$$

To find the wave speeds of an acceleration wave we begin with equations (7.2.5).

By the chain rule, employing the relations (7.2.6), system (7.2.5) may be rewritten as

$$\begin{aligned}
\rho\ddot{u} =& \frac{\partial^2 W}{\partial u_X \partial u_X} u_{XX} + \frac{\partial^2 W}{\partial p_X \partial u_X} p_{XX} + \frac{\partial^2 W}{\partial q_X \partial u_X} q_{XX} \\
&+ \frac{\partial^2 W}{\partial p \partial u_X} p_X + \frac{\partial^2 W}{\partial q \partial u_X} q_X - \beta p_X - \beta_p p_X p \\
&- \beta_q q_X p - \gamma q_X - \gamma_p p_X q - \gamma_q q_X q\ , \\
\alpha\dot{p} =& \frac{\partial J}{\partial u_X} u_{XX} + \frac{\partial J}{\partial p_X} p_{XX} + \frac{\partial J}{\partial q_X} q_{XX} + \frac{\partial J}{\partial p} p_X + \frac{\partial J}{\partial q} q_X \\
&- \lambda(p-q) - \beta \frac{\partial \dot{u}}{\partial X}\ , \\
\beta_1\dot{q} =& \frac{\partial M}{\partial u_X} u_{XX} + \frac{\partial M}{\partial p_X} p_{XX} + \frac{\partial M}{\partial q_X} q_{XX} + \frac{\partial M}{\partial p} p_X + \frac{\partial M}{\partial q} q_X \\
&+ \lambda(p-q) - \gamma \frac{\partial \dot{u}}{\partial X}.
\end{aligned} \tag{7.3.3}$$

To proceed we evaluate equations (7.3.3) on either side of S and in this way we take the jumps of equations (7.3.3), employing the definition of the acceleration wave S and the constitutive theory (7.2.6) to obtain

$$\begin{aligned}
\rho[u_{tt}] &= W_{,u_X u_X}[u_{XX}] + W_{,p_X u_X}[p_{XX}] + W_{,q_X u_X}[q_{XX}] \ , \\
0 &= \frac{\partial J}{\partial u_X}[u_{XX}] + \frac{\partial J}{\partial p_X}[p_{XX}] + \frac{\partial J}{\partial q_X}[q_{XX}] - \beta[u_{tX}] \ , \\
0 &= \frac{\partial M}{\partial u_X}[u_{XX}] + \frac{\partial M}{\partial p_X}[p_{XX}] + \frac{\partial M}{\partial q_X}[q_{XX}] - \gamma[u_{tX}].
\end{aligned} \tag{7.3.4}$$

Next, we employ the Hadamard relation, sometimes known as the kinematic condition of compatibility, cf. Truesdell and Toupin [116] and Chen [21],

$$\frac{\delta}{\delta t}[f] = \left[\frac{\partial f}{\partial t}\right] + V\left[\frac{\partial f}{\partial X}\right] \ , \tag{7.3.5}$$

where $\delta/\delta t$ denotes the time derivative at the wave and V is the speed of the wave. Since $u,\ p,\ q \in C^1(\mathcal{R})$, $[u_t] = 0,\ [u_X] = 0,\ [p_t] = 0,\ [p_X] = 0,\ [q_t] = 0,\ [q_X] = 0$, so by using the Hadamard relation (7.3.5),

$$\begin{aligned}
0 &= \frac{\delta}{\delta t}[u_t] = [u_{tt}] + V[u_{tX}] \ , \quad 0 = \frac{\delta}{\delta t}[u_X] = [u_{Xt}] + V[u_{XX}] \ , \\
0 &= \frac{\delta}{\delta t}[p_t] = [p_{tt}] + V[p_{tX}] \ , \quad 0 = \frac{\delta}{\delta t}[p_X] = [p_{Xt}] + V[p_{XX}] \ , \\
0 &= \frac{\delta}{\delta t}[q_t] = [q_{tt}] + V[q_{tX}] \ , \quad 0 = \frac{\delta}{\delta t}[q_X] = [q_{Xt}] + V[q_{XX}] \ .
\end{aligned} \tag{7.3.6}$$

Thus,

$$\begin{aligned}
[u_{tt}] &= -V[u_{tX}] = V^2[u_{XX}] \ , \\
[p_{tt}] &= -V[p_{tX}] = V^2[p_{XX}] \ , \\
[q_{tt}] &= -V[q_{tX}] = V^2[q_{XX}].
\end{aligned} \tag{7.3.7}$$

Employ relations (7.3.7) in equations (7.3.4) to derive the three jump equations

$$\begin{aligned}
\left(\rho V^2 - W_{u_X u_X}\right) a(t) &= W_{p_X u_X} P(t) + W_{q_X u_X} Q(t) \ , \\
\left(J_{u_X} + \beta V\right) a(t) &= -J_{p_X} P(t) - J_{q_X} Q(t) \ , \\
\left(M_{u_X} + \gamma V\right) a(t) &= -M_{p_X} P(t) - M_{q_X} Q(t).
\end{aligned} \tag{7.3.8}$$

Solving for $P(t)$ and $Q(t)$ in terms of $a(t)$ only, from equations $(7.3.8)_2$ and $(7.3.8)_3$ yields

$$P(t) = \frac{J_{q_X}\left(M_{u_X} + \gamma V\right) - M_{q_X}\left(J_{u_X} + \beta V\right)}{M_{q_X} J_{p_X} - J_{q_X} M_{p_X}} a(t) \ , \tag{7.3.9}$$

and

$$Q(t) = \frac{J_{p_X}\left(M_{u_X} + \gamma V\right) - M_{p_X}\left(J_{u_X} + \beta V\right)}{M_{p_X} J_{q_X} - J_{p_X} M_{q_X}} a(t) \ . \tag{7.3.10}$$

Substitute the expressions (7.3.9) and (7.3.10) into equation $(7.3.8)_1$ to obtain the 1-Dimensional wave speed equation

$$\begin{aligned}\left(\rho V^2 - W_{u_X u_X}\right) a(t) =& W_{p_X u_X} \frac{J_{q_X}\left(M_{u_X} + \gamma V\right) - M_{q_X}\left(J_{u_X} + \beta V\right)}{M_{q_X} J_{p_X} - J_{q_X} M_{p_X}} a(t) \\ &+ W_{q_X u_X} \frac{J_{p_X}\left(M_{u_X} + \gamma V\right) - M_{p_X}\left(J_{u_X} + \beta V\right)}{M_{p_X} J_{q_X} - J_{p_X} M_{q_X}} a(t).\end{aligned} \tag{7.3.11}$$

For a non-zero amplitude $a(t) = [u_{tt}]$ we see from (7.3.11), that

$$\begin{aligned}&\rho V^2 + \left[\frac{\beta}{\Xi}\left(W_{q_X u_X} M_{p_X} - W_{p_X u_X} M_{q_X}\right) + \frac{\gamma}{\Xi}\left(W_{p_X u_X} J_{q_X} - W_{q_X u_X} J_{p_X}\right)\right] V \\ &+ \frac{J_{u_X}}{\Xi}\left(W_{q_X u_X} M_{p_X} - W_{p_X u_X} M_{q_X}\right) + \frac{M_{u_X}}{\Xi}\left(W_{p_X u_X} J_{q_X} - W_{q_X u_X} J_{p_X}\right) - W_{u_X u_X} = 0 \ .\end{aligned} \tag{7.3.12}$$

Here $\Xi = M_{p_X} J_{q_X} - J_{p_X} M_{q_X}$.

Thus, the speed of the wave is

$$V = -\frac{E_1}{2\rho} + \sqrt{\frac{E_1^2}{4\rho^2} + \frac{E_2}{\rho}} \ , \tag{7.3.13}$$

where

$$E_1 = \left(\frac{\beta M_{p_X}}{\Xi} - \frac{\gamma J_{p_X}}{\Xi}\right) W_{q_X u_X} + \left(\frac{\gamma J_{q_X}}{\Xi} - \frac{\beta M_{q_X}}{\Xi}\right) W_{p_X u_X} \ , \tag{7.3.14}$$

and

$$\begin{aligned}E_2 = W_{u_X u_X} &+ \left(\frac{M_{u_X} J_{p_X}}{\Xi} - \frac{J_{u_X} M_{p_X}}{\Xi}\right) W_{q_X u_X} \\ &+ \left(\frac{J_{u_X} M_{q_X}}{\Xi} - \frac{M_{u_X} J_{q_X}}{\Xi}\right) W_{p_X u_X} \ .\end{aligned} \tag{7.3.15}$$

Actually, equation (7.3.12) allows for two waves, a right moving one and a left moving one. We here only deal with one, the one moving to the right.

Gentile and Straughan [35] chose the form of the fluxes as

$$J_{GS} = k(\chi) p \quad and \quad M_{GS} = m(\chi) q.$$

The jump reduces their system to

$$\begin{aligned}\rho[\ddot{u}] =& W_{u_X u_X}[u_{XX}] + W_{u_X p_X}[p_{XX}] + W_{u_X q_X}[q_{XX}] \ , \\ 0 =& k[p_{XX}] - \beta[\dot{u}_X] \ , \\ 0 =& m[q_{XX}] - \gamma[\dot{u}_X] \ ,\end{aligned} \tag{7.3.16}$$

and using the Hadamard relation gives the following forms of $P_{GS}(t)$ and $Q_{GS}(t)$

$$P_{GS}(t) = -\frac{\beta V_{GS}}{k}a(t) \;\; and \;\; Q_{GS}(t) = -\frac{\gamma V_{GS}}{m}a(t) \; ,$$

and the speed of the wave is

$$V_{GS} = -\frac{E_{GS}}{2\rho} + \sqrt{\frac{E_{GS}^2}{4\rho^2} + \frac{W_{u_X u_X}}{\rho}} \; ,$$

where

$$E_{GS} = \frac{\beta}{k}W_{u_X p_X} + \frac{\gamma}{m}W_{u_X q_X}.$$

Comparing our system (7.3.4) to (7.3.16) shows that $J_{u_X} = M_{u_X} = J_{q_X} = M_{p_X} = 0$, $J_{p_X} = k$, and $M_{q_X} = m$ in Gentile and Straughan [35].

7.4 Amplitude Equation

We may proceed to derive the amplitude equation for an acceleration wave by differentiating equation $(7.3.3)_1$ with respect to X and equations $(7.3.3)_2$ and $(7.3.3)_3$ with respect to t, and then take the jumps of the resulting equations. Moreover, to simplify the calculations we suppose that the state ahead of the wave is constant, *i.e.*, $p^+ = constant$, $q^+ = constant$, and $u^+_{,X} = constant$, which implies $p^+_{,X} = 0$, $p^+_{,XX} = 0$, $\dot{p}^+ = 0$, $q^+_{,X} = 0$, $q^+_{,XX} = 0$, $\dot{q}^+ = 0$, $u^+_{,XX} = 0$ and $\dot{u}^+_{,X} = 0$ and therefore many terms disappear. We employ the expressions obtained from the Hadamard relation (7.3.7) together with the product jump relation

$$[ab] = a^+[b] + b^+[a] - [a][b] \; . \tag{7.4.1}$$

One requires further relations and these may be obtained from the Hadamard relation as

$$\begin{aligned}
[u_{XXX}] &= -\frac{[\dot{u}_{XX}]}{V} + \frac{1}{V^3}\frac{\delta a}{\delta t} \; , & -[\dot{u}_{XX}] &= \frac{[\ddot{u}_X]}{V} + \frac{1}{V^2}\frac{\delta a}{\delta t} \; , \\
[u_{XXX}] &= \frac{[\ddot{u}_X]}{V^2} + \frac{2}{V^3}\frac{\delta a}{\delta t} \; , & [p_{XXX}] &= -\frac{[\dot{p}_{XX}]}{V} + \frac{1}{V^3}\frac{\delta P}{\delta t} \; , \\
-[\dot{p}_{XX}] &= \frac{[\ddot{p}_X]}{V} + \frac{1}{V^2}\frac{\delta P}{\delta t} \; , & [p_{XXX}] &= \frac{[\ddot{p}_X]}{V^2} + \frac{2}{V^3}\frac{\delta P}{\delta t} \; , \\
[q_{XXX}] &= -\frac{[\dot{q}_{XX}]}{V} + \frac{1}{V^3}\frac{\delta Q}{\delta t} \; , & -[\dot{q}_{XX}] &= \frac{[\ddot{q}_X]}{V} + \frac{1}{V^2}\frac{\delta Q}{\delta t} \; , \\
[q_{XXX}] &= \frac{[\ddot{q}_X]}{V^2} + \frac{2}{V^3}\frac{\delta Q}{\delta t} \; .
\end{aligned} \tag{7.4.2}$$

The jump of the X derivative of $(7.3.3)_1$ yields the equation

$$\begin{aligned}\rho[\ddot{u}_X] =& W_{u_Xu_X}[u_{XXX}] - W_{u_Xu_Xu_X}[u_{XX}]^2 \\ &- W_{u_Xu_Xp_X}[u_{XX}][p_{XX}] - W_{u_Xu_Xq_X}[u_{XX}][q_{XX}] \\ &+ W_{p_Xu_X}[p_{XXX}] - W_{p_Xu_Xu_X}[p_{XX}][u_{XX}] \\ &- W_{p_Xu_Xp_X}[p_{XX}]^2 - W_{p_Xu_Xq_X}[p_{XX}][q_{XX}] \\ &+ W_{q_Xu_X}[q_{XXX}] - W_{q_Xu_Xu_X}[u_{XX}][q_{XX}] \\ &- W_{q_Xu_Xp_X}[q_{XX}][p_{XX}] - W_{q_Xu_Xq_X}[q_{XX}]^2 \\ &+ W_{qu_X}[q_{XX}] + W_{pu_X}[p_{XX}] - \beta[p_{XX}] \\ &- \beta_p p^+[p_{XX}] - \beta_q p^+[q_{XX}] - \gamma[q_{XX}] \\ &- \gamma_p q^+[p_{XX}] - \gamma_q q^+[q_{XX}] \ .\end{aligned} \tag{7.4.3}$$

After taking the t derivative of $(7.3.3)_2$ we take the jump to arrive at the equation

$$\begin{aligned}\alpha[\ddot{p}] =& J_{u_X}[\dot{u}_{XX}] + J_{u_Xu_X}[u_{XX}][\dot{u}_X] - J_{u_Xp_X}[u_{XX}][\dot{p}_X] \\ &- J_{u_Xq_X}[u_{XX}][\dot{q}_X] + J_{p_X}[\dot{p}_{XX}] - J_{p_Xu_X}[\dot{u}_X][p_{XX}] \\ &- J_{p_Xp_X}[p_{XX}][\dot{p}_X] - J_{p_Xq_X}[p_{XX}][\dot{q}_X] + J_{q_X}[\dot{q}_{XX}] \\ &- J_{q_Xu_X}[q_{XX}][\dot{u}_X] - J_{q_Xp_X}[q_{XX}][\dot{p}_X] - J_{q_Xq_X}[q_{XX}][\dot{q}_X] \\ &+ J_p[\dot{p}_X] + J_q[\dot{q}_X] - \beta[\ddot{u}_X] \ .\end{aligned} \tag{7.4.4}$$

Further, the jump of the t derivative of $(7.3.3)_3$ yields

$$\begin{aligned}\beta_1[\ddot{q}] =& M_{u_X}[\dot{u}_{XX}] - M_{u_Xu_X}[u_{XX}][\dot{u}_X] - M_{u_Xp_X}[\dot{p}_X][u_{XX}] \\ &- M_{u_Xq_X}[\dot{q}_X][u_{XX}] + M_{p_X}[\dot{p}_{XX}] \\ &- M_{p_Xu_X}[p_{XX}][\dot{u}_X] - M_{p_Xp_X}[p_{XX}][\dot{p}_X] \\ &- M_{p_Xq_X}[p_{XX}][\dot{q}_X] + M_{q_X}[\dot{q}_{XX}] \\ &- M_{q_Xu_X}[\dot{u}_X][q_{XX}] - M_{q_Xp_X}[\dot{p}_X][q_{XX}] \\ &- M_{q_Xq_X}[\dot{q}_X][q_{XX}] + M_p[\dot{p}_X] + M_q[\dot{q}_X] - \gamma[\ddot{u}_X] \ .\end{aligned} \tag{7.4.5}$$

We have to remove the third derivative terms in equations (7.4.3), (7.4.4) and (7.4.5) by employing (7.3.7) together with (7.4.2). To achieve this we form the combination

$$(7.4.3)\times\Xi + (7.4.4)\times\frac{W_{q_Xu_X}M_{p_X} - W_{p_Xu_X}M_{q_X}}{V} + (7.4.5)\times\frac{W_{p_Xu_X}J_{q_X} - W_{q_Xu_X}J_{p_X}}{V} \ ,$$

where as defined in section (7.3) $\Xi = M_{p_X} J_{q_X} - J_{p_X} M_{q_X}$.

We then employ the wave speed equation (7.3.11) to show that $a(t)$ satisfies the amplitude equation

$$\frac{\delta a}{\delta t} + \frac{\alpha_2}{\alpha_1} a(t) + \frac{\alpha_3}{\alpha_1} a^2(t) = 0 \ , \tag{7.4.6}$$

where $\delta a/\delta t$ is the rate of change of the amplitude as seen by an observer moving with the wave and the coefficients $\alpha_i,\ i = 1, 2, 3$, are given by

$$\begin{aligned} \alpha_1 =& V\Xi^2 \left\{ W_{p_X u_X} (M_{q_X} \zeta_1 - J_{q_X} \zeta_2) + W_{q_X u_X} (J_{p_X} \zeta_2 - M_{p_X} \zeta_1) \right\} \\ &+ V\Xi^2 \left\{ 2W_{u_X u_X} \Xi + W_{q_X u_X} \zeta_5 + W_{p_X u_X} \zeta_6 \right\} \ , \end{aligned} \tag{7.4.7}$$

and

$$\begin{aligned} \alpha_2 =& V^2\Xi^2 (M_{q_X} \zeta_1 - J_{q_X} \zeta_2) \left\{ W_{pu_X} - \beta - \beta_p p^+ - \gamma_p q^+ \right\} \\ &+ V^2\Xi^2 (J_{p_X} \zeta_2 - M_{p_X} \zeta_1) \left\{ W_{qu_X} - \beta_q p^+ - \gamma - \gamma_q q^+ \right\} \\ &- \zeta_3 V\Xi (M_{q_X} \zeta_1 - J_{q_X} \zeta_2) \left\{ J_p V + \alpha V^2 \right\} \\ &- \zeta_3 V\Xi (J_{p_X} \zeta_2 - M_{p_X} \zeta_1) J_q V \\ &- \zeta_4 V\Xi (M_{q_X} \zeta_1 - J_{q_X} \zeta_2) M_p V \\ &- \zeta_4 V\Xi (J_{p_X} \zeta_2 - M_{p_X} \zeta_1) \left\{ M_q V + \beta_1 V^2 \right\} \end{aligned} \tag{7.4.8}$$

and

$$\begin{aligned}
\alpha_3 = &- \Xi^3 W_{u_X u_X u_X} - 2W_{u_X u_X p_X}\Xi^2(M_{q_X}\zeta_1 - J_{q_X}\zeta_2) \\
&- 2W_{u_X u_X q_X}\Xi^2(J_{p_X}\zeta_2 - M_{p_X}\zeta_1) \\
&- W_{p_X p_X u_X}\Xi(M_{q_X}\zeta_1 - J_{q_X}\zeta_2)^2 \\
&- 2W_{p_X q_X u_X}\Xi(M_{q_X}\zeta_1 - J_{q_X}\zeta_2)(J_{p_X}\zeta_2 - M_{p_X}\zeta_1) \\
&- W_{q_X q_X u_X}\Xi(J_{p_X}\zeta_2 - M_{p_X}\zeta_1)^2 \\
&+ \zeta_3\left\{J_{u_X u_X}\Xi^2 + 2J_{p_X u_X}\Xi(M_{q_X}\zeta_1 - J_{q_X}\zeta_2)\right\} \\
&+ 2J_{q_X u_X}\Xi\zeta_3(J_{p_X}\zeta_2 - M_{p_X}\zeta_1) \\
&+ J_{p_X p_X}\zeta_3(M_{q_X}\zeta_1 - J_{q_X}\zeta_2)^2 \\
&+ 2J_{p_X q_X}\zeta_3(M_{q_X}\zeta_1 - J_{q_X}\zeta_2)(J_{p_X}\zeta_2 - M_{p_X}\zeta_1) \\
&+ J_{q_X q_X}\zeta_3(J_{p_X}\zeta_2 - M_{p_X}\zeta_1)^2 \\
&+ \zeta_4\left\{M_{u_X u_X}\Xi^2 + 2M_{p_X u_X}\Xi(M_{q_X}\zeta_1 - J_{q_X}\zeta_2)\right\} \\
&+ 2M_{q_X u_X}\Xi\zeta_4(J_{p_X}\zeta_2 - M_{p_X}\zeta_1) \\
&+ M_{p_X p_X}\zeta_4(M_{q_X}\zeta_1 - J_{q_X}\zeta_2)^2 \\
&+ 2M_{p_X q_X}\zeta_4(M_{q_X}\zeta_1 - J_{q_X}\zeta_2)(J_{p_X}\zeta_2 - M_{p_X}\zeta_1) \\
&+ M_{q_X q_X}\zeta_4(J_{p_X}\zeta_2 - M_{p_X}\zeta_1)^2 \ ,
\end{aligned} \tag{7.4.9}$$

where

$$\begin{aligned}
\zeta_1 &= J_{u_X} + \beta V \ , \\
\zeta_2 &= M_{u_X} + \gamma V \ , \\
\zeta_3 &= W_{q_X u_X} M_{p_X} - W_{p_X u_X} M_{q_X} \ , \\
\zeta_4 &= W_{p_X u_X} J_{q_X} - W_{q_X u_X} J_{p_X} \ , \\
\zeta_5 &= M_{u_X} J_{p_X} - M_{p_X} J_{u_X} \ , \\
\zeta_6 &= M_{q_X} J_{u_X} - M_{u_X} J_{q_X}.
\end{aligned}$$

Equation (7.4.6) may be written as

$$\frac{\delta a}{\delta t} + \lambda_1 a(t) + \lambda_2 a^2(t) = 0 \ , \tag{7.4.10}$$

where $\lambda_1 = \alpha_2/\alpha_1$ and $\lambda_2 = \alpha_3/\alpha_1$. Under the conditions that V, λ_1 and λ_2 are constants ahead of the wave, equation (7.4.10) may be integrated to yield the amplitude

$a(t)$ as

$$a(t) = \frac{a(0)}{e^{\lambda_1 t} + (\lambda_2 a(0)/\lambda_1)\{e^{\lambda_1 t} - 1\}}. \tag{7.4.11}$$

The blow-up time is

$$T = \frac{1}{\lambda_1} ln \left(\frac{\frac{\lambda_2 a(0)}{\lambda_1}}{1 + \frac{\lambda_2 a(0)}{\lambda_1}} \right). \tag{7.4.12}$$

For the blow-up,

1) if $\lambda_2 a(0)/\lambda_1 < -1$, we need $\lambda_1 > 0$, which implies either

(a) $\lambda_2 < 0$ and $a(0) > 0$ such that $|\lambda_2 a(0)| > \lambda_1$, or

(b) $\lambda_2 > 0$ and $a(0) < 0$ such that $|\lambda_2 a(0)| > \lambda_1$,

2) if $\lambda_2 a(0)/\lambda_1 > 0$, we need $\lambda_1 < 0$, which implies either

(a) $\lambda_2 < 0$ and $a(0) > 0$, or

(b) $\lambda_2 > 0$ and $a(0) < 0$.

3) if $\lambda_1 = 0$, then $a(t)$ satisfies the amplitude equation

$$\frac{\delta a}{\delta t} + \lambda_2 a^2(t) = 0.$$

This gives

$$a(t) = \frac{a(0)}{1 + a(0)\lambda_2 t},$$

a similar case to this has been discussed in Straughan [100]. In which for the blow-up time, $T = -1/a(0)\lambda_2$,

if $a(0) < 0$, we need $\lambda_2 > 0$, and

if $a(0) > 0$, we need $\lambda_2 < 0$.

7.5 Special Case: Given Strain Energy Function

To solve (7.4.10) and obtain some useful information we need to know the strain energy function $W = W(\chi)$, the fluxes, $M(\chi), J(\chi)$, and the constitutive functions,

$\beta(p,q)$ *and* $\gamma(p,q)$. Suppose

$$\begin{aligned} W(\chi) =& \iota_1 u_X^2 + \iota_2 u_X p + \iota_3 u_X q + \iota_4 pq + \iota_5 p^2 + \iota_7 p_X^2 \\ &+ \iota_8 p_X q_X + \iota_9 q_X^2 \ , \\ M(\chi) =& \iota_{10} u_X^2 + \iota_{11} u_X p + \iota_{12} u_X q + \iota_{13} pq + \iota_{14} p^2 + \iota_{15} q^2 \\ &+ \iota_{16} p_X^2 + \iota_{17} p_X q_X + \iota_{18} q_X^2 \ , \\ J(\chi) =& \iota_{19} u_X^2 + \iota_{20} u_X p + \iota_{21} u_X q + \iota_{22} pq + \iota_{23} p^2 + \iota_{24} q^2 \\ &+ \iota_{25} p_X^2 + \iota_{26} p_X q_X + \iota_{27} q_X^2 \ , \\ \beta(p,q) =& \iota_{28} p^2 + \iota_{29} pq + \iota_{30} q^2 \ , \\ \gamma(p,q) =& \iota_{31} p^2 + \iota_{32} pq + \iota_{33} q^2 \ , \end{aligned} \tag{7.5.1}$$

for constants $\iota_1, \iota_2, ..., \iota_{33}$. Then,

$$\begin{aligned} & W_{u_X} = 2\iota_1 u_X + \iota_2 p + \iota_3 q \ , \\ & W_{u_X u_X} = 2\iota_1 \ , \\ & W_{u_X u_X u_X} = 0 \ , \\ & W_{u_X u_X p_X} = W_{u_X u_X q_X} = W_{p_X p_X u_X} = W_{p_X q_X u_X} = W_{q_X q_X u_X} = 0 \ , \\ & W_{p_X u_X} = W_{q_X u_X} = 0 \ , \\ & W_{p u_X} = \iota_2 \ , \\ & W_{q u_X} = \iota_3 . \end{aligned} \tag{7.5.2}$$

Moreover,

$$\begin{aligned} & M_{u_X} = 2\iota_{10} u_X + \iota_{11} p + \iota_{12} q \ , \\ & M_{u_X u_X} = 2\iota_{10} \ , \\ & M_{p_X u_X} = M_{q_X u_X} = 0 \ , \\ & M_{p_X} = 2\iota_{16} p_X + \iota_{17} q_X \ , \\ & M_{q_X} = \iota_{17} p_X + 2\iota_{18} q_X \ , \\ & M_p = \iota_{11} u_X + \iota_{13} q + 2\iota_{14} p \ , \\ & M_q = \iota_{12} u_X + \iota_{13} p + 2\iota_{15} q \ , \\ & M_{p_X p_X} = 2\iota_{16} \ , \\ & M_{p_X q_X} = \iota_{17} \ , \\ & M_{q_X q_X} = 2\iota_{18} \ , \end{aligned} \tag{7.5.3}$$

and

$$\begin{aligned}
J_{u_X} &= 2\iota_{19}u_X + \iota_{20}p + \iota_{21}q \ , \\
J_{u_Xu_X} &= 2\iota_{19} \ , \\
J_{p_Xu_X} &= J_{q_Xu_X} = 0 \ , \\
J_{p_X} &= 2\iota_{25}p_X + \iota_{26}q_X \ , \\
J_{q_X} &= \iota_{26}p_X + 2\iota_{27}q_X \ , \\
J_p &= \iota_{20}u_X + \iota_{22}q + 2\iota_{23}p \ , \\
J_q &= \iota_{21}u_X + \iota_{22}p + 2\iota_{24}q \ , \\
J_{p_Xp_X} &= 2\iota_{25} \ , \\
J_{p_Xq_X} &= \iota_{26} \ , \\
J_{q_Xq_X} &= 2\iota_{27}.
\end{aligned} \tag{7.5.4}$$

While the derivatives of the constitutive functions $\beta(p,q)$ and $\gamma(p,q)$ are

$$\begin{aligned}
\beta_p &= 2\iota_{28}p + \iota_{29}q \ , \\
\beta_q &= \iota_{29}p + 2\iota_{30}q \ , \\
\beta_{pq} &= \iota_{29} \ , \\
\gamma_p &= 2\iota_{31}p + \iota_{32}q \ , \\
\gamma_q &= \iota_{32}p + 2\iota_{33}q \ , \\
\gamma_{pq} &= \iota_{32}.
\end{aligned} \tag{7.5.5}$$

Then, by using (7.5.2)-(7.5.5), it follows that the wave speed is

$$V = \sqrt{\frac{2\iota_1}{\rho}}. \tag{7.5.6}$$

Whereas the amplitude equation is

$$\frac{\delta a}{\delta t} + \frac{\alpha_2}{\alpha_1}a(t) = \frac{\delta a}{\delta t} + \lambda_1 a(t) = 0 \ , \tag{7.5.7}$$

because $\alpha_3 = 0$ and

$$\begin{aligned}
\alpha_1 =& 2(2\iota_1)\Xi^3\sqrt{\frac{2\iota_1}{\rho}} \ , \\
\alpha_2 =& \frac{2\iota_1}{\rho}\Xi^2(M_{q_X}\zeta_1 - J_{q_X}\zeta_2)\left\{W_{pu_X} - \beta - \beta_p p^+ - \gamma_p q^+\right\} \\
&+ \frac{2\iota_1}{\rho}\Xi^2(J_{p_X}\zeta_2 - M_{p_X}\zeta_1)\left\{W_{qu_X} - \beta_q p^+ - \gamma - \gamma_q q^+\right\} \ ,
\end{aligned} \tag{7.5.8}$$

for

$$\begin{aligned}\Xi =&M_{p_X}J_{q_X} - J_{p_X}M_{q_X}\\ =&(2\iota_{16}\iota_{26} - 2\iota_{17}\iota_{25})p_X^2 + (4\iota_{16}\iota_{27} - 4\iota_{18}\iota_{25})p_Xq_X + (2\iota_{17}\iota_{27} - 2\iota_{18}\iota_{26})q_X^2 \ ,\end{aligned} \tag{7.5.9}$$

and

$$\begin{aligned}\zeta_1 =&2\iota_{19}u_X + \iota_{20}p + \iota_{21}q\\ &+ \sqrt{\frac{2\iota_1}{\rho}}(\iota_{28}p^2 + \iota_{29}pq + \iota_{21}q^2) \ ,\\ \zeta_2 =&2\iota_{10}u_X + \iota_{11}p + \iota_{12}q\\ &+ \sqrt{\frac{2\iota_1}{\rho}}(\iota_{31}p^2 + \iota_{32}pq + \iota_{33}q^2) \ ,\\ \zeta_3 =&\zeta_4 = 0 \ ,\\ \zeta_5 =&(4\iota_{10}\iota_{25} - 4\iota_{16}\iota_{19})u_Xp_X + (2\iota_{10}\iota_{26} - 2\iota_{17}\iota_{19})u_Xq_X\\ &+ (2\iota_{11}\iota_{25} - 2\iota_{16}\iota_{20})pp_X + (\iota_{11}\iota_{26} - \iota_{17}\iota_{20})pq_X\\ &+ (2\iota_{12}\iota_{25} - 2\iota_{16}\iota_{21})qp_X + (\iota_{12}\iota_{26} - \iota_{17}\iota_{21})qq_X \ ,\\ \zeta_6 =&(2\iota_{17}\iota_{19} - 2\iota_{10}\iota_{26})u_Xp_X + (4\iota_{18}\iota_{19} - 4\iota_{10}\iota_{27})u_Xq_X\\ &+ (\iota_{17}\iota_{20} - \iota_{11}\iota_{26})pp_X + (2\iota_{18}\iota_{20} - 2\iota_{11}\iota_{27})pq_X\\ &+ (\iota_{17}\iota_{21} - \iota_{12}\iota_{26})qp_X + (2\iota_{18}\iota_{21} - 2\iota_{12}\iota_{27})qq_X.\end{aligned} \tag{7.5.10}$$

Therefore, the amplitude equation (7.5.7) gives

$$ln\ a(t) - ln\ a(0) = -\lambda_1 t \ , \tag{7.5.11}$$

which implies

$$a(t) = a(0)e^{-\lambda_1 t}. \tag{7.5.12}$$

From (7.5.12), we see that $a(t)$ will decay exponentially in time if $\lambda_1 > 0$ and will grow up in time if $\lambda_1 < 0$.

Chapter 8

Three-Dimensional Acceleration Waves in Non-Linear Double Porosity Materials

8.1 Introduction

In the previous chapter (7), we derived the equations governing the wavespeed and the amplitudes of an acceleration wave in a one-dimensional model describing the behaviour of a nonlinear elastic body containing a double porosity structure. While this is very useful and leads to important results, the overall situation is more complicated as a wave moves in a three-dimensional body. Here, we are investigating the propagation of an acceleration wave in three-dimensional fully nonlinear model.

Let $\mathcal{B}_0$ be a body deformed from a reference configuration at time $t = 0$ into a new configuration at time t. Denote the points in the reference configuration by X_A, where $A = 1, 2, 3$. The mapping to the new configuration denoted by

$$x_i = x_i(X_A, t). \tag{8.1.1}$$

By referring to the reference configuration, the displacement $\mathbf{u}$ of a typical particle moving from $\mathbf{X}$ in the reference configuration to $\mathbf{x}$ at time t is

$$u_i(X_A, t) = x_i(X_A, t) - X_i. \tag{8.1.2}$$

The deformation gradient tensor is

$$F_{iA} = \frac{\partial x_i}{\partial X_A}, \tag{8.1.3}$$

which leads to the displacement gradient

$$u_{i,A} = \frac{\partial u_i}{\partial X_A} = \frac{\partial x_i}{\partial X_A} - \frac{\partial X_i}{\partial X_A} = F_{iA} - \delta_{iA}. \tag{8.1.4}$$

We consider the theory of double porosity elastic materials based on an internal strain energy function W. The basic equations involve the elastic displacement, $u_i(X_A, t)$, the fluid pressure associated with the macro pores, $p(X_A, t)$, and the fluid pressure associated with the micro pores, $q(X_A, t)$. The governing equations of double porosity elastic materials in three dimensions are

$$\begin{aligned} \rho\ddot{u}_i =& \frac{\partial}{\partial X_A}\left(\frac{\partial W}{\partial u_{i,A}}\right) - \frac{\partial}{\partial X_A}\left(\beta_{iA}p\right) - \frac{\partial}{\partial X_A}\left(\gamma_{iA}q\right), \\ \alpha\dot{p} =& \frac{\partial J_A}{\partial X_A} - \lambda(p-q) - \beta_{iA}\frac{\partial \dot{u}_i}{\partial X_A}, \\ \beta_1\dot{q} =& \frac{\partial M_A}{\partial X_A} + \lambda(p-q) - \gamma_{iA}\frac{\partial \dot{u}_i}{\partial X_A}. \end{aligned} \tag{8.1.5}$$

In these equations W is the strain energy function, J_A and M_A are the fluxes associated with the macro and micro pores, respectively, referred to the reference configuration. For constitutive theory, we use the list of variables

$$\chi = u_{i,A}\ ,\ p_{,A}\ ,\ q_{,A}\ ,\ p\ ,\ q\ ,$$

and suppose that

$$W = W(\chi),\ J_A = J_A(\chi),\ \textit{and}\ M_A = M_A(\chi)\ , \tag{8.1.6}$$

and

$$\beta_{iA} = \beta_{iA}(p,q)\ \textit{and}\ \gamma_{iA} = \gamma_{iA}(p,q). \tag{8.1.7}$$

8.2 Acceleration Waves

An acceleration wave for a system of a non-linear double porosity elastic material in three dimensions is defined as a surface S such that $u_i(X_A, t), p(X_A, t), q(X_A, t)$ are

C^1 everywhere and the second and higher derivatives of $u_i(X_A,t), p(X_A,t), q(X_A,t)$ are allowed to have finite discontinuities across the surface S.

The amplitudes $a_i(t), P(t), Q(t)$ of the three dimensional acceleration wave are defined by

$$a_i(t) = [\ddot{u}_i], P(t) = [\ddot{p}(t)], Q(t) = [\ddot{q}(t)].$$

To find the wave speed of an acceleration wave, we begin with equations (8.1.5). By the chain rule, employing the relations(8.1.6), system (8.1.5) may be rewritten as

$$\begin{aligned}
\rho\ddot{u}_i =& \frac{\partial^2 W}{\partial u_{i,A}\partial u_{j,B}}\frac{\partial^2 u_j}{\partial X_A \partial X_B} + \frac{\partial^2 W}{\partial u_{i,A}\partial p_{,B}}\frac{\partial^2 p}{\partial X_A \partial X_B} + \frac{\partial^2 W}{\partial u_{i,A}\partial q_{,B}}\frac{\partial^2 q}{\partial X_A \partial X_B} \\
&+ \frac{\partial^2 W}{\partial u_{i,A}\partial p}\frac{\partial p}{\partial X_A} + \frac{\partial^2 W}{\partial u_{i,A}\partial q}\frac{\partial q}{\partial X_A} - \beta_{iA}\frac{\partial p}{\partial X_A} - \frac{\partial \beta_{iA}}{\partial p}\frac{\partial p}{\partial X_A}p \\
&- \frac{\partial \beta_{iA}}{\partial q}\frac{\partial q}{\partial X_A}p - \gamma_{iA}\frac{\partial q}{\partial X_A} - \frac{\partial \gamma_{iA}}{\partial p}\frac{\partial p}{\partial X_A}q - \frac{\partial \gamma_{iA}}{\partial q}\frac{\partial q}{\partial X_A}q\ , \\
\alpha\dot{p} =& \frac{\partial J_A}{\partial u_{i,C}}\frac{\partial^2 u_i}{\partial X_C \partial X_K} + \frac{\partial J_A}{\partial p_{,C}}\frac{\partial^2 p}{\partial X_C \partial X_K} + \frac{\partial J_A}{\partial q_{,C}}\frac{\partial^2 q}{\partial X_C \partial X_K} + \frac{\partial J_A}{\partial p}\frac{\partial p}{\partial X_K} \\
&+ \frac{\partial J_A}{\partial q}\frac{\partial q}{\partial X_K} - \lambda(p-q) - \beta_{iA}\frac{\partial \dot{u}_i}{\partial X_A}\ , \\
\beta_1\dot{q} =& \frac{\partial M_A}{\partial u_{i,C}}\frac{\partial^2 u_i}{\partial X_C \partial X_K} + \frac{\partial M_A}{\partial p_{,C}}\frac{\partial^2 p}{\partial X_C \partial X_K} + \frac{\partial M_A}{\partial q_{,C}}\frac{\partial^2 q}{\partial X_C \partial X_K} + \frac{\partial M_A}{\partial p}\frac{\partial p}{\partial X_K} \\
&+ \frac{\partial M_A}{\partial q}\frac{\partial q}{\partial X_K} + \lambda(p-q) - \gamma_{iA}\frac{\partial \dot{u}_i}{\partial X_A}.
\end{aligned} \tag{8.2.1}$$

General compatibility relations for a function $f(\mathbf{X},t)$ are needed across the surface S, cf. Chen [21] and Straughan [100]. If f is continuous in $\mathcal{R}^3$ but its derivative is discontinuous across S then

$$[f_{,A}] = N^A B \quad where \quad B = [N^R f_{,R}]. \tag{8.2.2}$$

When $f \in C^1(\mathcal{R}^3)$ then

$$[f_{,AB}] = N^A N^B C \quad where \quad C = [N^R N^S f_{,RS}]. \tag{8.2.3}$$

In (8.2.2) and (8.2.3), N^A refers to the unit normal to S in the reference configuration and $[f]$ is the jump of a function across the wave as defined in chapter (7), equation (7.3.1).

To proceed we evaluate equations (8.2.1) on either side of S by taking the jump, employing the definition of the acceleration wave S, and the constitutive theory

(8.1.6) to obtain

$$\begin{aligned}
\rho[u_{i,tt}] &= W_{u_{i,A}u_{j,B}} N^A N^B [u_{j,RS} N^R N^S] \\
&\quad + W_{u_{i,A}p_{,B}} N^A N^B [p_{,RS} N^R N^S] \\
&\quad + W_{u_{i,A}q_{,B}} N^A N^B [q_{,RS} N^R N^S] \ , \\
0 &= \frac{\partial J_A}{\partial u_{i,C}} N^A N^C [u_{i,RS} N^R N^S] + \frac{\partial J_A}{\partial p_{,C}} N^A N^C [p_{,RS} N^R N^S] \\
&\quad + \frac{\partial J_A}{\partial q_{,C}} N^A N^C [q_{,RS} N^R N^S] - \beta_{iA} N^A [\dot{u}_{i,C} N^C] \ , \\
0 &= \frac{\partial M_A}{\partial u_{i,C}} N^A N^C [u_{i,RS} N^R N^S] + \frac{\partial M_A}{\partial p_{,C}} N^A N^C [p_{,RS} N^R N^S] \\
&\quad + \frac{\partial M_A}{\partial q_{,C}} N^A N^C [q_{,RS} N^R N^S] - \gamma_{iA} N^A [\dot{u}_{i,C} N^C].
\end{aligned} \tag{8.2.4}$$

The relation corresponding to the Hadamard formula (7.3.5) in three dimensions is

$$\frac{\delta}{\delta t}[f] = \left[\dot{f}\right] + U_N \left[N^A f_{,A}\right], \tag{8.2.5}$$

where $\delta/\delta t$ denotes the time derivative at the wave, $\dot{f} = \partial f/\partial t|_{\mathbf{X}}$, $f_{,A} = \partial f/\partial X_A$, and U_N is the speed at the point on S with unit normal N^A.

Since $u_i, p, q \in C^1(\mathcal{R}^3)$, $[u_{i,t}] = 0, [u_{i,A}] = 0, [p_t] = 0, [p_{,A}] = 0, [q_t] = 0, [q_{,A}] = 0$, so employing the Hadamard relation in three dimensions, *i.e.* equation (8.2.5), we obtain

$$\begin{aligned}
0 &= \frac{\delta}{\delta t}[u_{i,t}] = [u_{i,tt}] + U_N [N^A \dot{u}_{i,A}] \ , \quad 0 = \frac{\delta}{\delta t}[u_{i,A}] = [\dot{u}_{i,A}] + U_N [N^B u_{i,AB}] \ , \\
0 &= \frac{\delta}{\delta t}[p_{,t}] = [p_{,tt}] + U_N [N^A \dot{p}_{,A}] \ , \qquad 0 = \frac{\delta}{\delta t}[p_{,A}] = [\dot{p}_{,A}] + U_N [N^B p_{,AB}] \ , \\
0 &= \frac{\delta}{\delta t}[q_{,t}] = [q_{tt}] + U_N [N^A \dot{q}_{,A}] \ , \qquad 0 = \frac{\delta}{\delta t}[q_{,A}] = [\dot{q}_{,A}] + U_N [N^B q_{,AB}] \ .
\end{aligned} \tag{8.2.6}$$

Thus,

$$[\ddot{u}_i] = -U_N [N^A \dot{u}_{i,A}]. \tag{8.2.7}$$

which implies

$$[N^A \dot{u}_{i,A}] = -\frac{a_i}{U_N} \ , \tag{8.2.8}$$

and

$$[N^A \dot{u}_{i,A}] = -U_N [N^A N^B u_{i,AB}]. \tag{8.2.9}$$

Combining (8.2.7) and (8.2.9) gives

$$[\ddot{u}_i] = U_N^2 [N^A N^B u_{i,AB}], \tag{8.2.10}$$

likewise

$$[\ddot{p}] = U_N^2[N^A N^B p_{,AB}], \tag{8.2.11}$$

and

$$[\ddot{q}] = U_N^2[N^A N^B q_{,AB}]. \tag{8.2.12}$$

Using relations (8.2.7) – (8.2.12) in (8.2.4) we derive the three jump equations

$$\begin{aligned}
\left(\rho\delta_{ij}U_N^2 - W_{u_{i,A}u_{j,B}}N^A N^B\right)a_j(t) &= W_{u_{i,A}p,_B}N^A N^B P(t) + W_{u_{i,A}q,_B}N^A N^B Q(t)\ ,\\
\left(\frac{\partial J_A}{\partial u_{i,C}}N^A N^C + \beta_{iA}N^A U_N\right)a_i(t) &= -\frac{\partial J_A}{\partial p_{,C}}N^A N^C P(t) - \frac{\partial J_A}{\partial q_{,C}}N^A N^C Q(t)\ ,\\
\left(\frac{\partial M_A}{\partial u_{i,C}}N^A N^C + \gamma_{iA}N^A U_N\right)a_i(t) &= -\frac{\partial M_A}{\partial p_{,C}}N^A N^C P(t) - \frac{\partial M_A}{\partial q_{,C}}N^A N^C Q(t).
\end{aligned} \tag{8.2.13}$$

Let

$$\begin{gathered}
\xi_2 = \frac{\partial J_A}{\partial q_{,C}}N^A N^C\ , \quad \xi_1 = \frac{\partial J_A}{\partial p_{,C}}N^A N^C\ ,\\
\mu_2 = \frac{\partial M_A}{\partial p_{,C}}N^A N^C\ , \quad \mu_1 = \frac{\partial M_A}{\partial q_{,C}}N^A N^C\ ,\\
\Sigma = \xi_1\mu_1 - \xi_2\mu_2\ ,
\end{gathered}$$

$$\Gamma_i = Ł_i + \gamma_{iA}N^A U_N \quad \textit{and} \quad \Lambda_i = K_i + \beta_{iA}N^A U_N\ ,$$

where

$$K_i = \frac{\partial J_A}{\partial u_{i,C}}N^A N^C \quad \textit{and} \quad Ł_i = \frac{\partial M_A}{\partial u_{i,C}}N^A N^C\ .$$

Then equations (8.2.13) may be rewritten in the form

$$\begin{aligned}
\left(\rho\delta_{ij}U_N^2 - Q_{ij}\right)a_j(t) &= P_i P(t) + Q_i Q(t)\ ,\\
\Lambda_i a_i(t) &= -\xi_1 P(t) - \xi_2 Q(t)\ ,\\
\Gamma_i a_i(t) &= -\mu_2 P(t) - \mu_1 Q(t)\ ,
\end{aligned} \tag{8.2.14}$$

where the terms Q_{ij}, P_i, and Q_i are given by

$$Q_{ij} = W_{u_{i,A}u_{j,B}}N^A N^B\ , \quad P_i = W_{u_{i,A}p,_B}N^A N^B\ , \quad Q_i = W_{u_{i,A}q,_B}N^A N^B\ .$$

Solving for $P(t)$ and $Q(t)$ in terms of $a_i(t)$ only from equations $(8.2.14)_2$ and $(8.2.14)_3$, *i.e.*

$$\begin{pmatrix}\xi_1 & \xi_2\\ \mu_2 & \mu_1\end{pmatrix}\begin{pmatrix}P(t)\\ Q(t)\end{pmatrix} = \begin{pmatrix}-\Lambda_i a_i\\ -\Gamma_i a_i\end{pmatrix},$$

implies

$$\begin{pmatrix} P(t) \\ Q(t) \end{pmatrix} = \frac{1}{\Sigma} \begin{pmatrix} \mu_1 & -\xi_2 \\ -\mu_2 & \xi_1 \end{pmatrix} \begin{pmatrix} -\Lambda_i a_i \\ -\Gamma_i a_i \end{pmatrix},$$

which yields

$$P(t) = \left(\frac{\xi_2 \Gamma_i - \mu_1 \Lambda_i}{\Sigma} \right) a_i(t) \ , \tag{8.2.15}$$

and

$$Q(t) = \left(\frac{\mu_2 \Lambda_i - \xi_1 \Gamma_i}{\Sigma} \right) a_i(t) \ . \tag{8.2.16}$$

Substitute the expressions (8.2.15) and (8.2.16) into equation $(8.2.14)_1$ to obtain

$$\begin{aligned} \left(\rho \delta_{ij} U_N^2 - Q_{ij}\right) a_j(t) =& \frac{P_i}{\Sigma} \left\{ \xi_2 \left(\text{Ł}_j + \gamma_{jA} N^A U_N \right) - \mu_1 \left(K_j + \beta_{jA} N^A U_N \right) \right\} a_j(t) \\ &+ \frac{Q_i}{\Sigma} \left\{ \mu_2 \left(K_j + \beta_{jA} N^A U_N \right) - \xi_1 \left(\text{Ł}_j + \gamma_{jA} N^A U_N \right) \right\} a_j(t) \ , \end{aligned} \tag{8.2.17}$$

Equation (8.2.17) may be written as a wavespeed relation as follows

$$R_{ij} a_j = \rho \delta_{ij} U_N^2 a_j \ , \tag{8.2.18}$$

where

$$\begin{aligned} R_{ij} = Q_{ij} &+ \frac{P_i}{\Sigma} \left\{ \xi_2 \left(\text{Ł}_j + \gamma_{jA} N^A U_N \right) - \mu_1 \left(K_j + \beta_{jA} N^A U_N \right) \right\} \\ &+ \frac{Q_i}{\Sigma} \left\{ \mu_2 \left(K_j + \beta_{jA} N^A U_N \right) - \xi_1 \left(\text{Ł}_j + \gamma_{jA} N^A U_N \right) \right\} . \end{aligned} \tag{8.2.19}$$

Relation (8.2.18) is an eigenvalue/eigenvector equation. The wavespeeds U_N^2 are the eigenvalues of R_{ij} and a_j are the eigenvectors. This equation governs the propagation of a nonlinear acceleration wave and yields the wavespeed in three dimensions. Since the reference configuration $\mathcal{B}_0$ is deformed to a new current configuration $\mathcal{B}$, it means that there is an applied transformation to the surface S. Moreover, when applying a transformation to the surface S it is useful to derive normals n_i for the resulting surface s in the current configuration from the original normals N^A.

The transformation is well known, cf. Chen [21] Eq.(4.10) and Gentile & Straughan [35],

$$N^A = F_{iA} n_i \frac{|\nabla_{\mathbf{x}} s|}{|\nabla_{\mathbf{X}} S|} \ . \tag{8.2.20}$$

We use this in all the expressions in R_{ij} to write $R_{ij} = R_{ij}(n_i)$. So, we write

$$\begin{aligned} Q_{ij} &= \frac{\partial^2 W}{\partial u_{j,B} \partial u_{i,A}} N^A N^B \\ &= W_{u_{j,B} u_{i,A}} F_{rA} n_r F_{tB} n_t \left(\frac{|\nabla_{\mathbf{x}} s|}{|\nabla_{\mathbf{X}} S|} \right)^2 \\ &= Q_{ij}(n_i) \ . \end{aligned} \tag{8.2.21}$$

Then we have to write

$$\begin{aligned} P_i &= W_{u_{i,A} p_{,B}} N^A N^B \\ &= W_{u_{i,A} p_{,B}} F_{rA} n_r F_{tB} n_t \left(\frac{|\nabla_{\mathbf{x}} s|}{|\nabla_{\mathbf{X}} S|} \right)^2 \\ &= P_i(n_i) \ , \end{aligned} \tag{8.2.22}$$

and

$$\begin{aligned} Q_i &= W_{u_{i,A} q_{,B}} N^A N^B \\ &= W_{u_{i,A} q_{,B}} F_{rA} n_r F_{tB} n_t \left(\frac{|\nabla_{\mathbf{x}} s|}{|\nabla_{\mathbf{X}} S|} \right)^2 \\ &= Q_i(n_i) \ . \end{aligned} \tag{8.2.23}$$

Then we write $(8.2.14)_1$ as

$$\left(\rho \delta_{ij} U_N^2 - Q_{ij}(n_i) \right) a_j(t) = P_i(n_i) P(t) + Q_i(n_i) Q(t) \ , \tag{8.2.24}$$

and then

$$R_{ij}(\mathbf{n}) a_j = \rho \delta_{ij} U_N^2 a_j \ , \tag{8.2.25}$$

defines the correct relation from which we may deduce the existence of a plane acceleration wave that may propagate if a_j is an eigenvector of $R_{ij}(n_i)$.

The wavespeed may be calculated if we know the direction of an acceleration wave, say $a_j = a m_j$, where m_j is the unit vector in the direction of a_j.
Taking the inner product of (8.2.25) with m_i one may solve for the wavespeed as

$$U_N^2 = \frac{R_{ij} m_i m_j}{\rho} \ . \tag{8.2.26}$$

However, R_{ij} involves U_N so the wavespeed equation is

$$\begin{aligned}\rho U_N^2 =& Q_{ij}m_i m_j + \frac{P_i}{\Sigma}\left(\xi_2 \text{Ł}_j m_i m_j - \mu_1 K_j m_i m_j\right) \\ &+ \frac{Q_i}{\Sigma}\left(\mu_2 K_j m_i m_j - \xi_1 \text{Ł}_j m_i m_j\right) \\ &+ U_N \frac{P_i}{\Sigma}\left\{\xi_2 \gamma_{jA} N^A m_i m_j - \mu_1 \beta_{jA} N^A m_i m_j\right\} \\ &+ U_N \frac{Q_i}{\Sigma}\left\{\mu_2 \beta_{jA} N^A m_i m_j - \xi_1 \gamma_{jA} N^A m_i m_j\right\} \ ,\end{aligned} \tag{8.2.27}$$

which may be written as

$$\rho U_N^2 + A_1 U_N + A_2 = 0 \ , \tag{8.2.28}$$

thus, the speed of the wave is

$$U_N = -\frac{A_1}{2\rho} + \sqrt{\frac{A_1^2}{4\rho^2} + \frac{A_2}{\rho}} \ , \tag{8.2.29}$$

where

$$A_1 = \frac{P_i}{\Sigma}\left\{\mu_1 \beta_{jA} N^A m_i m_j - \xi_2 \gamma_{jA} N^A m_i m_j\right\} + \frac{Q_i}{\Sigma}\left\{\xi_1 \gamma_{jA} N^A m_i m_j - \mu_2 \beta_{jA} N^A m_i m_j\right\} \ ,$$

and

$$A_2 = Q_{ij} m_i m_j + \frac{P_i}{\Sigma}\left(\xi_2 \text{Ł}_j m_i m_j - \mu_1 K_j m_i m_j\right) + \frac{Q_i}{\Sigma}\left(\mu_2 K_j m_i m_j - \xi_1 \text{Ł}_j m_i m_j\right) \ .$$

Equation (8.2.28) allows for two waves, a right moving one and a left moving one.

Chapter 9

Conclusions and Future Work

Convection in porous media, particularly double-diffusive convection in porous media, has attracted our attention due to its wide range of applications in geological process and a variety of geotechnical applications, cf. Malashetty & Biradar [60].

We worked on a model of thermosolutal convection in porous media proposed by Pritchard & Richardson [83], Wang & Tan [124], and Malashetty & Biradar [60] and a generalization. They used the linear instability technique to investigate the stability of the systems. We used the energy method to obtain the space of definite stability because the linear instability technique guarantees instability but it does not specify any information about stability.

In chapters 2 and 3 we studied continuous dependence of the Darcy and the Brinkman thermosolutal convection on reaction. This investigation was needed to assess and study the properties of the models before the numerical work which follows in chapters 4 - 6. We obtained the nonlinear boundaries numerically using the energy method. Our study reveals regions of potential sub-critical instability when there is a reaction as we have shown in chapter 4 for the Darcy porous medium and chapter 5 for the Brinkman porous medium. In chapter 6 our investigation shows that the mechanical anisotropy parameter has opposite effect to that of the thermal anisotropy parameter on the stability of the Darcy thermosolutal convection system, in which we have restricted our consideration to the horizontal isotropic porous medium.

For further work, one may use the energy method to study the stability of the

reactive Brinkman thermosolutal convection with anisotropic permeability and thermal diffusivity. There are more than one form in which one may consider for the mechanical and thermal anisotropy parameters, the horizontal isotropic form $m_{ij} = diag\{m, m, m_{33}\}$ or the general form $m_{ij} = diag\{m_{11}, m_{22}, 1\}$. We may refer the reader to an article on nonlinear thermal convection in anisotropic porous media by Kvernvold & Tyvand [51] and the references therein. Moreover, one may consider the configuration of Tyvand & Storesletten [119] and Straughan & Walker [111] for the permeability. These writers studied a porous medium in which the permeability is transversely isotropic.

Regarding a deformed skeleton, we investigated the behaviour and the amplitude of a one-dimensional acceleration wave in non-linear double porosity materials in chapter 7 and we analysed the wave speed in three-dimensions in chapter 8. A further extension to this work is to obtain the amplitude equations for the three-dimensional acceleration waves in nonlinear double porosity materials, cf. Chen [21], Chen [20], and Lindsay & Straughan [55]. There are many application areas for multi-porosity elasticity, for example carbon sequestration in fissured aquifers, capacitive de-ionization water treatment process employing dual porosity electrodes, and many other applications, cf. Straughan [107] and the references therein.

Another possibility and interesting opportunity would be to study the behaviour of the acceleration waves in triple porosity elastic materials, cf. Straughan [108], Straughan [107], Svanadze [115], and Svanadze [114]. One may examine the behaviour of the acceleration waves for different forms of the terms representing connectivity between the pressures in the various pore scales as modelled by Straughan [107].

Bibliography

[1] Bushra Al-Sulaimi. The energy stability of Darcy thermosolutal convection with reaction. *International Journal of Heat and Mass Transfer*, 86:369–376, 2015.

[2] Bushra Al-Sulaimi. The non-linear energy stability of Brinkman thermosolutal convection with reaction. *Ricerche di Matematica*, pages 1–17, 2016.

[3] Giovambattista Amendola and Mauro Fabrizio. Thermal convection in a simple fluid with fading memory. *Journal of Mathematical Analysis and Applications*, 366(2):444–459, 2010.

[4] Giovambattista Amendola, Mauro Fabrizio, John Murrough Golden, and Adele Manes. Energy stability for thermo-viscous fluids with a fading memory heat flux. *Evolution Equations & Control Theory*, 4(3):265–279, 2015.

[5] Giovambattista Amendola, Mauro Fabrizio, and Adele Manes. On energy stability for a thermal convection in viscous fluids with memory. *Palestine Journal of Mathematics*, 2:144–158, 2013.

[6] K. A. Ames and B. Straughan. *Non-standard and improperly posed problems*, volume 194. Academic Press, 1997.

[7] GI Barenblatt, Iu P Zheltov, and IN Kochina. Basic concepts in the theory of seepage of homogeneous liquids in fissured rocks [strata]. *Journal of applied mathematics and mechanics*, 24(5):1286–1303, 1960.

[8] J. Bdzil and H. L. Frisch. Chemical instabilities. II. Chemical surface reactions and hydrodynamic instability. *Physics of Fluids (1958-1988)*, 14(3):475–482, 1971.

[9] J. Bdzil and H. L. Frisch. Chemically driven convection. *The Journal of Chemical Physics*, 72(3):1875–1886, 1980.

[10] James G Berryman and Herbert F Wang. Elastic wave propagation and attenuation in a double-porosity dual-permeability medium. *International Journal of Rock Mechanics and Mining Sciences*, 37(1):63–78, 2000.

[11] A. Berti, I. Bochicchio, and M. Fabrizio. Phase separation in quasi-incompressible fluids: Cahn Hilliard model in the Cattaneo Maxwell framework. ZAMP, 2014.

[12] V. Berti, M. Fabrizio, and D. Grandi. A phase field model for brine channels in sea ice. *Physica B*, 425:100–104, 2013.

[13] E. Bonetti, M. Fabrizio, and M. Frémond. A first order phase transition with non - constant density. *J. Math. Anal. Appl.*, 384:561–577, 2011.

[14] David Bourne. Hydrodynamic stability, the chebyshev tau method and spurious eigenvalues. *Continuum Mechanics and Thermodynamics*, 15(6):571–579, 2003.

[15] F Capone, V De Cataldis, and R De Luca. On the nonlinear stability of an epidemic SEIR reaction-diffusion model. *Ricerche di Matematica*, 62(1):161–181, 2013.

[16] F Capone, V De Cataldis, and R De Luca. On the stability of a SEIR reaction diffusion model for infections under Neumann boundary conditions. *Acta Applicandae Mathematicae*, 132(1):165–176, 2014.

[17] F Capone and R De Luca. On the stability-instability of vertical throughflows in double diffusive mixtures saturating rotating porous layers with large pores. *Ricerche di Matematica*, 63(1):119–148, 2014.

[18] Florinda Capone and Roberta De Luca. Coincidence between linear and global nonlinear stability of non-constant throughflows via the Rionero Auxiliary System Method. *Meccanica*, 49(9):2025–2036, 2014.

[19] S Chandrasekhar. Hydromagnetic and hydrodynamic stability. *Clarendon, Oxford*, 1961.

[20] Peter J Chen. The growth of acceleration waves of arbitrary form in homogeneously deformed elastic materials. *Archive for Rational Mechanics and Analysis*, 30(2):81–89, 1968.

[21] PJ Chen. Growth and decay of waves in solids(longitudinal and transverse shock and acceleration waves propagation and decay in anisotropic and isotropic elastic bodies based on theory of singular surfaces). *Solid-state mechanics 3.(A 73-45495 24-32) Berlin, Springer-Verlag, 1973,*, pages 303–402, 1973.

[22] DG Christopherson. Note on the vibration of membranes. *The Quarterly Journal of Mathematics*, 11:63–65, 1940.

[23] Michele Ciarletta, Francesca Passarella, and Merab Svanadze. Plane waves and uniqueness theorems in the coupled linear theory of elasticity for solids with double porosity. *Journal of Elasticity*, 114(1):55–68, 2014.

[24] Roberta De Luca. Global nonlinear stability and cold convection instability of non-constant porous throughflows, 2D in vertical planes. *Ricerche di Matematica*, pages 1–15, 2015.

[25] Roberta De Luca and Salvatore Rionero. Convection in multi-component rotating fluid layers via the Auxiliary System Method. *Ricerche di Matematica*, pages 1–17, 2015.

[26] J. J. Dongarra, B. Straughan, and D. W. Walker. Chebyshev Tau-QZ algorithm methods for calculating spectra of hydrodynamic stability problems. *Applied Numerical Mathematics*, 22(4):399–434, 1996.

[27] M. Fabrizio, C. Giorgi, and A. Morro. A thermodynamic approach to non-isothermal phase-field evolution in continuum physics. *Physica D*, 214:144–156, 2006.

[28] M. Fabrizio, C. Giorgi, and A. Morro. A continuum theory for first order phase transitions based on the balance of structure order. *Math. Meth. Appl. Sci.*, 31:627–653, 2008.

[29] M. Fabrizio, C. Giorgi, and A. Morro. Phase separation in quasi incompressible Cahn - Hilliard fluids. *European J. Mechanics, B/Fluids*, 30:281–287, 2011.

[30] SN Gaikwad and Irfana Begum. Onset of double-diffusive reaction–convection in an anisotropic rotating porous layer. *Transport in Porous Media*, 98(2):239–257, 2013.

[31] SN Gaikwad, MS Malashetty, and K Rama Prasad. An analytical study of linear and nonlinear double diffusive convection in a fluid saturated anisotropic porous layer with soret effect. *Applied Mathematical Modelling*, 33(9):3617–3635, 2009.

[32] SN Gaikwad, MS Malashetty, and K Rama Prasad. Linear and non-linear double diffusive convection in a fluid-saturated anisotropic porous layer with cross-diffusion effects. *Transport in porous media*, 80(3):537–560, 2009.

[33] J. E. Gatica, H. J. Viljoen, and V. Hlavacek. Interaction between chemical reaction and natural convection in porous media. *Chemical Engineering Science*, 44(9):1853–1870, 1989.

[34] JE Gatica, H Viljoen, and V Hlavacek. Stability analysis of chemical reaction and free convection in porous media. *International Communications in Heat and Mass Transfer*, 14(4):391–403, 1987.

[35] M Gentile and B Straughan. Acceleration waves in nonlinear double porosity elasticity. *International Journal of Engineering Science*, 73:10–16, 2013.

[36] M. Gentile and B. Straughan. Structural stability in resonant penetrative convection in a Forchheimer porous material. *Nonlinear Analysis, Real World Applications*, 14:397–401, 2013.

[37] D. Gilbarg and N.S. Trudinger. *Elliptic partial differential equations of second order*. Springer, Berlin - Heidelberg - New York, 1977.

[38] D. Gutkowicz-Krusin and J. Ross. Rayleigh–Bénard instability in reactive binary fluids. *The Journal of Chemical Physics*, 72(6):3577–3587, 1980.

[39] M. W. Hirsch and S. Smale. *Differential equations, dynamical systems, and linear algebra*. Academic Press, New York, 1974.

[40] C. W. Horton and F. T. Rogers. Convection currents in a porous medium. *Journal of Applied Physics*, 16(6):367–370, 1945.

[41] D Ieşan. Method of potentials in elastostatics of solids with double porosity. *International Journal of Engineering Science*, 88:118–127, 2015.

[42] D Ieşan and R Quintanilla. On a theory of thermoelastic materials with a double porosity structure. *Journal of Thermal Stresses*, 37(9):1017–1036, 2014.

[43] Dorin Iesan. *Thermoelastic models of continua*, volume 118. Springer Science & Business Media, 2013.

[44] DB Ingham and I Pop. Transport phenomenon in porous media, vol. i, 1998.

[45] Derek B Ingham and Ioan Pop. *Transport phenomena in porous media III*, volume 3. Elsevier, 2005.

[46] Jena Jeong, Paul Sardini, Hamidréza Ramézani, Marja Siitari-Kauppi, and Holger Steeb. Modeling of the induced chemo-mechanical stress through porous cement mortar subjected to co_2: enhanced micro-dilatation theory and 14 c-pmma method. *Computational Materials Science*, 69:466–480, 2013.

[47] Jihoon Kim and George J Moridis. Numerical analysis of fracture propagation during hydraulic fracturing operations in shale gas systems. *International Journal of Rock Mechanics and Mining Sciences*, 76:127–137, 2015.

[48] R. J. Knops and L. E. Payne. Continuous data dependence for the equations of classical elastodynamics. *Proc. Camb. Phil. Soc.*, 66:481–491, 1969.

[49] R. J. Knops and L. E. Payne. Improved estimates for continuous data dependence in linear elastodynamics. *Math. Proc. Camb. Phil. Soc.*, 103:535–559, 1988.

[50] Rajneesh Kumar, Richa Vohra, and MG Gorla. State space approach to boundary value problem for thermoelastic material with double porosity. *Applied Mathematics and Computation*, 271:1038–1052, 2015.

[51] Oddmund Kvernvold and Peder A Tyvand. Nonlinear thermal convection in anisotropic porous media. *Journal of Fluid Mechanics*, 90(04):609–624, 1979.

[52] ER Lapwood. Convection of a fluid in a porous medium. *Proceedings of the Cambridge*, 44:508–521, 1948.

[53] C. Lin and L. E. Payne. Structural stability for a Brinkman fluid. *Math. Meth. Appl. Sci.*, 30:567–578, 2007.

[54] C. Lin and L. E. Payne. Structural stability for the Brinkman equations of flow in double diffusive convection. *J. Math. Anal. Appl.*, 325:1479–1490, 2007.

[55] KA Lindsay and B Straughan. Propagation of mechanical and temperature acceleration waves in thermoelastic materials. *Zeitschrift für angewandte Mathematik und Physik ZAMP*, 30(3):477–490, 1979.

[56] KA Lindsay and B Straughan. Penetrative convection in a micropolar fluid. *International Journal of Engineering Science*, 30(12):1683–1702, 1992.

[57] Y. Liu, Y. Du, and C. H. Lin. Convergence and continuous dependence results for the Brinkman equations. *Applied Mathematics and Computation*, 215:4443–4455, 2010.

[58] S Lombardo and G Mulone. Induction magnetic stability with a two-component velocity field. *Mechanics Research Communications*, 62:89–93, 2014.

[59] M Malashetty and S Gaikwad. Onset of convective instabilities in a binary liquid mixtures with fast chemical reactions in a porous medium. *Heat and mass transfer*, 39(5-6):415–420, 2003.

[60] M. S. Malashetty and B. S. Biradar. The onset of double diffusive reaction - convection in an anisotropic porous layer. *Phys. Fluids*, 23:064102, 2011.

[61] MS Malashetty and Rajashekhar Heera. The effect of rotation on the onset of double diffusive convection in a horizontal anisotropic porous layer. *Transport in Porous Media*, 74(1):105–127, 2008.

[62] MS Malashetty and Mahantesh Swamy. The onset of convection in a binary fluid saturated anisotropic porous layer. *International Journal of Thermal Sciences*, 49(6):867–878, 2010.

[63] M Mamou. Stability analysis of double-diffusive convection in porous enclosures. *Transport phenomena in porous media II*, page 113, 2002.

[64] M Marin, S Vlase, and M Paun. Considerations on double porosity structure for micropolar bodies. *AIP Advances*, 5(3):037113, 2015.

[65] D Masin, V Herbstová, and J Bohác. Properties of double porosity clayfills and suitable constitutive models. In *PROCEEDINGS OF THE INTERNATIONAL CONFERENCE ON SOIL MECHANICS AND GEOTECHNICAL ENGINEERING*, volume 16, page 827. AA BALKEMA PUBLISHERS, 2005.

[66] Ian Masters, William KS Pao, and RW Lewis. Coupling temperature to a double-porosity model of deformable porous media. *International Journal for Numerical Methods in Engineering*, 49(3):421–438, 2000.

[67] Cleve B Moler and Gilbert W Stewart. An algorithm for generalized matrix eigenvalue problems. *SIAM Journal on Numerical Analysis*, 10(2):241–256, 1973.

[68] A. Morro and B. Straughan. Convective instabilities for reacting viscous flows far from equilibrium. *J. Non-Equilib. Thermodyn.*, 15:139–150, 1990.

[69] D. A. Nield. Onset of thermohaline convection in a porous medium. *Water Resources Research*, 4(3):553–560, 1968.

[70] D. A. Nield and A. Barletta. The Horton–Rogers–Lapwood problem revisited: the effect of pressure work. *Transport in Porous Media*, 77(2):143–158, 2009.

[71] D. A. Nield and A. Bejan. *Convection in porous media*. springer, 2006.

[72] Jace W Nunziato and Stephen C Cowin. A nonlinear theory of elastic materials with voids. *Archive for Rational Mechanics and Analysis*, 72(2):175–201, 1979.

[73] Steven A Orszag. Accurate solution of the orr–sommerfeld stability equation. *Journal of Fluid Mechanics*, 50(04):689–703, 1971.

[74] L. E. Payne. On geometric and modeling perturbations in partial differential equation. In R. J. Knops and A. A. Lacey, editors, *Proceedings of the LMS Symposium on Non-Classical Continuum Mechanics*, pages 108–128, Cambridge, 1987. Cambridge University Press.

[75] L. E. Payne. On stabilizing ill-posed problems against errors in geometry and modeling. In H. Engel and C. W. Groetsch, editors, *Proceedings of the Conference on Inverse and Ill-posed Problems: Strobhl*, pages 399–416, New York, 1987. Academic Press.

[76] L. E. Payne. Continuous dependence on geometry with applications in continuum mechanics. In G. A. C. Graham and S. K. Malik, editors, *Continuum Mechanics and its Applications*, pages 877–890, Washington, DC, 1989. Hemisphere Publ. Co.

[77] L. E. Payne, J. F. Rodrigues, and B. Straughan. Effect of anisotropic permeability on Darcy's law. *Math. Meth. Appl. Sci.*, 24:427–438, 2001.

[78] L. E. Payne, J. C. Song, and B. Straughan. Continuous dependence and convergence results for Brinkman and Forchheimer models with variable viscosity. *Proc. Roy. Soc. London A*, 455:2173–2190, 1999.

[79] L. E. Payne and B. Straughan. Stability in the initial-time geometry problem for the Brinkman and Darcy equations of flow in porous media. *J. Math. Pures et Appl.*, 75:225–271, 1996.

[80] L. E. Payne and B. Straughan. Analysis of the boundary condition at the interface between a viscous fluid and a porous medium and related modelling questions. *J. Math. Pures et Appl.*, 77:317–354, 1998.

[81] L. E. Payne and B. Straughan. Convergence and continuous dependence for the Brinkman - Forchheimer equations. *Stud. Appl. Math.*, 102:419–439, 1999.

[82] L. E. Payne and H. F. Weinberger. New bounds for solutions of second order elliptic partial differential equations. *Pacific J. Math.*, 8:551–573, 1958.

[83] D. Pritchard and C. N. Richardson. The effect of temperature - dependent solubility on the onset of thermosolutal convection in a horizontal porous layer. *J. Fluid Mech.*, 571:59–95, 2007.

[84] M. H. Protter and H. F. Weinberger. *Maximum Principles in Differential Equations*. PRENTICE-HALL, INC. Englewood Cliffs, New Jersey, 1967.

[85] Salvatore Rionero. Long-time behaviour of multi-component fluid mixtures in porous media. *International Journal of Engineering Science*, 48(11):1519–1533, 2010.

[86] Salvatore Rionero. Global nonlinear stability for a triply diffusive convection in a porous layer. *Continuum Mechanics and Thermodynamics*, 24(4-6):629–641, 2012.

[87] Salvatore Rionero. Multicomponent diffusive-convective fluid motions in porous layers: Ultimately boundedness, absence of subcritical instabilities, and global nonlinear stability for any number of salts. *Physics of Fluids (1994-present)*, 25(5):054104, 2013.

[88] Salvatore Rionero. Soret effects on the onset of convection in rotating porous layers via the Auxiliary System Method. *Ricerche di Matematica*, 62(2):183–208, 2013.

[89] Salvatore Rionero. Heat and mass transfer by convection in multicomponent Navier–Stokes Mixtures: Absence of subcritical instabilities and global nonlinear stability via the Auxiliary System Method. *Rendiconti Lincei-Matematica e Applicazioni*, 25(4):369–412, 2014.

[90] Salvatore Rionero. Lˆ2-energy decay of convective nonlinear PDEs reaction–diffusion systems via Auxiliary ODEs systems. *Ricerche di Matematica*, 64(2):251–287, 2015.

[91] Salvatore Rionero and Isabella Torcicollo. Stability of a Continuous Reaction-Diffusion Cournot-Kopel Duopoly Game Model. *Acta Applicandae Mathematicae*, 132(1):505–513, 2014.

[92] N. Rudraiah, P. G. Siddheshwar, and T. Masuoka. Nonlinear convection in porous media: a review. *Journal of Porous Media*, 6(1):1–32, 2003.

[93] P Sarma and K Aziz. New transfer functions for simulation of naturally fractured reservoirs with dual porosity models. SPEJ 11 (3): 328–340. Technical report, SPE-90231-PA. DOI: 10.2118/90231-PA, 2006.

[94] Edoardo Scarpetta and Merab Svanadze. Uniqueness theorems in the quasi-static theory of thermoelasticity for solids with double porosity. *Journal of Elasticity*, 120(1):67–86, 2015.

[95] Atul K Srivastava and P Bera. Influence of chemical reaction on stability of thermo-solutal convection of couple-stress fluid in a horizontal porous layer. *Transport in Porous Media*, 97(2):161–184, 2013.

[96] V. Steinberg and H. R. Brand. Convective instabilities of binary mixtures with fast chemical reaction in a porous medium. *The Journal of Chemical Physics*, 78(5):2655–2660, 1983.

[97] V. Steinberg and H. R. Brand. Amplitude equations for the onset of convection in a reactive mixture in a porous medium. *The Journal of Chemical Physics*, 80(1):431–435, 1984.

[98] L Storesletten. Effects of anisotropy on convective flow through porous media. *Transport phenomena in porous media*, pages 261–283, 1998.

[99] B. Straughan. *The energy method, stability, and nonlinear convection*, volume 91 of *Applied Mathematical Sciences*. Springer, New York, second edition, 2004.

[100] B. Straughan. *Stability and wave motion in porous media*, volume 165 of *Applied Mathematical Sciences*. Springer, New York, 2008.

[101] B. Straughan. Thermal convection with the cattaneo–christov model. *International Journal of Heat and Mass Transfer*, 53(1):95–98, 2010.

[102] B. Straughan. Continuous dependence on the heat source in resonant porous penetrative convection. *Studies in Applied Mathematics*, 1:1–13, 2011.

[103] B. Straughan. *Heat Waves*, volume 177 of *Applied Mathematical Sciences*. Springer, New York, 2011.

[104] B. Straughan. Stability and uniqueness in double porosity elasticity. *International Journal of Engineering Science*, 65:1–8, 2013.

[105] B. Straughan. Nonlinear stability in microfluidic porous convection problems. *Ricerche di Matematica*, 63(1):265–286, 2014.

[106] B. Straughan. Shocks and acceleration waves in modern continuum mechanics and in social systems. *Evolution Equations & Control Theory*, 3(3), 2014.

[107] B. Straughan. Modelling questions in multi-porosity elasticity. *Meccanica*, pages 1–10, 2016.

[108] B. Straughan. Waves and uniqueness in multi-porosity elasticity. *Journal of Thermal Stresses*, 39(6):704–721, 2016.

[109] B. Straughan and Bushra Al Sulaimi. Structural stability for Brinkman convection with reaction. *Bollettino dell'Unione Matematica Italiana*, 7(3):243–251, 2014.

[110] B. Straughan and K. Hutter. A priori bounds and structural stability for double diffusive convection incorporating the Soret effect. *Proc. Roy. Soc. London A*, 455:767–777, 1999.

[111] B. Straughan and DW Walker. Anisotropic porous penetrative convection. In *Proceedings of the Royal Society of London A: Mathematical, Physical and Engineering Sciences*, volume 452, pages 97–115. The Royal Society, 1996.

[112] Merab Svanadze. Plane waves and boundary value problems in the theory of elasticity for solids with double porosity. *Acta applicandae mathematicae*, 122(1):461–471, 2012.

[113] Merab Svanadze. Uniqueness theorems in the theory of thermoelasticity for solids with double porosity. *Meccanica*, 49(9):2099–2108, 2014.

[114] Merab Svanadze. Fundamental solutions in the theory of elasticity for triple porosity materials. *Meccanica*, pages 1–13, 2015.

[115] Merab Svanadze. External boundary value problems in the quasi static theory of elasticity for triple porosity materials. *PAMM*, 16(1):495–496, 2016.

[116] Clifford Truesdell and Richard Toupin. *The classical field theories*. Springer, 1960.

[117] I Tsagareli and L Bitsadze. Explicit solution of one boundary value problem in the full coupled theory of elasticity for solids with double porosity. *Acta Mechanica*, 226(5):1409–1418, 2015.

[118] H. Tu and C. Lin. Continuous dependence for the Brinkman equations of flow in double-diffusive convection. *Electronic Journal of Differential Equations*, 2007:1–9, 2007.

[119] Peder A Tyvand and Leiv Storesletten. Onset of convection in an anisotropic porous medium with oblique principal axes. *J. Fluid Mech*, 226:371–382, 1991.

[120] Peter Vadász. *Emerging Topics in Heat and Mass Transfer in Porous Media: From Bioengineering and Microelectronics to Nanotechnology*, volume 22. Springer Science & Business Media, 2008.

[121] K Vafai. Handbook of porous media, marcel dekker, new york, 2000.

[122] Kambiz Vafai. *Handbook of porous media*. Crc Press, 2005.

[123] H. J. Viljoen, J. E. Gatica, and V. Hlavacek. Bifurcation analysis of chemically driven convection. *Chemical Engineering Science*, 45(2):503–517, 1990.

[124] S. Wang and W. Tan. The onset of Darcy-Brinkman thermosolutal convection in a horizontal porous media. *Physics Letters A*, 373:776–780, 2009.

[125] D. J. Wollkind and H. L. Frisch. Chemical instabilities: I. A heated horizontal layer of dissociating fluid. *Physics of Fluids (1958-1988)*, 14(1):13–18, 1971a.

[126] D. J. Wollkind and H. L. Frisch. Chemical instabilities. III. Nonlinear stability analysis of a heated horizontal layer of dissociating fluid. *Physics of Fluids (1958-1988)*, 14(3):482–487, 1971b.

[127] Ying Zhao and Mian Chen. Fully coupled dual-porosity model for anisotropic formations. *International Journal of Rock Mechanics and Mining Sciences*, 43(7):1128–1133, 2006.

Appendix A

Useful Expressions

In section 1.1, we recalled two *lemmas* due to their usefulness in the qualitative stability analysis. Here, we are introducing the derivation of the identities used in our qualitative analysis by providing the proofs of the *lemmas*.

A.1 The Proof of *lemma 1*

Proof: To derive the *Rellich Identity* we begin by writing

$$\int_{\Omega} x_i \phi_{,i} \Delta\phi = 0, \tag{A.1.1}$$

which can be written as

$$\int_{\Omega} x_i \phi_{,i} \phi_{,kk} = 0, \tag{A.1.2}$$

upon integration of (A.1.2) by parts, we obtain

$$\int_{\Omega} \frac{\partial}{\partial x_k} \left(x_i \phi_{,i} \phi_{,k} \right) dV - \int_{\Omega} \phi_{,k} \frac{\partial}{\partial x_k} \left(x_i \phi_{,i} \right) dV = 0,$$

using the *Divergence Theorem*, implies

$$\oint_{\Gamma} x_i \phi_{,i} n_k \phi_{,k} dA - \int_{\Omega} \phi_{,k} \phi_{,i} x_{i,k} dV - \int_{\Omega} \phi_{,k} x_i \phi_{,ik} dV = 0,$$

which can be written as

$$\oint_{\Gamma} x_i \phi_{,i} n_k \phi_{,k} dA - \int_{\Omega} \phi_{,k} \phi_{,i} x_{i,k} dV - \frac{1}{2} \int_{\Omega} x_i \frac{\partial}{\partial x_i} \left(\phi_{,k} \phi_{,k} \right) dV = 0. \tag{A.1.3}$$

Integrating by parts on the last term of (A.1.3) and with the aid of the *Divergence Theorem*, we obtain

$$\oint_\Gamma x_i\phi_{,i}n_k\phi_{,k}dA - \int_\Omega \phi_{,k}\phi_{,i}x_{i,k}dV - \frac{1}{2}\oint_\Gamma x_i n_i\phi_{,k}\phi_{,k}dA + \frac{1}{2}\int_\Omega x_{i,i}\phi_{,k}\phi_{,k}dV = 0.$$

Using the fact that $x_{i,k} = \delta_{ik}$, we see

$$\oint_\Gamma x_i\phi_{,i}\frac{\partial\phi}{\partial n}dA + \frac{1}{2}\int_\Omega \phi_{,k}\phi_{,k}dV - \frac{1}{2}\oint_\Gamma x_i n_i\phi_{,k}\phi_{,k}dA = 0,$$

which can be written as

$$\oint_\Gamma x_i\phi_{,i}\frac{\partial\phi}{\partial n}dA + \frac{1}{2}\|\nabla\phi\|^2 - \frac{1}{2}\oint_\Gamma x_i n_i|\nabla\phi|^2dA = 0. \tag{A.1.4}$$

Employing the fact that on the boundary Γ, the gradient of ϕ is defined as

$$\nabla\phi = \nabla_s\phi + \mathbf{n}\frac{\partial\phi}{\partial n}, \tag{A.1.5}$$

where $\nabla_s\phi$ are the components of the surface gradient vector. Using (A.1.5) in (A.1.4), we obtain

$$\oint_\Gamma x_i n_i\left(\frac{\partial\phi}{\partial n}\right)^2 dA + \oint_\Gamma \mathbf{x}.\nabla_s\phi\frac{\partial\phi}{\partial n}dA + \frac{1}{2}\|\nabla\phi\|^2 - \frac{1}{2}\oint_\Gamma x_i n_i|\nabla\phi|^2dA = 0. \tag{A.1.6}$$

Squaring both sides of (A.1.5), leads to

$$|\nabla\phi|^2 = |\nabla_s\phi|^2 + 2\nabla_s\phi.\mathbf{n}\frac{\partial\phi}{\partial n} + \left(\frac{\partial\phi}{\partial n}\right)^2, \tag{A.1.7}$$

since $\nabla_s\phi$ and $n_i\frac{\partial\phi}{\partial n}$ are orthogonal vectors on the surface, their product is zero. Therefore, (A.1.7) will be

$$|\nabla\phi|^2 = |\nabla_s\phi|^2 + \left(\frac{\partial\phi}{\partial n}\right)^2. \tag{A.1.8}$$

Now, employing (A.1.8) in (A.1.6) we obtain

$$\begin{aligned}&\oint_\Gamma x_i n_i\left(\frac{\partial\phi}{\partial n}\right)^2 dA + \oint_\Gamma \mathbf{x}.\nabla_s\phi\frac{\partial\phi}{\partial n}dA + \frac{1}{2}\|\nabla\phi\|^2\\ &-\frac{1}{2}\oint_\Gamma x_i n_i|\nabla_s\phi|^2dA - \frac{1}{2}\oint_\Gamma x_i n_i\left(\frac{\partial\phi}{\partial n}\right)^2 dA = 0,\end{aligned} \tag{A.1.9}$$

which can be written as

$$\begin{aligned}\frac{1}{2}\oint_\Gamma x_i n_i\left(\frac{\partial\phi}{\partial n}\right)^2 dA + \frac{1}{2}\|\nabla\phi\|^2 &= \frac{1}{2}\oint_\Gamma x_i n_i|\nabla_s\phi|^2dA - \oint_\Gamma \mathbf{x}.\nabla_s\phi\frac{\partial\phi}{\partial n}dA\\ &\leq \frac{1}{2}\oint_\Gamma x_i n_i|\nabla_s\phi|^2dA\end{aligned} \tag{A.1.10}$$

Assume that Ω is star shaped so that $x_i n_i \geq K_0 > 0$ on Γ and also $x_i n_i \leq B_0$ on Γ, where K_0 *and* B_0 are constants. Therefore, from inequality (A.1.10) we may show that

$$\begin{aligned} K_0 \oint_\Gamma \left(\frac{\partial \phi}{\partial n}\right)^2 dA + \|\nabla\phi\|^2 &\leq \oint_\Gamma x_i n_i \left(\frac{\partial \phi}{\partial n}\right)^2 dA + \|\nabla\phi\|^2 \\ &\leq \oint_\Gamma x_i n_i |\nabla_s \phi|^2 dA \\ &\leq B_0 \oint_\Gamma |\nabla_s \phi|^2 dA, \end{aligned}$$

from which we conclude that

$$\|\nabla\phi\|^2 + K_0 \oint_\Gamma \left(\frac{\partial \phi}{\partial n}\right)^2 dA \leq B_0 \oint_\Gamma |\nabla_s \phi|^2 dA. \tag{A.1.11}$$

This ends the proof. □

A.2 The Proof of *lemma 2*

Proof: To prove the inequality (1.1.9), we begin by writing

$$\int_\Omega \psi\phi\Delta\phi dV = 0.$$

Using integration by parts, gives

$$\int_\Omega \frac{\partial}{\partial x_i}\left(\psi\phi\frac{\partial\phi}{\partial x_i}\right) dV - \int_\Omega \frac{\partial}{\partial x_i}(\psi\phi)\frac{\partial\phi}{\partial x_i} dV = 0. \tag{A.2.1}$$

Applying the *Divergence Theorem* to the first term, we obtain

$$\oint_\Gamma \psi\phi\frac{\partial\phi}{\partial n} dV - \int_\Omega \frac{\partial}{\partial x_i}(\psi\phi)\frac{\partial\phi}{\partial x_i} dV = 0. \tag{A.2.2}$$

Since $\psi = 0$ *on* Γ, condition $(1.1.8)_2$, the first term of (A.2.2) is zero, implying that

$$\int_\Omega \frac{\partial}{\partial x_i}(\psi\phi)\frac{\partial\phi}{\partial x_i} dV = 0. \tag{A.2.3}$$

Equation (A.2.3) may be written as

$$\int_\Omega \psi_{,i}\phi\phi_{,i} dV + \int_\Omega \psi\phi_{,i}\phi_{,i} dV = 0. \tag{A.2.4}$$

Handling the first term of (A.2.4), we see

$$\int_\Omega \psi_{,i}\phi\phi_{,i} dV = \int_\Omega \frac{\partial}{\partial x_i}(\psi_{,i}\phi\phi)\, dV - \int_\Omega \psi_{,ii}\phi^2 dV - \int_\Omega \psi_{,i}\phi_{,i}\phi dV,$$

which implies that

$$2\int_{\Omega}\psi_{,i}\phi\phi_{,i}dV=\int_{\Omega}\frac{\partial}{\partial x_i}\left(\psi_{,i}\phi^2\right)dV-\int_{\Omega}\psi_{,ii}\phi^2dV. \tag{A.2.5}$$

Applying the *Divergence Theorem* to the first term in the right hand side of (A.2.5) and employing condition $(1.1.8)_1$ to the second term, we obtain

$$\int_{\Omega}\psi_{,i}\phi\phi_{,i}dV=\frac{1}{2}\oint_{\Gamma}\phi^2\frac{\partial\psi}{\partial n}dA+\frac{1}{2}\int_{\Omega}\phi^2dV. \tag{A.2.6}$$

Substituting (A.2.6) in (A.2.4), gives

$$\frac{1}{2}\oint_{\Gamma}\phi^2\frac{\partial\psi}{\partial n}dA+\frac{1}{2}\int_{\Omega}\phi^2dV+\int_{\Omega}\psi\phi_{,i}\phi_{,i}dV=0, \tag{A.2.7}$$

which can be written as

$$\begin{aligned}2\left(\psi\nabla\phi,\nabla\phi\right)+\|\phi\|^2&=-\oint_{\Gamma}\phi^2\frac{\partial\psi}{\partial n}dA\\&\leq\psi_1\oint_{\Gamma}M^2dA,\end{aligned}$$

in which (1.1.10) and $(1.1.6)_2$ have been used.

This ends the proof. □

Appendix B

The Chebyshev Tau Method

Throughout this thesis, we have used the Chebyshev Tau method to solve the eigenvalue problems numerically. In this appendix we will introduce the Chebyshev polynomials and their properties which make them useful to apply and solve the equations. Then we will show how this technique work by applying it to a differential system of equations.

B.1 Chebyshev Polynomials

Chebyshev polynomials are a sequence of orthogonal polynomials which are related to de Moivre's formula and which can be defined recursively. In the study of differential equations they arise as the solution to the Chebyshev differential equations

$$(1-x^2)y'' - xy' + n^2 y = 0.$$

The Chebyshev polynomials of the n^{th} degree, $T_n : [-1,1] \to [-1,1]$, are defined by

$$T_n(\cos(\theta)) = cos(n\theta); \quad n = \{0,1,2,3,...\}. \tag{B.1.1}$$

The first two polynomials, the polynomial of degree 0 and the polynomial of degree 1, are defined by setting $n = 0$ and $n = 1$ respectively in (B.1.1) to find that

$$\begin{aligned} T_0 &= 1, \\ T_1 &= \cos(\theta). \end{aligned} \tag{B.1.2}$$

Then to define the higher degree Chebyshev polynomials recursively, we start by defining T_{n+1} and T_{n-1} using the known trigonometric identities, to find that

$$\begin{aligned} T_{n+1}(\cos(\theta)) &= \cos((n+1)\theta) = \cos(n\theta)\cos(\theta) - \sin(n\theta)\sin(\theta) \ , \\ T_{n-1}(\cos(\theta)) &= \cos((n-1)\theta) = \cos(n\theta)\cos(\theta) + \sin(n\theta)\sin(\theta) \ . \end{aligned} \tag{B.1.3}$$

Adding $(B.1.3)_1$ and $(B.1.3)_2$, we obtain the recurrence relation

$$T_{n+1}(\cos(\theta)) + T_{n-1}(\cos(\theta)) = 2\cos(n\theta)\cos(\theta). \tag{B.1.4}$$

We now use the known polynomials, *i.e.* T_0 and T_1, in (B.1.4) to find the higher degree Chebyshev polynomials. Setting $x = \cos(\theta)$, (B.1.4) may be written as

$$T_{n+1}(x) + T_{n-1}(x) = 2xT_n(x). \tag{B.1.5}$$

It follows that the full set of Chebyshev polynomials is

$$\begin{aligned} T_0(x) =& 1 \ , \\ T_1(x) =& x \ , \\ T_2(x) =& 2x^2 - 1 \ , \\ T_3(x) =& 4x^3 - 3x \ , \\ T_4(x) =& 8x^4 - 8x^2 + 1 \ , \\ T_5(x) =& 16x^5 - 20x^3 + 5x \ , \\ & \textit{etc.} \end{aligned} \tag{B.1.6}$$

B.2 Roots and Extrema

A Chebyshev polynomial of degree n has n different roots in the interval $[-1, 1]$. Using the trigonometric definition and the fact that

$$\cos\left(\frac{\pi}{2}(2k+1)\right) = 0 \ ,$$

one can easily prove that the roots of T_n are

$$x_k = \cos\left(\frac{\pi}{2}\frac{2k-1}{n}\right) \ ; \quad k = 1, 2, ..., n.$$

The extrema of T_n on the interval $-1 \leq x \leq 1$ are located at

$$x_k = \cos\left(\frac{k}{n}\pi\right) \ ; \quad k = 0, 1, ..., n.$$

The Chebyshev polynomials have extrema at the endpoints, given by

$$\begin{aligned} T_n(1) &= 1 \ , \\ T_n(-1) &= (-1)^n. \end{aligned} \tag{B.2.1}$$

One unique property of the Chebyshev polynomials is that on the interval $-1 \leq x \leq 1$ all of the extrema have values that are either -1 or 1.

B.3 Orthogonality

The fact that the Chebyshev polynomials form a sequence of orthogonal polynomials is employed in the Chebyshev Tau method. In this section we explore the orthogonality property of the Chebyshev polynomials. We start by considering a weighted integral of $T_n T_m$ over the interval $[-1, 1]$.

$$\begin{aligned} \int_{-1}^{1} \frac{T_n(x)T_m(x)}{\sqrt{1-x^2}} dx &= \int_0^{\pi} \cos(n\theta)\cos(m\theta) d\theta \\ &= \frac{1}{2}\int_0^{\pi} \left[\cos\left((n+m)\theta\right) + \cos\left(|n-m|\theta\right)\right] d\theta. \end{aligned} \tag{B.3.1}$$

We consider three cases, $n \neq m$, $n = m = 0$, and $n = m \neq 0$.

Case 1: $n \neq m$

In this case, we integrate (B.3.1) to obtain

$$\begin{aligned} \int_{-1}^{1} \frac{T_n(x)T_m(x)}{\sqrt{1-x^2}} dx &= \int_0^{\pi} \cos(n\theta)\cos(m\theta) d\theta \\ &= \frac{1}{2}\int_0^{\pi} \left[\cos\left((n+m)\theta\right) + \cos\left(|n-m|\theta\right)\right] d\theta \\ &= \frac{1}{2}\left[\frac{\sin\left((n+m)\theta\right)}{n+m} + \frac{\sin\left(|n-m|\theta\right)}{|n-m|}\right]_0^{\pi} \\ &= 0 \ . \end{aligned} \tag{B.3.2}$$

Case 2: $n = m = 0$

Here, in order to avoid the division by zero we simplify our expression to obtain

$$\begin{aligned} \int_{-1}^{1} \frac{T_n(x)T_m(x)}{\sqrt{1-x^2}} dx &= \int_0^{\pi} \cos(n\theta)\cos(m\theta) d\theta \\ &= \frac{1}{2}\int_0^{\pi} [1+1] d\theta \\ &= \pi \ . \end{aligned} \tag{B.3.3}$$

Case 3: $n = m \neq 0$

In this case, we have to simply the second term before integrating it to avoid the division by zero.

$$\begin{aligned}\int_{-1}^{1} \frac{T_n(x)T_m(x)}{\sqrt{1-x^2}}dx &= \int_0^{\pi} \cos(n\theta)\cos(m\theta)d\theta \\ &= \frac{1}{2}\int_0^{\pi} \left[\cos\left((n+m)\theta\right)+1\right]d\theta \\ &= \frac{1}{2}\left[\frac{\sin\left((n+m)\theta\right)}{n+m}+\theta\right]_0^{\pi} \\ &= \frac{\pi}{2}\ .\end{aligned} \tag{B.3.4}$$

Therefore, the Chebyshev polynomials are orthogonal with respect to the weighted inner product in $L^2(-1,1)$ so that

$$\langle T_n(x), T_m(x)\rangle = \int_{-1}^{1} \frac{T_n(x)T_m(x)}{\sqrt{1-x^2}}dx = \begin{cases} 0\ ; & n \neq m\ , \\ \pi\ ; & n = m = 0\ , \\ \frac{\pi}{2}\ ; & n = m \neq 0\ . \end{cases}$$

B.4 Chebyshev Differential Matrices

In this section we will derive the coefficient of the Chebyshev differential matrix D. A continuously differentiable function defined in $(-1,1)$ may be expanded in terms of Chebyshev polynomials such that

$$f(x) = \sum_{n=0}^{\infty} f_n T_n(x)\ , \tag{B.4.1}$$

where f_n are the coefficients of the expansion. If f is a polynomial of degree n, then the series will be finite, truncating at $n = N^{th}$ term. The derivatives of f take similar form to (B.4.1), so that in general

$$f^{(k)}(x) = \sum_{n=0}^{\infty} f_n^{(k)} T_n(x)\ , \tag{B.4.2}$$

where $f^{(k)}$ is the k^{th} derivative of f, with $f^{(0)} = f$, and $f_n^{(k)}$ are the coefficients related to the Chebyshev expansion of the k^{th} derivative of f.

We start by differentiating $T_n(x)$ with respect to x so that

$$\begin{aligned}\frac{dT_n(x)}{dx} &= \frac{dT_n}{d\theta}\frac{d\theta}{dx} \\ &= \frac{n\sin(n\theta)}{\sin(\theta)},\end{aligned} \tag{B.4.3}$$

from which we obtain

$$\begin{aligned}\frac{1}{n+1}T_{n+1}^{\backprime}(x) - \frac{1}{n-1}T_{|n-1|}^{\backprime}(x) &= \frac{1}{\sin(\theta)}\{\sin\left((n+1)\theta\right) - \sin\left((n-1)\theta\right)\} \\ &= 2\cos(n\theta) \\ &= 2T_n(x)\ ,\ n \geq 2.\end{aligned} \tag{B.4.4}$$

When $n = 0$ we have

$$T_1^{\backprime}(x) + T_1^{\backprime}(x) = 2T_0(x)\ , \tag{B.4.5}$$

and when $n = 1$, we need to multiply (B.4.4) by $n - 1$ we find that

$$T_0^{\backprime}(x) = 0. \tag{B.4.6}$$

Use of (B.1.6) shows that (B.4.5) and (B.4.6) are true and therefore

$$2T_n(x) = \frac{1}{n+1}T_{n+1}^{\backprime}(x) - \frac{1}{n-1}T_{|n-1|}^{\backprime}(x)\ ,\ for\ n \geq 0. \tag{B.4.7}$$

Therefore,

$$\begin{aligned}\frac{d}{dx}\sum_{n=0}^{\infty} f_n T_n(x) &= \sum_{n=0}^{\infty} f_n^{(1)} T_n(x) \\ &= \frac{1}{2}\sum_{n=0}^{\infty} f_n^{(1)}\left\{\frac{1}{n+1}T_{n+1}^{\backprime}(x) - \frac{1}{n-1}T_{|n-1|}^{\backprime}(x)\right\} \\ &= \frac{1}{2}\frac{d}{dx}\sum_{n=0}^{\infty} f_n^{(1)}\left\{\frac{1}{n+1}T_{n+1}(x) - \frac{1}{n-1}T_{|n-1|}(x)\right\}.\end{aligned} \tag{B.4.8}$$

So

$$\begin{aligned}2\frac{d}{dx}\left(f_0T_0 + f_1T_1 + ...\right) &= \frac{d}{dx}\left(f_0^{(1)}\left(T_1 + T_1\right) + f_1^{(1)}\left(\frac{T_2}{2}\right) + f_2^{(1)}\left(\frac{T_3}{3} - T_1\right) + \cdots\right) \\ &= \frac{d}{dx}\left(T_1(2f_0^{(1)} - f_2^{(1)}) + \frac{T_2}{2}(f_1^{(1)} - f_3^{(1)}) + \frac{T_3}{3}(f_2^{(1)} - f_4^{(1)}) + \cdots\right),\end{aligned} \tag{B.4.9}$$

where we have used (B.4.7) and (B.4.6). Equating the coefficients of T_i we have that

$$\begin{aligned}
2f_0 &= 0 \ , \\
2f_1 &= 2f_0^{(1)} - f_2^{(1)} \ , \\
2f_2 &= \frac{1}{2}(f_1^{(1)} - f_3^{(1)}) \ , \\
2f_3 &= \frac{1}{3}(f_2^{(1)} - f_4^{(1)}) \ , \\
2f_4 &= \frac{1}{4}(f_3^{(1)} - f_5^{(1)}) \ , \\
2f_5 &= \frac{1}{5}(f_4^{(1)} - f_6^{(1)}) \ , \\
&\textit{etc.}
\end{aligned} \tag{B.4.10}$$

which leads to the recurrence relation

$$2jf_j = c_{j-1}f_{j-1}^{(1)} - f_{j+1}^{(1)} \ for \ \ j \geq 1 \ , \tag{B.4.11}$$

where $c_0 = 2$ and $c_j = 1$ for $j \geq 1$.

Taking the sum of both sides of (B.4.11) from $j = n+1$ to $j = \infty$ where $n \geq 0$ such that $j + n$ is odd, *i.e.*

$$\begin{aligned}
2 \sum_{\substack{j=n+1 \\ j+n=odd}}^{\infty} jf_j &= \sum_{\substack{j=n+1 \\ j+n=odd}}^{\infty} c_{j-1}f_{j-1}^{(1)} - f_{j+1}^{(1)} \\
&= (c_n f_n^{(1)} - f_{n+2}^{(1)}) + (c_{n+2}f_{n+2}^{(1)} - f_{n+4}^{(1)}) + (c_{n+4}f_{n+4}^{(1)} - f_{n+6}^{(1)}) + \cdots \\
&= c_n f_n^{(1)} \ ,
\end{aligned} \tag{B.4.12}$$

where we have used the fact that $c_i = 1$ for $i \geq 1$, and we have cancelled all the terms except the first term. It follows that

$$f_n^{(1)} = \frac{2}{c_n} \sum_{\substack{j=n+1 \\ j+n=odd}}^{\infty} jf_j \ . \tag{B.4.13}$$

Therefore, in general

$$f_n^{(k)} = \frac{2}{c_n} \sum_{\substack{j=n+1 \\ j+n=odd}}^{\infty} jf_j^{(k-1)} \ , \quad n \geq 0 \ . \tag{B.4.14}$$

The Chebyshev expansion of $f^{(k)}(x)$ is now truncated at $n = N$ term to find that

$$f^{(k)}(x) = \sum_{n=0}^{N} f_n^{(k)} T_n(x) + e_{N+1}(x) \ , \tag{B.4.15}$$

where e_{N+1} is the error which is assumed to be small and that there exist a function $\tilde{f}^{(k)}(x)$ which approximate $f^{(k)}(x)$ so that

$$\tilde{f}^{(k)}(x) = \sum_{n=0}^{N} \tilde{f}_n T_n(x).$$

If we define a vector $\tilde{f}^{(k)} = (\tilde{f}_0^{(k)}, \tilde{f}_1^{(k)}, \tilde{f}_2^{(k)}, \tilde{f}_3^{(k)}, \cdots, \tilde{f}_N^{(k)})^T$ and then substitute into the expression (B.4.14) to obtain

$$\tilde{f}_n^{(k)} = \frac{2}{c_n} \sum_{\substack{j=n+1 \\ j+n=odd}}^{N} j f_j^{(k-1)} \ , \quad n \geq 0 \ . \tag{B.4.16}$$

Then we may construct an $(N+1) \times (N+1)$ upper triangular matrix D such that $\tilde{f}^{(k)} = D\tilde{f}^{(k-1)}$ where the matrix D is given by

$$D = \begin{pmatrix} 0 & 1 & 0 & 3 & 0 & 5 & 0 & 7 & 0 & ... \\ 0 & 0 & 4 & 0 & 8 & 0 & 12 & 0 & 16 & ... \\ 0 & 0 & 0 & 6 & 0 & 10 & 0 & 14 & 0 & ... \\ 0 & 0 & 0 & 0 & 8 & 0 & 12 & 0 & 16 & ... \\ 0 & 0 & 0 & 0 & 0 & 10 & 0 & 14 & 0 & ... \\ ... & ... & ... & ... & ... & ... & ... & ... & ... & ... \end{pmatrix} . \tag{B.4.17}$$

(B.4.17) is the first Chebyshev differential matrix. The second differential matrix D^2 is defined by $\tilde{f}^{(k)} = D^2\tilde{f}^{(k-2)}$. By matrix multiplication, we expect D^2 to be

$$D^2 = D \times D = \begin{pmatrix} 0 & 0 & 4 & 0 & 32 & 0 & 108 & ... \\ 0 & 0 & 0 & 24 & 0 & 120 & 0 & ... \\ 0 & 0 & 0 & 0 & 48 & 0 & 192 & ... \\ ... & ... & ... & ... & ... & ... & ... & ... \end{pmatrix} . \tag{B.4.18}$$

To verify this we start from (B.4.14)

$$
\begin{aligned}
f_n^{(2)} =& \frac{2}{c_n} \sum_{\substack{j=n+1 \\ j+n=odd}}^{\infty} j f_j^{(1)} \\
=& \frac{2}{c_n} \sum_{\substack{j=n+1 \\ j+n=odd}}^{\infty} j \frac{2}{c_j} \sum_{\substack{p=j+1 \\ p+j=odd}}^{\infty} p f_p \\
=& \frac{4}{c_n} \sum_{\substack{j=n+1 \\ j+n=odd}}^{\infty} j \sum_{\substack{p=j+1 \\ p+j=odd}}^{\infty} p f_p \ , \ c_{j\geq 1} = 1 \\
=& \frac{4}{c_n}(n+1)\left[(n+2)f_{n+2} + (n+4)f_{n+4} + (n+6)f_{n+6} + \cdots\right] \\
&+ \frac{4}{c_n}(n+3)\left[(n+4)f_{n+4} + (n+6)f_{n+6} + (n+8)f_{n+8} + \cdots\right] \\
&+ \frac{4}{c_n}(n+5)\left[(n+6)f_{n+6} + (n+8)f_{n+8} + (n+10)f_{n+10} + \cdots\right] \\
&+ \cdots \\
=& \frac{4}{c_n}(n+1)(n+2)f_{n+2} \\
&+ \frac{4}{c_n}\left[(n+1) + (n+3)\right](n+4)f_{n+4} \\
&+ \frac{4}{c_n}\left[(n+1) + (n+3) + (n+5)\right](n+6)f_{n+6} \\
&+ \frac{4}{c_n}\left[(n+1) + (n+3) + (n+5) + (n+7)\right](n+8)f_{n+8} \\
&+ \cdots \\
=& \frac{4}{c_n} \sum_{\substack{j=n+2 \\ j+n=even}}^{\infty} j f_j \sum_{\substack{p=n+1 \\ p+n=odd}}^{j-1} p \ .
\end{aligned}
\tag{B.4.19}
$$

We may simplify the finite sum as

$$\begin{aligned}
\sum_{\substack{p=n+1\\ p+n=odd}}^{j-1} p &= (n+1)+(n+3)+(n+5)+(n+7)+\cdots+(j-1)\\
&= \sum_{q=0}^{\frac{1}{2}(j-n-2)} (n+2q+1)\\
&= (n+1)\sum_{q=0}^{\frac{1}{2}(j-n-2)} 1 + 2\sum_{q=0}^{\frac{1}{2}(j-n-2)} q\\
&= (n+1)\left(\frac{1}{2}(j-n)\right) + 2\left(\frac{1}{2}(j-n-2)\right)\frac{1}{2}\left(\frac{1}{2}(j-n)\right)\\
&= \frac{1}{2}(j-n)\left[(n+1)+\left(\frac{1}{2}(j-n)-1\right)\right]\\
&= \frac{1}{2}(j-n)\left[\frac{1}{2}n+\frac{1}{2}j\right]\\
&= \frac{1}{4}(j^2-n^2).
\end{aligned} \tag{B.4.20}$$

Employing (B.4.20) in (B.4.19), it follows that

$$f_n^{(2)} = \frac{1}{c_n}\sum_{\substack{j=n+2\\ j+n=even}}^{\infty} j(j^2-n^2)f_j \ , \ n \geq 0 \ , \tag{B.4.21}$$

from which we find that

$$\begin{aligned}
f_0^{(2)} &= 4f_2 + 32f_4 + 108f_6 + \cdots\\
f_1^{(2)} &= 24f_3 + 120f_5 + \cdots\\
f_2^{(2)} &= 48f_4 + 192f_6 + \cdots\\
&\quad etc.
\end{aligned} \tag{B.4.22}$$

Similar expressions to (B.4.21) may be found for higher derivatives. Following the truncation method procedure used to obtain the first differentiation matrix, we find that (B.4.21) approves the matrix (B.4.18).

The Chebyshev tau method may be used to compute higher order derivative matrices, detailed explanation of the technique may be found in Dongarra *et al.* [26].

B.5 Application of Chebyshev Tau Method

In this section, we will show how to apply the Chebyshev-Tau method to solve the system (1.2.25) introduced in chapter 1 which is

$$\begin{aligned}(\hat{D}^2 - a^2)^2 W - Ra^2\Theta = 0 \\ (\hat{D}^2 - a^2)\Theta + RW = 0 \ ,\end{aligned} \tag{B.5.1}$$

where W is the velocity in the $\hat{z}$ direction, Θ is the temperature, a is the wave number, and R is the Rayleigh number. The corresponding boundary conditions

$$\hat{D}W = W = \Theta = 0 \ on \ \hat{z} = 0, 1. \tag{B.5.2}$$

We have to make the transformation from $\hat{z} \in (0,1) \rightarrow z \in (-1,1)$, *i.e.* $z = 2\hat{z} - 1$. Under this transformation $D = d/dz = 2d/d\hat{z}$. We have to introduce a variable χ such that $\chi = \Delta w$. Then equations (B.5.1) will be

$$\begin{aligned}(4D^2 - a^2)W - \chi = 0 \\ (4D^2 - a^2)\chi - Ra^2\Theta = 0 \\ (4D^2 - a^2)\Theta + RW = 0 \ ,\end{aligned} \tag{B.5.3}$$

we consider (B.5.3) to be an eigenvalue problem with eigenvalue R, and we have to obtain the critical Rayleigh number R_c.

We expand the functions W, χ, Θ in terms of Chebyshev polynomials such that

$$W(z) = \sum_{n=0}^{\infty} W_n T_n(z), \ \chi(z) = \sum_{n=0}^{\infty} \chi_n T_n(z), \ \Theta(z) = \sum_{n=0}^{\infty} \Theta_n T_n(z),$$

$$W''(z) = \sum_{n=0}^{\infty} W_n^{(2)} T_n(z), \ \chi''(z) = \sum_{n=0}^{\infty} \chi_n^{(2)} T_n(z), \ \Theta''(z) = \sum_{n=0}^{\infty} \Theta_n^{(2)} T_n(z) \ ,$$

where W_n, Θ_n, and χ_n are the coefficients of the expansions. Truncating the expansions in the $n = N^{th}$ term, so that the functions are approximated as

$$\begin{aligned}\tilde{W}(z) = \sum_{n=0}^{N} W_n T_n(z), \ \tilde{\chi}(z) = \sum_{n=0}^{N} \chi_n T_n(z), \ \tilde{\Theta}(z) = \sum_{n=0}^{N} \Theta_n T_n(z), \\ \tilde{W}''(z) = \sum_{n=0}^{N} W_n^{(2)} T_n(z), \ \tilde{\chi}''(z) = \sum_{n=0}^{N} \chi_n^{(2)} T_n(z), \ \tilde{\Theta}''(z) = \sum_{n=0}^{N} \Theta_n^{(2)} T_n(z) \ .\end{aligned} \tag{B.5.4}$$

The error resulting from this truncation may be expressed as

$$\begin{aligned}
\tilde{W}^{(2)}(z) - a^2\tilde{W}(z) - \tilde{\chi}(z) &= \tau_1 T_{N-1} + \tau_2 T_N \ , \\
\tilde{\chi}^{(2)}(z) - a^2\tilde{\chi}(z) - Ra^2\tilde{\Theta}(z) &= \tau_3 T_{N-1} + \tau_4 T_N \ , \\
\tilde{\Theta}^{(2)}(z) - a^2\tilde{\Theta}(z) - R\tilde{W}(z) &= \tau_5 T_{N-1} + \tau_6 T_N \ ,
\end{aligned} \tag{B.5.5}$$

where the $\tau_i' s$ are the error measurements.

Taking the weighted inner product of (B.5.5) with T_j for $j = 0, 1, 2, ..., N-2$ and using the orthogonality property of the Chebyshev polynomial on $L^2(-1, 1)$ to remove the $\tau_i' s$. In this way we obtain $(2N - 2)$ equations. Then we define vectors $\tilde{W} = (W_0, W_1, W_2, ..., W_N)^T$, $\tilde{\chi} = (\chi_0, \chi_1, \chi_2, ..., \chi_N)^T$, and $\tilde{\Theta} = (\Theta_0, \Theta_1, \Theta_2, ..., \Theta_N)^T$, and make the substitution $\tilde{W}^{(2)} = 4D^2\tilde{W}$, $\tilde{\chi}^{(2)} = 4D^2\tilde{\chi}$, and $\tilde{\Theta}^{(2)} = 4D^2\tilde{\Theta}$. We may then write our system in the form

$$\begin{aligned}
4D^2\tilde{W} - a^2\tilde{W} - \tilde{\chi} &= 0 \ , \\
4D^2\tilde{\chi} - a^2\tilde{\chi} &= Ra^2\tilde{\Theta} \ , \\
4D^2\tilde{\Theta} - a^2\tilde{\Theta} &= R\tilde{W} \ .
\end{aligned} \tag{B.5.6}$$

We have to add two rows of zeros to the bottom of the matrix D^2 To make the matrix square. Then we have to overwrite these two rows by the boundary conditions, in which we have to employ the property of the Chebyshev polynomials at -1 and 1, that

$$T_n(\pm 1) = (\pm 1)^n \ , \quad T_n^{\backprime}(\pm 1) = (\pm 1)^{n-1} n^2 \ ,$$

so that the boundary conditions may be expressed in the form

$$\sum_{n=0}^{N} W_n = 0 \ , \ \sum_{n=0}^{N} (-1)^n W_n = 0 \ ,$$

$$\sum_{n=0}^{N} \Theta_n = 0 \ , \ \sum_{n=0}^{N} (-1)^n \Theta_n = 0 \ ,$$

$$\sum_{n=0}^{N} n^2 W_n = 0 \ , \ \sum_{n=0}^{N} (-1)^{n-1} n^2 W_n = 0 \ .$$

Our system is now in the form of a generalised eigenvalue problem, in the form $Ax = RBx$, and can be solved using the QZ algorithm, cf. Moler & Stewart

[67], where $x = (W_0, W_1, W_2, ..., W_N, \chi_0, \chi_1, \chi_2, ..., \chi_N, \Theta_0, \Theta_1, \Theta_2, ..., \Theta_N)$ and the matrices A and B are given by

$$A = \begin{pmatrix} 4D^2 - a^2 I & -I & 0 \\ 1, 1, 1, 1, ..., 1 & 0 \cdots 0 & 0 \cdots 0 \\ 1, -1, 1, ..., (-1)^N & 0 \cdots 0 & 0 \cdots 0 \\ 0 & 4D^2 - a^2 I & 0 \\ 0, 1, 4, 9, ..., (N)^2 & 0 \cdots 0 & 0 \cdots 0 \\ 0, 1, -4, 9, -16, ..., (-1)^{N-1} N^2 & 0 \cdots 0 & 0 \cdots 0 \\ 0 & 0 & 4D^2 - a^2 I \\ 0 \cdots 0 & 0 \cdots 0 & 1, 1, 1, 1, ..., 1 \\ 0 \cdots 0 & 0 \cdots 0 & 1, -1, 1, ..., (-1)^N \end{pmatrix},$$

$$B = \begin{pmatrix} 0 & 0 & 0 \\ 0 \cdots 0 & 0 \cdots 0 & 0 \cdots 0 \\ 0 \cdots 0 & 0 \cdots 0 & 0 \cdots 0 \\ 0 & 0 & a^2 I \\ 0 \cdots 0 & 0 \cdots 0 & 0 \cdots 0 \\ 0 \cdots 0 & 0 \cdots 0 & 0 \cdots 0 \\ I & 0 & 0 \\ 0 \cdots 0 & 0 \cdots 0 & 0 \cdots 0 \\ 0 \cdots 0 & 0 \cdots 0 & 0 \cdots 0 \end{pmatrix}.$$

For more details, explanation, examples, and implementation of the Chebyshev-Tau method, we refer the reader to the books of Straughan [99,100], Dongarra *et al.* [26], Bourne [14], and Orszag [73].

Appendix C

The Compound Matrix Method

In chapter 5, we employed the Compound Matrix method to solve the Brinkman thermosolutal convection with reaction system. Below is the list of the 70 Compound Matrix variables which we generated:

$$y_1 = W_1W_2^{\prime}W_3^{\prime\prime}W_4^{\prime\prime\prime} + \cdots \quad y_2 = W_1W_2^{\prime}W_3^{\prime\prime}\Theta_4 + \cdots \quad y_3 = W_1W_2^{\prime}W_3^{\prime\prime}\Theta_4^{\prime} + \cdots$$

$$y_4 = W_1W_2^{\prime}W_3^{\prime\prime}\Phi_4 + \cdots \quad y_5 = W_1W_2^{\prime}W_3^{\prime\prime}\Phi_4^{\prime} + \cdots \quad y_6 = W_1W_2^{\prime}W_3^{\prime\prime\prime}\Theta_4 + \cdots$$

$$y_7 = W_1W_2^{\prime}W_3^{\prime\prime\prime}\Theta_4^{\prime} + \cdots \quad y_8 = W_1W_2^{\prime}W_3^{\prime\prime\prime}\Phi_4 + \cdots \quad y_9 = W_1W_2^{\prime}W_3^{\prime\prime\prime}\Phi_4^{\prime} + \cdots$$

$$y_{10} = W_1W_2^{\prime}\Theta_3\Theta_4^{\prime} + \cdots \quad y_{11} = W_1W_2^{\prime}\Theta_3\Phi_4 + \cdots \quad y_{12} = W_1W_2^{\prime}\Theta_3\Phi_4^{\prime} + \cdots$$

$$y_{13} = W_1W_2^{\prime}\Theta_3^{\prime}\Phi_4 + \cdots \quad y_{14} = W_1W_2^{\prime}\Theta_3^{\prime}\Phi_4^{\prime} + \cdots \quad y_{15} = W_1W_2^{\prime}\Phi_3\Phi_4^{\prime} + \cdots$$

$$y_{16} = W_1W_2^{\prime\prime}W_3^{\prime\prime\prime}\Theta_4 + \cdots \quad y_{17} = W_1W_2^{\prime\prime}W_3^{\prime\prime\prime}\Theta_4^{\prime} + \cdots \quad y_{18} = W_1W_2^{\prime\prime}W_3^{\prime\prime\prime}\Phi_4 + \cdots$$

$$y_{19} = W_1W_2^{\prime\prime}W_3^{\prime\prime\prime}\Phi_4^{\prime} + \cdots \quad y_{20} = W_1W_2^{\prime\prime}\Theta_3\Theta_4^{\prime} + \cdots \quad y_{21} = W_1W_2^{\prime\prime}\Theta_3\Phi_4 + \cdots$$

$$y_{22} = W_1W_2^{\prime\prime}\Theta_3\Phi_4^{\prime} + \cdots \quad y_{23} = W_1W_2^{\prime\prime}\Theta_3^{\prime}\Phi_4 + \cdots \quad y_{24} = W_1W_2^{\prime\prime}\Theta_3^{\prime}\Phi_4^{\prime} + \cdots$$

$$y_{25} = W_1W_2^{\prime\prime}\Phi_3\Phi_4^{\prime} + \cdots \quad y_{26} = W_1W_2^{\prime\prime}\Theta_3\Theta_4^{\prime} + \cdots \quad y_{27} = W_1W_2^{\prime\prime\prime}\Theta_3\Phi_4 + \cdots$$

$$y_{28} = W_1W_2^{\prime\prime\prime}\Theta_3\Phi_4^{\prime} + \cdots \quad y_{29} = W_1W_2^{\prime\prime\prime}\Theta_3^{\prime}\Phi_4 + \cdots \quad y_{30} = W_1W_2^{\prime\prime\prime}\Theta_3^{\prime}\Phi_4^{\prime} + \cdots$$

$$y_{31} = W_1W_2^{\prime\prime\prime}\Phi_3\Phi_4^{\prime} + \cdots \quad y_{32} = W_1\Theta_2\Theta_3^{\prime}\Phi_4 + \cdots \quad y_{33} = W_1\Theta_2\Theta_3^{\prime}\Phi_4^{\prime} + \cdots$$

$$y_{34} = W_1\Theta_2\Phi_3\Phi_4^{\prime} + \cdots \quad y_{35} = W_1\Theta_2^{\prime}\Phi_3\Phi_4^{\prime} + \cdots \quad y_{36} = W_1^{\prime}W_2^{\prime\prime}W_3^{\prime\prime\prime}\Theta_4 + \cdots$$

$$y_{37} = W_1^{\prime}W_2^{\prime\prime}W_3^{\prime\prime\prime}\Theta_4^{\prime} + \cdots \quad y_{38} = W_1^{\prime}W_2^{\prime\prime}W_3^{\prime\prime\prime}\Phi_4 + \cdots \quad y_{39} = W_1^{\prime}W_2^{\prime\prime}W_3^{\prime\prime\prime}\Phi_4^{\prime} + \cdots$$

$$y_{40} = W_1^{\prime}W_2^{\prime\prime}\Theta_3\Theta_4^{\prime} + \cdots \quad y_{41} = W_1^{\prime}W_2^{\prime\prime}\Theta_3\Phi_4 + \cdots \quad y_{42} = W_1^{\prime}W_2^{\prime\prime}\Theta_3\Phi_4^{\prime} + \cdots$$

$$y_{43} = W_1^{\backprime} W_2^{\backprime\backprime} \Theta_3^{\backprime} \Phi_4 + \cdots \quad y_{44} = W_1^{\backprime} W_2^{\backprime\backprime} \Theta_3^{\backprime} \Phi_4^{\backprime} + \cdots \quad y_{45} = W_1^{\backprime} W_2^{\backprime\backprime} \Phi_3 \Phi_4^{\backprime} + \cdots$$

$$y_{46} = W_1^{\backprime} W_2^{\backprime\backprime\backprime} \Theta_3 \Theta_4^{\backprime} + \cdots \quad y_{47} = W_1^{\backprime} W_2^{\backprime\backprime\backprime} \Theta_3 \Phi_4 + \cdots \quad y_{48} = W_1^{\backprime} W_2^{\backprime\backprime\backprime} \Theta_3 \Phi_4^{\backprime} + \cdots$$

$$y_{49} = W_1^{\backprime} W_2^{\backprime\backprime\backprime} \Theta_3^{\backprime} \Phi_4 + \cdots \quad y_{50} = W_1^{\backprime} W_2^{\backprime\backprime\backprime} \Theta_3^{\backprime} \Phi_4^{\backprime} + \cdots \quad y_{51} = W_1^{\backprime} W_2^{\backprime\backprime\backprime} \Phi_3 \Phi_4^{\backprime} + \cdots$$

$$y_{52} = W_1^{\backprime} \Theta_2 \Theta_3^{\backprime} \Phi_4 + \cdots \quad y_{53} = W_1^{\backprime} \Theta_2 \Theta_3^{\backprime} \Phi_4^{\backprime} + \cdots \quad y_{54} = W_1^{\backprime} \Theta_2 \Phi_3 \Phi_4^{\backprime} + \cdots$$

$$y_{55} = W_1^{\backprime} \Theta_2^{\backprime} \Phi_3 \Phi_4^{\backprime} + \cdots \quad y_{56} = W_1^{\backprime\backprime\backprime} W_2^{\backprime\backprime\backprime} \Theta_3 \Theta_4^{\backprime} + \cdots \quad y_{57} = W_1^{\backprime\backprime} W_2^{\backprime\backprime\backprime} \Theta_3 \Phi_4 + \cdots$$

$$y_{58} = W_1^{\backprime\backprime} W_2^{\backprime\backprime\backprime} \Theta_3 \Phi_4^{\backprime} + \cdots \quad y_{59} = W_1^{\backprime\backprime} W_2^{\backprime\backprime\backprime} \Theta_3^{\backprime} \Phi_4 + \cdots \quad y_{60} = W_1^{\backprime\backprime} W_2^{\backprime\backprime\backprime} \Theta_3^{\backprime} \Phi_4^{\backprime} + \cdots$$

$$y_{61} = W_1^{\backprime\backprime} W_2^{\backprime\backprime\backprime} \Phi_3 \Phi_4^{\backprime} + \cdots \quad y_{62} = W_1^{\backprime\backprime} \Theta_2 \Theta_3^{\backprime} \Phi_4 + \cdots \quad y_{63} = W_1^{\backprime\backprime} \Theta_2 \Theta_3^{\backprime} \Phi_4^{\backprime} + \cdots$$

$$y_{64} = W_1^{\backprime\backprime} \Theta_2 \Phi_3 \Phi_4^{\backprime} + \cdots \quad y_{65} = W_1^{\backprime\backprime} \Theta_2^{\backprime} \Phi_3 \Phi_4^{\backprime} + \cdots \quad y_{66} = W_1^{\backprime\backprime\backprime} \Theta_2 \Theta_3^{\backprime} \Phi_4 + \cdots$$

$$y_{67} = W_1^{\backprime\backprime\backprime} \Theta_2 \Theta_3^{\backprime} \Phi_4^{\backprime} + \cdots \quad y_{68} = W_1^{\backprime\backprime\backprime} \Theta_2 \Phi_3 \Phi_4^{\backprime} + \cdots \quad y_{69} = W_1^{\backprime\backprime\backprime} \Theta_2^{\backprime} \Phi_3 \Phi_4^{\backprime} + \cdots$$

$$y_{70} = \Theta_1 \Theta_2^{\backprime} \Phi_3 \Phi_4^{\backprime} + \cdots$$

The above 70 variables satisfy the 70 differential equations

$$y_1^{\backprime} = R_E R \frac{a^2}{\tilde{\gamma}} y_2 - R_E R_s \frac{a^2}{\tilde{\gamma}} \left(\frac{1 \mp \lambda}{2} \right) y_4$$

$$y_2^{\backprime} = y_3 + y_6$$

$$y_3^{\backprime} = y_7 + a^2 y_2 - R_E \frac{h\lambda}{2} y_4$$

$$y_4^{\backprime} = y_8 + y_5$$

$$y_5^{\backprime} = y_9 + (a^2 + \eta) y_4 - R_E \frac{h}{2} y_2$$

$$y_6^{\backprime} = y_7 + y_{16} + \left(2a^2 + \frac{1}{\tilde{\gamma}} \right) y_2 + R_E R_s \frac{a^2}{\tilde{\gamma}} \left(\frac{1 \mp \lambda}{2} \right) y_{11}$$

$$y_7^{\backprime} = y_{17} + \left(2a^2 + \frac{1}{\tilde{\gamma}} \right) y_3 + R_E R \frac{a^2}{\tilde{\gamma}} y_{10} + a^2 y_6 - R_E \left(\frac{h\lambda}{2} \right) y_8 + R_E R_s \frac{a^2}{\tilde{\gamma}} \left(\frac{1 \mp \lambda}{2} \right) y_{13}$$

$$y_8^{\backprime} = y_9 + y_{18} + \left(2a^2 + \frac{1}{\tilde{\gamma}} \right) y_4 + R_E R \frac{a^2}{\tilde{\gamma}} y_{11}$$

$$y_9^{\backprime} = y_{19} + \left(2a^2 + \frac{1}{\tilde{\gamma}} \right) y_5 + R_E R \frac{a^2}{\tilde{\gamma}} y_{12} - R_E R_s \frac{a^2}{\tilde{\gamma}} \left(\frac{1 \mp \lambda}{2} \right) y_{15} + (a^2 + \eta) y_8 - R_E \frac{h}{2} y_6$$

$$y_{10}^{\backprime} = y_{20} - R_E \left(\frac{h\lambda}{2} \right) y_{11}$$

$$y_{11}^{\backprime} = y_{12} + y_{13} + y_{21}$$

$$y_{12}^{\backprime} = y_{14} + y_{22} + (a^2 + \eta)y_{11}$$

$$y_{13}^{\backprime} = y_{14} + y_{23} + a^2 y_{11}$$

$$y_{14}^{\backprime} = y_{24} + a^2 y_{12} - R_E \left(\frac{h\lambda}{2}\right) y_{15} + (a^2 + \eta)y_{13} + R_E \frac{h}{2} y_{10}$$

$$y_{15}^{\backprime} = y_{25} + R_E \frac{h}{2} y_{11}$$

$$y_{16}^{\backprime} = y_{17} + y_{36} + R_E R_s \frac{a^2}{\tilde{\gamma}} \left(\frac{1 \mp \lambda}{2}\right) y_{21}$$

$$y_{17}^{\backprime} = y_{37} + R_E R \frac{a^2}{\tilde{\gamma}} y_{20} + a^2 y_{16} - R_E \frac{h\lambda}{2} y_{18} + R_E R_s \frac{a^2}{\tilde{\gamma}} \left(\frac{1 \mp \lambda}{2}\right) y_{23}$$

$$y_{18}^{\backprime} = y_{19} + y_{38} + R_E R \frac{a^2}{\tilde{\gamma}} y_{21}$$

$$y_{19}^{\backprime} = y_{39} + R_E R \frac{a^2}{\tilde{\gamma}} y_{22} - R_E R_s \frac{a^2}{\tilde{\gamma}} \left(\frac{1 \mp \lambda}{2}\right) y_{25} + (a^2 + \eta)y_{18} - R_E \frac{h}{2} y_{16}$$

$$y_{20}^{\backprime} = y_{40} + y_{26} - R_E \frac{h\lambda}{2} y_{21}$$

$$y_{21}^{\backprime} = y_{41} + y_{27} + y_{23} + y_{22}$$

$$y_{22}^{\backprime} = y_{42} + y_{28} + y_{24} + (a^2 + \eta)y_{21}$$

$$y_{23}^{\backprime} = y_{43} + y_{29} + y_{24} + a^2 y_{21}$$

$$y_{24}^{\backprime} = y_{44} + y_{30} + a^2 y_{22} - R_E \frac{h\lambda}{2} y_{25} + (a^2 + \eta)y_{23} + R_E \frac{h}{2} y_{20}$$

$$y_{25}^{\backprime} = y_{45} + y_{31} + R_E \frac{h}{2} y_{21}$$

$$y_{26}^{\backprime} = y_{46} + \left(2a^2 + \frac{1}{\tilde{\gamma}}\right) y_{20} - R_E \left(\frac{h\lambda}{2}\right) y_{27} - R_E R_s \frac{a^2}{\tilde{\gamma}} \left(\frac{1 \mp \lambda}{2}\right) y_{32}$$

$$y_{27}^{\backprime} = y_{47} + y_{29} + y_{28} + \left(2a^2 + \frac{1}{\tilde{\gamma}}\right) y_{21}$$

$$y_{28}^{\backprime} = y_{48} + y_{30} + (a^2 + \eta)y_{27} + \left(2a^2 + \frac{1}{\tilde{\gamma}}\right) y_{22} + R_E R_s \frac{a^2}{\tilde{\gamma}} \left(\frac{1 \mp \lambda}{2}\right) y_{34}$$

$$y_{29}^{\backprime} = y_{49} + y_{30} + a^2 y_{27} + \left(2a^2 + \frac{1}{\tilde{\gamma}}\right) y_{23} + R_E R \frac{a^2}{\tilde{\gamma}} y_{32}$$

$$y_{30}^{\backprime} = y_{50} + \left(2a^2 + \frac{1}{\tilde{\gamma}}\right) y_{24} + R_E R \frac{a^2}{\tilde{\gamma}} y_{33} + a^2 y_{28} - R_E \left(\frac{h\lambda}{2}\right) y_{31} + (a^2 + \eta)y_{29}$$
$$+ R_E R_s \frac{a^2}{\tilde{\gamma}} \left(\frac{1 \mp \lambda}{2}\right) y_{35} + R_E \frac{h}{2} y_{26}$$

$$y_{31}^{\backprime} = y_{51} + \left(2a^2 + \frac{1}{\tilde{\gamma}}\right) y_{25} + R_E R \frac{a^2}{\tilde{\gamma}} y_{34} + R_E \frac{h}{2} y_{27}$$

$$y_{32}^{\backprime} = y_{33} + y_{52}$$

$$y_{33}^{\backprime} = y_{53} - R_E \left(\frac{h\lambda}{2}\right) y_{34} + (a^2 + \eta) y_{32}$$

$$y_{34}^{\backprime} = y_{54} + y_{35}$$

$$y_{35}^{\backprime} = y_{55} + a^2 y_{34} - R_E \frac{h}{2} y_{32}$$

$$y_{36}^{\backprime} = y_{37} - \left(a^4 + \frac{a^2}{\tilde{\gamma}}\right) y_2 + R_E R_s \frac{a^2}{\tilde{\gamma}} \left(\frac{1 \mp \lambda}{2}\right) y_{41}$$

$$y_{37}^{\backprime} = R_E R \frac{a^2}{\tilde{\gamma}} y_{40} + a^2 y_{36} - R_E \left(\frac{h\lambda}{2}\right) y_{38} - \left(a^4 + \frac{a^2}{\tilde{\gamma}}\right) y_3 + R_E R_s \frac{a^2}{\tilde{\gamma}} \left(\frac{1 \mp \lambda}{2}\right) y_{43} + R_E R y_1$$

$$y_{38}^{\backprime} = y_{39} + R_E R \frac{a^2}{\tilde{\gamma}} y_{41} - \left(a^4 + \frac{a^2}{\tilde{\gamma}}\right) y_4$$

$$y_{39}^{\backprime} = R_E R \frac{a^2}{\tilde{\gamma}} y_{42} - R_E R_s \frac{a^2}{\tilde{\gamma}} \left(\frac{1 \mp \lambda}{2}\right) y_{45} + (a^2 + \eta) y_{38} - R_E \frac{h}{2} y_{36} - \left(a^4 + \frac{a^2}{\tilde{\gamma}}\right) y_5 - R_E R_s \left(\frac{1 \mp \lambda}{2\lambda}\right) y_1$$

$$y_{40}^{\backprime} = y_{46} - R_E \left(\frac{h\lambda}{2}\right) y_{41} + R_E R y_2$$

$$y_{41}^{\backprime} = y_{47} + y_{43} + y_{42}$$

$$y_{42}^{\backprime} = y_{48} + y_{44} + (a^2 + \eta) y_{41} - R_E R_s \left(\frac{1 \mp \lambda}{2\lambda}\right) y_2$$

$$y_{43}^{\backprime} = y_{49} + y_{44} + a^2 y_{41} - R_E R y_4$$

$$y_{44}^{\backprime} = y_{50} + a^2 y_{42} - R_E \left(\frac{h\lambda}{2}\right) y_{45} + (a^2 + \eta) y_{43} - R_E R y_5 + R_E \frac{h}{2} y_{40} - R_E R_s \left(\frac{1 \mp \lambda}{2\lambda}\right) y_3$$

$$y_{45}^{\backprime} = y_{51} + R_E \frac{h}{2} y_{41} - R_E R_s \left(\frac{1 \mp \lambda}{2\lambda}\right) y_4$$

$$y_{46}^{\backprime} = y_{56} - R_E \left(\frac{h\lambda}{2}\right) y_{47} + \left(2a^2 + \frac{1}{\tilde{\gamma}}\right) y_{40} + R_E R y_6 + \left(a^4 + \frac{a^2}{\tilde{\gamma}}\right) y_{10} - R_E R_s \frac{a^2}{\tilde{\gamma}} \left(\frac{1 \mp \lambda}{2}\right) y_{52}$$

$$y_{47}^{\backprime} = y_{57} + y_{49} + y_{48} + \left(2a^2 + \frac{1}{\tilde{\gamma}}\right) y_{41} + \left(a^4 + \frac{a^2}{\tilde{\gamma}}\right) y_{11}$$

$$y_{48}^{\backprime} = y_{58} + y_{50} + (a^2+\eta)y_{47} + \left(2a^2 + \frac{1}{\tilde{\gamma}}\right) y_{42} - R_E R_s \left(\frac{1 \mp \lambda}{2\lambda}\right) y_6 + \left(a^4 + \frac{a^2}{\tilde{\gamma}}\right) y_{12}$$
$$+ R_E R_s \frac{a^2}{\tilde{\gamma}} \left(\frac{1 \mp \lambda}{2}\right) y_{54}$$

$$y_{49}^{\backprime} = y_{59} + y_{50} + a^2 y_{47} + \left(2a^2 + \frac{1}{\tilde{\gamma}}\right) y_{43} + R_E R \frac{a^2}{\tilde{\gamma}} y_{52} - R_E R y_8 + \left(a^4 + \frac{a^2}{\tilde{\gamma}}\right) y_{13}$$

$$y_{50}^{\backprime} = y_{60} + \left(2a^2 + \frac{1}{\tilde{\gamma}}\right) y_{44} + R_E R \frac{a^2}{\tilde{\gamma}} y_{53} + a^2 y_{48} - R_E \left(\frac{h\lambda}{2}\right) y_{51} + (a^2+\eta) y_{49}$$
$$+ \left(a^4 + \frac{a^2}{\tilde{\gamma}}\right) y_{14} + R_E R_s \frac{a^2}{\tilde{\gamma}} \left(\frac{1 \mp \lambda}{2}\right) y_{55} - R_E R y_9 + R_E \frac{h}{2} y_{46} - R_E R_s \left(\frac{1 \mp \lambda}{2\lambda}\right) y_7$$

$$y_{51}^{\backprime} = y_{61} + \left(2a^2 + \frac{1}{\tilde{\gamma}}\right) y_{45} + R_E R \frac{a^2}{\tilde{\gamma}} y_{54} + \left(a^4 + \frac{a^2}{\tilde{\gamma}}\right) y_{15} + R_E \frac{h}{2} y_{47} - R_E R_s \left(\frac{1 \mp \lambda}{2\lambda}\right) y_8$$

$$y_{52}^{\backprime} = y_{62} + y_{53} - R_E R y_{11}$$

$$y_{53}^{\backprime} = y_{63} - R_E \left(\frac{h\lambda}{2}\right) y_{54} + (a^2+\eta) y_{52} - R_E R y_{12} - R_E R_s \left(\frac{1 \mp \lambda}{2\lambda}\right) y_{10}$$

$$y_{54}^{\backprime} = y_{64} + y_{55} - R_E R_s \left(\frac{1 \mp \lambda}{2\lambda}\right) y_{11}$$

$$y_{55}^{\backprime} = y_{65} + a^2 y_{54} + R_E R y_{15} - R_E \frac{h}{2} y_{52} - R_E R_s \left(\frac{1 \mp \lambda}{2\lambda}\right) y_{13}$$

$$y_{56}^{\backprime} = \left(a^4 + \frac{a^2}{\tilde{\gamma}}\right) y_{20} - R_E \left(\frac{h\lambda}{2}\right) y_{57} - R_E R_s \frac{a^2}{\tilde{\gamma}} \left(\frac{1 \mp \lambda}{2}\right) y_{62} + R_E R y_{16}$$

$$y_{57}^{\backprime} = y_{59} + y_{58} + \left(a^4 + \frac{a^2}{\tilde{\gamma}}\right) y_{21}$$

$$y_{58}^{\backprime} = y_{60} + (a^2+\eta) y_{57} - R_E R_s \left(\frac{1 \mp \lambda}{2\lambda}\right) y_{16} + \left(a^4 + \frac{a^2}{\tilde{\gamma}}\right) y_{22} + R_E R_s \frac{a^2}{\tilde{\gamma}} \left(\frac{1 \mp \lambda}{2}\right) y_{64}$$

$$y_{59}^{\backprime} = y_{60} + a^2 y_{57} + R_E R \frac{a^2}{\tilde{\gamma}} y_{62} - R_E R y_{18} + \left(a^4 + \frac{a^2}{\tilde{\gamma}}\right) y_{23}$$

$$y_{60}^{\backprime} = R_E R \frac{a^2}{\tilde{\gamma}} y_{63} + a^2 y_{58} - R_E \left(\frac{h\lambda}{2}\right) y_{61} + (a^2+\eta) y_{59} + \left(a^4 + \frac{a^2}{\tilde{\gamma}}\right) y_{24}$$
$$+ R_E R_s \frac{a^2}{\tilde{\gamma}} \left(\frac{1 \mp \lambda}{2}\right) y_{65} - R_E R y_{19} + R_E \frac{h}{2} y_{56} - R_E R_s \left(\frac{1 \mp \lambda}{2\lambda}\right) y_{17}$$

$$y_{61}^{\backprime} = R_E R \frac{a^2}{\tilde{\gamma}} y_{64} + \left(a^4 + \frac{a^2}{\tilde{\gamma}}\right) y_{25} + R_E \frac{h}{2} y_{57} - R_E R_s \left(\frac{1 \mp \lambda}{2\lambda}\right) y_{18}$$

$$y_{62}^{\backprime} = y_{66} + y_{63} - R_E R y_{21}$$

$$y_{63}^{\backprime} = y_{67} - R_E \left(\frac{h\lambda}{2}\right) y_{64} + (a^2+\eta) y_{62} - R_E R y_{22} - R_E R_s \left(\frac{1 \mp \lambda}{2\lambda}\right) y_{20}$$

$$
\begin{aligned}
y_{64}^{\backprime} &= y_{68} + y_{65} - R_E R_s \left(\frac{1 \mp \lambda}{2\lambda}\right) y_{21} \\
y_{65}^{\backprime} &= y_{69} + a^2 y_{64} + R_E R y_{25} - R_E \frac{h}{2} y_{62} - R_E R_s \left(\frac{1 \mp \lambda}{2\lambda}\right) y_{23} \\
y_{66}^{\backprime} &= -\left(a^4 + \frac{a^2}{\tilde{\gamma}}\right) y_{32} + \left(2a^2 + \frac{1}{\tilde{\gamma}}\right) y_{62} + y_{67} - R_E R y_{27} \\
y_{67}^{\backprime} &= -\left(a^4 + \frac{a^2}{\tilde{\gamma}}\right) y_{33} + \left(2a^2 + \frac{1}{\tilde{\gamma}}\right) y_{63} - R_E \left(\frac{h\lambda}{2}\right) y_{68} + (a^2 + \eta) y_{66} \\
&\quad - R_E R_s \frac{a^2}{\tilde{\gamma}} \left(\frac{1 \mp \lambda}{2}\right) y_{70} - R_E R y_{28} - R_E R \left(\frac{1 \mp \lambda}{2\lambda}\right) y_{26} \\
y_{68}^{\backprime} &= -\left(a^4 + \frac{a^2}{\tilde{\gamma}}\right) y_{34} + \left(2a^2 + \frac{1}{\tilde{\gamma}}\right) y_{64} + y_{69} - R_E R_s \left(\frac{1 \mp \lambda}{2\lambda}\right) y_{27} \\
y_{69}^{\backprime} &= -\left(a^4 + \frac{a^2}{\tilde{\gamma}}\right) y_{35} + \left(2a^2 + \frac{1}{\tilde{\gamma}}\right) y_{65} + R_E R \frac{a^2}{\tilde{\gamma}} y_{70} + a^2 y_{68} + R_E R y_{31} \\
&\quad - R_E \frac{h}{2} y_{66} - R_E R_s \left(\frac{1 \mp \lambda}{2\lambda}\right) y_{29} \\
y_{70}^{\backprime} &= R_E R y_{34} - R_E R_s \left(\frac{1 \mp \lambda}{2\lambda}\right) y_{32}
\end{aligned}
$$